NASA-CR-54037

N64-26580

ALKALI METALS BOILING AND CONDENSING INVESTIGATIONS

Quarterly Progress Report 6

Volume I

EDITED BY J. LONGO, JR.

prepared for
NATIONAL AERONAUTICS AND SPACE ADMINISTRATION

SPACE POWER AND PROPULSION SECTION
MISSILE AND SPACE DIVISION
GENERAL ELECTRIC
CINCINNATI 15, OHIO

ALKALI METALS BOILING AND CONDENSING INVESTIGATIONS
VOLUME I

QUARTERLY PROGRESS REPORT 6
Covering the Period
October 1, 1963 to December 31, 1963

edited by
J. Longo, Jr.
Manager, Heat Transfer Project

prepared for

NATIONAL AERONAUTICS AND SPACE ADMINISTRATION

Contract NAS 3-2528
April 20, 1964

Technical Management
NASA - Lewis Research Center
Nuclear Power Technology Branch
Ruth N. Weltmann

SPACE POWER AND PROPULSION SECTION
MISSILE AND SPACE DIVISION
GENERAL ELECTRIC COMPANY
Cincinnati 15, Ohio, 45215

FOREWORD

The investigation described herein is being performed by the General Electric Company under the sponsorship of the National Aeronautics and Space Administration under contract NAS 3-2528.

Its purpose is to accumulate information pertinent to heat transfer phenomena, two-phase pressure drop, and stability characteristics of boiling and condensing potassium and sodium. Studies are to be executed at conditions approximately those anticipated in space turboelectric systems exceeding 100 kw electric output.

The quarterly report of the Alkali Metals Boiling and Condensing Investigations, extending from October 1, 1963 through December 31, 1963, is presented in two volumes. Volume I documents the general plan of investigation, operation of the facilities, results of the investigations, supporting instrumentation and materials effort, and, also, the tabulated heat transfer data obtained from the 100 kw and 50 kw facilities. Volume II documents the 300 kw heat transfer data, including discussion of the data as well as calculational procedures.

TABLE OF CONTENTS

		Page No.
FOREWORD		iii
TABLE OF CONTENTS		v
LIST OF TABLES		vii
LIST OF ILLUSTRATIONS		viii
NOMENCLATURE		xiii
SECTION		
	SUMMARY	1
I.	300 KW FACILITY	3
	300 KW Operations	3
	Data Analysis	7
IA.	300 KW FACILITY MULTITUBE BOILER TEST SECTION	15
	Requirements	15
	Thermal Analyses	17
II.	100 KW FACILITY	27
	100 KW Operation	27
	Data Analysis	32
III.	50 KW FACILITY	35
	50 KW Operation	35
	Data Analysis	37
	Calorimetric Flowmeter	43
IV.	POOL BOILING HEAT TRANSFER INVESTIGATIONS	45
V.	ANALYSIS	47
	General Considerations	47
	Acceleration Pressure Drop	52
	Elevation Pressure Drop	55
	Other Quantities of Interest	57
	Summary	58
VI.	INSTRUMENTATION	61
	300 KW Facility	61
	100 KW Facility	63
	50 KW Facility	63

TABLE OF CONTENTS (CONT'D)

	Page No.
VII. MATERIALS SUPPORT	65
300 KW Facility	65
100 KW Facility	65
50 KW Facility	65
TABLES	67
ILLUSTRATIONS	75
REFERENCES	154
APPENDICES	
A. Evaluation of the 300 KW Facility Multitube Boiler Concept	159
B. 100 KW Facility Heat Transfer Data	161
C. 50 KW Facility Heat Transfer Data	195
D. A Calorimetric Method for the Measurement of Alkali Metal Flow Rate	273
E. Derivation of the Expression for the Two-Phase Gradient from Continuity and Momentum Considerations	279
F. Derivation of the Relationship between Slip, Void Fraction, and Flowing Quality	283
G. Expressions for the Slip and Shape Factor in Terms of the Entrainment Fraction for the Modified Annular Flow Model	285
H. The Determination of Expressions for Several of the Densities in Terms of the Slip Ratio	289
I. The Determination of the Derivative of $1/\hat{\rho}$ with Respect to the Slip Ratio	291
J. The Relationship between the Slip Ratio and the Acceleration Factor	293
K. Proof that the Value of $1/\hat{\rho}$ is Identical for a Slip of one and a Slip equal to ρ_f/ρ_g.	295

LIST OF TABLES

Table		Page
1	Conditions for Film Boiling Runs	67
2	Properties of L-605 at Elevated Temperatures	68
3	Measurements of L-605 Alloy Tube for 300 KW Test Section.	69
4	300 KW Facility Instrumentation Locations.	70

LIST OF ILLUSTRATIONS

Figure		Page
1.	Primary Shell Wall Temperature Vs. Length - 300 KW System Film Boiling Run 5/11 1856.	75
2.	Primary Shell Wall Temperature Vs. Length - 300 KW System Film Boiling Run 5/11 1955.	76
3.	Primary Shell Wall Temperature Vs. Length - 300 KW System Film Boiling Run 5/11 2056.	77
4.	Primary Shell Wall Temperature Vs. Length - 300 KW System Film Boiling Run 5/11 2256.	78
5.	Primary Shell Wall Temperature Vs. Length - 300 KW System Film Boiling Run 5/22 0250.	79
6.	Primary Shell Wall Temperature Vs. Length - 300 KW System Film Boiling Run 5/22 0310.	80
7.	Primary Shell Wall Temperature Vs. Length - 300 KW System Film Boiling Run 5/22 0330.	81
8.	Primary Shell Wall Temperature Vs. Length - 300 KW System Film Boiling Run 5/22 0348.	82
9.	Primary Shell Wall Temperature Vs. Length - 300 KW System Film Boiling Run 5/23 0018.	83
10.	Primary Shell Wall Temperature Vs. Length - 300 KW System Film Boiling Run 5/23 0051.	84
11.	Primary Shell Wall Temperature Vs. Length - 300 KW System Film Boiling Run 5/23 0118.	85
12.	Primary Shell Wall Temperature Vs. Length - 300 KW System Film Boiling Run 5/23 0144.	86
13.	Primary Shell Wall Temperature Vs. Length - 300 KW System Film Boiling Run 5/23 0214.	87
14.	Primary Shell Wall Temperature Vs. Length - 300 KW System Film Boiling Run 5/23 2205.	88
15.	Primary Shell Wall Temperature Vs. Length - 300 KW System Film Boiling Run 5/23 2221.	89

LIST OF ILLUSTRATIONS (CONT.)

Figure		Page
16.	Primary Shell Wall Temperature Vs. Length - 300 KW System Film Boiling Run 5/23 2351.	90
17.	Primary Shell Wall Temperature Vs. Length - 300 KW System Film Boiling Run 5/24 0032.	91
18.	Primary Shell Wall Temperature Vs. Length - 300 KW System Film Boiling Run 5/24 1345.	92
19.	Primary Shell Wall Temperature Vs. Length - 300 KW System Film Boiling Run 6/27 0815.	93
20.	Primary Shell Wall Temperature Vs. Length - 300 KW System Film Boiling Run 6/27 0845.	94
21.	Primary Shell Wall Temperature Vs. Length - 300 KW System Film Boiling Run 6/27 0915.	95
22.	Primary Shell Wall Temperature Vs. Length - 300 KW System Film Boiling Run 6/27 0945.	96
23.	Primary Shell Wall Temperature Vs. Length - 300 KW System Film Boiling Run 6/27 1030.	97
24.	Primary Shell Wall Temperature Vs. Length - 300 KW System Film Boiling Run 6/27 1100.	98
25.	Primary Shell Wall Temperature Vs. Length - 300 KW System Film Boiling Run 6/28 0202.	99
26.	Primary Shell Wall Temperature Vs. Length - 300 KW System Film Boiling Run 6/28 0300.	100
27.	Film Boiling Heat Flux Vs. Liquid Velocity - 300 KW System.	101
28.	Primary Shell Wall Temperature Vs. Length - 300 KW System Film Boiling Run 5/23 1000.	102
29.	Required Power Vs. Potassium Flow Rate for Superheat of 50°F - 300 KW System.	103
30.	Required Heat Transfer Area Vs. Potassium Inlet Saturation Temperature and Flow Rate For 100% Quality at Boiler Exit - 300 KW System.	104

LIST OF ILLUSTRATIONS (CONT.)

Figure		Page
31.	Two-Phase Friction and Momentum Pressure Drop Vs. Mass Velocity and Tube Diameter.	105
32.	Potassium Outlet Temperature at 100% Quality Vs. Tube Diameter, Potassium Mass Velocity Flow Rate and Tube Diameter.	106
33.	Coiled Tube Configuration - 300 KW System.	107
34.	Tubing Bend Radius Relationship.	108
35.	Straight Tube Configuration - 300 KW System.	109
36.	Straight Tube, Floating Header Multitube Boiler - 300 KW System.	110
37.	"U" Tube Test Boiler - 300 KW System.	111
38.	Multiple Coil Tube Test Boiler - 300 KW System.	112
39.	Heat Loss From the Transducer Line at the Boiler Exit of the 100 KW loop.	113
40.	Operating Limits of Present 100 KW System.	114
41.	100 KW Liquid Potassium Data.	118
42.	Heat Flux versus ΔT for Boiling Potassium in the 100 KW System.	119
43.	Heat Flux versus ΔT for Boiling Potassium in the 100 KW System.	120
44.	Heat Flux versus ΔT for Boiling Potassium in the 100 KW System.	121
45.	Heat Flux versus ΔT for Boiling Potassium in the 100 KW System.	122
46.	Heat Flux versus ΔT for Boiling Potassium in the 100 KW System.	123
47.	Heat Flux versus ΔT for Boiling Potassium in the 100 KW System.	124

LIST OF ILLUSTRATIONS (CONT.)

Figure		Page
48.	Heat Flux versus ΔT for Boiling Potassium in the 100 KW System.	125
49.	Heat Transfer Coefficients for Boiling Potassium in the 100 KW System.	126
50.	Heat Transfer Coefficients for Boiling Potassium in the 100 KW System.	127
51.	Heat Transfer Coefficients for Boiling Potassium in the 100 KW System.	128
52.	Heat Transfer Coefficients for Boiling Potassium in the 100 KW System.	129
53.	Heat Transfer Coefficients for Boiling Potassium in the 100 KW System.	130
54.	Heat Transfer Coefficients for Boiling Potassium in the 100 KW System.	131
55.	Heat Transfer Coefficients for Boiling Potassium in the 100 KW System.	132
56.	Liquid Heat Transfer Results for Potassium in a 5/8" Diameter Vertical Tube - 50 KW System.	133
57.	Comparison of Wall Radial Temperature Profile with Varying Sodium Reynolds Number - 50 KW System.	134
58.	Local Condensing Heat Transfer Results for Potassium Vapor - 50 KW System.	135
59.	Comparison of Radial Temperature Profiles at Top and Bottom Axial Stations - 50 KW System.	136
60.	Condensing Heat Transfer Results - 50 KW System.	137
61.	Hypothetical Liquid Vapor Distribution Over a Cross Section.	138
62.	The System Under Investigation.	139
63.	$\left(\frac{\rho_f}{\rho_g}\right)^m$ vs. Saturation Temperature (m = 1, 1/2, 1/3, 0).	140
64.	Minimum Value of the Acceleration Pressure Drop with Quality as a Parameter.	141

LIST OF ILLUSTRATIONS (CONT.)

Figure		Page
65.	Slip Ratio Vs. Acceleration Factor for a Density Ratio of Ten.	142
66.	Ratio of Slip to the Superficial Slip Vs. the Acceleration Factor (any fluid).	143
67.	Dimensionless Acceleration Pressure Drop Vs. Slip for a Density Ratio of 10.	144
68.	Dimensionless Acceleration Pressure Drop for a Slip of One with Quality as a Parameter.	145
69.	Comparison of Dimensionless Acceleration Pressure Drops for Slip Ratios of 1.0 and $(\frac{\rho_f}{\rho_g})^{\frac{1}{2}}$.	146
70.	Percentage Error in the Acceleration Pressure Drop Due to the Uncertainty in the Slip Ratio.	147
71.	Dimensionless Elevation Pressure Drop (Slip Ratio = 1.0).	148
72.	Dimensionless Elevation Pressure Drop $\left[\text{Slip Ratio} = (\frac{\rho_f}{\rho_g})^{\frac{1}{2}}\right]$.	149
73.	Void Fraction Vs. Quality for Potassium (Slip Ratio = 1.0).	150
74.	Void Fraction Vs. Quality for Potassium $\left[\text{Slip Ratio} = (\frac{\rho_f}{\rho_g})^{\frac{1}{2}}\right]$.	151
75.	Boiler Inlet Pressure Gage Calibration - 300 KW System.	152
76.	Boiler Exit Pressure Gage Calibration - 300 KW System.	153

NOMENCLATURE

Symbols	Quantity	Unit
a	acceleration factor; $a = V_{f2}/V_{f1}$	dimensionless
A	area	ft_2
A'	constant in least squares equation	dimensionless
B	magnetic flux density	gauss
B'	constant in least squares equation	dimensionless
c	tube to shell diametrical clearance	inch
C	correction factor to E.M. flowmeter signal	dimensionless
C_2	thickness of partition plate	inch
C_p	specific heat	$Btu/lb_m\text{-}^oF$
D	diameter	inch
E	entrainment factor	dimensionless
E'	output voltage from E.M. flowmeter	mv
f	friction factor	dimensionless
F	a function of	dimensionless
g	acceleration due to gravity	ft/sec^2
g_c	conversion factor	$lb_m\text{-}ft/lb_f\text{-}sec^2$
G	mass velocity	$lb_m/ft^2\text{-}sec$
h	heat transfer coefficient	$Btu/hr\text{-}ft^2\text{-}^oF$
h'	distance from edge of circle to tube row in straight tube arrangement	inch
H_{fg}	latent heat of vaporization	Btu/lb vapor
K	slip ratio; $K = V_g/V_f$	dimensionless

NOMENCLATURE (CONT'D)

Symbols	Quantity	Unit
K'	modified slip; $K' = V_g/V_{f(a)}$	dimensionless
K_s	superficial slip ratio; $K_s = V_{gs}/V_{fl} = X\rho_f/\rho_g$	dimensionless
kw	thermal conductivity	Btu/hr-ft-^oF
ln	natural log	dimensionless
L	length	inch
m	mass flow rate	lb_m/sec
n	number	dimensionless
n'	number of runs	dimensionless
p	pitch	inch
p'	wetted perimeter	inch
P	pressure	psia
P'	distance between tube centers in any row	inch
q	heat transferred	Btu/sec
Q	heat transferred	kw
r	distance between tube centers from row to row	inch
R	radial coordinate	ft
R_f	liquid fraction	dimensionless
R_g	vapor or void fraction	dimensionless
S	tube to tube spacing	inch
S_n	chord length of nth row	inch
t	tube wall thickness	inch
t'	time	hrs

NOMENCLATURE (CONT'D)

Symbols	Quantity	Unit
T	temperature	^{o}F
U	over-all heat transfer coefficient	Btu/hr-ft^2-^{o}F
V	velocity	ft/sec
W	weight flow rate	lbs/sec
X	flowing quality	lb vapor/sec per lb mixture/sec
X'	nonflowing quality	lb vapor/lb mixture
z	vertical distance	inch
Z	available heat transfer shell length	inch

Vector Quantities

Symbols	Quantity	Unit
$\bar{A}$	vector area	ft^2
$\bar{F}$	force	lb_f
$\bar{V}$	vector velocity	ft/hr

Greek Symbols	Quantity	Unit
σ	standard error	%
β	shape factor	dimensionless
τ_w	wall shear stress	lb/ft^2
ρ	density	lb_m/ft^3
ρ_t	density of fluid at temperature T	lb/ft^3
ϕ'	helix angle formed in coiled tube geometry	radians
θ	angular coordinate	radians

NOMENCLATURE (CONT'D)

Greek Symbols (Cont'd)	Quantity	Unit
ϕ	angle of the pipe axis with horizontal	radians
K	tube bending constant	dimensionless
Δ	difference	dimensionless
μ	molecular viscosity	lb_m/ft-hr
Σ	summation	dimensionless
ρ'	electrical resistivity	micro-ohm - cm
ν	kinematic viscosity	ft^2/hr
Γ	mass flowrate per unit width	lbs_m/hr-ft

Subscripts	Quantity
a	annulus
A	air
c	condenser
co	coil
e	elevation
f	fluid
g	gas
h	partition plates
H	hydraulic
HT	heat transfer
i	inside wall
in	inlet

NOMENCLATURE (CONT'D)

Subscripts (Cont'd)	Quantity
K	Potassium
lm	log-mean
L	Loss
LF	loss from facility
LSH	loss from superheater
n	number
Na	sodium
Nu	Nusselt number
o	outside wall
ot	outer tube circle
out	outlet
p	passes
Pe	Peclet number
Pr	primary
r	row
R	required
Re	Reynolds
s	shell
t	tubes
T	total
v	vapor
w	wall

NOMENCLATURE (CONT'D)

Subscripts (Cont'd)	Quantity
(fa)	liquid not entrained with vapor
(fg)	liquid entrained with vapor
1	inlet
2	outlet

SUMMARY

The program reviewed in this report is conducted for the National Aeronautics and Space Administration under Contract NAS-3-2528 to obtain two-phase heat transfer data for sodium and potassium under conditions of boiling and condensing. In addition, information related to pressure drop and flow stability are to be obtained. Test section development and materials studies pertinent to the experimental work are conducted as a support effort.

300 KW Facility

During this report period, additional boiling potassium data with a helical swirl generator insert were obtained. The data from ninety-eight runs obtained in the previous quarter are presented in Volume II of this report. Analyses of the boiling potassium data for a 1.0-inch nominal diameter tube without an insert have continued. A significant relationship for the initiation of film boiling heat flux was determined as a function of the liquid velocity (based on a slip ratio = $\sqrt[3]{\rho_f / \rho_g}$) and is reported.

300 KW Facility Multitube Boiler Test Section

A new task, leading to a multitube boiler for potassium testing, was initiated during this period. This work effort will indicate the adequacy of extending data obtained on simple geometries to the more complex systems. In addition the problems associated with a multitube system, e.g., stability between tubes connected to common headers, which cannot be investigated with single tube test sections, can now be investigated. Testing a more advanced boiler geometry provides the next step in the boiling potassium program. This program will lead eventually to a full scale boiler and is implemented by the increased boiling potassium data obtained. Thermal and geometric parameter studies have been performed and three boiler concepts are reviewed.

100 KW Facility

The 100 kw facility reached 2625 hours of operation above 800°F (most of the operation above 1500°F) during this reporting period. In addition, boiling potassium data at 2200°F was obtained for the first time. Forty-nine stable boiling runs were obtained in the 3/8-inch diameter test section. This completed the 3/8-inch diameter test section investigation and a 3/4-inch diameter test section was installed. Field welding of the large diameter test section was successfully accomplished.

50 KW Facility

Eighteen condensing runs were obtained; the facility has now operated for 440 hours above 800°F. A significant improvement in

the determination of the potassium flow rate was made during this period with the successful testing of a calorimetric flowmeter which gave flow measurements approximately 15% higher than those obtained with the electromagnetic type flowmeter and significantly improved the facility heat balance. Evaluation of the data obtained in the 50 kw facility show

1) Local liquid potassium heat transfer coefficients, especially at low Peclet numbers, fall below predictions based on both theory and empirical correlations.

2) Local condensing potassium heat transfer coefficients obtained between 1170°F and 1260°F ranged from 4000 to 9000 Btu/hr-ft^2-°F with an apparent increase in the condensing coefficient with increasing temperature.

Pool Boiling

Installation and instrumentation problems continue to delay boiling operations. Calibration runs have been initiated.

Analyses

The work effort under this task during the present reporting period entailed determining the range and magnitude of the acceleration and elevation pressure drops in a two-phase potassium system. Maximum and minimum acceleration and elevation pressure drops are presented. For exit qualities greater than 25% and potassium temperatures greater than 1400°F, the maximum possible error in determining the acceleration pressure drop was less than 70%. Increasing quality and/or potassium temperature decreased this error.

Instrumentation

Instrumentation activities on the 300 kw facility during this reporting period were primarily maintenance type. Secondary boiler inlet and outlet pressure gage calibrations were performed. In the 100 kw facility, a new instrumentation feed-through from the vacuum chamber, which substantially increases the number of thermocouples that can be utilized, was designed.

Materials Support

The principal work effort was the repair of the 300 kw test boiler and the installation of a 3/4-inch diameter test boiler for the 100 kw system. Field welding the 3/4-inch diameter Cb-1Zr test boiler was performed successfully for the first time.

I. 300 KW FACILITY

J. Longo, Jr.

The 300 kw facility is used to obtain potassium boiling and condensing heat transfer data. Both the boiling and condensing test sections are controlled temperature types, i.e., the temperatures of the heat acceptance (Sodium) and rejection (Air) fluids rather than the heat generator are controlled. Reference 1 presents a detailed description of the facility.

This section, covering the 300 kw operation from October 1, 1963 through December 31, 1963, describes the maintenance, modification, and operating cycle of the facility as well as the data and results obtained. During this period, the 300 kw facility operated above 800°F for 235 hours; effective January 1, 1964, total loop operating time above 800°F was 2200 hours. Current 300 kw facility effort is directed at obtaining heat transfer performance data in a 1.0-inch nominal diameter boiler tube with a helical swirl generator insert. Additionally, data analysis of the heat transfer performance of a 1.0-inch nominal diameter tube without an insert has continued. Film boiling conditions for the no-insert data are presented in this report.

300 KW Operations

As reported in reference 2, the 300 kw boiler had failed because of a leak at the bimetallic braze joining the 1.0-inch nominal diameter, Mo-.5 Ti boiler tube to the L-605 extension tube. The boiler was removed from the facility and a new 1.0-inch nominal diameter, L-605 tube replaced the Mo-.5Ti tube. Reference 2 discusses the tube qualification procedure and the limitations resulting from the use of an L-605 tube in the 300 kw facility. The 300 kw operating log is abstracted below:

10/1/63	Boiler removed from 300 kw facility.
10/7/63	Hot trapping of alkali metals. Working on boiler repair.
10/17/63	Welding of boiler initiated. Radiograph of root welds completed.
10/17/63	All bench welds on boiler completed and passed radiographs.

10/19/63	Installed repaired boiler in facility. Completed root welds of four connections. Radiographs made and passed.
10/23/63	Welding of boiler in 300 kw facility completed. Welds passed radiograph. Adjusted boiler hangers. Boiler auxillary heaters installed and checked. Checked boiler thermocouples and noted some requiring repair
10/24/63	Transferred clean sodium (<30 ppm O_2) from shipping container to primary dump tank. Started to heat up system.
10/25/63	All thermocouples repaired. Boiler ready for insulation.
10/26/63	Boiler insulated. Transferred clean potassium (<30 ppm O_2) from hot trap to secondary dump tank. Instrumentation checkout and repair of loop instruments completed. Pressure gauge calibrations initiated.
10/27/63	Pulled vacuum on loops and filled primary and secondary loops. Sodium and potassium flowing in primary and secondary loops, respectively. Loops being heated to 1100°F.
10/29/63	Completed flushing of loops and dumped both loops. Primary equalizer line is plugged. Preparing to take sodium and potassium samples.
10/30/63	Drained secondary dump tank and refilled with clean potassium. Drained primary dump tank and refilled with clean sodium. Filled primary and secondary loops and initiated second flush.
10/31/63	Completed flushing and dumped both loops. Primary equalizer line is plugged. Secondary equalizer line is sluggish.
11/1/63	Took samples of primary and secondary fluids. Made pressure check on boiler ($\sim$50 psi). No indication of leakage in 3 hours.
11/2/63	Filled primary loop and initiated calibration runs at 1200°F.

11/3/63	Completed calibration runs on primary loop at 1800°F. Cooling down to fill potassium loop.
11/4/63	Filled secondary loop and established flow. Primary pump trouble. Capacitor on primary pump power line bad. Dumped both loops.
11/6/63	Venting lines removed and cleaned. New capacitor on primary pump power line installed.
11/26/63	All venting and fill lines cleaned, unplugged, and rewelded.
11/27/63	Ran pressure gauge calibration check again.
11/29/63	Loop filled and being flushed.
12/2/63	Took primary and secondary samples, filled loop and circulated flow. Primary flow is low. Temperature increased to 1100°F to try to increase flow.
12/3/63	Dumped both loops at 1000°F in order to hot trap.
12/14/63	Secondary fill line plugged.
12/15/63	Cut secondary fill line and found plug.
12/17/63	Fill line to secondary loop welded back in place after removing plug. All welds passed radiograph tests.
12/18/63	Transferred potassium from hot trap to dump tank.
12/19/63	Filled both loops and initiated flushing at 1000°F. Secondary flow erratic. Heating loop up slowly.
12/20/63	Dumped both loops in order to hot trap in dump tanks.
12/26/63	Emptied secondary dump tank and refilled with clean potassium. Both loops filled, flowing, and heating up. Initiated boiling runs.
12/31/63	Secondary control valve bellows leak necessitated shutdown after 144 hours of boiling at primary temperature of 1850°F.

Interestingly, once again, the failure of one component, the boiler, seems to have triggered other failures, the primary pump and the plugged secondary fill line.

Although obtaining boiling heat transfer performance data with the helical swirl generator insert remained important, major emphasis was placed on determining the limitations of the facility in terms of the capability of the furnace and condenser to provide and remove 300 kw. For the approximate 100 hours of boiling runs obtained during this quarter, therefore, the system was operated at the maximum power capability. The range of operating conditions covered during this test program were:

Primary inlet temperature, ^{o}F	1400 - 1863
Primary exit temperature, ^{o}F	1383 - 1823
Primary flow rate, lbs/sec	6.4 - 11.3
Secondary flow rate, lbs/sec	0.015 - 1.875
Secondary inlet temperature, ^{o}F	856 - 1620
Secondary exit temperature, ^{o}F	1353 - 1742
Secondary quality, %	0 - 98
Condenser air flow rate, lbs/sec	0 - 0.5
Maximum power input, kw	163.5

Because of the inability to increase the condenser air flow, the maximum power input was limited to 163.5 kw. The air is delivered to the 300 kw facility in a 6-inch pipe at approximately 90 psig. The air then passes through a steam heat exchanger that can be used to heat the inlet air to the condenser and thereby prevent possible plugging in the facility at low power operation. From the heat exchanger, two separate 3-inch lines lead to the horizontal and vertical condensers, respectively. A large pressure drop, approximately 60 psi, at the air-flows used during the testing program, occurred across the steam heat exchanger, thereby restricting the air flow to the condensers.

Operation, after the installation of the steam heat exchanger has indicated that this equipment is unnecessary and, therefore, will be cut from the system. Preliminary evaluation of the air flow rate capability with the steam heat exchanger removed shows that the air flowrate will be approximately 8 lbs/sec.

The heat transfer capability of the condenser for a 1600°F potassium temperature and a 100°F inlet air temperature is given by:

$$q_c = W_A \, C_{PA} \left[1500 - 10^{\,3.176 - \frac{UA_c}{8280\, W_A C_{PA}}} \right] \qquad (1)$$

The air side heat transfer coefficient is controlling and, therefore, an over-all heat transfer coefficient of 100 Btu/hr-ft^2-^{o}F at an air flow of 4 lbs/sec was determined. The horizontal condenser heat transfer area is 7.17 ft^2. These values, together with equation 1, indicate that the horizontal condenser alone could remove approximately 300 kw at an air flow rate of 4 lbs/sec. Thus, when the vertical condenser is used, in addition to the horizontal condenser the heat removal capacity of the 300 kw system will not be limiting.

Because of the air flow limitation, the maximum capacity of the gas fired furnace could not be determined. However, the fuel valve was only one quarter open when supplying $\sim$180 kw (total). Thus, the furnace should be capable of supplying the rated 300 kw.

Data Analysis

The data from the 98 boiling runs obtained with the 1.0-inch nominal diameter Mo-0.5 Ti boiler tube with the helical swirl generator insert from July, 1963 to October, 1963 have been reduced. These data and the data from the ten liquid runs are presented in Volume II of this report. The data from the 67 boiling runs obtained with the 1.0-inch nominal diameter L-605 boiler tube during the current reporting period will be presented in the next quarterly report.

The major effort under this task has been concentrated on analyzing the boiling data obtained without an insert. The data that are used in this analyses were reported in reference 2, Volume II, and consist of 174 boiling runs. The following range of variables were covered by these boiling runs:

Boiling fluid	Potassium
Outlet potassium temperature, ^{o}F	715 - 1777
Potassium flow rate, lbs/sec	0.058 - 0.87
Boiler power, kw	to 133
Outlet potassium quality, %	0 - 89
Inlet primary temperature, ^{o}F.	732 - 1849
Transient Operation, ^{o}F/hr	$<$ 50

A significant correlation between the film boiling heat flux and the liquid velocity was obtained. The term film boiling heat flux as used in this report is that heat flux above which a marked decrease in the heat transfer rate is observed. The measurements used in the analysis were:

1) The shell temperatures measured by 65 thermocouples located along the length of the boiler shell which forms the outside wall of the primary fluid annulus.

2) The primary and secondary, inlet and outlet bulk fluid temperatures measured by three thermocouples at each of these locations.

3) The primary and secondary flow rates measured by an electromagnetic flow meter located in each of the primary and secondary loops.

Supporting measurements used in the analysis were the inlet and outlet secondary pressures.

The calibration of the primary fluid thermocouples was accomplished by a series of liquid runs in which the primary flow rate and temperature level were changed with no secondary fluid in the boiler tube. Using the primary inlet bulk fluid temperature as the reference, a best fit straight line was then drawn on the plot of temperature versus position along the boiler length. With this procedure, the primary thermocouples could be corrected as a function of temperature level and primary flow rate. The heat loss per unit length, which was calculated from the primary flow rate, the primary bulk inlet temperature, and the corrected primary bulk outlet temperature was, therefore, assumed to be constant along the boiler length.

The secondary fluid thermocouples were calibrated by a series of liquid-liquid runs in which the primary fluid flow was intentionally set at a low flow rate (to obtain maximum temperature differential for determining the heat given up by the primary) and the potassium flow rate was set at a high level (to obtain minimum temperature differential for calibration). With no air flow on the condenser (in these runs, the condenser would act as a simple heat sink), the heat input to the secondary fluid is equal to the secondary system heat losses. The secondary fluid outlet thermocouple was then corrected relative to the secondary fluid inlet thermocouple using the anticipated temperature rise, calculated from the measured secondary fluid flow rate and the heat input. The heat input to the secondary fluid was determined from the heat given up by the primary fluid minus the boiler heat loss at that temperature level. Before installation into the facility, the secondary fluid inlet thermocouple was calibrated relative to the primary fluid inlet thermocouple as a function of temperature. Thus, the primary and secondary thermocouples are internally consistent.

The secondary fluid inlet and outlet pressure gages were calibrated by pressurizing the secondary loop with argon without any potassium in the loop and determining millivolt signal versus pressure. The electromagnetic flow meters were only calibrated indirectly, relative to each other, by noting primary and secondary temperature decreases and increases, respectively, for the liquid-liquid runs.

These measurement corrections and calibrations have been included in the data reported in reference 2. The corrected boiler shell temperatures for all the runs reported in reference 2 were plotted as a function of length.

From the boiler shell temperature versus length plots, twenty-six runs were selected on the following basis:

1) It was assumed that temperature changes of less than $50^{o}F/hr$ behaved essentially as steady state runs. Steady state conditions are required to ensure that fluid temperature changes reflected in changing thermal driving forces do not simulate apparent decreases in the heat transfer coefficient.

2) The plot of the shell temperature versus length showed a minimum of two different slopes where the slope near the primary inlet (secondary outlet) was smaller than the slope further downstream. For the film boiling runs selected, the slope of the shell temperature versus length in the primary inlet region was negligible.

Figures 1 through 26 are plots of boiler shell temperature versus boiler length where the length is measured from reference plane B in Figure 15 of reference 3. The active heat transfer length of the boiler extends from 24 inches to 91.5 inches.

The film boiling heat flux was calculated from the slope of the shell temperatures downstream of the film boiling region, the primary flow rate and the heat transfer area over which the slope was constant. Using the slope of the shell temperatures downstream of the film boiling region to infer the primary bulk temperature gradient is correct only for a constant heat flux system. Its use in this particular case is based on the following argument.

1) The slope was measured approximately 1 foot downstream of the point at which a definite change of axial temperature gradient becomes apparent.

2) In the nucleate boiling region of the boiler, the boiling heat transfer coefficient is so large that the primary fluid and tube wall are the controlling resistance (reference 3). Thus, the resistance to heat transfer can be considered constant over the nucleate boiling length and the heat flux is proportional to the temperature differential between the primary and secondary fluids.

3) The decrease in secondary fluid pressure with length, caused by momentum drop, was less than 3 psi, or less than $20^{o}F$ change in the secondary temperature, while the primary fluid temperature decrease was less than $20^{o}F$ in the boiling regime. In the counterflow heat exchanger of the 300 kw test boiler and with an average thermal driving force of approximately $100^{o}F$, a change in heat flux of less than 40% along the boiling length could be expected. The two-phase frictional pressure drop will increase this difference in

heat flux, but the magnitude of the drop is a strong function of quality. The greatest two phase frictional pressure drop would, therefore, occur at the exit of the boiler and not in the nucleate boiling region.

4) Finally, and most important for design considerations, the film boiling heat flux calculated in the preceding manner would be the minimum heat flux that would induce film boiling at the particular condition tested.

The quality, temperature and pressure of the secondary fluid at the point of film boiling initiation were assumed equal to these same properties at the boiler exit. This was necessary since these parameters were measured, or in the case of quality, calculated from measurements, at the boiler exit.

The assumption of temperature and pressure of the secondary fluid at the point of the inception of film boiling being equal to the measured quantities at the boiler exit will introduce an error in the determination of fluid properties such as density. In order to assess the magnitude of this possible error, the maximum pressure drop measured over the boiler length in these tests was assumed to occur over the film boiling region. This pressure drop was $\sim$ 5 psi. At the temperatures of this investigation, the vapor density change was determined to be less than 15% due to the 5 psi pressure drop. Thus the magnitude of the errors on fluid properties, introduced by utilizing the measurements obtained at the boiler exit, appear quite small.

The effect of the 5 psi pressure drop on the quality introduces an error less than 1% in the determination of this quantity while the heat added after the film boiling inception point could introduce another 1% error in the value of the quality at the point of film boiling inception.

Thus the assumption of secondary fluid properties at the boiler exit being equal to those at the point of film boiling inception appears justifiable.

The test plan used to obtain the 174 boiling runs on the 1.0-inch nominal diameter, Mo-0.5 Ti boiler tube was established on the basis of determining over-all boiler performance as a function of primary and secondary flow rates, boiler power and operating temperature. Because film boiling could not be detected definitely until after the temperature gradient along the shell wall was plotted, no rigorous testing procedure could be used to investigate film boiling initiation conditions. Sufficient film boiling data were obtained, however, to draw some conclusions about the effect of such variables as secondary flow, pressure and quality on the burnout heat flux. Table I presents data on the pertinent variables for the 26 film

boiling runs studied. The effects of the following variables on the inception of film boiling heat flux were examined.

1. Effect of Quality

   a. Code numbers 14* and 15 versus code numbers 18 and 22
   b. Code number 3 versus code number 4
   c. Code number 9 versus code number 12

   Increasing quality increased film boiling heat flux

2. Effect of Potassium Flow Rate

   a. Code number 16 versus code number 22
   b. Code number 7 versus code number 10

   Increasing flow rate increased film boiling heat flux

3. Effect of Pressure

   a. Code number 18 versus code number 22
   b. Code number 4 versus code number 24
   c. Code number 25 versus code number 26
   d. Code number 16 versus code number 17

   Except for item d, increasing pressure increased film boiling heat flux.

4. Effect of Length of Film Boiling

   a. Code numbers 5 and 6 versus code numbers 7 and 8
   b. Code number 13 versus code number 24

   No significant effect could be determined.

The corresponding increase in the film boiling heat flux with the increase in quality was surprising, since the predeominant opinion is that increases in quality tend to lower the film boiling heat flux. Several investigators (references 4, 5, and 6) however, have reported this same phenomenon in film boiling experiments with water. Reference 4 concludes that:

1) The burnout heat flux is not a single valued function of quality.

2) A maximum in the film boiling heat flux is reached at a certain quality.

---

* See Table 1 for corresponding run numbers.

Reference 5 reports a maxima in the heat flux versus quality but notes that the experiments showing this maxima may have been taken during oscillating or unstable flow conditions. Reference 6 has noted direct evidence that upstream film boiling conditions did occur. After detailed investigation, it was concluded that this occurred while the system pressure and flow were steady; compressibility effects in the inlet piping did not induce upstream film boiling.

The effect of increased flow rate in increasing the film boiling heat flux has been determined by a number of authors (e.g., reference 7). However, reference 5 has found that the film boiling heat flux decreases with increasing mass velocity.

The effect of pressure on film boiling has also been determined in film boiling studies with water. Again, however, two divergent views are reported. For example, reference 7 notes an increase in film boiling heat flux with increasing pressure; reference 5 conversely, reports a decrease in film boiling heat flux with increasing pressure. As noted above, this study observed both an increase and a decrease in the film boiling heat flux with increasing pressures.

Recognizing the film boiling studies with water and the different results reported, an attempt was initiated to postulate a model for film boiling which could explain most of the apparent anomalies in film boiling studies and still account for the results found in this investigation. The model which appears most reasonable at this time is that at least two types of film boiling, with the liquid film as the controlling parameter, occur.

In the first type film boiling, the liquid film is relatively thick and offers a resistance to the vapor emanating from the wall. The net result is that the vapor blankets the surface. In this condition, there may be a critical ratio of vapor generation rate, as measured by the radial vapor velocity to the liquid velocity. Also, in this region, factors tending to increase the liquid velocity, such as increases in flow rate, pressure and quality would permit an increase in the heat flux before film boiling was initiated.

The second type initiation of film boiling would occur because the vapor velocity is so large that waves are created on the liquid layer adjacent to the wall. As the vapor velocity increased, the crest of the waves would increase; finally, patches of liquid would be torn from the wall, thus causing film boiling. In this region, increases in the liquid velocity, i.e., increases in flow rate, pressure and quality, would decrease the film boiling heat flux.

With this model in mind, the first type film boiling would occur at low liquid velocities; the second type, at higher liquid velocities. To check the adequacy of this model on the film boiling data obtained in the 1.0-inch nominal diameter, Mo-.5 Ti tube with no insert, a plot of film boiling heat flux versus liquid velocity was constructed.

The determination of the liquid velocity was made in several ways, i.e.:

1) Assuming a slip ratio of 1.0

2) Assuming a slip ratio of $\sqrt{\rho_f/\rho_v}$

3) Assuming a slip ratio of $\sqrt[3]{\rho_f/\rho_v}$

Possibly, neither of the above methods for calculating the slip ratio, the ratio of the vapor to liquid velocities, is strictly correct. (See Section V. Analysis.) To obtain an empirical type relationship between the film boiling heat flux and the liquid velocity, however, they should be adequate. Figure 27 is a plot of film boiling heat flux versus liquid velocity, which was calculated assuming a slip ratio equal to the cube root of the density ratio. The film boiling heat flux varied from 200,000 to 500,000 Btu/hr-ft^2 and reached a maximum at a liquid velocity of 45 fps. To provide a stronger justification for the model, attempts to correlate film boiling data from water studies in this manner will be initiated.

One interesting side light to this study was the consideration that if the model were correct, then film boiling could occur upstream of the nucleate boiling region. All the data used in this study were deliberately chosen so that film boiling would occur downstream of the nucleate boiling region. A review of the temperature profiles of the remaining 148 boiling runs showed that some runs had regions at the boiler tube inlet where negligible transfer occurred. Figure 28 presents a typical plot of this condition. Originally, it was postulated that superheating the potassium liquid could account for these upstream, low heat transfer regions. However, as noted in reference 3, the testing was carried out under a slow transient. It was found in several runs, which exhibited negligible heat transfer at the boiler tube inlet, that the run just previous to it was in nucleate boiling. The change in conditions was accomplished by decreasing the condenser air flow thus lowering the heat flux. Thus, a condition of negligible heat transfer occurred at the boiler inlet, whereas immediately before this, (in time) vapor bubbles were present to provide nucleation sites. A detailed review of this aspect of the boiling studies, to determine if those runs showing regions of negligible heat transfer at the boiler tube inlet were in film boiling, is planned. Determining whether the film

boiling relationship presented in Figure 27 also applies to these inlet, low heat transfer conditions will afford one check on this.

Since all the film boiling data were obtained with one test section, no geometry effects can be determined. An effort to determine length effects on film boiling, was inconclusive. The performance of the boiler constituted one reason for the inconclusive results. The length effect was examined by noting the length over which film boiling occurred. For a constant length test section, this would be proportional to a nucleate boiling length effect on film boiling. However, when film boiling occurred over a significant length of the boiler, heat was transferred to the potassium fluid upstream of the boiler in the region of the inlet thermal barrier. Figures 3 and 9 indicate this effect. In Figure 3, the film boiling occurs over a fairly small length of the boiler and the sodium outlet temperature is approximately equal to the temperature measured on the boiler shell wall at the end of the active heat transfer length. In Figure 9, the film boiling occurs over a major portion of the boiler tube and the sodium outlet temperature is significantly below that temperature measured as the boiler shell wall at the end of the active heat transfer length. Thus, some heat must have been rejected by the primary fluid beyond the active heat transfer region. The net result of the boiler performance was that the boiler tube heat transfer length was not constant, thus defeating any attempts to determine length effects in film boiling initiation.

Summarizing, a film boiling relationship has been postulated which significantly correlates potassium film boiling data.

Although limited in geometry effects, the testing conditions investigated, are

Heat flux, Btu/hr-ft^2.	204,000 - 498,000
Secondary flow rate, lb/sec.	0.0853 - 0.5997
Quality, %	21.9 - 89.6
Exit fluid temperature, ^{o}F	1497 - 1753

These test conditions cover a wide range and should make this relationship useful for design calculations.

I. A. 300 KW FACILITY MULTITUBE BOILER TEST SECTION

J. Longo, Jr., D. Ferguson, and R. Stankiewicz

This task was established to provide a more advanced boiler geometry (multitube) for testing in the 300 kw facility than the present single tube boiler designs afford. The purpose of testing this more advanced boiler geometry will be

1. To determine the capability of extending present single tube heat transfer performance data to predict the heat transfer performance of a multitube boiler.

2. To determine potential problem areas and feasible solutions that cannot be assessed with the single tube test boilers. Those areas which must be covered before reliable predictions on boiler performance can be made are

   a. Pressure differences arising from flow maldistribution in the boiler headers.
   b. Effect of primary temperature distribution on multitube performance.
   c. Stability criteria between parallel boiler tubes connected to common headers.

The testing of a more advanced boiler geometry provides the next step in the boiling potassium program leading eventually to a full scale boiler and is possible due to the increased boiling potassium data obtained by the Space Power and Propulsion Section, General Electric Company, under NASA contract NAS 3-2528.

A by-product of the multitube boiler testing will, of necessity, be a design procedure for fabricating potassium multitube boilers. The work expended on this task during the reporting period was concerned with this phase of the study. Parametric studies, both thermal and geometric, which were initiated during this period, and three boiler design concepts are discussed.

Requirements

Before initiating the actual analysis and design of a multitube boiler, specifications were established. These preliminary specifications are enumerated on the following pages.

Performance

1. Power level: 200 to 300 kw.

2. Life: 1000 hrs with 50 room to operating temperature cycles.

3. Temperature: 1850°F shell temperatures continuously and 2000°F transient.

4. Pressure: 80 psia continuous shell pressure and 150 psia transient.

5. Primary fluid: sodium

   a. Inlet temperature: 1800-1850°F.
   b. Inlet pressure: 40-60 psia.
   c. Flow rate: 7 to 14 lb/sec.
   d. Pressure drop: 10 psi maximum.

6. Secondary fluid: potassium

   a. Inlet temperature: 1100-1500°F.
   b. Inlet pressure: 40-60 psia.
   c. Exit temperature: 1650°F.
   d. Flow rate: .08-.13 lb/sec/tube.
   e. Pressure drop: 10 psi maximum.
   f. Exit quality: 98-100%.

In general, this unit shall be compatible with 300 kw facility components, i.e., pumps, flowmeters, etc.

Configuration

1. Boiler tube diameter shall be equal to or less than 1 inch.

2. Quantity of tubes shall be less than 6 but more than 2.

3. The unit diameter and length shall accommodate installation into the existing 300 kw facility.

4. The unit shall be sized and mounted so that bending of the boiler shell will not occur.

5. The minimum criteria for instrumentation is that these items will be measured:

   a. Secondary fluid inlet and exit temperature and pressure.
   b. Primary fluid inlet and exit temperature and pressure.
   c. Secondary fluid exit temperature of each tube.
   d. Shell wall axial temperature gradient.

6. The unit shall be oriented so that it is in a vertical operating position.

7. Servicing the unit shall include these considerations:

   a. Provisions for lifting and normal handling.
   b. Provisions for drainage of liquid metal from all cavities.
   c. Capability of tube inspection, repair and/or replacement.

8. Liquid metal to air wall thickness at any point shall not be less than .030 inch and, for safety, double containment is preferred in these areas.

9. The unit shall be designed so that basic modifications to the facility will not impede the installation of a superheater at a later date.

Materials and Fabrication

1. All shell components shall be constructed from L-605.

2. Tubes shall be constructed from material compatible with the specified liquid metals and the L-605 shell.

3. All welds will be full penetration, crevice free.

4. All critical welds will be X-rayed and leak tested.

5. Tube to header and bimetallic joints, if used, shall be tested in mock-up for elevated temperature operation and thermal cycle life.

Thermal Analyses

Before initiating actual design calculations, a parametric study is being conducted to determine the quantitative effects of variations in significant system variables such as power, heat transfer coefficients, tube diameter, tube length, and boiler pressure drop.

The basic approach to establishing pertinent design parameters was to select a range of mass velocity over which the performance of the multitube boiler would be investigated. The mass velocity is related to the potassium flow rate, the tube diameter and the number of tubes by

$$G = \frac{576\ W_K}{\pi\ D_t^{\ 2}\ N_t} \qquad (2)$$

The requirement of 50°F superheat also relates the potassium flow rate to the facility power capability, i.e.,

$$Q_R = 1.05\ W_K \left[X\ H_{fg} + C_{p_v}\ (50) \right] + Q_{LF} + Q_{LSH} = KW \quad (3)$$

where Q_{LF} is the heat loss in the facility with the exception of the superheater and Q_{LSH} is the heat loss from the superheater. Alternatively, Q_{LF} can be considered as the sensible heat required to bring the inlet fluid temperature to the saturation temperature at the boiler exit.

Figure 29 is a graph of equation 3 in terms of the superheat requirements, the boiler requirements, and the summation of these, which must equal the facility requirements. This relationship was determined by assuming

$X = 1.0$
$Q_{LF} = 50$ kw
$Q_{LSH} = 5$ kw
H_{fg} = latent heat of vaporization of potassium at 1650°F
Cp_v = specific heat of potassium vapor at 1800°F

Thus a conservative relationship, i.e., highest heat requirements for a particular flow rate, is obtained. Once the facility capability is known, the maximum allowable potassium flow rate can be determined from Figure 29.

The relationship of boiler geometry to heat transfer area is

$$A_{HT} = \frac{\pi}{144}\ N_t\ D_t\ L_t \quad (4)$$

Therefore, the heat transfer area can be related to the potassium mass velocity and flow rate using 2 and 4, i.e.,

$$\frac{G}{4\ W_K} = \frac{L_t}{A_{HT}\ D_t} \quad (5)$$

The heat transfer area required can be determined if the following items are known:

1) Primary inlet temperature.

2) Heat load, which is equal to $X\ W_K\ H_{(fg)}$ for the boiler alone.

3) Primary flow rate.

4) Over-all heat transfer coefficient as a function of fluid condition along the tube.

5) Secondary temperature along the boiler.

To determine the heat transfer area, the following assumptions were made:

1) The primary inlet temperature is 1850°F.

2) The primary flow rate is 24 lbs/sec.

3) The over-all heat transfer coefficient is equal to 3000 Btu/hr-ft^2°F for qualities up to 70% and 200 Btu/hr-ft^2°F for qualities from 70-100%.

Figure 30 depicts the required heat transfer area as a function of the secondary inlet temperature and flow rate using these assumptions.

A primary flow rate equal to 24 lbs/sec exceeds the facility capability and efforts to determine the proper value is proceeding. Also, new data, presented in this report, will invalidate assumption 3. The present parametric study is, therefore, being revised to reflect these changes.

Using the heat transfer area as determined above, the ratio of boiler tube length to diameter is given in equation 5, i.e.,

$$\frac{L_t}{D_t} = \frac{G\ A_{HT}}{4\ W_K} \tag{6}$$

The pressure drop across the boiler tube on the secondary side is given by the following equation:

$$\Delta P = \frac{f}{144}\ \frac{L}{D}\ \frac{G^2}{2 g_c \rho_v} + \frac{G^2}{144 g_c}\left(\frac{1}{\rho_v} - \frac{1}{\rho_f}\right) \tag{7}$$

It is conservatively assumed that the friction portion of the pressure drop is equal to that value calculated as though 100% vapor passed the length of the tube. Also, the friction factor from reference 8 is

$$f = \frac{0.316}{(N_{Re})^{.25}} = 0.316 \left(\frac{12\,\mu_v}{G D_t}\right)^{0.25} \tag{8}$$

Substituting equations 6 and 8 into equation 7, the pressure drop relation becomes

$$\Delta P = \frac{(12)^{0.25}(0.316)G^{2.75} A_{HT} (\mu_v)^{0.25}}{288\,(4)\,W_K\,\rho_v\,g_c\,(D_t)^{0.25}} + \frac{G^2}{144\,g_c}\left(\frac{1}{\rho_v} - \frac{1}{\rho_f}\right) \tag{9}$$

Taking fluid properties at the saturation temperature of the secondary inlet fluid at the initiation of boiling, the pressure drop across the boiler tube on the secondary side can be calculated.

The exit temperature is then determined from the following equation:

$$T_{K\text{-}out} = F\,[P_{in} - \Delta P] \tag{10}$$

where the vapor pressure vs. temperature data from reference 9 are used.

Note that the diameter is still present in equation 9 and should be accounted for. Figure 31 presents the friction and momentum pressure drops as a function of secondary mass velocity and tube diameter. The large diameter effect shown is somewhat misleading and must be considered in the light of the momentum pressure drop. For example, until the tube length is equal to 10 ft, the momentum pressure drop is controlling and changes in diameter are insignificant.

Figure 32 presents the exit potassium temperature as a function of potassium mass velocity, flow rate, and tube diameter for a potassium inlet saturation temperature of 1700°F. Up to a mass velocity equal to 30 lbs/ft^2-sec, a diameter change from 1.0 inch to 0.25 inch decreased the exit potassium temperature by less than 10°F.

In summary,

- The 300 kw facility appears capable of generating and removing 300 kw at 1850°F. (See Section I. 300 KW Facility.)

- The maximum allowable potassium flow rate for this power is 0.3 lbs/sec wtihout a superheater and 0.28 lbs/sec with a superheater requirement of 50°F.

- The primary flow rate capability must be determined before the design can be set.

- The revised heat transfer area required will be calculated using the data reported in the 300 kw facility analyses section of this report and the primary flow rate capability.

- Curves similar to Figure 32 will be obtained and, for the desired exit temperature and secondary flow rate, the required potassium inlet temperature and mass velocity combination can be determined.

- For a particular inlet temperature, then, the combination of number of tubes (N_t), tube length (L_t), and tube diameter (D_t), which provides fabrication and design simplicity consistent with facility space accommodations, can be chosen.

Geometric Study

In conjunction with the performance parametric study, a geometric investigation was also performed. Appropriate design equations were developed to determine boiler configuration and arrangement for a coiled and a straight bundle. The relationships consider such factors as tube diameter, quantity, length, spacing, and available boiling section envelope. These equations, instrumental in the current design, will also be useful in future multiple tube investigations.

Coiled Tube Geometry. Figure 33 illustrates a typical coiled tube arrangement. The minimum practical coil diameter (D_{co}) is a function of the tube diameter (D_t), the tube wall thickness (t), and helix angle (Ø). Figure 34 is a bend radius curve for a material comparable to L-605. From this, the following tube bending equation was derived:

$$D_{co} = \frac{2 \mathcal{K} D_t^2}{t} \cos \phi \tag{11}$$

where $\mathcal{K}$ is a tube bending constant; it was selected to give a value which is relatively conservative for normal forming of L-605 material.

From geometric relationship, the pitch (p) for a given tube is

$$p = N_t \ (D_t + S) \tag{12}$$

where N_t is the number of tubes in the bundle and S is the tube to tube spacing. By geometric relationship, the length per coil is

$$L_{co} = \sqrt{p^2 + (\pi D_{co})^2} \tag{13}$$

The number of coils for each tube (n) and the total tube length (L_t), respectively, are

$$n = \frac{Z}{p} \quad ; \qquad L_t = L_{co}\, n = \frac{L_c Z}{p} \tag{14}$$

where Z is the available heat transfer shell length.

Re-arranging, substituting, and solving for Z gives

$$Z = \frac{L}{\sqrt{1 + \left[\frac{2 \mathcal{K} \pi D_t^2 \cos \phi}{t \ N \ (D_t + S)}\right]^2}} \tag{15}$$

Also, the minimum shell inside diameter is

$$D_s = D_{co} + D_t + c$$

or, substituting,

$$D_s = \frac{2 \mathcal{K} D_t^2 \cos \phi}{t} + D_t + c \tag{16}$$

where c is the tube to shell diametrical clearance.

Straight Tube Geometry. In Figure 35 a typical straight tube arrangement for a two pass system is illustrated. Relationships can be developed between tube diameter (D_t), tube to shell diametrical clearance (c), number of tube passes (N_p), number of tubes (N_t) that will fit within a given shell diameter (D_s), and tube to tube clearance (P') and (r). The distance between tube centers in any row is designated P' and the distance between tube centers from row to row is designated r. The relationships obtained require an iterative process for solution and are applicable to computer techniques. The number of tube passes (N_p), is determined from the active heat transfer length (Z), permissible from facility considerations, and the desired boiler tube length (L_t), from heat transfer considerations. The relationship is

$$N_p = \frac{L_t}{Z} \tag{17}$$

The number of partition plates (N_h) required is one less than the number of passes, i.e.,

$$N_h = \frac{L_t}{Z} - 1 \tag{18}$$

Referring to Figure 35, the outer tube circle diameter (D_{ot}) can be related to the shell diameter by the following relationship:

$$D_{ot} = D_s - (c + D_t) \tag{19}$$

The number of tubes that can be positioned in a shell is based on calculating, row by row, the number of tubes which could be placed in the chord of the circle defined by D_{ot}.

The first row of the tube centerlines ($n_r = 1$) is located at r/2 from the center line of the circle and each successive tube row is located at r distance from the preceding one. Thus, the distance from the edge of the circle to the n_rth row (h'_n) is

$$h'_n = \frac{D_{ot} - r}{2} - \frac{c_2}{2} - (n_r - 1) r \tag{20}$$

where n_r is the row number and C_2 is the thickness of the partition. For more than a two pass system, the above equation does not apply.

The chord length of the nth row is then

$$S_n = 2\sqrt{h_n (D_{ot} - h'_{n_r})} \tag{21}$$

and the number of tubes is then

$$N_t = 2 \sum_{n_r = 1}^{n_r = N} \frac{S_n}{P'} \tag{22}$$

where each term S_n/P' is rounded off to the next lower integer. The limiting row count (N) is reached when $S_n/P' < 1$

Structural Analysis

Basic structural components of a coiled tube and a straight tube boiler are being investigated in the following areas:

1) Static pressure stresses.

2) Boiler tube buckling criteria.

3) Thermal stresses.

4) Thermal expansion and associated stresses.

5) Thermal transient stresses.

Table 2 summarizes applicable L-605 properties which are being used in the structural analyses. These properties were obtained from references 10 and 11.

Design Discussion

Based upon the above analyses, three design configuration are being considered. They are

1) Straight tube, floating header (Figure 36).

2) Straight tube, hairpin bend (Figure 37).

3) Coil tube, single pass (Figure 38).

Both the straight tube configurations are two tube pass, two shell pass heat exchanger configurations. A two pass arrangement should provide sufficient boiler tube length. Primary and secondary fluid design arrangements are shown in Figures 36 and 37. The design differs basically in the method of transition from the first to the second tube pass. The configuration shown in Figure 38 is a one tube pass, one shell pass arrangement.

For purposes of comparison, the advantages and disadvantages of the straight tube configurations and coil tube arrangement are presented in Appendix A. Current technology from the present 300 kw single tube test boiler has been factored into the designs cited.

II. 100 KW FACILITY

J. A. Bond

The 100 kw facility is a single loop system used to study alkali metals boiling heat transfer at temperatures up to 2200°F. The electrically heated boiling test section is a vertical section of 3/8 inch schedule 80, Cb-1Zr pipe. Thermocouples are attached along the outer wall of the test section at intervals of approximately 3 inches. A preheater, located upstream of and in series with the test section, controls the boiler inlet subcooling. Reference 1 gives a detailed description of the 100 kw facility, which differs from the 300 kw system in four major areas:

1) The boiling test section is a uniform heat flux type.

2) Designed to exceed the 1850°F limitation of the 300 kw facility, the 100 kw facility has operated successfully up to 2200°F.

3) Heat is rejected from the system by radiation to the water-cooled walls of the enclosure.

4) Because it is smaller in size and power rating, this loop is operated more easily and is, therefore, particularly attractive for development work.

This section covers the 100 kw system operation and the data obtained from October 1, 1963 through December 31, 1963. A review of problem areas associated with loop operation and instrumentation with proposed solutions is also included.

100 KW Operation

Operation with potassium as the working fluid continued during this report period. The facility operated at fluid temperatures above 800°F for 579 hours; total facility operating time above 800°F is now 2625 hours. In December, the facility was shutdown for the reasons which are enumerated and discussed below.

1) Installation of a new 3/4 inch schedule 80 test section.

2) Replacement of the W vs. W + 26% Re thermocouples with W + 3% Re vs. W + 26% Re thermocouples.

3) Installation of a new power measuring system.

The 100 kw facility was first operated with stable boiling in February 1963. Previously, problems pertinent to heat transfer measurement were secondary to initiating loop operation. Although stability continues to be a major problem area, considerable stable boiling data have been obtained. Examination of these data has revealed several problem areas:

- Temperature measurement
- Power measurement
- Flow measurement
- Stability

Temperature Measurement. The fluid temperature is measured at the the preheater inlet, the boiler inlet and after a mixer located downstream of the test section. The preheater and boiler inlet temperatures are measured with thermocouples attached to the outer wall of the pipe. Although the pipe is insulated, there is always some heat loss and assuming the wall temperature is equal to the fluid temperature could introduce significant errors. To determine the inlet fluid temperature more accurately, a thermocouple well has been installed at the inlet of the new 3/4 inch test section.

The mixer, located approximately 15 inches from the boiler exit, consists of two baffle plates. The thermocouple used to measure the boiler exit temperature is located in a well downstream of the mixer.

Measuring the potassium temperature at the mixer imposes two problems, one during boiling operation and one during liquid testing. During boiling operation, the fluid entering the mixer is a two-phase mixture. Consequently, the pressure drop across the baffle plates is accompanied by a corresponding decrease in the fluid temperature. During liquid operation, because of heat loss, the temperature measured in the mixer is lower than the fluid temperature at the test section exit. The pipe connecting the test section and mixer is insulated. However, the pipe leading to the differential pressure transducer, which is located between the mixer and the test section, cannot be insulated because it has a bimetallic joint that must be kept cool. The transducer line, then, acts as a radiating fin through which heat is lost from the fluid.

To determine the heat loss from this fin, thermocouples were attached at the base and tip of the transducer line. Using the radiating fin analysis of reference 12, these measured temperatures were used to calculate the heat loss. Figure 39 shows the calculated heat loss as a function of the temperature at the base of the fin. The loss, although small, could lead to large errors in

liquid temperature because of the low flow rate and low specific heat of potassium. For example, at 1400°F the heat loss is approximately .04 Btu/sec and the specific heat is approximately .192 Btu/lb-°F. For a typical flow rate of .04 lb/sec, this represents a temperature drop of 5.2°F; for lower flow rates and/or higher temperatures, the error is even greater. To reduce errors in fluid temperature measurement, the mixer was removed and a thermocouple well installed 4 7/8 inches downstream of the test section exit.

Temperatures on the wall of the boiling test section are measured with thermocouples attached to the outer wall. As cited previously in reference 3, the major operational problem is thermocouple failure. Failure is usually caused by separation of the pure tungsten wire from the boiler tube at the weld junction. Two possible replacement thermocouples have been tested in the boiling test section. The results of these tests indicated that the failure rate will be reduced significantly if the W vs. W + 26% Re thermocouples were replaced by W + 3% Re vs. W + 26% Re thermocouples. At the end of this reporting period, therefore, a complete reinstrumentation was proceeding. A measurement problem in the test section wall thermocouples, caused by radiation effects from the radiant heaters is being reviewed currently. Further changes, especially in the manner of shielding these thermocouples, may be desirable.

Power Measurement. Electrical power input to the 100 kw test section is calculated from the measured values of voltage and amperage. The current is measured with a current transformer whose accuracy is 3% of the full scale reading which is 350 amps. At low power levels in the range of 0 to 4 kw (gross), errors as large as 20% in the power measurement could occur. A calibrated polyphase wattmeter with an accuracy of .75% has been obtained from the Advanced Technology Laboratory, General Electric Company. This wattmeter will be used in future tests.

Flow Measurement. The flow rate in the facility is obtained from the output signal of an electromagnetic flowmeter. The room temperature magnetic flux density of the magnet is 895 gauss. Because of the low flow rates, the resulting flowmeter output signal is approximately 0.1 milivolts. In some cases, the noise level can be a significant fraction of the total measured signal. Since this signal is proportional to the magnetic flux density at a given flow rate, installing a new magnet with a higher flux density is planned.

Stability. In reference 2 a system operating envelope, which indicated the regions outside of which it is impossible to operate, was determined. This envelope indicates the operating limits imposed by thermodynamic and heat transfer considerations, and shows an estimated heater capacity of 50 kw. A more thorough analysis has shown the heater capacity to be 35 kw. This limit was obtained as follows: measured values of line current were plotted as a function of the corresponding line-to-line voltage as shown in Figure 40A. This data was obtained during actual boiling operation. The current is not a linear function of voltage because the heater resistance

increases with temperature. The line current in the three phase "Y" connected heater circuit is given by:

$$I_A = \frac{5\ V_{AB}}{\sqrt{3}\ R} \qquad (1)$$

where,

I_A = Line current

V_{AB} = Line-to-line voltage

R = Electrical resistance of one tungsten rod at temperature. Each phase of the circuit consists of 5 rods in parallel.

The variation of resistance with temperature is given by:

$$R = R_o \left[1 + \alpha\ t_c\right] \qquad (2)$$

where,

R_o = Room temperature resistance of one rod.

α = Temperature coefficient of resistance.

t_c = Tungsten rod temperature.

Combining (1) and (2) and solving for t_c:

$$t_c = \frac{1}{\alpha}\left[\frac{5\ V_{AB}}{\sqrt{3}\ I_A\ R_o} - 1\right] \qquad (3)$$

Thus, the tungsten rod temperature can be deduced from the measured values of V_{AB}, I_A and R_o. The power is obtained from V_{AB} and I_A:

$$P = \sqrt{3}\ V_{AB}\ I_A \qquad (4)$$

Figure 40B is a plot of heater power as a function of rod temperature as obtained by the above procedure. This shows a maximum heater capacity of 35 kw at a rod temperature of 5900°F. Figure 40C is the revised system operating envelope as determined by thermodynamic and/or heat transfer considerations. The system operation is further limited by instabilities in the loop which are described later in this report.

Figure 40D is a plot showing combinations of net boiler power and flow that can be achieved in the present 100 kw facility. The vertical line at W = 0.087 lb/sec represents the maximum flow obtainable with the present orifice installed. This limit was obtained by circulating liquid potassium (no boiler power) in the loop with the power to the pump at its maximum setting. To operate at higher flows, the orifice diameter must be increased. As power is increased, boiling begins in the test section and the friction pressure drop increases with a resultant decrease in flow. The slanting dashed line shows the decrease in flow with power at a loop pressure of 140 inch Hg; this line was drawn through the one measured point as shown. The horizontal line at 22.8 kw represents the net power limit imposed by the present heater. This is based on a gross power input of 35 KW and a heat loss equal to 35% of gross. The rectangle A-B-C-D defines the power and flow limits of the present system. To operate at higher flows, the orifice diameter must be increased and, if higher power is desired, the heater must be replaced.

The cross hatched area in Figure 40D shows those combinations of flow rate and power at which stable boiling data have been obtained to date. Even in this region, the system is not always stable because the loop pressure affects stability. The upper and lower limits of the "stable boiling region" are best described by considering the sequence of events as the flow and loop pressure are held constant and the boiler power is slowly increased:

1) Initially, with no boiler power, the fluid is all liquid with a steady flow rate and pressure.

2) As the boiler power is increased, the fluid temperature at the boiler exit approaches the saturation temperature corresponding to the loop pressure at that point.

3) When the power is increased sufficiently to initiate boiling at the test section exit, the liquid at this point frequently begins to superheat. During the superheating process, the flow and pressure remain constant as the liquid temperature rises above the saturation temperature. Finally, a critical superheat is reached (usually between 50°F and 200°F). Here, the liquid flashes and the temperature drops sharply to saturation. Simultaneously, a sudden decrease in flow is observed. This "bumping" often initiates pressure oscillations in the dump tank. The flow then oscillates a few times and the superheating process recurs. This cyclic process continues until operator action is taken.

4) As the power is again increased, a point is reached at which stable boiling begins, as indicated by the stability of the flow rate, loop temperatures, and dump tank pressure measurements.

5) Stable boiling continues as power is increased. Finally, a power level is reached at which unstable boiling occurs again.

6) As power is increased further, the system remains unstable up to the maximum power limit.

To extend the region of stable boiling, installing a valve between the dump tank and the loop is being considered. This valve would enable the loop to be hydraulically separated from the dump tank during operation and thus prevent amplification of the loop oscillations by the dump tank.

Data Analysis

The operation of the 100 kw facility can be separated into two categories: liquid operation, in which the data taken were used to evaluate the heat loss from the transducer line and calibrate the instrumentation; boiling operation, in which the data taken were used to determine boiling heat transfer coefficients. The liquid data are included in Appendix B. Figure 41 is a plot of Nusselt number versus Peclet number for these data. The low values of the Nusselt number are probably caused by errors in temperature measurement. The measured fluid temperature is low because of the heat loss in the transducer line discussed above. Direct radiation from the tungsten heating rods may cause the measured tube wall temperature to be high. Both these effects combine to give an erroneously large temperature difference and, hence, the Nusselt number is low. The thermocouple wells in the new test section at the inlet and outlet should eliminate the large fluid temperature error. A method, which has been devised to determine the error caused by radiation will be checked and reported in the next quarterly report.

Forty-nine points were taken during stable boiling of potassium in this quarter. The results of these tests are presented in Appendix B. The calculation procedure has been reported in reference 3. Because of changes in the location of instrumentation, the data are reported in two parts. The ranges of variables covered in these tests are:

Heat flux, Btu/hr-ft^2	34,000 to 160,000
Mass flux, lb/hr ft^2	54,000 to 240,000
Boiler outlet temperature, ^{o}F	1560 to 2202
Quality, %	2 to 54

These constitute the first stable boiling potassium data obtained in the 100 kw facility with fluid temperatures of 2200°F. Figures 42 through 48 are plots of heat flux versus temperature differential (ΔT) between the inside wall and mixer based on the data reported. The inside wall temperature was determined from the heat flux and the outside wall temperature measured by thermocouple number 13 located 4 7/8 inches upstream of the boiler exit. Each plot includes data taken at a constant pressure with mass velocity (G) as a constant parameter. Apparently, increasing G increases the heat flux (q/A) for a given ΔT at the lower pressures. The effect of quality, however, is combined with the effect of G in these plots. This trend, increasing q/A with increasing G at a given ΔT, is not clearly evident at the high pressures.

In Figures 49 through 55, the same data are plotted as heat transfer coefficient versus boiler exit quality. Each of these plots includes data taken at constant mass flux with pressure as a constant parameter. The heat transfer coefficient apparently increases with quality over the ranges studied. Again, in these plots, the effects of G and quality cannot be separated. The effect of pressure is clearly evident at low mass fluxes.

A comparison of the boiling heat transfer data taken during this quarter and those taken previously is currently being conducted. The results will be reported in future quarterly reports.

III. 50 KW FACILITY

S. G. Sawochka

The 50 kw facility is used to obtain condensing data for alkali metals. To obtain a wide range of condensing heat flux over a range of coolant temperatures, this two-loop system uses a sodium cooling loop. The test section is a vertical, annular configuration with potassium condensing inside a thick-walled nickel tube and sodium coolant flowing in the annulus. Except for the test section, the potassium and sodium loops of the facility are constructed of Type 316 SS; loop operation, therefore, is limited to 1600°F.

This section, covering the 50 kw operation from September 1963 through December 1963, details the maintenance, modification and operating cycle of the facility as well as the data obtained. During this period, the 50 kw facility was operated above 800°F for 100 hours; total loop operating time above 800°F effective December 31, 1963 was 440 hours. In this quarter, 128 runs were made on the 5/8" ID test section. Of these, 18 were condensing runs and the remainder were heat loss determination, thermocouple standardizations and liquid-liquid runs. The data from the condensing and liquid-liquid runs are presented in Appendix C of this report. With the installation of a calorimetric flowmeter the determination of the potassium flow rate improved significantly during this period. The need for the calorimetric flowmeter as well as the design and the error analyses of the installed version are discussed in this quarterly report. An evaluation of the data obtained in the 50 kw testing indicate the following results, which are detailed later in this section:

1) Local liquid potassium heat transfer coefficients, especially at low Peclet numbers, fall below predictions based on both theory and empirical correlations, reference 14.

2) Local condensing potassium heat transfer coefficients determined between 1170°F and 1260°F ranged from 4000 to 9000 Btu/hr-ft^2-°F, with an apparent increase in the condensing coefficient with an increasing inlet vapor temperature.

50 KW Operation

The 50 kw operating log covering this reporting period is abstracted below.

10/1/63 10/2/63	Sodium and potassium liquid heat loss and thermocouple standardizations, 650-850°F.

10/3/63 10/5/63	Liquid-liquid data runs for local heat transfer coefficient determinations.
10/6/63	Reworked sodium pump wiring for higher flow capacity. Installed second electromagnetic flowmeter on potassium loop and second set of electrodes on the original flowmeter.
10/24/63	Circulated potassium loop to compare flowmeter readings.
10/25/63 10/31/63	Loop dumped and cooled in preparation for installation of thermal calorimeter flowmeter.
11/1/63 11/6/63	Calorimetric flowmeter assembled and bench welded.
11/7/63 11/16/63	Calorimetric flowmeter welded in place. (See Appendix D for location and description.) Instrumentation installed and checked out.
11/17/63 11/18/63	Calorimetric and EM flowmeters tested by circulating potassium at 650-750°F.
11/19/63 11/30/63	Potassium boiler emptied and refilled twice with hot trapped potassium ($<$30 ppm O_2). Inability to obtain flow indicated braze failure of pump duct to the electrode in the potassium loop MSA electromagnetic pump.
12/1/63 12/4/63	Completed high temperature heat loss and sodium Thermocouple standardizations at 950 and 1050°F.
12/5/63	Completed potassium vapor thermocouple standardizations and began condensing experiments at 1150-1250°F. Low power runs successful, but pin hole leak was indicated by smoke from bottom of test section. Shutdown facility to dismantle test section and determine cause of leak.
12/8/63 12/31/63	Test section dismantled. Pin holes through seal weld of sheet insert in the slotted section of Ni tube determined as the location of the leak.

The latest failure of the condenser test section had been repaired by modifying the joint between the junction of the thick-walled nickel tube and the 1/2-inch Type 316 SS (reference 3). This fix was a success. Although the 1/2-inch pipe at the bottom of the test section, where this repair was made, was bent approximately 15°, the brazed joint did not fail.

Data Analysis

The test program presently being conducted in the 50 kw facility comprises two phases; a liquid-liquid test program and a condensing test program. The liquid-liquid test program that has been carried out (although necessarily limited because the prime objective of this program is the determination of condensing heat transfer coefficients), has fulfilled the initial objectives of the program. Namely:

1) To evaluate instrumentation reliability and accuracy

2) To ensure that the radial wall temperature profile provided an accurate indication of the local heat flux

3) To determine test section heat balances

The method of thermocouple standardization discussed in previous quarterly reports, references 3 and 8, has been completed. In order to assist the reader, and avoid having to review past quarterly reports, the standardization procedure together with the important results are presented below. The term standardization is used rather than calibration since the method employed in correcting the thermocouples was to reference them to a particular thermocouple installed in the facility rather than to a primary reference.

The procedure used to standardize the sodium, potassium and test section thermocouples is presented below:

1. The sodium inlet and outlet thermocouples are standardized to one of the sodium inlet well thermocouples. The test procedure is to determine the sodium inlet and outlet thermocouples readings at various temperature levels and at least two sodium flowrates per temperature level with the potassium loop evacuated.

   Thus for any run, the thermocouple standardization factor for a particular thermocouple is given by

$$q_{L_1} = W_1 C_p \left[T_m - T_R + \epsilon \right]_1 \tag{1}$$

   at the same temperature level but at sodium flowrate W_2, the standardization factor for the same thermocouple is given by

$$q_{L_2} = W_2 C_p \left[T_m - T_R + \epsilon \right]_2 \tag{2}$$

also the heat loss (q_L) is given by

$$q_L = UA\left[T_{Na} - T_a\right] \tag{3}$$

If the air side resistance is controlling then $q_L \neq F\ (W_{Na})$ and q_{L1} in equation 1 is equal to q_{L2} in equation 2. Further if the standardization factor is assumed to be only a function of temperature level then equation 1 and 2 can be combined to give

$$\frac{q_{L1}}{(WC_p)_1} - (T_m - T_R)_1 = \frac{q_{L1}}{(WC_p)_2} - (T_m - T_R)_2 \tag{4}$$

Solving for q_L

$$q_{L1} = \frac{(T_m - T_R)_1 - (T_m - T_R)_2}{\frac{1}{(WC_p)_1} - \frac{1}{(WC_p)_2}} \tag{5}$$

and the standardization factor for the particular thermocouple can be obtained from equations 5 and 1.

Therefore at each temperature level, each sodium thermocouple will have a standardization factor referenced to the inlet sodium reference thermocouple. By noting the reference sodium thermocouple reading, the standardization factor for another sodium thermocouple is then known. Thus, when determining the heat given up or accepted by the sodium, the following relationship is used

$$q_{Na} = (WC_p)_{Na}\left[T_{Na_o} + \epsilon_o - T_{Na_m} - \epsilon_i\right] \tag{6}$$

where ϵ_o and ϵ_i apply to the outlet and inlet thermocouples respectively and are both standardized to the same reference thermocouple.

2. The potassium inlet and outlet thermocouples are standardized to one of the potassium inlet thermocouples. The test procedure is to determine the potassium inlet and outlet thermocouple readings at various temperature levels and at least two potassium flowrates per temperature level with the sodium loop evacuated.

Thus, in the same manner as detailed for the sodium thermocouples, the standardization factor for each potassium thermocouple referenced to a potassium inlet thermocouple is determined for each temperature level.

3. The test section wall thermocouples are standardized to the same potassium inlet thermocouple used to standardize the potassium thermocouples. The test procedure is to determine the test section wall thermocouples and reference potassium inlet thermocouple readings at various temperature levels with low velocity potassium at high quality and with the sodium loop evacuated. The test section outside shell is maintained at the potassium vapor temperature for the high temperature runs with electrical heating. This eliminated the necessity of considering heat losses in determining the standardization factor for the test section wall thermocouples.

The important results of the standardizing procedure were

1. Standardization factors for the sodium thermocouples were obtained at 600°F, 700°F and 780°F. There were no detectable trends of standardization factor with temperature level. The standardization factors for the thermocouple exhibiting the greatest deviation were 3.3°F, 3.0°F and 3.5°F for temperature levels of 600°F, 700°F and 780°F respectively.

2. Standardization factors for the potassium thermocouples were obtained at 660°F, 770°F and 850°F. There was a detectable trend of standardization factor with temperature level. The standardization factors for the thermocouple exhibiting the greatest deviation were -0.9°F, 1.3°F and 2.5°F for temperature levels of 660°F, 770°F and 850°F respectively.

3. Standardization factors for the test section wall thermocouples were obtained at 1160°F and 1260°F. There was no detectable trend of standardization factor with temperature level. The standardization factors for the thermocouple exhibiting the greatest deviation were 1.3°F and 1.2°F at 1160°F and 1260°F respectively.

The changes in the standardization factors for the potassium thermocouples are probably due to the probe measuring a local temperature along a radial profile rather than the bulk mean temperature. This is indicated by the potassium thermocouple data taken during the standardization of the test section wall thermocouples. In these runs, heat loss was prevented by maintaining the wall at the potassium vapor temperature, and the potassium thermocouple standardization factors did not vary with temperature level. The maximum deviation was 1.3°F and was constant from 1160°F to 1260°F. With no heat transfer occuring, the potassium temperature does not vary with radius and thus the local temperature is indicative of the bulk temperature.

Another factor pointing towards the probe measuring a local temperature along a radial profile rather than the bulk mean temperature is

provided by comparing the standardization factor for the sodium and potassium thermocouples. The apparent change in the standardization factor with temperature level occured in the loop which had no mixing baffles (potassium) while the loop which had mixing baffles (sodium) did not exhibit this effect.

Since the standardization factor of the potassium and test section wall thermocouples were less than 1.3^{o}F in the no heat loss standardization runs, it was decided to reduce the data without thermocouple corrections. Note that the liquid-liquid analyses will be affected by the uncertainty in the outlet potassium bulk temperature; for condensing runs however, this is not a serious consideration.

The data reduction procedure and the results of the liquid tests are presented in Appendix C. The following observations are pertinent.

Runs 1 Through 93

1) Since in these liquid runs, the test section performs as a cocurrent heat exchanger, the overall temperature differential between the sodium and potassium is greater at the first axial station (L/D=19) than at the second axial station (L/D=38). Thus the heat flux and the temperature difference between the potassium and the inner wall is also greater at the first axial position. For this reason, the calculated liquid heat transfer coefficient at the first axial station is more accurate, in some cases by a factor of 2, than the heat transfer coefficient determined at the second axial station.

2) Four wall thermocouples were operating at the first axial station while only three were operating at the second axial station. Thus the extrapolation of the wall thermocouple readings to infer the inner wall temperature has one more degree of freedom at the first axial position.

3) The outer wall to sodium temperature difference is much smaller than that of the potassium to inner wall temperature difference at either station due to the larger (1.72") diameter at the sodium-wall interface as compared to the diameter (0.625") at the potassium-wall interface. In addition, the outer wall temperature to sodium temperature difference is smaller than that of the inner wall to potassium temperature difference at the same Peclet number due to the higher thermal conductivity of the sodium as compared to the potassium.

   The sodium liquid heat transfer results are therefore not as accurate as the potassium liquid heat transfer data.

4) The agreement between the measured potassium heat transfer coefficient at the two axial stations, as shown in Figure 56 and presented in Appendix C, is excellent, considering the qualifications cited in items 1 and 2, above.

5) As indicated by the dates of the liquid data, three repetitive print outs of the system thermocouples were taken at each data point. This procedure was followed to alleviate erroneous results caused by a print out mistake on any of the repetitive readings.

Runs 94 Through 110

1) These runs, taken during initial testing, show a non uniform circumferential temperature condition on the sodium side. The fact that the measured temperature profile in the nickel tube wall does not have a straight line profile, when plotted as the logarithmic location of the wall thermocouples, evidences

this non-uniformity in radial temperature distribution. As the sodium flow rate was increased the measured temperature profile approached the linear logarithmic relationship expected. Figure 57, shows the measured temperature profile for a high and low sodium flow rate. Extrapolation of the logarithmic wall profile to obtain inner and outer wall temperature is, therefore, unjustified for the runs at low sodium flow rates as indicated by comparing the potassium Nusselt number results with those of the first 93 data runs.

2) This non uniform circumferential temperature of the sodium condition indicated that maintaining high sodium flows was necessary during all further testing of either liquid or condensing heat transfer.

A plot of the liquid Nusselt number versus the Peclet number for both axial stations for runs 1 through 93 is depicted in Figure 56. Because of the accuracy qualifications discussed, the L/D effect seemingly indicated here is not considered meaningful. For comparison, the analytical prediction of Lyon (reference 13) and the empirical correlation of Lubarsky (reference 14) are shown in the figure; as shown, the results are lower than those which would be estimated by either correlation. Axial conduction, nonwetting, gas on oxide films, or inaccuracies in the experimental procedure are not considered acceptable explanations for the relatively low values of the Nusselt number. Minor distortions of the velocity profile, however, can have sufficient effect to account for the difference between the experimental results and theory. To support this hypothesis further, the results of Johnson et al. (references 15 and 16) seem to indicate a difference in Nusselt numbers for the same Peclet number caused by flow direction, i.e., up or down.

Also, if the potassium outlet thermocouples are not measuring bulk conditions, especially at the low velocities lower Nusselt numbers would result for the low Peclet numbers than those predicted.

Condensing Runs

The data reduction procedure and the results of the condensing runs are also included in Appendix C. Again, no thermocouple corrections were added to the measured values. Because of the low boiler power which was selected to initiate the condensing test plan, the potassium flow rate was very low approximately 10 lb/hr. This produced condensing heat fluxes from 15,000 to 24,000 Btu/hr-ft^2 with local condensing heat transfer coefficients from 4000 - 9000 Btu/hr-ft^2-^{o}F. In the condensing runs, the test section is a countercurrent heat exchanger where the potassium vapor enters at the top of the test section while the sodium enters at the bottom. In these runs four wall thermocouples at each axial location were operable.

For comparison to theory, the results are plotted in Figure 58 as local condensing ratio versus local film Reynolds number. Only the

top axial position (L/D=19) results are considered reliable within ±30%. The bottom axial position (L/D=38) results are not considered as reliable because of the scatter in the wall thermocouple readings. Figure 59 is a typical plot of the radial temperature profile. The bottom profile is, no doubt, distorted because of the sodium leakage and subsequent breakdown of the thermocouples near the bottom of the test section which ultimately caused the test section failure. Using the high reliability measurements at the top axial position, Figure 60 is obtained by plotting the condensing ratio versus the inlet potassium temperature. Although the film Reynolds number variation is only ±11%, the condensing ratio exhibits a definite increase with temperature. This is in contrast to the result which could be anticipated if a thinning of the film by vapor shear were occurring, since the vapor velocity is higher at the lower temperature. A possible mechanism for the increase of condensing ratio with temperature is the existence of a vapor to liquid interfacial heat transfer "resistance". Although this presupposes a nonequilibrium thermodynamic condition at the gas-liquid interface, it is not unlikely. This type heat transfer resistance has not been noted with high Prandtl number fluids, but it has been suggested and detected experimentally by Bonilla (reference 17) with Mercury. The existence of interfacial resistance would be impossible to detect, except with low Prandtl number fluids, since the film resistance would be large by comparison.

In this series of testing, although the temperature range was relatively small, 1170-1260°F, the vapor pressure and density vary approximately by a factor of two. Interestingly, these variations roughly correspond to the increase in condensing ratio with temperature.

The condensing pressure drop was calculated by taking the difference in saturation pressures corresponding to the measured potassium vapor temperatures at the test section inlet and outlet. The pressure drop varied from 0.017 to 0.037 psi over the testing range, the higher drop corresponding to the lower temperature. Consideration and interpretation of the pressure drop results will require further analyses and will be reported in the next quarterly report.

Calorimetric Flowmeter

When the liquid-liquid data were reduced, a definite error in either temperature or flow measurement was indicated. This error became evident in two ways:

1) An average test section heat balance error of approximately 15% was obtained for all the runs by comparing the heat lost by the potassium to the sum of that gained by the sodium and the test section heat loss.

2) The heat flux obtained from the slope of the line drawn through the wall thermocouples and that calculated from the equations defining the cocurrent exchanger did not agree by 10-20%.

An effort to prove the validity of the heat flux, calculated from the wall radial temperature profile in the reduction of the condensing data, required that the reason for the discrepancy between the calculated and measured values be determined.

Since the sodium and potassium bulk fluid thermocouples had been relatively calibrated as accurately as possible, it was postulated that the discrepancy in heat flux could be caused by an error in flow measurement. To determine if the flow measurement were in error, an independent check on the potassium flow rate was necessary. A calorimetric flowmeter was designed and used as described in Appendix D. The results showed that, when all corrections had been applied to the theoretical flow equation of the EM flowmeter, this flowmeter gave readings which were approximately 14.5% lower than that obtained with the calorimetric flowmeter. The potassium flow rate obtained by the two methods is tabulated below.

Test Number	Flow Rate, lb/sec		Ratio, Calorimetric to Electromagnetic
	Calorimetric	Electromagnetic	
1	.141	.122	1.156
2	.306	.271	1.129
3	.311	.275	1.131
4	.312	.268	1.164

Use of the flow measurements obtained with the calorimetric flowmeter eliminated those factors which previously had provided an indication of an error in flow measurement.

IV. POOL BOILING HEAT TRANSFER INVESTIGATION

C. F. Bonilla

The pool boiling studies will provide basic data for understanding and correlating alkali metal heat transfer mechanisms, rather than design data as obtained in the 300, 100, and 50 kw facilities. Such information as surface effects, i.e., roughness, wettability, etc can be obtained more readily with pool boiling investigations than with forced circulation boiling loops.

During this report period, problems associated with the checkout of the pool boiling apparatus and with the instrumentation have continued and boiling operation, consequently, has been delayed.

V. ANALYSIS

G.L. Converse

The data obtained in the 300, 100 and 50 kw facilities are not, in themselves, directly applicable to design. The analyses task was established to combine the data generated by these separate facilities and arrive at meaningful design specifications. This section describes the analytical methods that were employed and the results that were obtained in arriving at the desired alkali metal heat transfer characteristics from the data generated in the separate facilities. The work effort during this quarter concentrated on determining the range and magnitude of the acceleration and elevation pressure drops in a boiling potassium system.

In proceeding from two-phase pressure drop testing to establishing correlations from which the two phase pressure drop can be predicted, a major problem is the contribution of the elevation and acceleration pressure drops to the total pressure drop measured. Since the fluid and vapor velocities are probably different, using the flowing quality to obtain vapor fraction and, thus, the mean density at any point can lead to serious errors in the determination of the acceleration and elevation pressure drops. These errors, in turn, affect the two-phase frictional pressure drop, which is obtained from the total measured drop minus the acceleration and elevation pressure drops.

This study was conducted to indicate the magnitude of the acceleration and elevation pressure drops and the possible error in their determination introduced by uncertainty in the fluid and vapor velocities.

General Considerations

Selection of Model. Several mathematical models (reference 19), to obtain a satisfactory method of predicting two-phase pressure drops, have been proposed although none are completely satisfactory at the present time. One of the simplest models proposed is the so-called annular flow model. In this model, the velocity and density distributions within each phase of the two-phase mixture are assumed uniform over the plane of a section. The manner in which the individual phases are distributed over the cross section is immaterial as long as the angular momentum equation is not violated. For a horizontal cross section, this implies a radially symmetric distribution of the individual phases. The term annular flow is derived from the fact that the physical flow pattern that appears to approximate the mathematical model most closely is one in which the liquid flows in an annulus surrounding a core of vapor.

This model, it should be noted, also approximates closely the case of fog flow, a flow pattern in which the liquid is dispersed in small droplets within the vapor.

The use of the annular flow model is based on the premise that obtaining some information about two-phase pressure drop may be possible without a detailed knowledge of the particular flow patterns that may exist in the system. In the modified annular flow model, which is sometimes called the quasi-annular flow model, a fraction (E) of the liquid flow rate is assumed to be dispersed in small droplets in the vapor flow and traveling with the vapor velocity. The remaining liquid flows with its own velocity (V_{fa}) in an annular flow pattern around the central vapor core. Annular flow, then, is a special case of modified annular flow in which none or, in the case of fog flow, all of the liquid is entrained in the vapor. Figure 61 is a sketch of a typical flow pattern for the modified annular flow model.

The present analysis will be confined to the annular flow model almost exclusively, and, specifically, to the acceleration and elevation pressure drops. The system to be investigated together with the basic assumptions and conditions of the analysis are depicted in Figure 62. Only the continuity equation and the equation of linear momentum will be used in the analysis. The information obtainable from the angular momentum equation and the first and second laws of thermodynamics will be given at a later date.

Derivation of the Expression for the Two-Phase Pressure Gradient from Continuity and Momentum Considerations. The first step in the analysis is to employ continuity and momentum principles to derive an expression for the two-phase pressure gradient. The detailed derivation is presented in Appendix E. The resultant equation for the total pressure gradient is

$$\frac{dP}{dL} = -\frac{G^2}{144 g_c}\frac{d}{dL}\left[\frac{(1-X)^2}{\rho_f R_f \beta_f} + \frac{X^2}{\rho_g R_g \beta_g}\right] - \frac{4\tau_w}{D_H (12)}$$

$$-\left(\frac{g}{g_c}\sin\phi\right)\left(\rho_g R_g + \rho_f R_f\right)\left(\frac{1}{1728}\right) \qquad (1)$$

The total pressure gradient, therefore, comprises three separate components, i.e., the acceleration gradient

$$\left(\frac{dP}{dL}\right)_{\text{acceleration}} = -\frac{G^2}{144 g_c}\frac{d}{dL}\left[\frac{(1-x)^2}{\rho_f R_f \beta_f} + \frac{x^2}{\rho_g R_g \beta_g}\right] \quad \text{(1a)}$$

the friction pressure gradient

$$\left(\frac{dP}{dL}\right)_{\text{friction}} = -\frac{4}{D_H (12)} \tau_w \quad \text{(1b)}$$

and the elevation pressure gradient

$$\left(\frac{dP}{dL}\right)_{\text{elevation}} = -\left(\frac{g}{g_c}\sin\phi\right)\left(\rho_g R_g + \rho_f R_f\right)\left(\frac{1}{1728}\right) \quad \text{(1c)}$$

Equation 1 can be simplified somewhat by introducing the following densities:

$$\frac{1}{\hat{\rho}} = \frac{(1-x)^2}{\rho_f R_f \beta_f} + \frac{x^2}{\rho_g R_g \beta_g} \quad \text{(2)}$$

$$\frac{1}{\bar{\rho}} = \frac{1}{\rho_f R_f + \rho_g R_g} \quad \text{(3)}$$

$$\frac{1}{\rho_H} = \frac{1-x}{\rho_f} + \frac{x}{\rho_g} \quad \text{(4)}$$

Substituting equations 2 and 3 into equation 1 yields the following equation:

$$\frac{dP}{dL} = -\frac{G^2}{144 g_c}\frac{d}{dL}\left(\frac{1}{\hat{\rho}}\right) - \left(\frac{g}{g_c}\frac{\sin\phi}{1728}\right)\left(\bar{\rho}\right) - \frac{4}{D_H (12)}\tau_w \quad \text{(5)}$$

A quantity known as the slip ratio will now be introduced. Let

$$K = \text{slip ratio} = V_g/V_f \tag{6}$$

where V_g and V_f are the average velocities of the vapor and liquid phases, i.e.,

$$V_g = \frac{m_g}{\rho_g A_g} = \frac{\int_{A_g} V_g \, dA_g}{\int_{A_g} dA_g} \tag{6a}$$

$$V_f = \frac{m_f}{\rho_f A_f} = \frac{\int_{A_f} V_f \, dA_f}{\int_{A_f} dA_f} \tag{6b}$$

The use of the assumptions and geometry conditions given in Figure 62 together with the slip ratio as defined yields the following relationships between slip (K), void fraction (R_g), and flowing quality (X): (See Appendix F for detailed derivation.)

$$R_f = 1 - R_g \tag{7}$$

$$K = \left(\frac{\rho_f}{\rho_g}\right)\left(\frac{X}{1-X}\right)\left(\frac{R_f}{R_g}\right) \tag{8}$$

$$R_g = \frac{1}{1 + K\left(\frac{\rho_g}{\rho_f}\right)\left(\frac{1-X}{X}\right)} \tag{9}$$

$$\frac{\rho_f}{\rho_g} = \left(\frac{1}{K}\right)\left(\frac{X}{1-X}\right)\left(\frac{R_f}{R_g}\right) \tag{10}$$

$$X = \frac{1}{1 + \frac{1}{K}\left(\frac{\rho_f}{\rho_g}\right)\left(\frac{R_f}{R_g}\right)} \tag{11}$$

Equations 7 through 11 show that any three of the five quantities X, R_g, R_f, ρ_f/ρ_g, and K determine the remaining two.

All the preceding equations are valid for either annular or modified annular flow. For modified annular flow, these additional relationships may be useful: (See Appendix G for derivations).

$$E = \frac{m_{f(g)}}{m_f} \quad \text{(Entrainment fraction)} \tag{12}$$

$$\beta_f = \frac{K - E}{K\,[1 + E\,(K-2)]} \tag{13}$$

$$\beta_g = 1 \tag{14}$$

$$K' = \frac{V_g}{V_{f(a)}} = \frac{K - E}{1 - E} \tag{15}$$

In the following analyses, only annular flow will be considered. Note that for annular flow

$$\beta_f = 1 \tag{16}$$

$$\beta_g = 1 \tag{17}$$

Using equations 7 and 9 in equations 2 through 4, the densities may be expressed in terms of the slip in the following manner: (See Appendix H for deviation).

$$\frac{1}{\hat{\rho}} = \frac{1}{\rho_g}\left[(1-X)\frac{\rho_g}{\rho_f} + \frac{X}{K}\right]\left[1 + (X)(K-1)\right] \tag{18}$$

$$\frac{1}{\bar{\rho}} = \frac{1}{\rho_g}\left[(1-X)\frac{\rho_g}{\rho_f} + \frac{X}{K}\right]\frac{K}{X + K\,(1-X)} \tag{19}$$

$$\frac{1}{\rho_H} = \frac{1}{\rho_g}\left[(1-x)\frac{\rho_g}{\rho_f} + x\right] \tag{20}$$

Note that $\hat{\rho} = \bar{\rho} = \rho_H$, when K = 1. The slip ratio is generally assumed to be 1 in the so-called homogeneous model.

If an expression for the slip ratio (K), in terms of known system parameters (e.g., pressure and quality), could be determined, then the acceleration pressure drop could be obtained directly from equation 1a. The determination of such an expression constitutes one of the central problems in the prediction of two-phase pressure drops.

The Acceleration Pressure Drop

Minimum Value of the Acceleration Pressure Drop. As shown in equation 5, the acceleration pressure gradient can be written

$$\left(\frac{dP}{dL}\right)_{\text{acceleration}} = -\frac{G^2}{144\, g_c}\frac{d}{dL}\left(\frac{1}{\hat{\rho}}\right)$$

If the important case in which the fluid enters the accelerating section (the boiler) as a saturated liquid is considered, then the over-all acceleration pressure drop is

$$P_2 - P_1 = \Delta P = -\frac{G^2}{144\, g_c}\left[\frac{1}{\hat{\rho}_2} - \frac{1}{\hat{\rho}_1}\right] \tag{21}$$

$$\Delta P = -\frac{G^2}{144\, g_c}\left[\frac{1}{\hat{\rho}_2} - \frac{1}{\rho_{f_1}}\right] \tag{22}$$

$$|\Delta P| = \frac{G^2}{144\, g_c}\left[\frac{1}{\hat{\rho}_2} - \frac{1}{\rho_{f_1}}\right] \tag{23}$$

The minimum value of $|\Delta P|$ will occur at the minimum value of $1/\hat{\rho}_2$ consistent with the given quality at station 2. Appendix I shows

$$\frac{\partial(1/\hat{\rho})}{\partial K} = (X - X^2)\left(\frac{1}{\rho_f} - \frac{1}{K^2 \rho_g}\right) \tag{24}$$

$$\therefore \frac{\partial(1/\hat{\rho})}{\partial K} = 0 \quad \text{when} \quad K = \sqrt{\frac{\rho_f}{\rho_g}} \tag{25}$$

The minimum value of $1/\hat{\rho}_2$ for a given quality can now be determined by substituting the slip ratio given by equation 25 into equation 19. Therefore, the minimum acceleration pressure drop for a prescribed exit quality and a state of saturated liquid at inlet is given by

$$\Delta P_{min} = -\frac{G^2}{144 g_c}\left[\left(\frac{1}{\hat{\rho}_2}\right)_{K=\sqrt{\rho_f/\rho_g}} - \frac{1}{\rho_{f1}}\right] \tag{26}$$

Note that, unless it is assumed that the densities of the individual phases do not vary over the accelerating length, it will be necessary to iterate to obtain $\Delta P_{minimum}$ from the inlet pressure or temperature.

Figure 63 shows the slip ratio for potassium given by equation 25. In Figure 64, the dimensionless acceleration pressure drop for potassium has been plotted for $K = \sqrt{\rho_f/\rho_g}$ versus the temperature for various qualities. The dimensionless acceleration pressure drop is defined

$$-\frac{g_c \rho_{f1} \Delta P (144)}{G^2} = \frac{\rho_{f1}}{\hat{\rho}} - 1 \tag{27}$$

Since iteration was not used in determining the acceleration pressure drop, the temperature which is given should be regarded the exit temperature in the test section. The assumption of a constant liquid density, i.e., $\rho_{f2} = \rho_{f1}$ should be recognized when using Figure 64.

<u>An Estimated Maximum Value of the Acceleration Pressure Drop.</u> Consider the case in which the fluid enters the accelerating section as a saturated liquid and the density of the liquid phase is constant over the accelerating length. Assuming, further, that

1) $K \geq 1$
2) $V_{f2} \geq V_{f1}$

it can be shown that the acceleration pressure drop does not exceed the homogeneous value, i.e., that which is calculated for a slip ratio of one, even when $K \geq 1$. To do this, an acceleration factor is defined as

$$a = V_{f2} / V_{f1} \tag{28}$$

Then assumption 2 requires that $a \geq 1$. Appendix J shows that the relationship between a and K is given by the following equation:

$$K = \left(\frac{\rho_{f2}}{\rho_{g2}}\right)\left(\frac{X}{a - (1 - X)}\right) \tag{29}$$

Equation 29 has been plotted in Figure 65 for a density ratio of ten. It can also be written

$$\frac{K}{\left(\frac{\rho_f}{\rho_g}\right)_2 X} = \frac{K}{K_s} = \frac{1}{a - (1 - X)} \tag{30}$$

In this form, the relationship between K/K_s and a is independent of the particular fluid. Equation 30 is plotted in Figure 66.

As indicated in Figure 65, if $K \geq 1$ and $a \geq 1$, then $K \leq \rho_f/\rho_g$. Thus K lies between 1 and ρ_f/ρ_g when a and K are assumed $\geq$ 1.0. Figure 67 shows the dimensionless momentum pressure drop as a function of K for a density ratio of 10. The minimum dimensionless momentum pressure drop for any quality occurs here at a K = 3.165 or the square root of the density ratio of 10. Since the curve is double valued, the maximum acceleration pressure drop occurs at K equal the density ratio (10.0) and also at K equal 1.0.

The value of the momentum pressure drop, therefore, is between the values calculated for K equal to 1 (or ρ_f/ρ_g) and K equal to $\sqrt{\rho_f/\rho_g}$. The dimensionless acceleration pressure drop for a slip ratio of 1 is shown for potassium in Figure 68. In Figure 69 the minimum and estimated maximum values of the acceleration pressure drop are shown on the same plots as functions of quality and temperature of potassium.

<u>The Estimated Error in the Calculation of the Acceleration Pressure Drop Due to the Uncertainty of the Slip.</u> In Figure 70 the percentage error in the acceleration pressure drop caused by the uncertainty in the slip has been plotted. Note that the error decreases with increasing quality and for X = 1, is zero.

For a given quality, the error decreases as temperature increases and at the critical temperature is zero. Generally, the percentage error decreases with increasing quality and/or increasing temperature.

The Homogeneous Acceleration Pressure Drop. The homogeneous acceleration pressure drop is defined generally as the acceleration pressure drop for a slip ratio of one. This case has been discussed above; however, it is quite pertinent to observe that a slip ratio of one approximates the slip expected with a fog flow pattern (liquid dispersed in small droplets in the vapor and moving with the vapor velocity).

An Estimate of the Acceleration Pressure Drop. An estimation of the acceleration pressure drop can be obtained from equation 21 with the following additional assumptions.

1) ρ_g and ρ_f are constant
2) $K = [\rho_f / \rho_g]^m$
3) $m = 1/3$

In general, the acceleration pressure drop calculated in this manner will fall between the maximum and minimum values which have been estimated. References 18 and 19 suggest that, for an idealized system, $K = (\rho_f / \rho_g)\ 1/3$

The Elevation Pressure Drop

The Maximum and Minimum Values of the Elevation Pressure Drop. The elevation pressure gradient has been given by equation 1c, i.e.,

$$\left(\frac{dP}{dL}\right)_{\text{elevation}} = -\left(\frac{g}{g_c}\ \frac{\sin\phi}{1728}\right)\left(\rho_g R_g + \rho_f R_f\right)$$

Equation 5 demonstrated that the elevation pressure drop could be expressed in terms of the slip with the following expression:

$$\left(\frac{dP}{dL}\right)_{\text{elevation}} = -\left(\frac{g}{g_c}\ \frac{\sin\phi}{1728}\right)\left(\bar{\rho}\right)$$

where, from equation 19,

$$\frac{1}{\bar{\rho}} = \frac{1}{\rho_g}\left[(1-x)\frac{\rho_g}{\rho_f} + \frac{x}{K}\right]\left[\frac{K}{x + K\ (1-x)}\right]$$

Therefore, the elevation pressure drop can be written

$$\left(\frac{dP}{dL}\right)_{\text{elevation}} = \left(-\frac{g}{g_c}\,\frac{\sin\phi}{1728}\right)\left(\rho_g\right)\left(\frac{X+K(1-X)}{X+K(1-X)(\rho_g/\rho_f)}\right) \quad (31)$$

The elevation pressure drop can be obtained by integrating equation 31, i.e.,

$$P_2 - P_1 = \int_0^L \left[\left(-\frac{g}{g_c}\,\frac{\sin\phi}{1728}\right)\left(\rho_g\right)\left(\frac{X+K(1-X)}{X+K(1-X)(\rho_g/\rho_f)}\right)\right] dL \quad (32)$$

Dividing both sides of equation 32 by $1/\rho_f$ and re-arranging, the maximum value of the elevation pressure drop can be obtained as follows:

$$-\frac{g_c}{g}\,\frac{\Delta P(1728)}{\rho_f \sin\phi} = \frac{1}{\rho_f}\int_0^L \rho_g\left(\frac{X+K(1-X)}{X+K(1-X)(\rho_g/\rho_f)}\right) dL$$

$$-\frac{g_c}{g}\,\frac{\Delta P(1728)}{\rho_f \sin\phi} = \frac{1}{\rho_f}\int_0^L \rho_f\left[\frac{\frac{X}{K(1-X)}+1}{\frac{X}{K(1-X)}\left(\frac{\rho_f}{\rho_g}\right)+1}\right] dL$$

Since $\rho_f \geq \rho_g$; $\dfrac{\frac{X}{K(1-X)}+1}{\frac{X}{K(1-X)}\left(\frac{\rho_f}{\rho_g}\right)+1} \leq 1$

$$\therefore\ \Delta P_{max} = -g/g_c\ \rho_f\ (\sin\phi)\ L/1728 \quad (33)$$

The minimum value of the elevation pressure drop is obtained in a similar manner, i.e.,

$$-\frac{g_c \Delta P(1728)}{g\,\rho_g \sin\phi} = \frac{1}{\rho_g}\int_0^L \rho_g\left[\frac{\frac{X}{K(1-X)}+1}{\frac{X}{K(1-X)}+\rho_g/\rho_f}\right] dL$$

Since $\rho_f \geq \rho_g$; $\dfrac{[X/K(1-X)]+1}{[X/K(1-X)]+\rho_g/\rho_f} \geq 1$

$$\therefore\ \Delta P_{min} = -g/g_c\ \rho_g\ (\sin\phi)\ L/1728 \quad (34)$$

It is worth while noting that $\partial(\Delta P \text{ elevation})/\partial K$ approaches zero as K approaches infinity, and does not possess a local minimum with respect to the slip as does the acceleration pressure drop.

The Effect of Slip on the Elevation Pressure Gradient. The dimensionless elevation pressure gradient is obtained by dividing both sides of equation 5 by ρ_f:

$$\frac{-(1728)\frac{g_c}{g}\left(\frac{dP}{dL}\right)_{elevation}}{\rho_f \sin\phi} = \frac{\bar{\rho}}{\rho_f} \tag{35}$$

Equation 35 has been plotted for potassium as a function of temperature in Figures 71 and 72 for K = 1 and $K = \sqrt{\rho_f/\rho_g}$, respectively. Note that the dimensionless elevation pressure gradient increases as the slip increases. The dimensionless elevation pressure gradient approaches one as K approaches infinity. In general,

$$\frac{\rho_g}{\rho_f} \leq \frac{-(1728)\frac{g_c}{g}\left(\frac{dP}{dL}\right)_{elevation}}{\rho_f \sin\phi} \leq 1 \tag{36}$$

The line for a quality of one in Figures 71 and 72 is identical with lower bounds in equation 36 while the upper bounds is equal to one.

An Estimate of the Elevation Pressure Drop. An estimate of the elevation pressure drop can be obtained from equation 32, if the quality dependence upon the length is known and the following assumptions are made:

1) ρ_g and ρ_f are constant along the length
2) $K = (\rho_f/\rho_g)^m$
3) $m = 1/3$

Using assumptions 1 through 3 and the known or assumed relationship between quality and length, the elevation pressure drop can be estimated by carrying out the indicated integration in equation 32.

Other Quantities of Interest

Superficial Slip. The superficial slip may be regarded either as an arbitrary correlation parameter [it has been used, for example, in the correlation of void fraction (R_g)] or as a first estimate of the slip. The slip might be estimated in the succeeding manner.

Underestimate the vapor velocity at the section of interest.

$$\text{Since } V_g = \frac{X m}{\rho_g A_g} \text{ and } V_{g(s)} = \frac{X m}{\rho_g A_T} \quad \therefore V_g > V_{g(s)} \tag{37}$$

assuming $a \geq 1$, then $V_{f1} \leq V_{f2}$. With this assumption, V_{f1} underestimates the liquid velocity:

$$K_s = \frac{\text{Superficial Vapor Velocity}}{\text{Inlet Liquid Velocity}}$$

$$K_s = \frac{V_{g(s)}}{V_{f1}} \qquad \frac{\text{Underestimate of } V_g}{\text{Underestimate of } V_f} \tag{38}$$

$$K_s = X \frac{\rho_f}{\rho_g} \tag{39}$$

Void Fraction. The relationship between the void fraction and the slip ratio is given by equation 8. In Figures 73 and 74 the void fraction for potassium has been plotted for slip ratios of 1 and the square root of the density ratio, respectively.

Summary

1) The two-phase acceleration pressure drop can be calculated from

$$\Delta P_{acc} = \frac{-G^2}{(144)\, g_c} \left[\frac{1}{\hat{\rho}_2} - \frac{1}{\hat{\rho}_1} \right]$$

where

$$\frac{1}{\hat{\rho}} = \frac{1}{\rho_g} \left[(1-x)\frac{\rho_g}{\rho_f} + \frac{x}{K} \right] \left[(1+x)(K-1) \right]$$

and the value of ΔP_{acc} is between that calculated for $K = 1$ and $K = \sqrt{\rho_f / \rho_g}$.

2) The minimum and maximum acceleration pressure drop for the case where the potassium enters the boiler as a saturated liquid and the liquid density can be assumed constant with length is given in Figures 64 and 68 respectively, as a function of potassium exit temperature and quality.

3) For exit qualities greater than 25% and temperatures greater than 1400°F, the maximum error in determining the acceleration pressure drop, by assuming either $K = 1$ or $K = \sqrt{\rho_f / \rho_g}$, is less than 70%. Using $K = \sqrt{\rho_f / \rho_g}$ will minimize this error.

4) The two-phase elevation pressure drop can be calculated from

$$\Delta P_{el} = -\frac{g}{g_c} \sin \phi \, (\bar{\rho})$$

where $$\frac{1}{\bar{\rho}} = \left[(1-x)\frac{\rho_g}{\rho_f} + \frac{x}{K}\right]\left[\frac{K}{x + K(1-x)}\right]$$

5) The minimum and maximum two-phase elevation pressure drops are

$$(\Delta P_{el})_{min} = \frac{-g}{g_c}\,\rho_g\left(\frac{\sin\phi}{1728}\right)L$$

$$(\Delta P_{el})_{max} = \frac{-g}{g_c}\,\rho_f\left(\frac{\sin\phi}{1728}\right)L$$

VI. INSTRUMENTATION

W.H. Bennethum

Before meaningful data can be obtained, accurate measurements are required for heat transfer investigations. The problems of instrumentation, to provide the desired information and accuracy for heat transfer investigations with alkali metals, are increased because of the boiling alkali metal environment. The instrumentation task was established to ensure that this desired data and required accuracy are achieved. This section describes the type, design, development, and application of the instrumentation pertinent to the heat transfer investigations reported.

300 KW Facility

Sensor locations have remained essentially unchanged during this quarter. The arrangement of all thermocouples located on the test boiler, including the insert, is described in reference 2. To accomodate limitations in the data reduction program, several minor changes in sensor location were made.

Eight new chromel-alumel thermocouples were added to the boiler shell in an attempt to define the magnitude of the error caused by the Pt vs. Pt + 10% Rh lead wire mismatch. This error, a function of temperature level in the enclosure, possibly can be determined by these chromel-alumel thermocouples, which are not as susceptible to lead wire mismatch. Four new thermocouples were added to the horizontal condenser cooling air exit stream to measure the bulk exit temperature of the air more precisely. The two thermocouples previously used for this purpose were located several inches from the liquid potassium pipe, one in each leg of the flow path, and were subject to radiation error. Two new thermocouples, one chromel-alumel and the other Pt vs. Pt + 10% Rh, were located several feet downstream of the cooling air exit in a common 4-inch diameter duct. Several feet further downstream, a second pair of chromel-alumel thermocouples was installed to measure heat loss in the exit duct. Table 4 is a complete list of all instrumentation locations in the 300 kw facility used for data obtained from December 9, 1963 to January 1, 1964.

By the last week of December, it was apparent that the insert thermocouples were not functioning. The loop was operated approximately 2 days following the failure of all seven insert thermocouples before being shut down for major repair activity. Subsequent removal of the insert from the test boiler indicated that a failure had occurred in the weld between the .500-inch OD by .049-inch wall tube at the exit of the 1-inch diameter boiling tube (Figure 20,

reference 3). This point was located in a region of high turbulence and vibratory forces probably caused the failure. Failure at this point permitted alkali metal to enter the center body of the insert and a major leak would have developed if the thermocouple sheaths had not been brazed into the upper cap. To avoid a recurrence, a replacement insert with a much stiffer upper section, fabricated from 1 1/8-inch OD by 3/4-inch ID tube, was designed. The helical ribbon was extended to cover the entire .250-inch OD by .049-inch wall tube and thus afford additional support over the last foot of 1-inch boiling tube. A detailed drawing of the modified insert will be included in the next progress report.

Significant emphasis was placed on achieving accurate pressure measurements at the inlet and exit of the boiler secondary fluid stream. Repeated over-pressurization caused by loop transient conditions had precluded attempts to measure pressure drop across the condensing test sections with low range, back-loaded transducers. The boiler inlet and exit pressure gages were encased in calrod heating units and insulation, so that the transducer temperature could be controlled over narrow temperature limits during loop operation. In-place calibrations were performed at two temperatures to determine the effects of temperature on the pressure gage output curve, and the results are presented in Figures 75 and 76. During the December data runs, both pressure gages were operated between the temperature limits stated on the calibration curves. To verify the curves shown in Figures 75 and 76, another partial calibration was performed December 8, 1963. There was excellent agreement between the two calibrations.

During the December data runs, the boiler exit pressure gage ceased to function properly for unknown causes. Following loop shutdown, an in-place calibration was performed January 4, 1964 which verified that the boiler exit pressure gage was not functioning properly. It also indicated that the boiler inlet pressure gage had undergone a substantial zero shift change. Such a change could have been caused by operating the transducer at elevated temperatures under high vacuum conditions or by some malfunction in the strain gage transducer used to convert the pressure signal into an electrical signal.

Following removal from the loop piping system, the boiler exit pressure gage was examined further to determine the cause of failure more specifically. The results indicated that contamination of the sodium-potassium filling material in the capillary tubing, connecting the rear side of the diaphragm sensing head to the bourdon spring, had occurred. This could have been caused either by a leak in the capillary system, including the sensing head, or by a concentration of contaminants present in the initial filling material. This same type malfunction has been cited in four of

the nine transducers used on the loop. Determining the precise cause is impossible without cutting apart the transducer. The faulty units will be returned to the manufacturer, Taylor Instrument Company, to determine the exact cause for failure and, thereby, prevent future interruptions in data acquisition.

100 KW Facility

Instrumentation sensor locations are essentially those illustrated in Figure 23, reference 8. A new instrumentation feed-through was designed which will accomodate approximately twice the temperature sensing elements on the facility. Seven, twenty-one hollow pin, glass-to-metal seal feed-through flanges replaced, at the same locations, three, twenty-one pin feed-throughs which had been used previously. To preclude stringing the refractory thermocouple wires over great distances, special copper lead wire in quartz insulation was run from the feed-through flange to a reference block inside the vacuum chamber. This approach was taken to eliminate the frequent breakage in the thermocouple leads caused by excessive handling and temperature cycling. The reference junction blocks consisted of terminal strip made from 1/2 inch square boron nitride bar stock. The thermocouple alloy and copper wires were twisted together and positioned with a stainless steel screw. The entire assembly was then insulated from loop radiation with a cylindrical shield wrapped with several layers of dimpled foil.

To measure the reference junction temperatures, three copper constantan thermocouples were installed on each terminal strip. The copper constantan thermocouples were referenced to an ice bath outside the loop chamber. Preliminary tests of this configuration, during loop operations, indicated that a temperature gradient of 15 to 20°F could be expected from one end of the terminal strip to the other. The three thermocouple junctions on the terminal strip will be used to determine the actual reference junction temperature at any point on the strip.

Because of the increased reliability of the W + 3% Re wire, as determined from its operation in the hot zone of the boiler for the past 6 months, i.e., no failures, the W + 3% Re vs. W + 26% Re will be used as the thermocouple alloy for the entire loop. This material will be installed during the next reporting period.

50 KW Facility

There was essentially no change in the instrumentation for the 50 kw facility during this reporting period. There was a significant problem associated with determining the accuracy of the potassium loop permanent magnet flowmeter. Test data indicated that a shift in calibration of the flowmeter had occurred. Examination of the

meter indicated that there was no reasonable cause for such a shift since all elements of the flowmeter, including the magnetic flux density, were unchanged. An attempt to resolve this problem by installing a second permanent magnet flowmeter in series with the original was unsuccessful. The output of the second flowmeter was extremely erratic and approximately one-fourth the expected value.

No reasonable explanation for this significant discrepancy has been determined. There is a discontinuity in the piping system in the area in which the flowmeters are located; it is not probable, however, that this is the cause. All the anticipated causes for such disagreement, i.e., mismatch between the pipe and electrode materials and nonuniform flux fields, were checked and eliminated. Presumably, therefore, the problem has been caused by some phenomenon, such as a partially filled duct or some change in the duct configuration. Build-up of foreign material or scale would invalidate the assumptions made in deriving the calculated flow meter sensitivity. Whenever testing schedule permits, the pipe section in the region of the flowmeter will be cut out and examined in order to arrive at an explanation of this discrepancy. In the meantime, a calorimetric technique has been used to measure flow. This device described in Section III, has been installed in the loop.

VII. MATERIALS SUPPORT

W. R. Young

300 KW Facility

A failure occurred in the test section at the bottom (inlet) bimetallic joint between the L-605 and the Mo-0.5 Ti alloy tubing. The failure was attributed to bending stresses transmitted to the Mo-0.5 Ti tube from the outer L-605 alloy pipe which bent during service. Since the 300 kw loop design could not readily be modified to eliminate bending of the test section, the Mo-0,5 Ti alloy tube was replaced with an L-605 alloy tube.

Three welded L-605 alloy tubes, 1.0-inch outside diameter with a 0.039-inch wall thickness, were inspected using an ultrasonic standard with test notches equivalent to 5% and 15% of the wall thickness. No indications were found on the tube designated number 1, which was used subsequently for fabrication of the new test section. The tube designated number 2 had one circumferential defect on the outside diameter, 43.25 inches from the index end; the tube designated number 3 could not be inspected because an uneven outside diameter at the weld seam area distorted the ultrasonic signal, negating a reliable inspection.

The new test section was reassembled in accordance with accepted welding procedures. The measurements of tube number 1 are given in Table 3. The helical swirl device was positioned inside the L-605 alloy tube and seal welded at the top of the test section.

100 KW Facility

A new Cb-1Zr alloy, 3/4-inch schedule 80 pipe, test section was fabricated, and installed in the 100 kw loop. The test section was welded and heat-treated in accordance with General Electric specification SPPS-3B "Welding of Columbium-1% Zirconium Alloy by the Inert Gas Tungsten Arc Process."

Installing the test section in the 100 kw loop required that a field welding procedure for Cb-1Zr, 3/4-inch schedule 80 pipe be developed. Since the wall thickness and, therefore, the heat input were greater than previous welds, a new inert gas shield was constructed using a design similar to that employed in prior field welding of Cb-1Zr, 3/8-inch schedule 80 pipe. Several trial welds were made which simulated the conditions of field welding; i.e., the pipe could not be rotated. These tests afforded the welding parameters and techniques needed to minimize atmospheric contamination. The two field welds required for test section installation were made without difficulty.

50 KW Facility

No work was performed on this facility during the quarterly period reported.

TABLE 1: CONDITIONS FOR FILM BOILING RUNS

Code Number	Run Number Date	Run Number Time	Potassium Flow Rate, lbs/sec	Potassium Temp., °F Inlet	Potassium Temp., °F Outlet	Film Boiling Length, Inches	Quality, %	Calc. Film Boiling Heat Flux, 10^6 Btu/hr-ft^2
1	5/11/63	1856	.1252	895	1497	26.0	77.5	.344
2		1955	.1659	1126	1515	16.0	70.2	.311
3		2056	.1809	1188	1544	10.0	66.6	.325
4		2256	.1720	1229	1565	23.0	75.6	.365
5	5/22/63	0250	.0853	1385	1742	23.5	82.1	.254
6		0310	.0856	1404	1737	23.0	80.8	.225
7		0330	.0856	1415	1721	45.0	81.1	.204
8		0348	.0856	1418	1711	49.0	83.5	.239
9	5/23/63	0018	.1401	1506	1681	45.0	79.9	.338
10		0051	.1399	1496	1675	40.0	81.7	.338
11		0118	.1399	1495	1675	43.0	81.2	.377
12		0144	.1399	1496	1670	42.0	89.6	.339
13		0214	.1418	1492	1667	46.0	88.1	.414
14		2205	.2129	1574	1650	40.0	74.0	.498
15		2221	.2150	1559	1643	39.0	71.4	.446
16		2351	.1235	1480	1664	14.0	46.2	.206
17	5/24/63	0032	.1235	1444	1586	14.0	39.0	.259
18		1343	.2052	1660	1753	14.0	48.4	.293
19	6/27/63	0815	.2461	1543	1665	17.0	32.6	.214
20		0845	.2406	1561	1679	16.0	32.3	.229
21		0915	.2498	1572	1689	11.0	32.6	.242
22		0945	.2104	1557	1676	13.0	45.9	.269
23		1030	.1794	1519	1662	11.0	59.9	.296
24		1100	.1506	1484	1641	20.0	81.4	.376
25	6/28/63	0202	.5997	1548	1626	26.0	23.7	.464
26		0300	.5997	1509	1591	26.0	21.9	.399

TABLE 2: PROPERTIES OF L-605 AT ELEVATED TEMPERATURES
(Data from Reference 10)

Property	Temperature 1600°F	1800°F	1850°F
Ultimate Tensile Strength, psi	35,000	22,700	20,000
Yield Strength ($\leq$1 hr), psi	25,000	20,500	14,000
Rupture Strength (1000 hr), psi	8,400	2,800	1,900
Thermal Conductivity, Btu/hr-°F-ft^2	15.0	16.0	16.0
Modulus of Elasticity, (10^6 psi)	24.9	22[a]	20[a]
Coefficient of Thermal Expansion, (10^{-6} inch/inch-°F)	9.0	9.41	9.5
Potassium/Sodium Corrosion Rate, inch/1000 hr	---	---	.005[b]
Oxidation Rate, inch/1000 hr	---	---	.003[b]
Design Stress (noncritical)=Rupture Strength/2, psi	4,200	1,400	950
Design Stress (critical)=Rupture Strength/3, psi	2,700	930	630

[a] Extrapolated from Haynes Stellite data, reference 10.
[b] General Electric test data, reference 11.

TABLE 3: MEASUREMENTS OF L-605 ALLOY TUBE FOR 300 KW TEST SECTION
(Tube No. 1; Wall Thickness, 0.039 Inch)

Distance from Top Joint, inches	Outside Diameter, inches	
	Angular 0°	Rotation 90°
0	1.000	1.004
4	1.002	1.002
8	1.002	1.002
12	1.002	1.002
16	1.001	1.002
20	1.002	1.003
24	1.002	1.002
28	1.002	1.002
32	1.002	1.001
36	1.002	1.001
40	1.001	1.002
44	1.002	1.002
48	1.002	1.003
52	1.001	1.002
56	1.002	1.001
60	1.002	1.000
64	1.002	1.001
68	1.002	1.002
72	1.001	1.002
76	1.000	1.001
80	1.002	1.002
84	1.002	1.003
88	1.001	1.001
92	1.002	1.002
96	1.001	1.001
100	1.002	1.001
104	1.001	1.000

TABLE 4: 300 KW FACILITY INSTRUMENTATION LOCATIONS
(December 9, 1963 Through January 1, 1964)

Sensor Location	Thermocouple Code Number	Ref.[1] Temp.	Rubicon Switch	Digital Scanner Channel
Cats block 1-1A(K)		ICE	H5	02
Cats block 1-1B(K)		ICE	H6	03
Cats block 1-2(CC)		ICE	H7	04
Cats block 1-3(CC)		ICE	H8	05
Cats block 1-4(CC)		ICE	H9	06
Cats block 2-1(CC)		ICE	H10	07
Cats block 2-2A(K)		ICE	H11	08
Cats block 2-2B(K)		ICE	H12	09
Hor. cond. exit well	3-112-G-S-H13	ICE	H13	10
Secondary inlet well	1-102-P-S-H1	ICE	H1	11
Secondary exit well	1-104-Z-S-H2	ICE	H2	12
Primary inlet well	1-106-W-S-H3	ICE	H3	13
Primary exit well	1-107-T-S-H4	ICE	H4	14
Not used				15
Not used				16
Secondary inlet well	1-102-N-S-B34	1-3	B34	17
Secondary inlet well	1-102-O-S-B35	1-3	B35	18
Secondary exit well	1-104-X-S-B37	1-3	B37	19
Secondary exit well	1-104-Y-S-B39	1-3	B39	20
Primary inlet well	1-106-U-S-C1	1-3	C1	21
Primary inlet well	1-106-V-S-C2	1-3	C2	22
Primary exit well	1-107-R-S-C4	1-3	C4	23
Primary exit well	1-107-S-S-C5	1-3	C5	24
Boiler shell (new ungrounded)	1-25-1.5-S-C7	1-3	C7	25
↓	1-25-5.5-S-C8	1-3	C8	26
	1-36-1.5-S-C9	1-3	C9	27
	1-36-5.5-S-C10	1-3	C10	28
	1-47-1.5-S-C11	1-3	C11	29
	1-47-5.5-S-C12	1-3	C12	30
	1-58-1.5-S-C13	1-3	C13	31
	1-58-5.5-S-C14	1-3	C14	32
Thermal pressure sensor		1-3	C15	33
Thermal pressure sensor braze		1-3	C16	34
Insert leak indicator		1-3	C17	35
Boiler shell (bottom)	1-91-2-S-C18	1-3	C18	36
↓	1-91-3-S-C19	1-3	C19	37
	1-91-4-S-C20	1-3	C20	38
	1-91-5-S-C21	1-3	C21	39
	1-91-6-S-C22	1-3	C22	40
	1-91-7-S-C23	1-3	C23	41
Boiler shell (bottom)	1-91-8-S-C24	1-3	C24	42

[1] Ice refers to ice bath at 32°F.

TABLE 4: 300 KW FACILITY INSTRUMENTATION LOCATIONS
(December 9, 1963 Through January 1, 1964)

Sensor Location	Thermocouple Code Number	Ref. Temp.	Rubicon Switch	Digital Scanner Channel
Boiler shell	1-80-1-S-C25	1-3	C25	43
	1-80-2-S-C26	1-3	C26	44
	1-80-3-S-C27	1-3	C27	45
	1-80-4-S-C28	1-3	C28	46
	1-80-5-S-C29	1-3	C29	47
	1-80-6-S-C30	1-3	C30	48
	1-80-7-S-C31	1-3	C31	49
	1-80-8-S-C32	1-3	C32	50
	1-69-1-S-C33	1-3	C33	51
	1-69-2-S-C34	1-3	C34	52
	1-69-3-S-C35	1-3	C35	53
	1-69-4-S-C36	1-3	C36	54
	1-69-5-S-C37	1-3	C37	55
	1-69-6-S-C38	1-3	C38	56
	1-69-7-S-C39	1-3	C39	57
	1-69-8-S-C40	1-3	C40	58
	1-58-1-S--	1-3	--	59
	1-58-2-S-F1	1-4	F1	60
	1-58-3-S-F2	1-4	F2	61
	1-58-4-S-F3	1-4	F3	62
	1-58-5-S-F4	1-4	F4	63
	1-58-6-S-F5	1-4	F5	64
	1-58-7-S-F6	1-4	F6	65
	1-58-8-S-F7	1-4	F7	66
	1-47-1-S-F8	1-4	F8	67
	1-47-2-S-F9	1-4	F9	68
	1-47-3-S-F10	1-4	F10	69
	1-47-4-S-F11	1-4	F11	70
	1-47-5-S-F12	1-4	F12	71
	1-47-6-S-F13	1-4	F13	72
	1-47-7-S-F14	1-4	F14	73
	1-47-8-S-F15	1-4	F15	74
	1-36-1-S-F16	1-4	F16	75
	1-36-2-S-F17	1-4	F17	76
	1-36-3-S-F18	1-4	F18	77
	1-36-4-S-F19	1-3	F19	78
	1-36-5-S-F20	1-4	F20	79
	1-36-6-S-F21	1-4	F21	80
	1-36-7-S-F22	1-4	F22	81
Boiler shell	1-36-8-S-F23	1-4	F23	82

TABLE 4: 300 KW FACILITY INSTRUMENTATION LOCATIONS
(December 9, 1963 Through January 1, 1964)

Sensor Location	Thermocouple Code Number	Ref. Temp.	Rubicon Switch	Digital Scanner Channel
Boiler shell top	1-25-1-S-F24	1-4	F24	83
	1-25-2-S-F25	1-4	F25	84
	1-25-3-S-G1	1-4	G1	85
	1-25-4-S-G2	1-4	G2	86
	1-25-5-S-G3	1-4	G3	87
	1-25-6-S-G4	1-4	G4	88
	1-25-7-S-G5	1-4	G5	89
	1-25-8-S-G6	1-4	G6	90
Vert. cond. inlet well	2-109-M-S-H26	ICE	H26	91
Vert. cond. exit well	2-111-H-S-H25	ICE	H25	92
Primary std-sec inlet well		ICE	G9	93
Cats block 1-1 (new cc)		ICE	G10	94
Short circuit			G11	95
Cats block 2-2 (new cc)		ICE	G12	96
Not used			G13	97
Primary flowmeter			G14	98
Secondary flowmeter			G15	99
Short circuit				100
Vertical condenser tube wall	2-1-12-S-B13	2-1	B13	101
	2-7-4:30-S-B18	2-1	B18	102
	2-5-7:30-S-B16	2-1	B16	103
	2-5-1:30-S-B17	2-1	B17	104
	2-1-6-S-B14	2-1	B14	105
	2-3-10:30-S-B15	2-1	B15	106
	2-9-3-S-B19	2-1	B19	107
Vertical condenser tube wall	2-9-9-S-B20	2-1	B20	108
Vertical condenser inlet well	2-109-L-S-B24	2-1	B24	109
Vertical condenser inlet well	2-109-M-S-B11	2-1	B11	110
Hor.cond.bulk air exit(at hood-S)		2-1	B12	111
Not Used			B21	112
Vertical cond. exit well	2-111-J-S-B22	2-1	B22	113
Vertical cond. exit well	2-111-K-S-B23	2-1	B23	114
Hor. cond. exit well	3-112-G-S-B32	2-1	B32	115
Hor. cond. exit well (new)	3-112-E-S-B33	2-1	B33	116
Sec. pump exit press. gage T/C		1-1	B25	117
Sec. pump inlet press. gage T/C		1-1	B26	118
Primary pump inlet press. gage T/C		1-1	B27	119
Primary pump exit press. gage T/C		1-1	B28	120
Vert. condenser inlet pressure			N1	121
Vert. condenser exit pressure			N2	122
Hor. condenser exit pressure			N3	123
Boiler exit pressure			N4	124
Primary pump exit pressure			N5	125

TABLE 4: 300 KW FACILITY INSTRUMENTATION LOCATIONS
(December 9, 1963 Through January 1, 1964)

Sensor Location	Thermocouple Code Number	Ref. Temp.	Rubicon Switch	Digital Scanner Channel
Primary pump inlet pressure			N6	126
Sec. pump inlet pressure			N7	127
Sec. pump exit pressure			N8	128
Boiler inlet pressure			N9	129
Short Circuit			--	130
Hor. cond. inlet pressure gage	T/C	1-1	A1	131
Vertical cond. annulus air	2-2-9-K-A2	2-2	A2	132
↓	2-4-3-K-A3	2-2	A3	133
↓	2-4-9-K-A4	2-2	A4	134
↓	2-6-3-K-A5	2-2	A5	135
Hor. cond. bulk air exit(at hood-k)		2-2	A6	136
Vert. cond. annulus air	2-8-3-K-A7	2-2	A7	137
Vert. cond. annulus air	2-8-9-K-A8	2-2	A8	138
Boiler shell(new ungrounded K)	1-25-3.5-K-A9	1-1	A9	139
↓	1-25-7.5-K-A10	1-1	A10	140
↓	1-36-3.5-K-A11	1-1	A11	141
↓	1-36-7.5-K-A12	1-1	A12	142
↓	1-47-3.5-K-A13	1-1	A13	143
↓	1-47-7.5-K-A14	1-1	A14	144
↓	1-58-3.5-K-A15	1-1	A15	145
↓	1-58-7.5-K-A16	1-1	A16	146
Hor.cond.bulk air exit(under hood-west)		2-2	A17	147
Hor.cond.bulk air exit(under hood-north)		2-2	A18	148
Vert. condenser bulk air in	2-L-6-K-A19	2-2	A19	149
Vert. condenser bulk air in	2-M-6-K-A20	2-2	A20	150
Vert. condenser bulk air out	2-N-6-K-A21	2-2	A21	151
Vert. condenser bulk air out	2-D-6-K-A22	2-2	A22	152
Hor. condenser bulk air in	3-S-12-K-A23	2-2	A23	153
Hor. condenser bulk air in	3-T-6-K-A24	2-2	A24	154
Hor. condenser annulus air	3-1-3-K-A25	2-2	A25	155
↓	3-1-9-K-A26	2-2	A26	156
↓	3-2-3-K-A27	2-2	A27	157
↓	3-2-9-K-A28	2-2	A28	158
↓	3-4-3-K-A29	2-2	A29	159
↓	3-4-9-K-A30	2-2	A30	160
↓	3-4-6-K-A31	2-2	A31	161
Boiler insert No. 7		1-1	A32	162
Hor. condenser annulus air	3-7-3-K-A33	2-2	A33	163
Vert. cond. cooling air orifice B		2-2	A34	164
Hor. cond. annulus air	3-8-3-K-A35	2-2	A35	165
Hor. cond. annulus air	3-8-9-K-A36	2-2	A36	166
Vert. cond. inlet press gage T/C		1-1	A37	167
Boiler exit pressure gage T/C		1-1	A38	168

TABLE 4: 300 KW FACILITY INSTRUMENTATION LOCATIONS
(December 9, 1963 Through January 1, 1964)

Sensor Location	Thermocouple Code Number	Ref. Temp.	Rubicon Switch	Digital Scanner Channel
Hor. cond. cooling air orifice	A	2-2	A39	169
Hor. cond. annulus air	3-13-9-K-B1	2-2	B1	170
Hor. cond. cooling air orifice	B	2-2	B2	171
Hor. cond. annulus air	3-12-9-K-B3	2-2	B3	172
Vert. cond. cooling air orifice	A	2-2	B4	173
Hor. cond. annulus air	3-13-9-K-B5	2-2	B5	174
↓	3-15-3-K-B6	2-2	B6	175
	3-15-9-K-B7	2-2	B7	176
Hor. cond. bulk air exit upper	3-U-12-K-B8	2-2	B8	177
Hor. cond. bulk air exit lower	3-V-6-K-B9	2-2	B9	178
Primary flowmeter stream temp.		1-1	E2	179
Primary flowmeter magnet temp.		1-1	E2	180
Secondary flowmeter stream temp.		1-1	E3	181
Secondary flowmeter magnet temp.		1-1	E4	182
Vert. cond. outer skin upstream temp.		1-1	E5	183
Vert. cond. outer skin downstream temp.		1-1	E6	184
Hor. cond. outer skin upstream temp.		1-1	E7	185
Hor. cond. outer skin downstream temp.		1-1	E8	186
Hor. cond. exit press. gage T/C		1-1	E9	187
Boiler inlet press. gage T/C		1-1	E10	188
Boiler insert No. 1 (lowest)		1-1	E11	189
No. 2		1-1	E12	190
No. 3		1-1	E13	191
No. 4		1-1	E14	192
No. 5		1-1	E15	193
No. 6		1-1	E16	194

Code Number Description

Test Section { 1 = Boiler; 2 = Horizontal Condenser; 3 = Vertical Condenser }

Distance from reference plane

Circumferential position: Quadrant-O'clock-Degrees

T/C alloy: S = Pt vs. Pt + 10% Rh; K = Chromel-Alumel; CC = Copper Constantan

Rubicon Switch Position

1 - 80 - 1 - S - C25

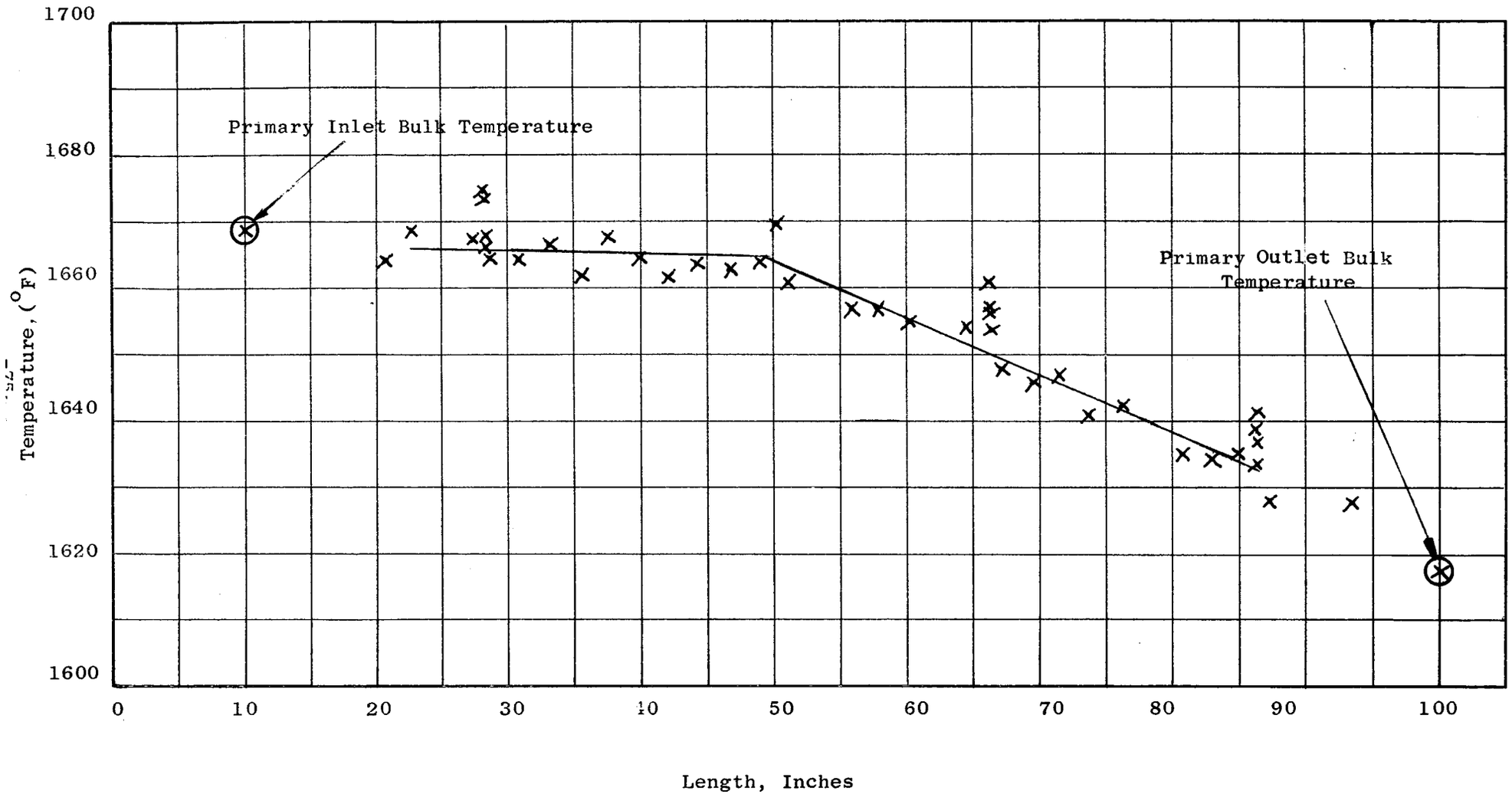

Figure 1. Primary Shell Wall Temperature vs Length - 300 KW System
Film Boiling Run 5/11 1856

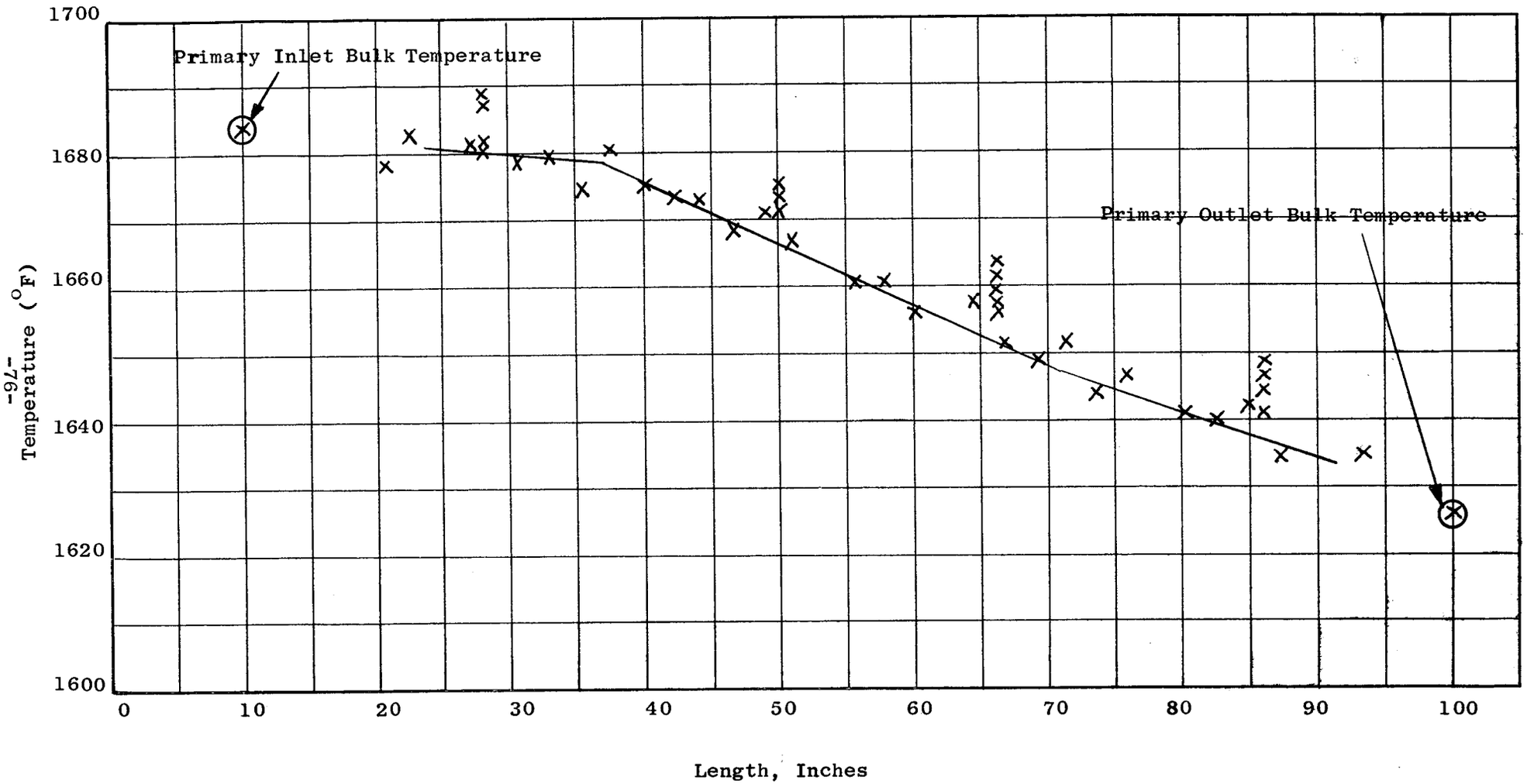

Figure 2. Primary Shell Wall Temperature vs Length - 300 KW System
Film Boiling Run 5/11 1955

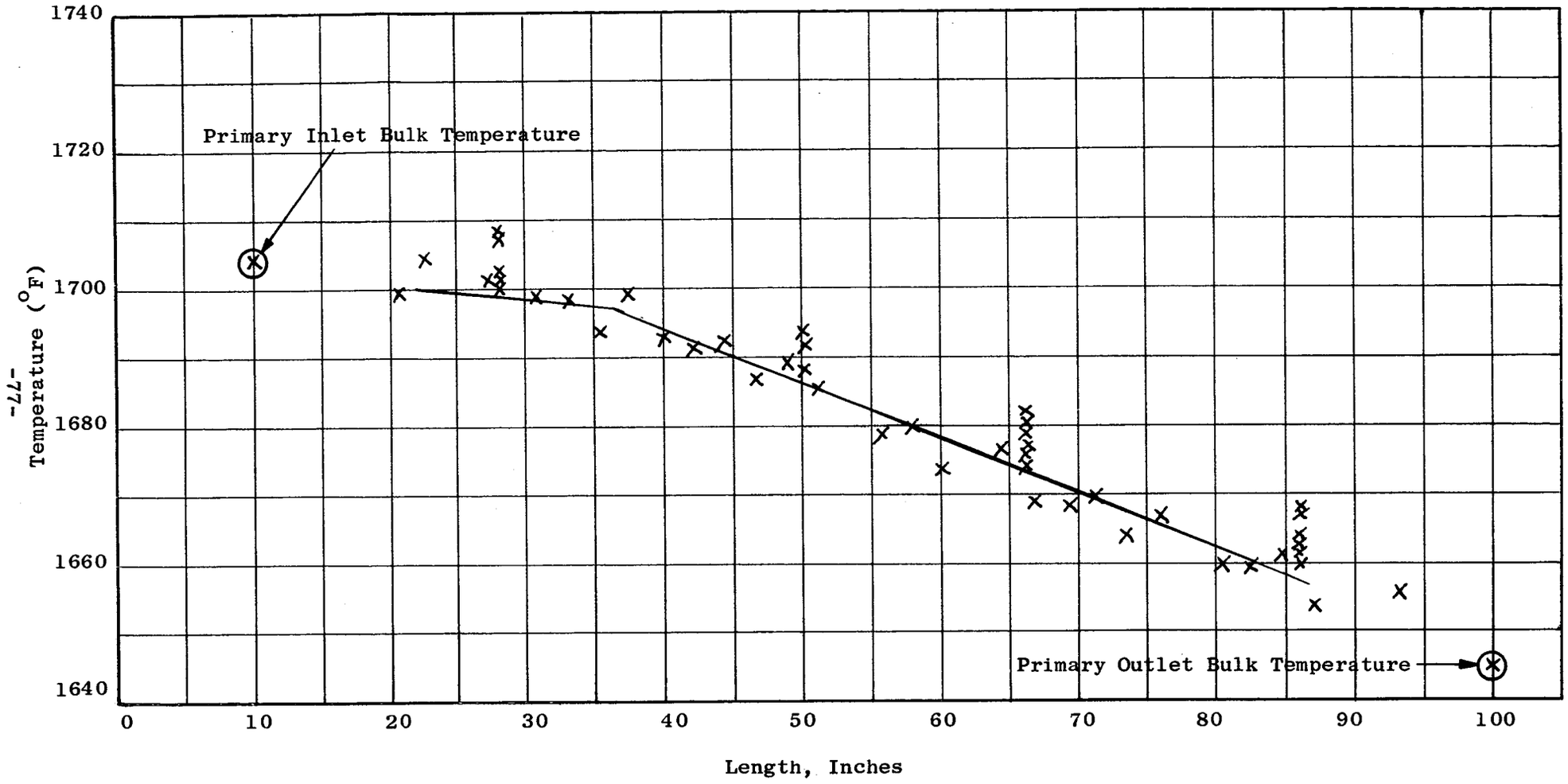

Figure 3. Primary Shell Wall Temperature vs Length - 300 KW System
Film Boiling Run 5/11 2056

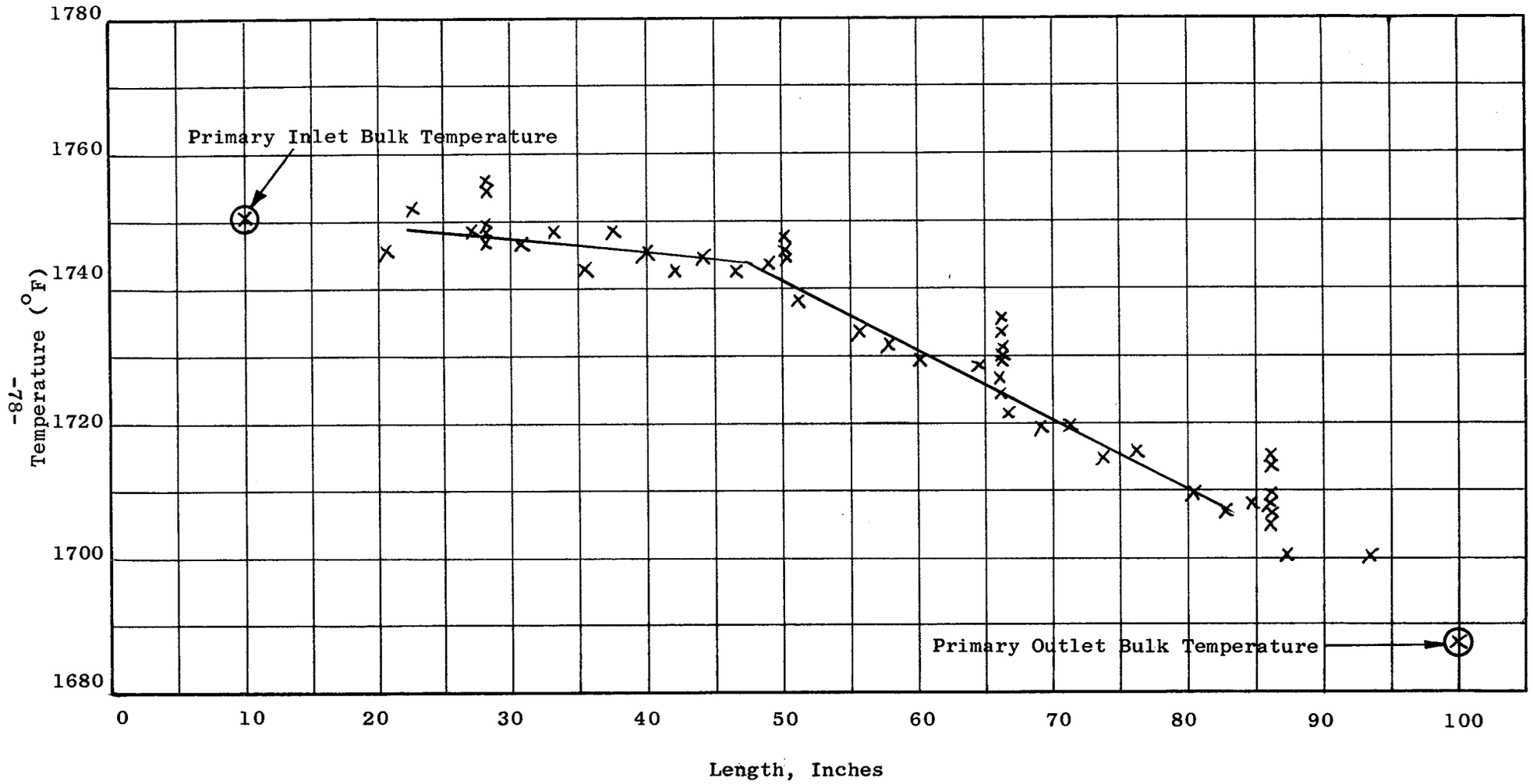

Figure 4. Primary Shell Wall Temperature vs Length - 300 KW System
Film Boiling Run 5/11 2256

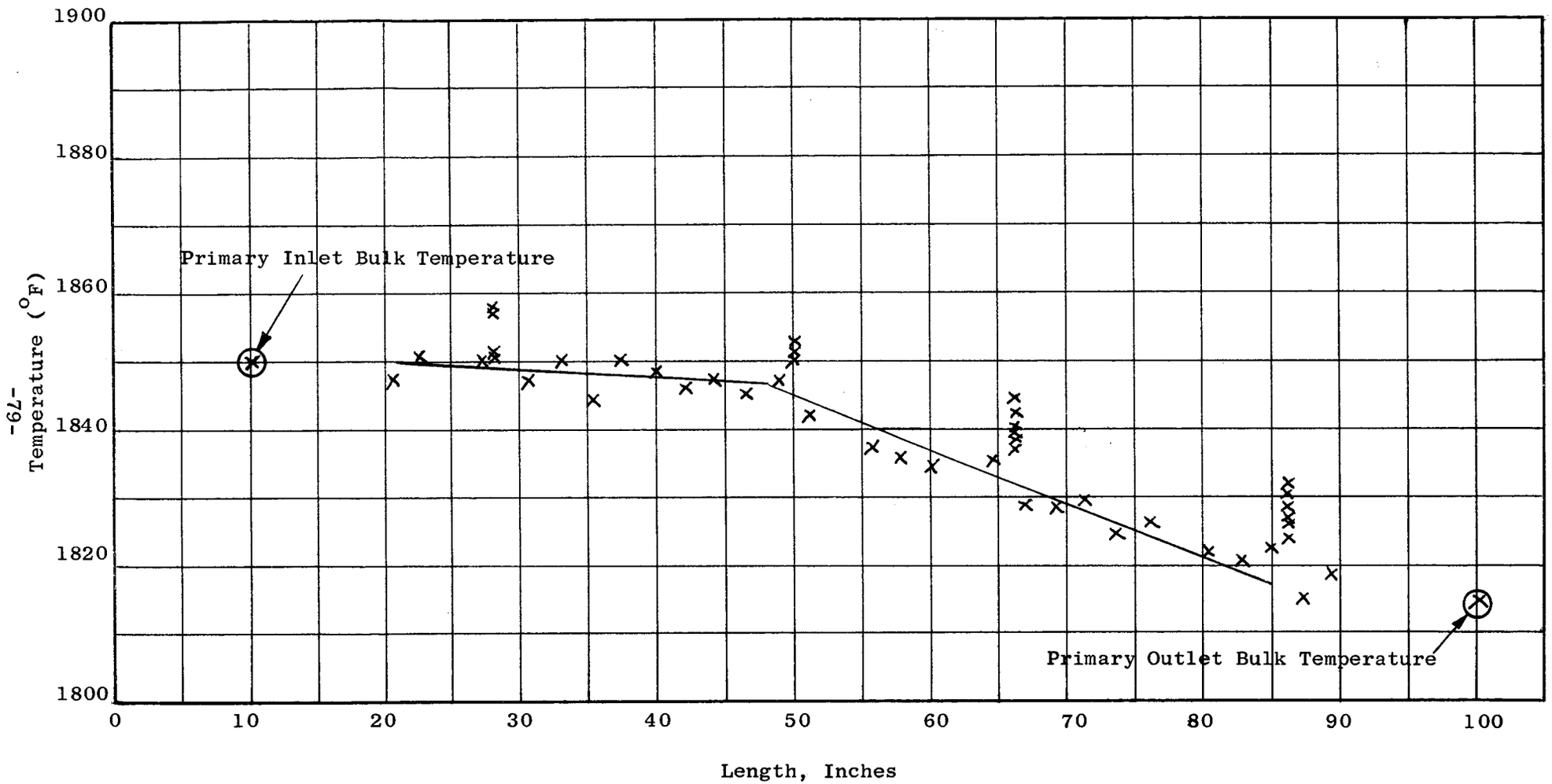

Figure 5. Primary Shell Wall Temperature vs Length - 300 KW System
Film Boiling Run 5/22 0250

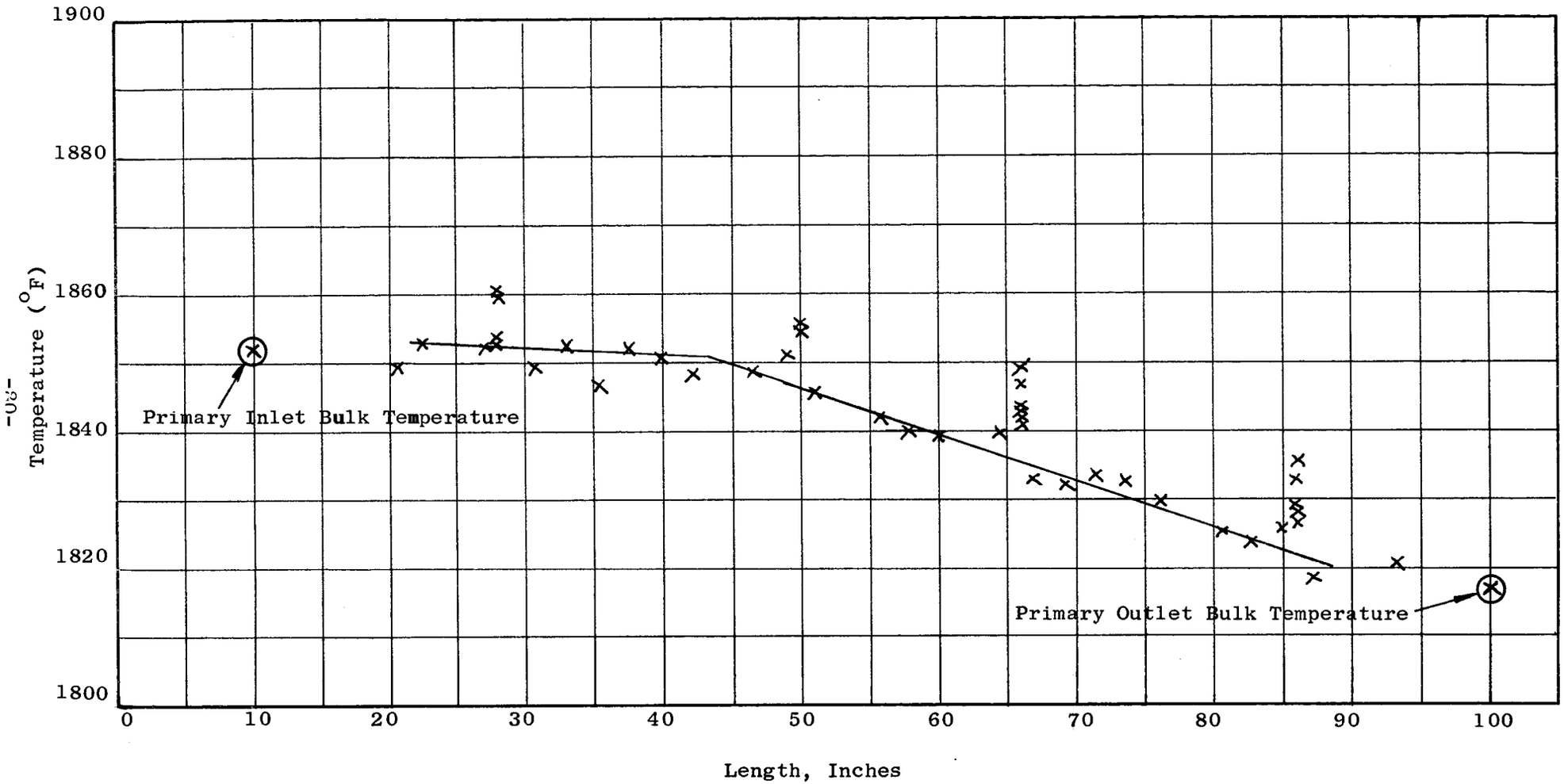

Figure 6. Primary Shell Wall Temperature vs Length - 300 KW System
Film Boiling Run 5/22 0310

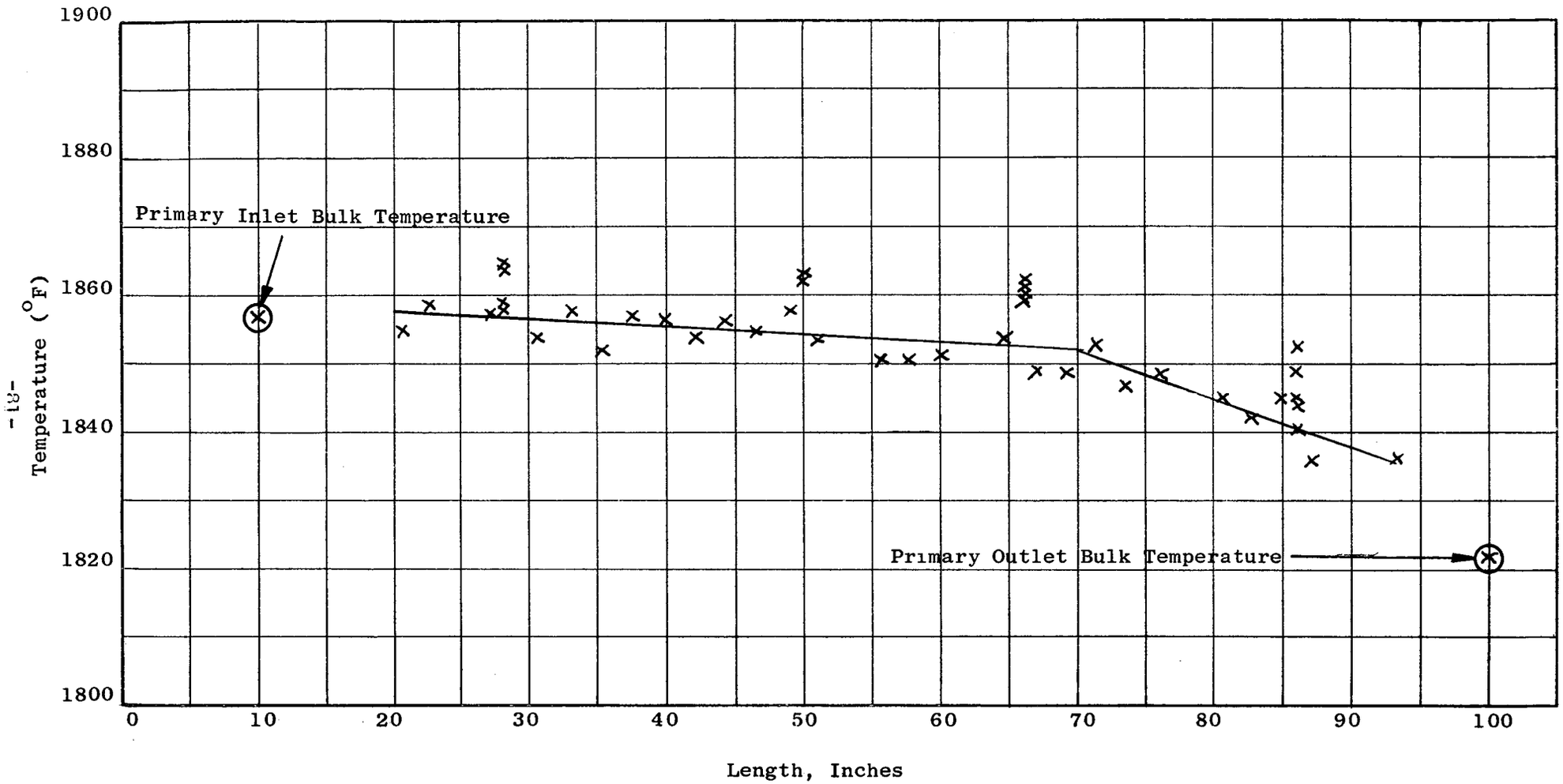

Figure 7. Primary Shell Wall Temperature vs Length - 300 KW System
Film Boiling Run 5/22 0330

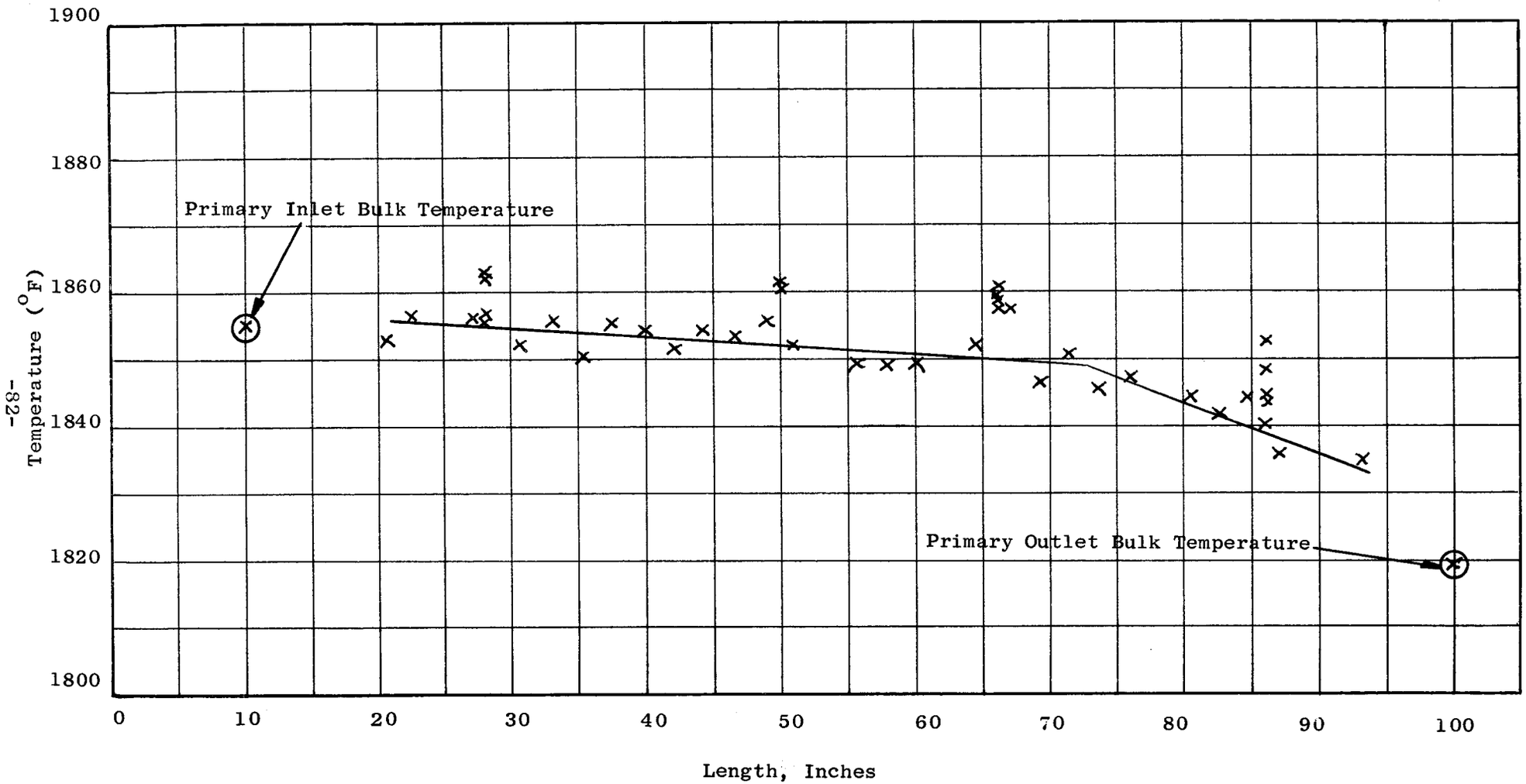

Figure 8. Primary Shell Wall Temperature vs Length - 300 KW System
Film Boiling Run 5/22 0348

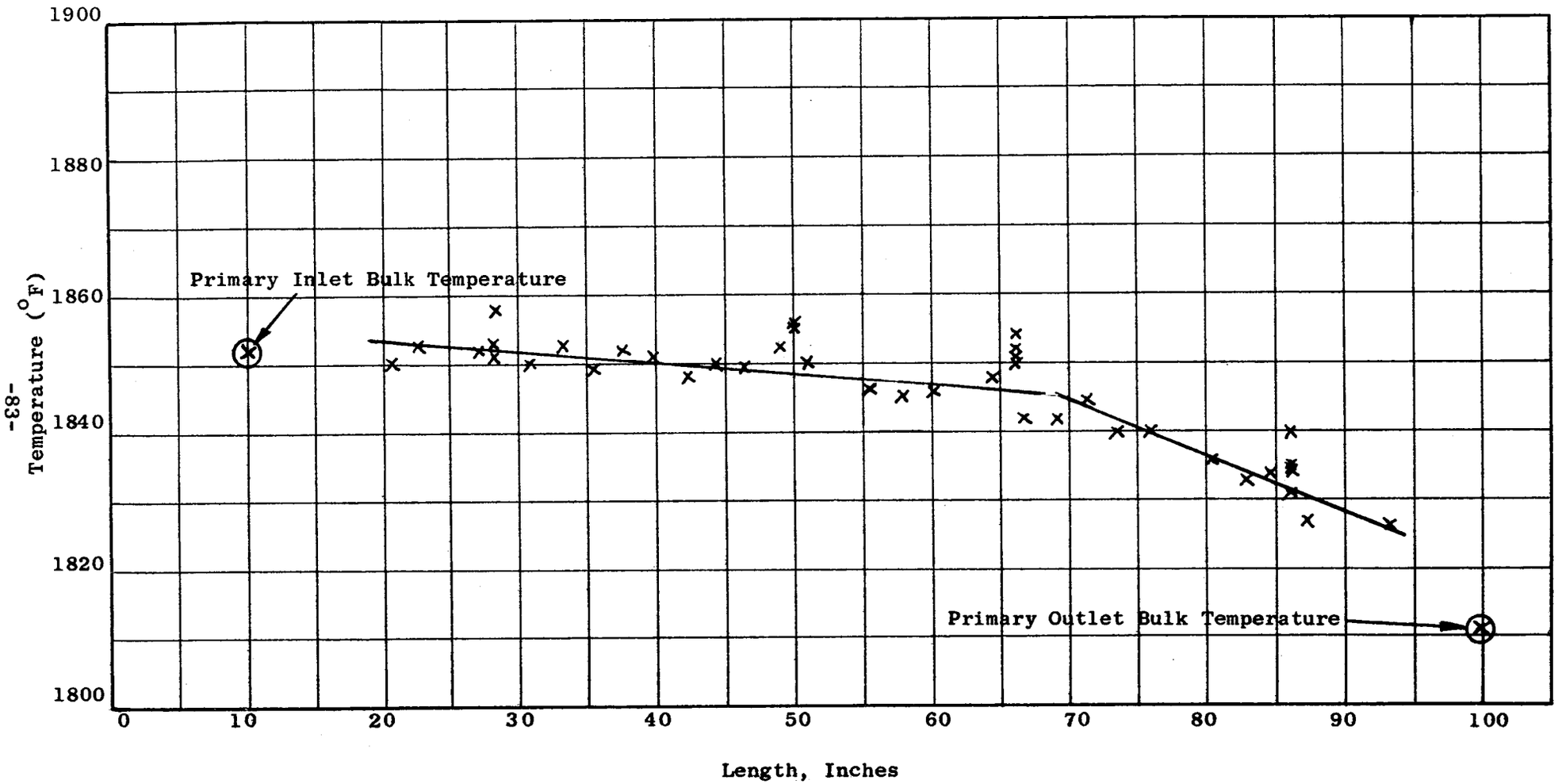

Figure 9. Primary Shell Wall Temperature vs Length - 300 KW System
Film Boiling Run 5/23 0018

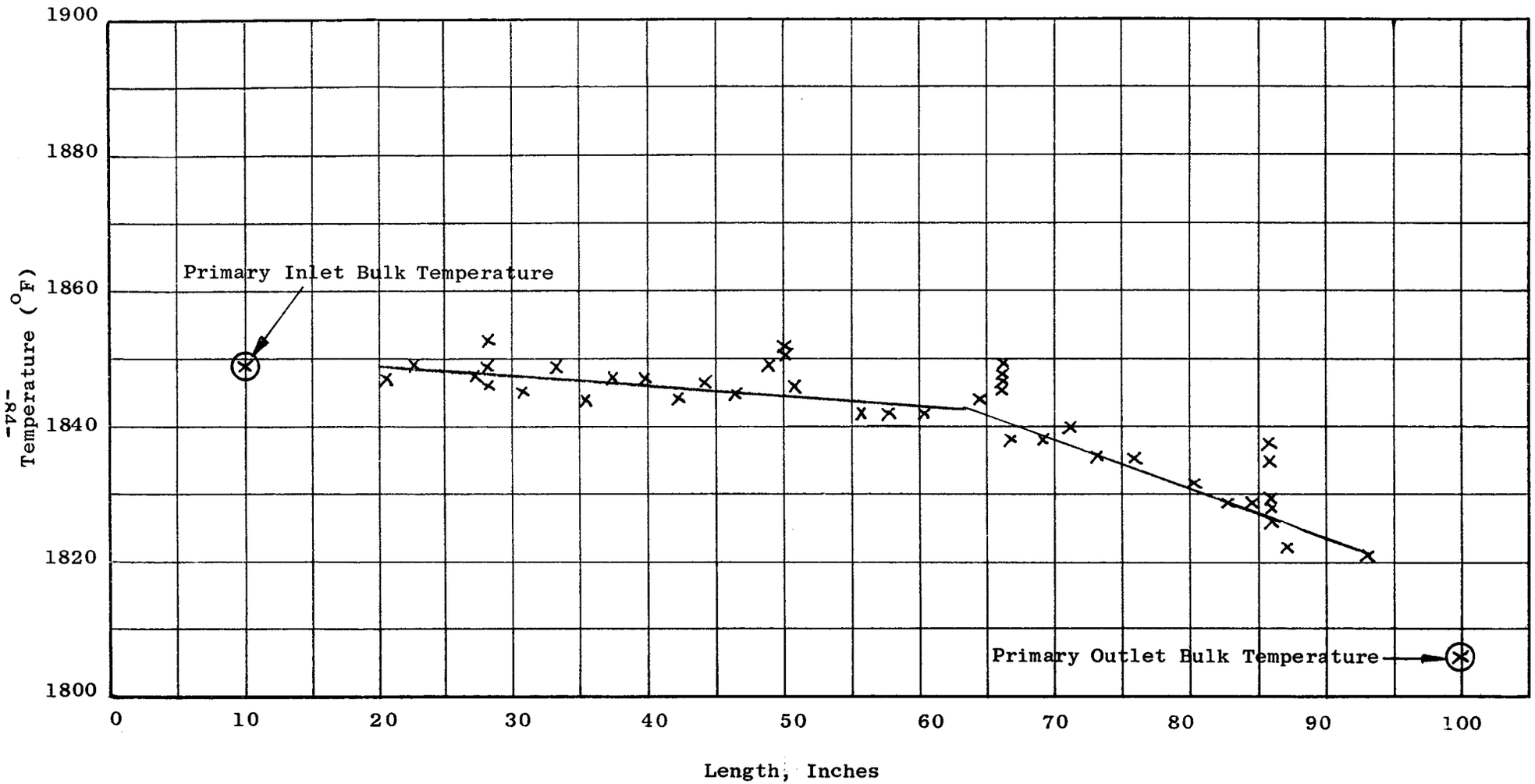

Figure 10. Primary Shell Wall Temperature vs Length - 300 KW System
Film Boiling Run 5/23 0051

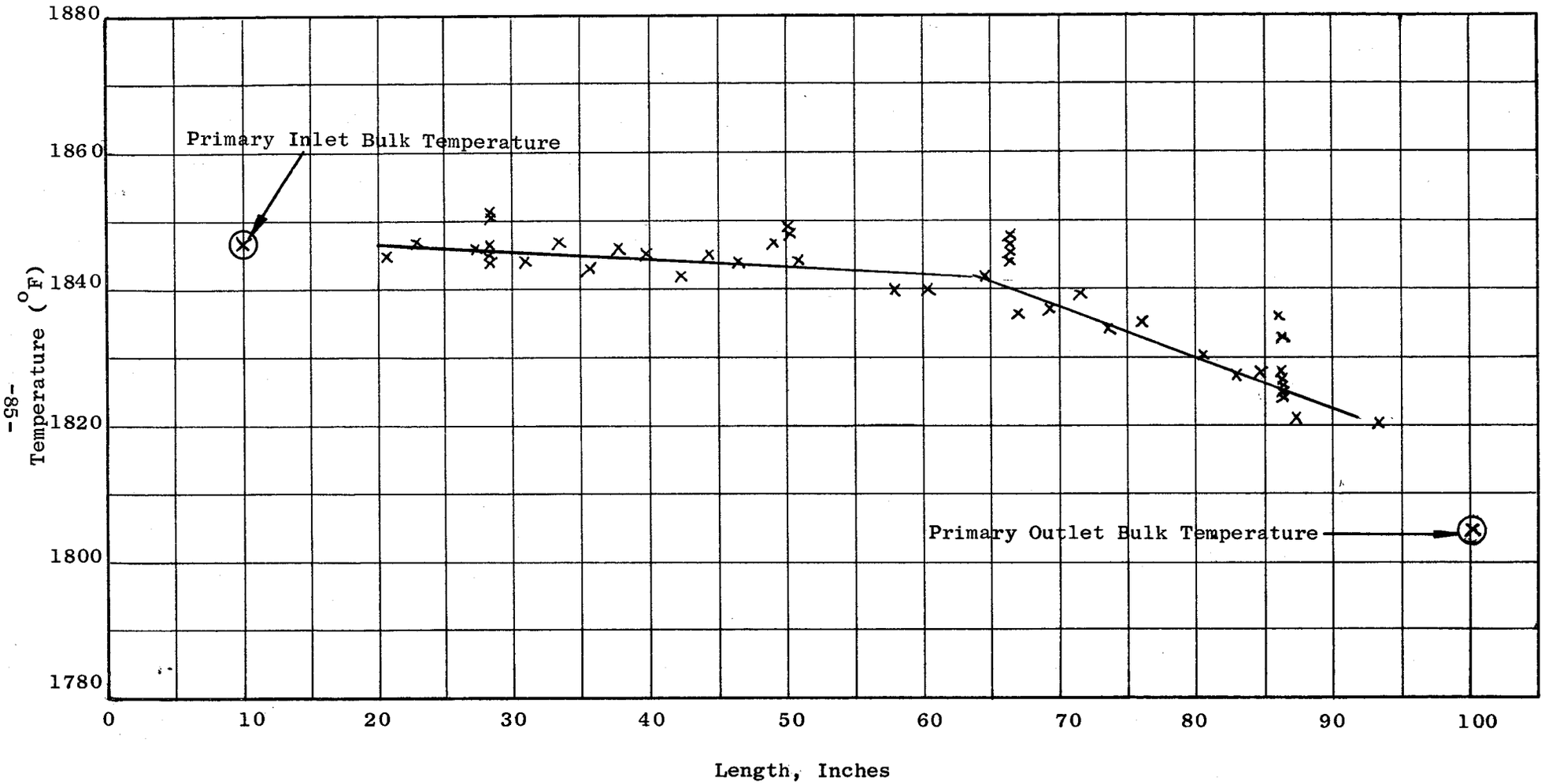

Figure 11. Primary Shell Wall Temperature vs Length - 300 KW System
Film Boiling Run 5/23 0118

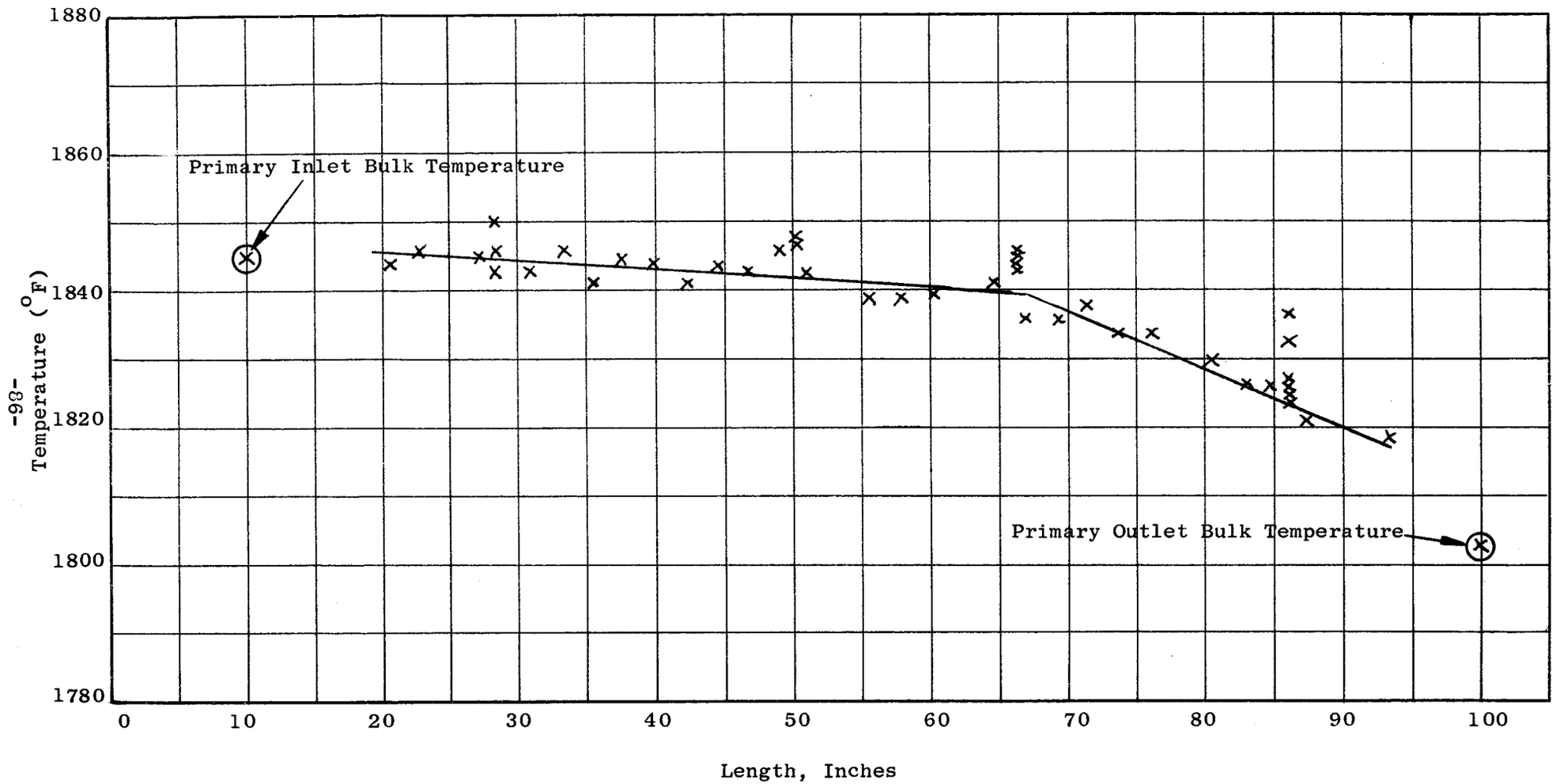

Figure 12. Primary Shell Wall Temperature vs Length - 300 KW System
Film Boiling Run 5/23 0144

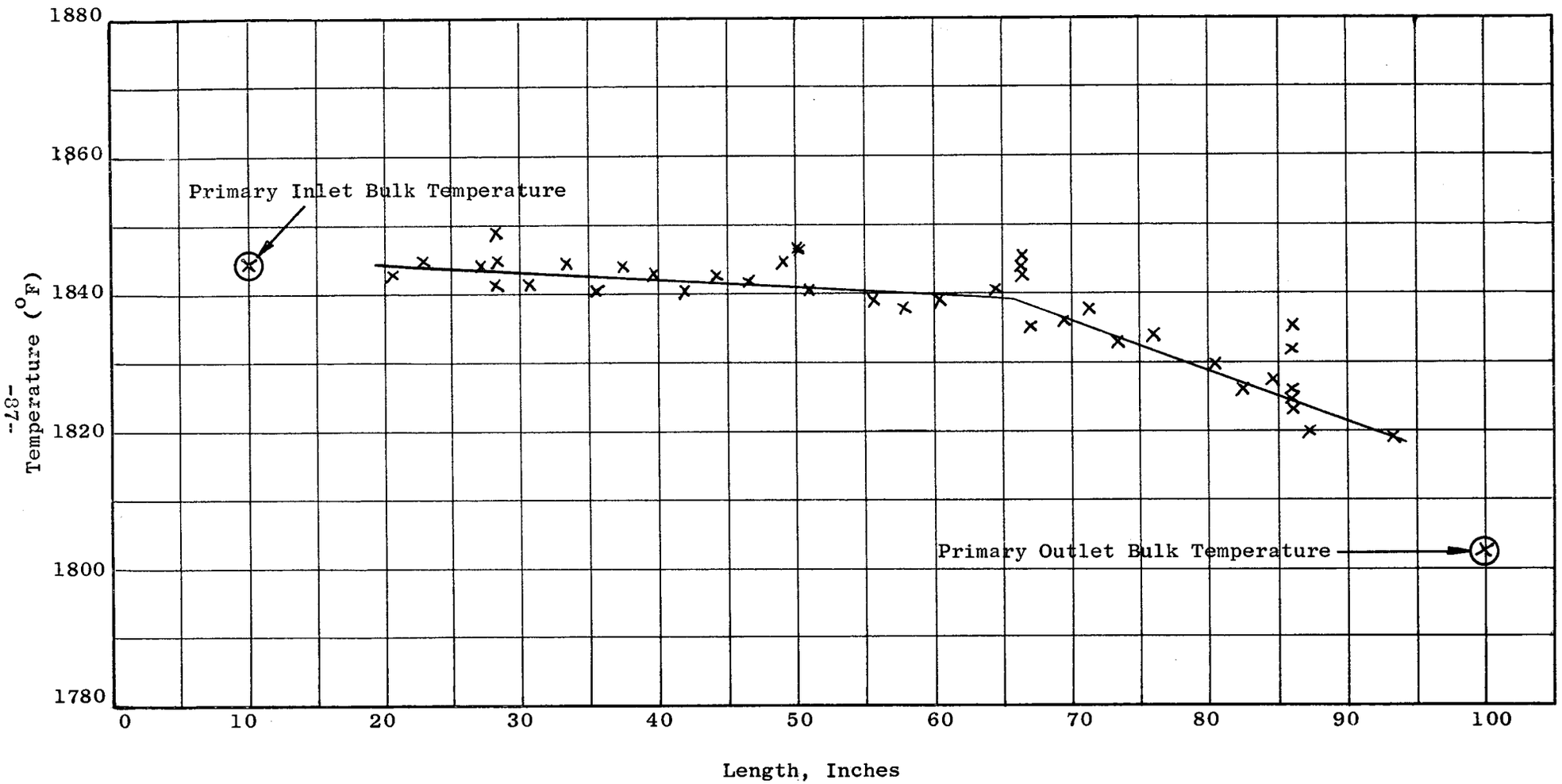

Figure 13. Primary Shell Wall Temperature vs Length - 300 KW System
Film Boiling Run 5/23 0214

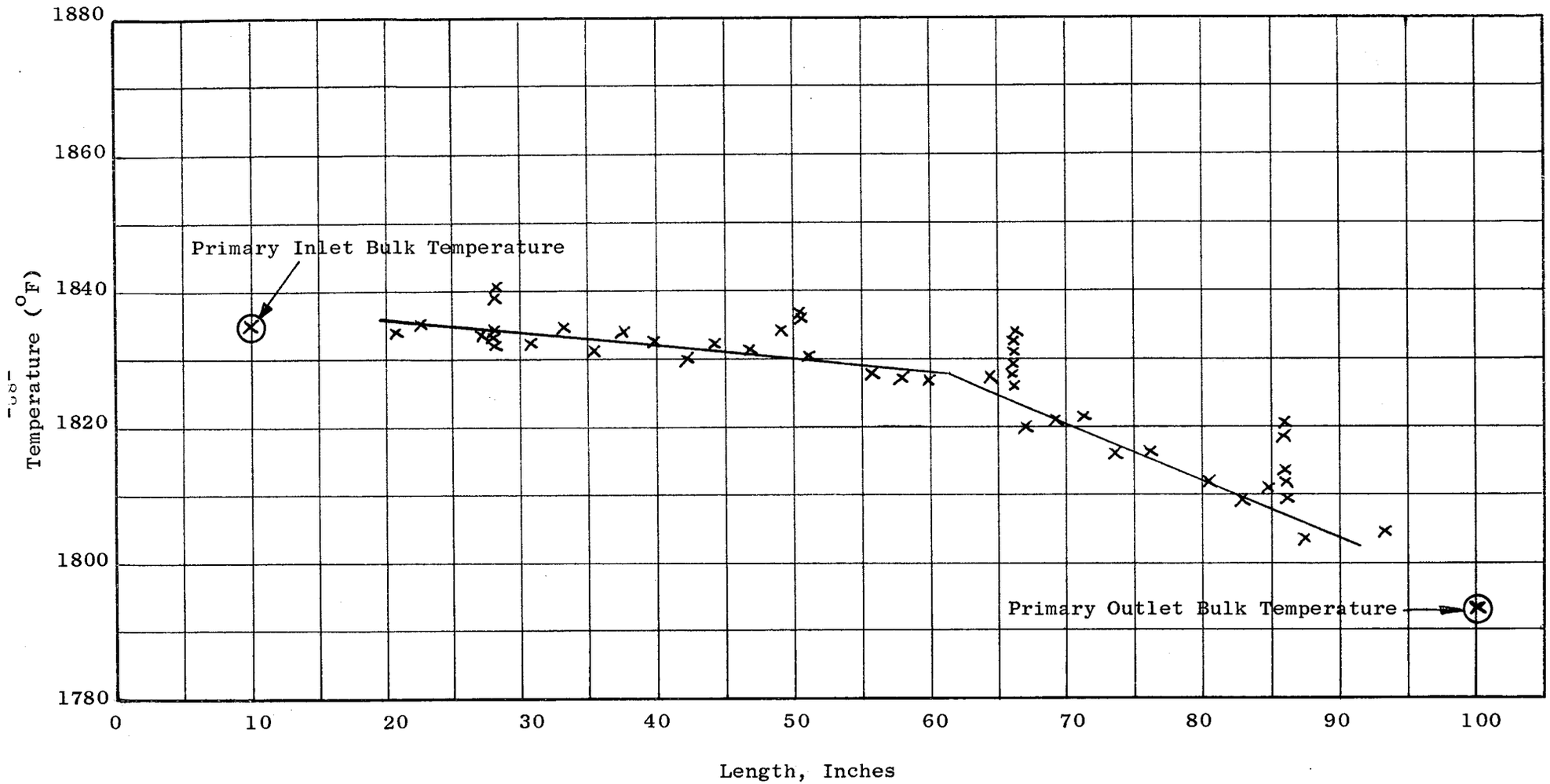

Figure 14. Primary Shell Wall Temperature vs Length - 300 KW System
Film Boiling Run 5/23 2205

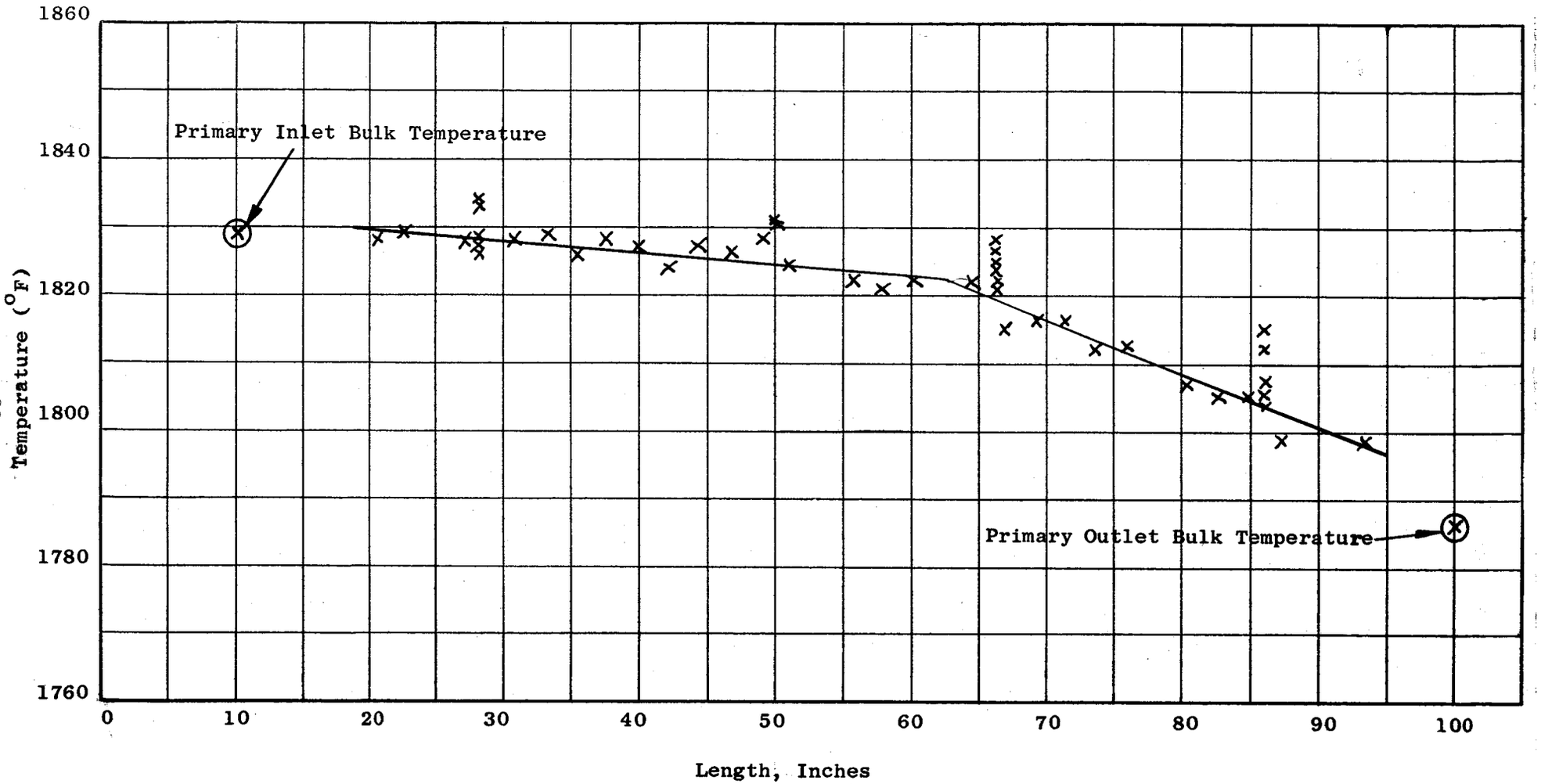

Figure 15. Primary Shell Wall Temperature vs Length - 300 KW System
Film Boiling Run 5/23 2221

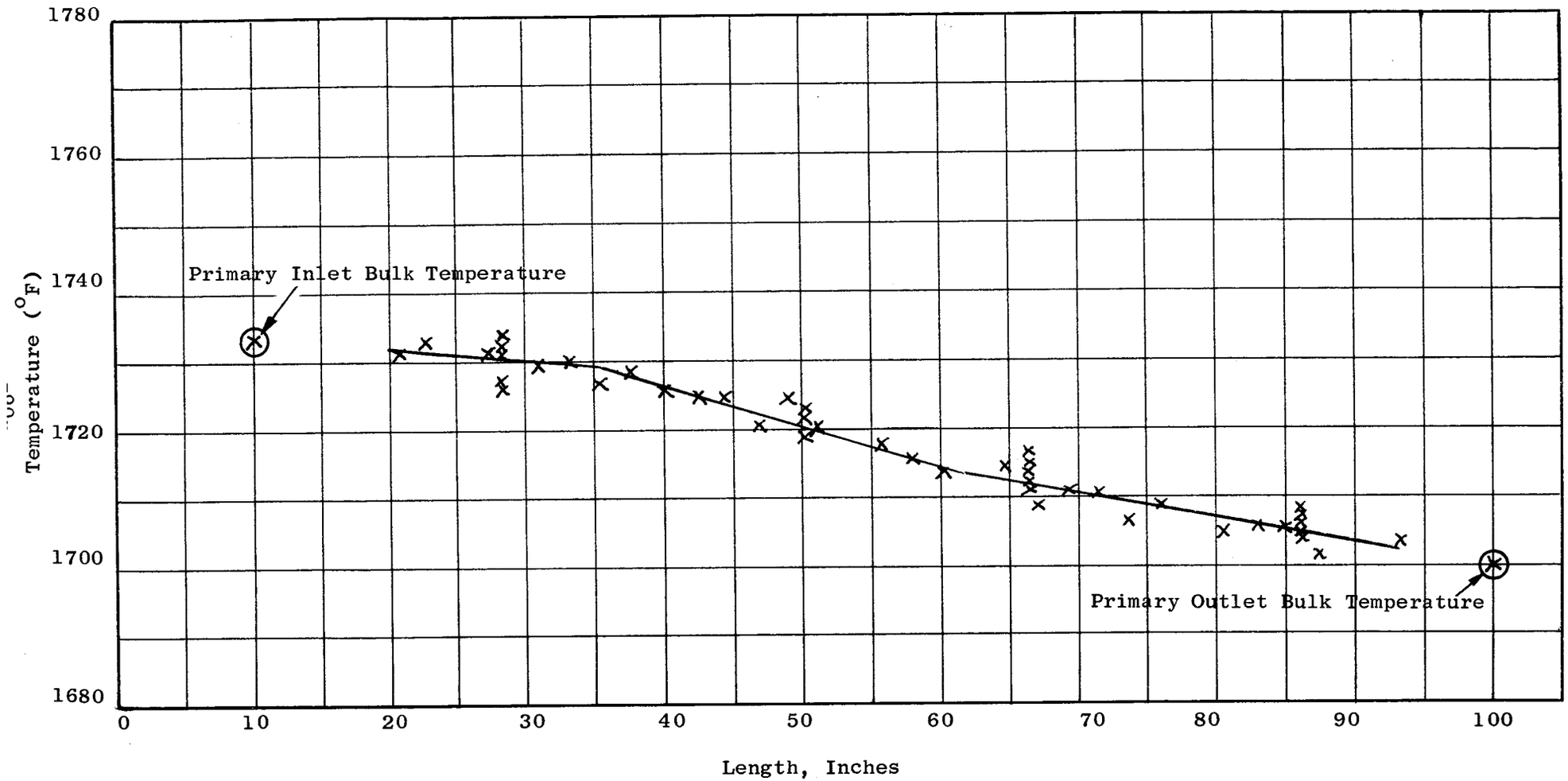

Figure 16. Primary Shell Wall Temperature vs Length - 300 KW System
Film Boiling Run 5/23 2351

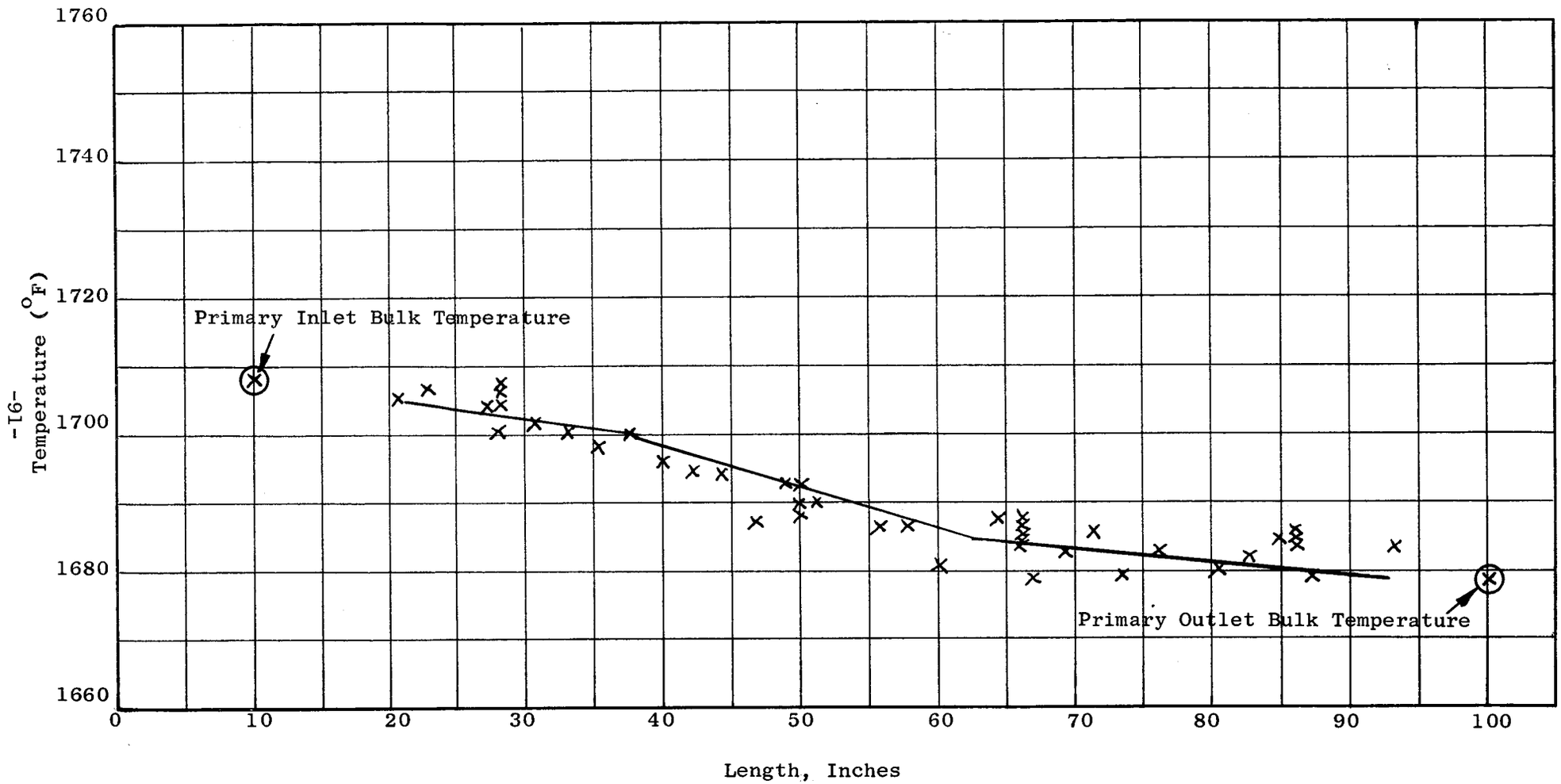

Figure 17. Primary Shell Wall Temperature vs Length - 300 KW System
Film Boiling Run 5/24 0032

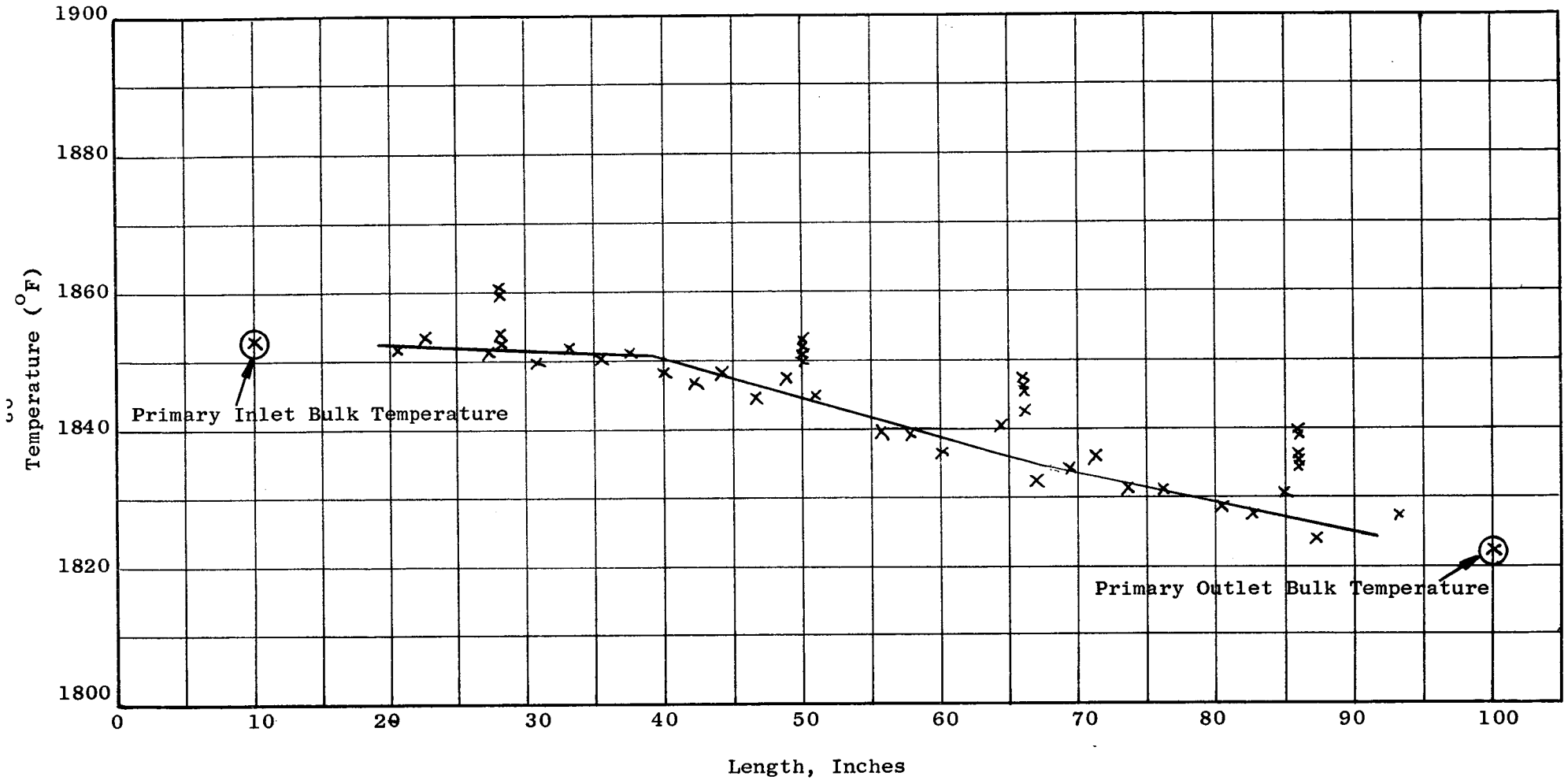

Figure 18. Primary Shell Wall Temperature vs Length - 300 KW System
Film Boiling Run 5/24 1345

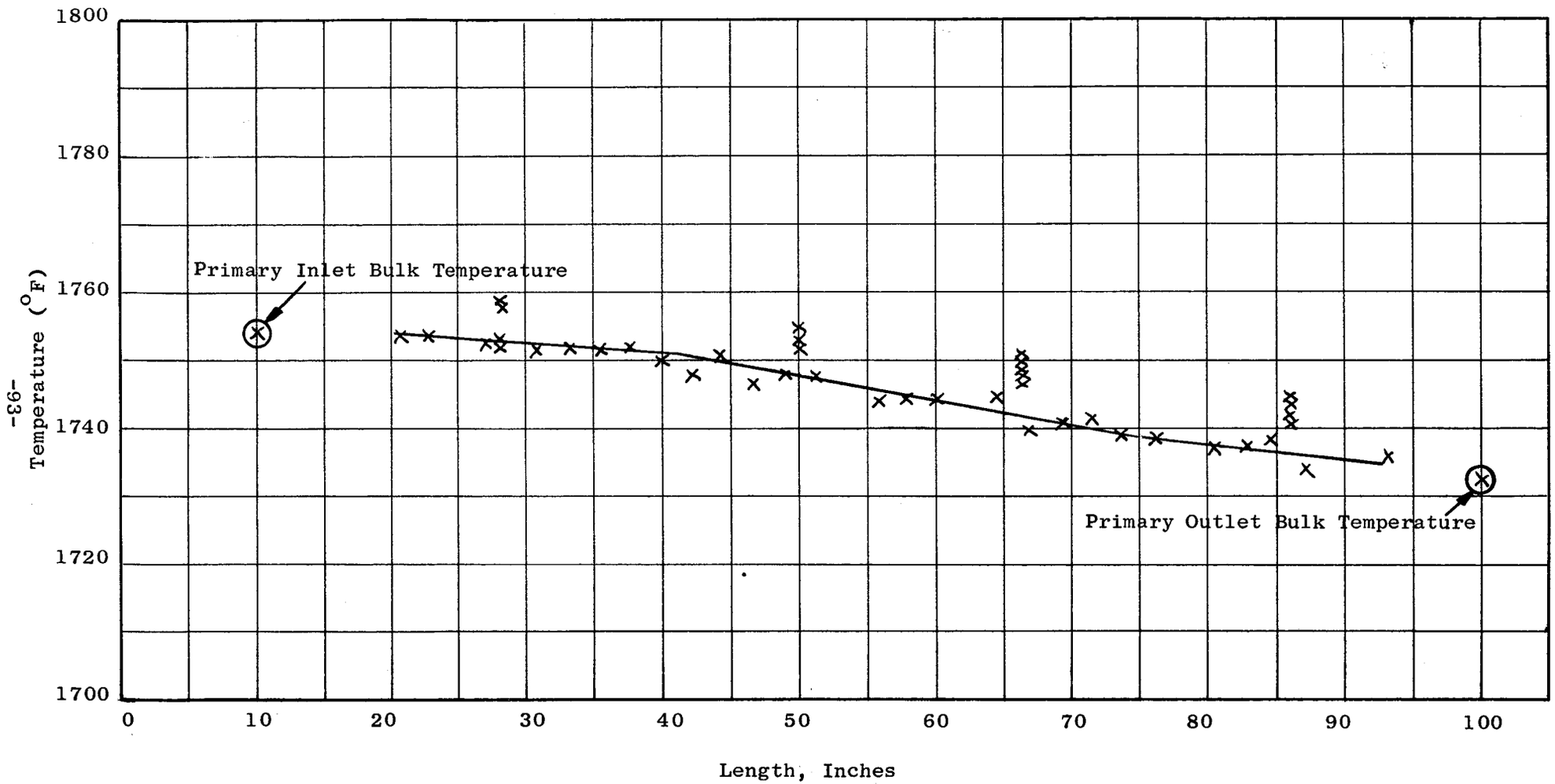

Figure 19. Primary Shell Wall Temperature vs Length - 300 KW System
Film Boiling Run 6/27 0815

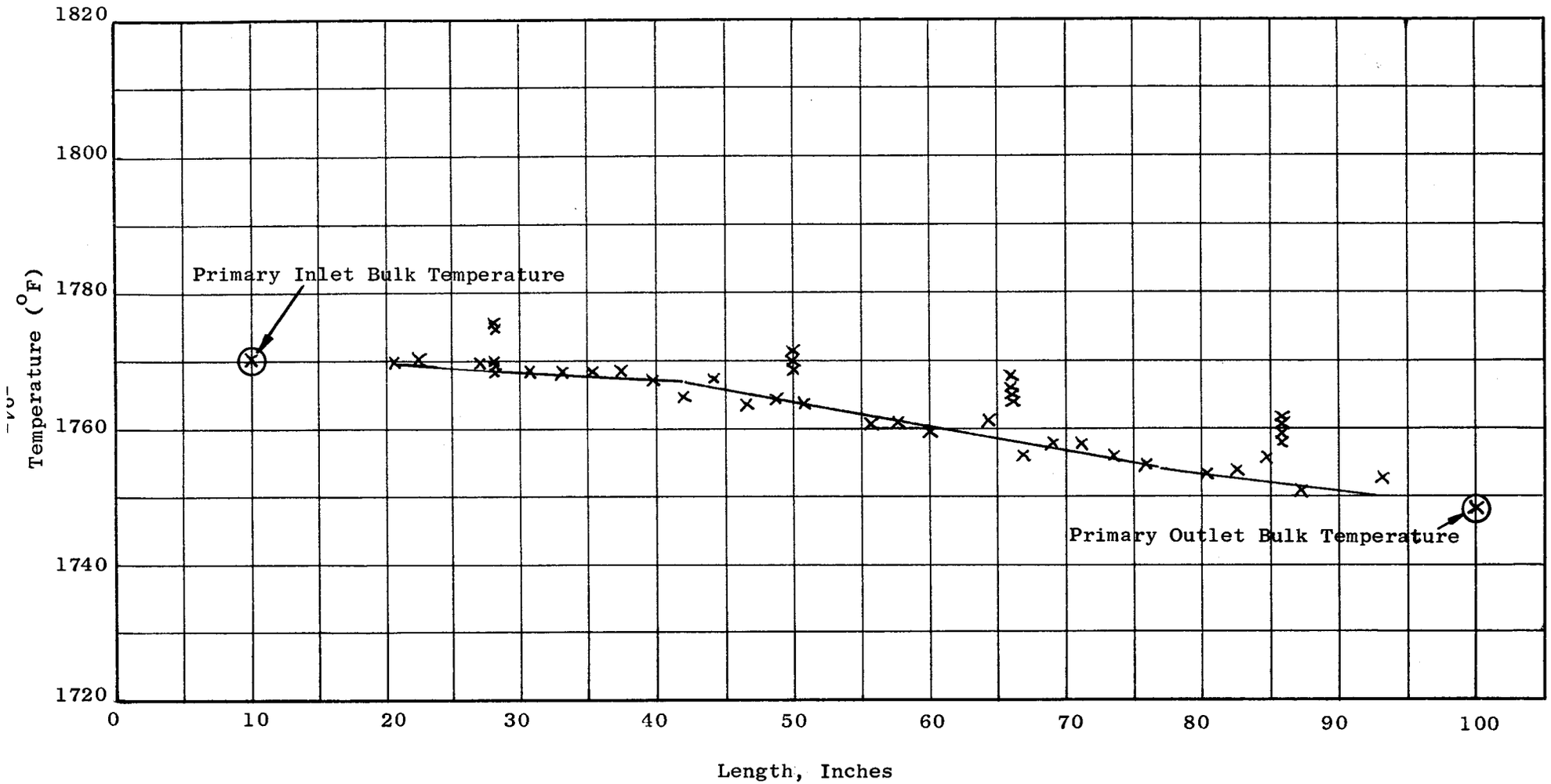

Figure 20. Primary Shell Wall Temperature vs Length - 300 KW System
Film Boiling Run 6/27 0845

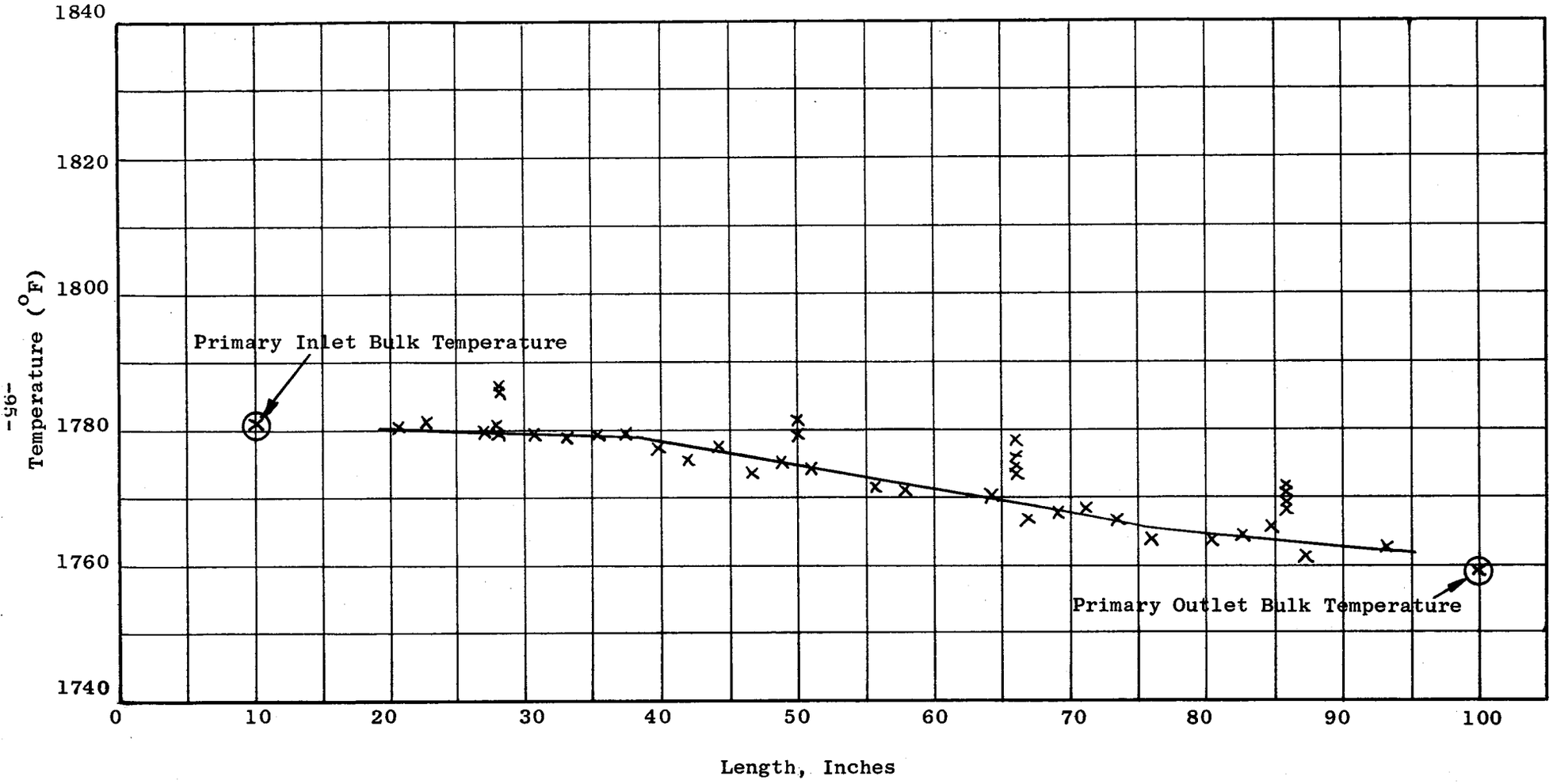

Figure 21. Primary Shell Wall Temperature vs Length - 300 KW System
Film Boiling Run 6/27 0915

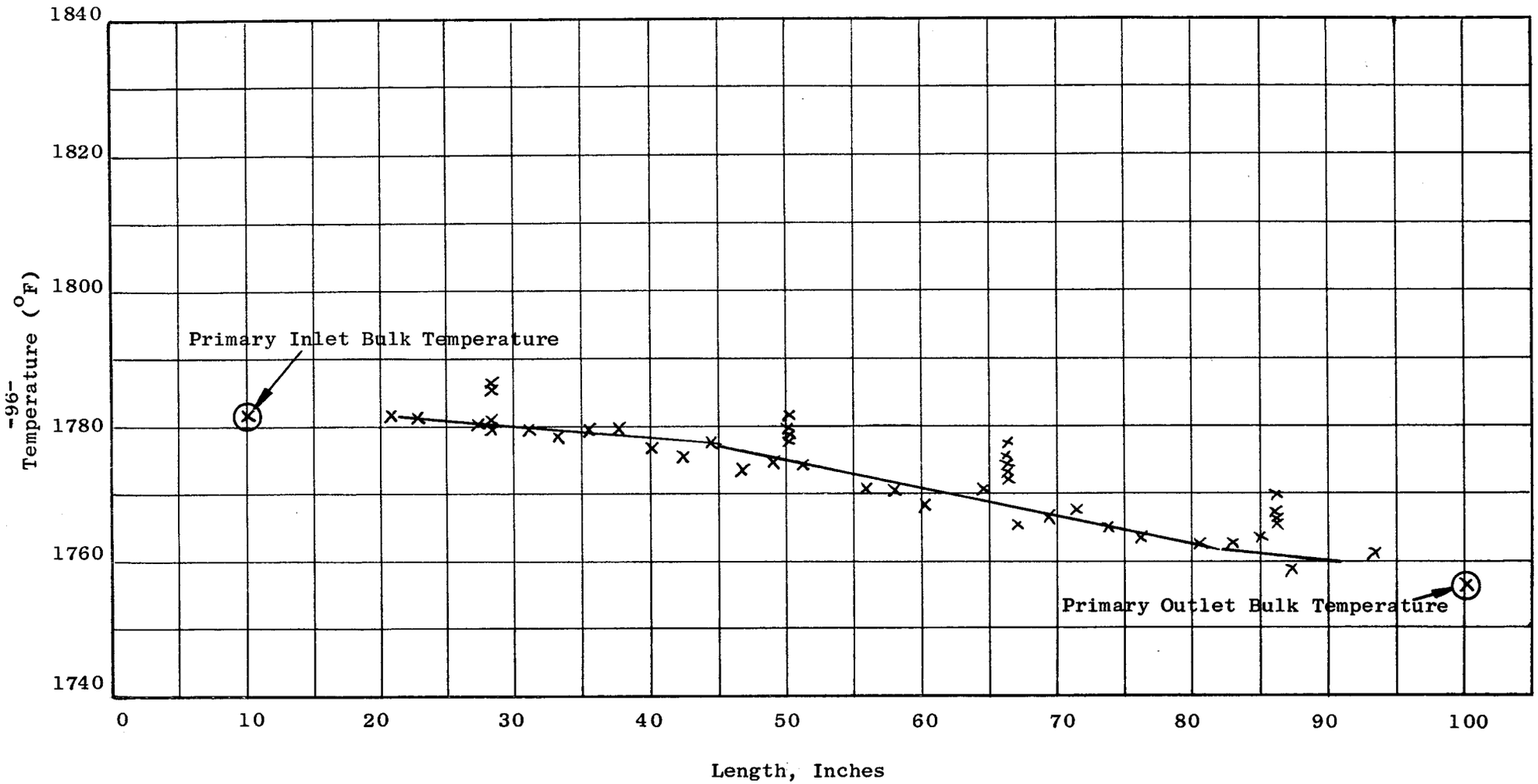

Figure 22. Primary Shell Wall Temperature vs Length - 300 KW System
Film Boiling Run 6/27 0945

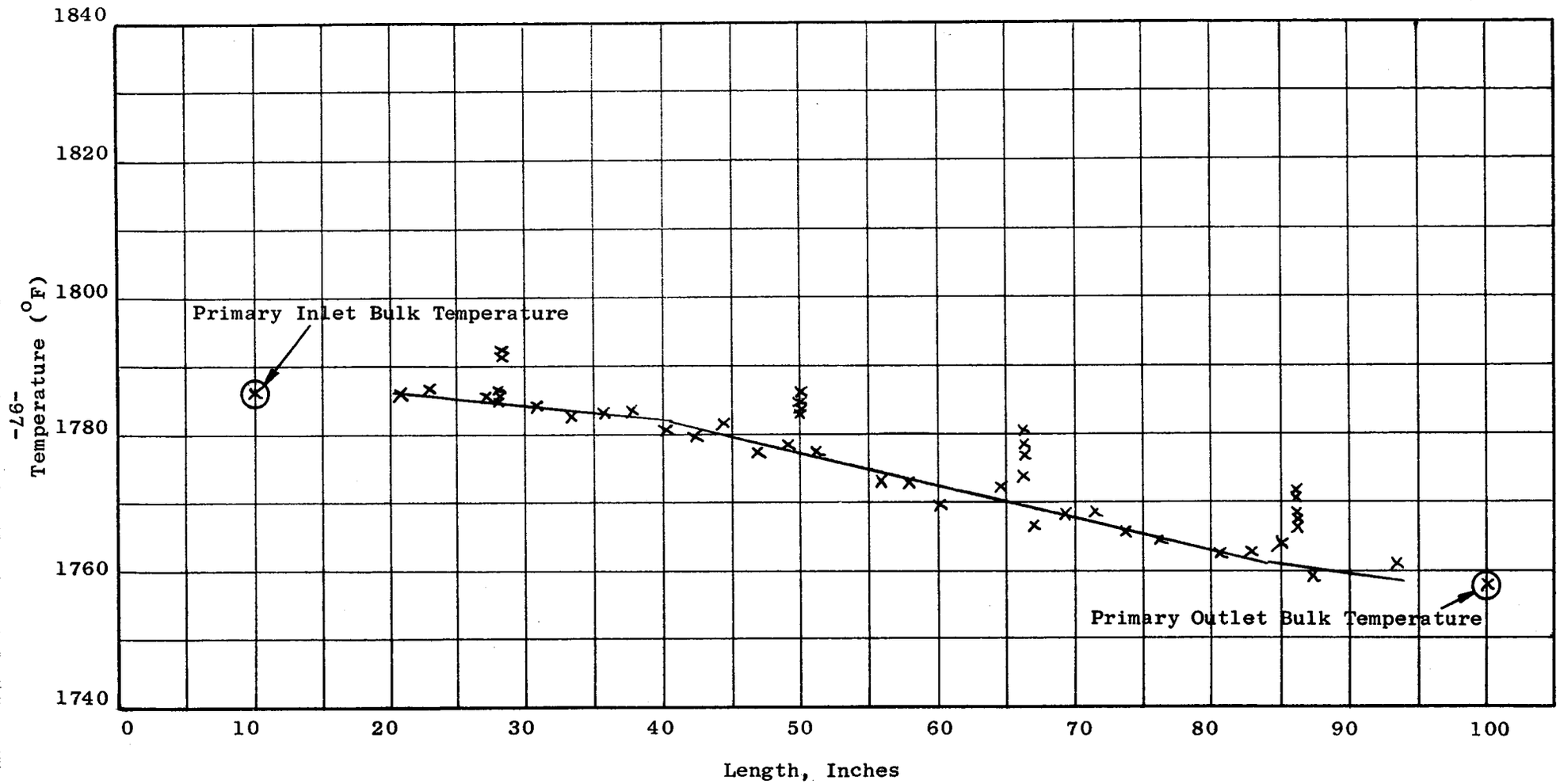

Figure 23. Primary Shell Wall Temperature vs Length - 300 KW System
Film Boiling Run 6/27 1030

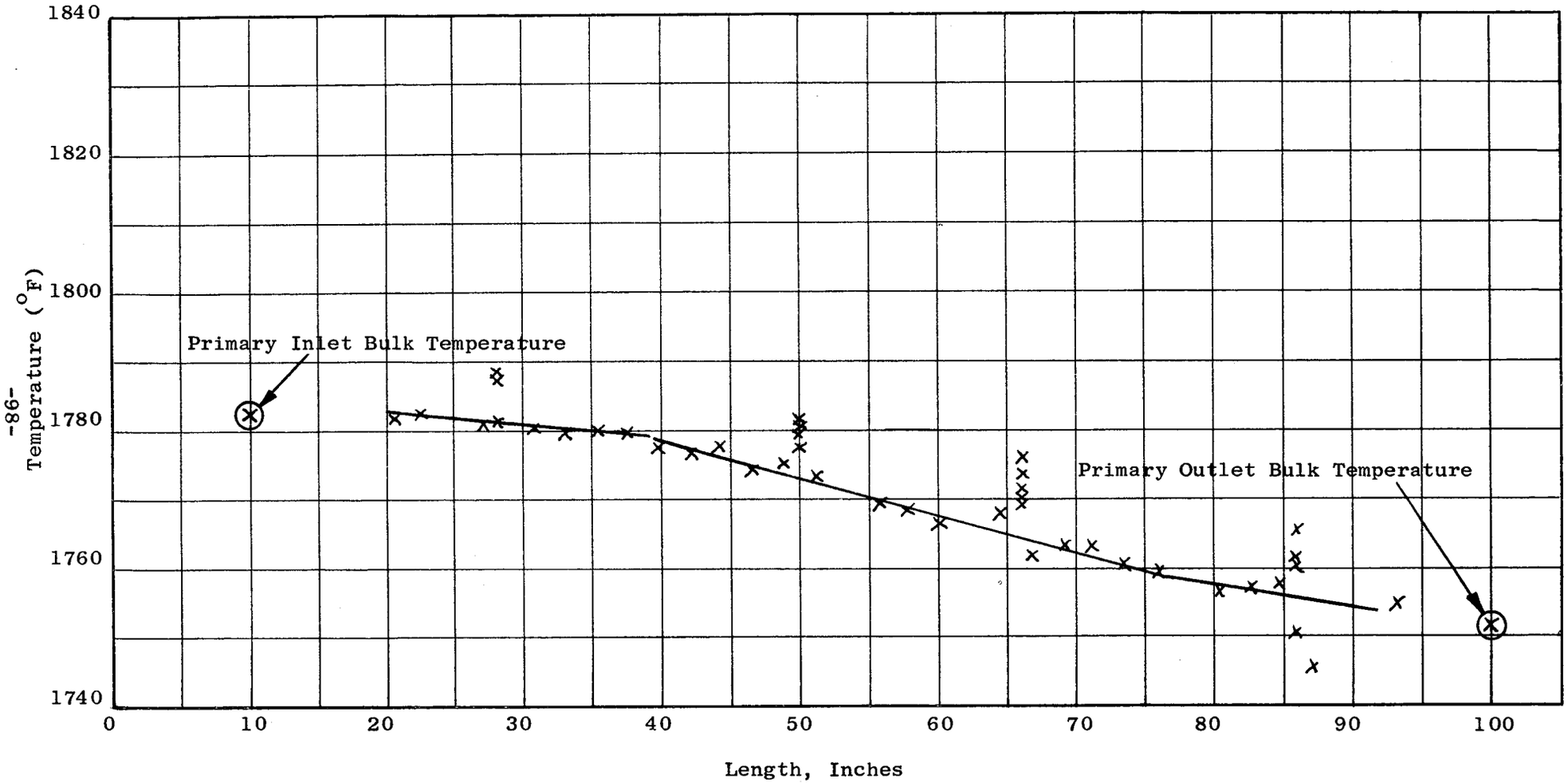

Figure 24. Primary Shell Wall Temperature vs Length - 300 KW System
Film Boiling Run 6/27 1100

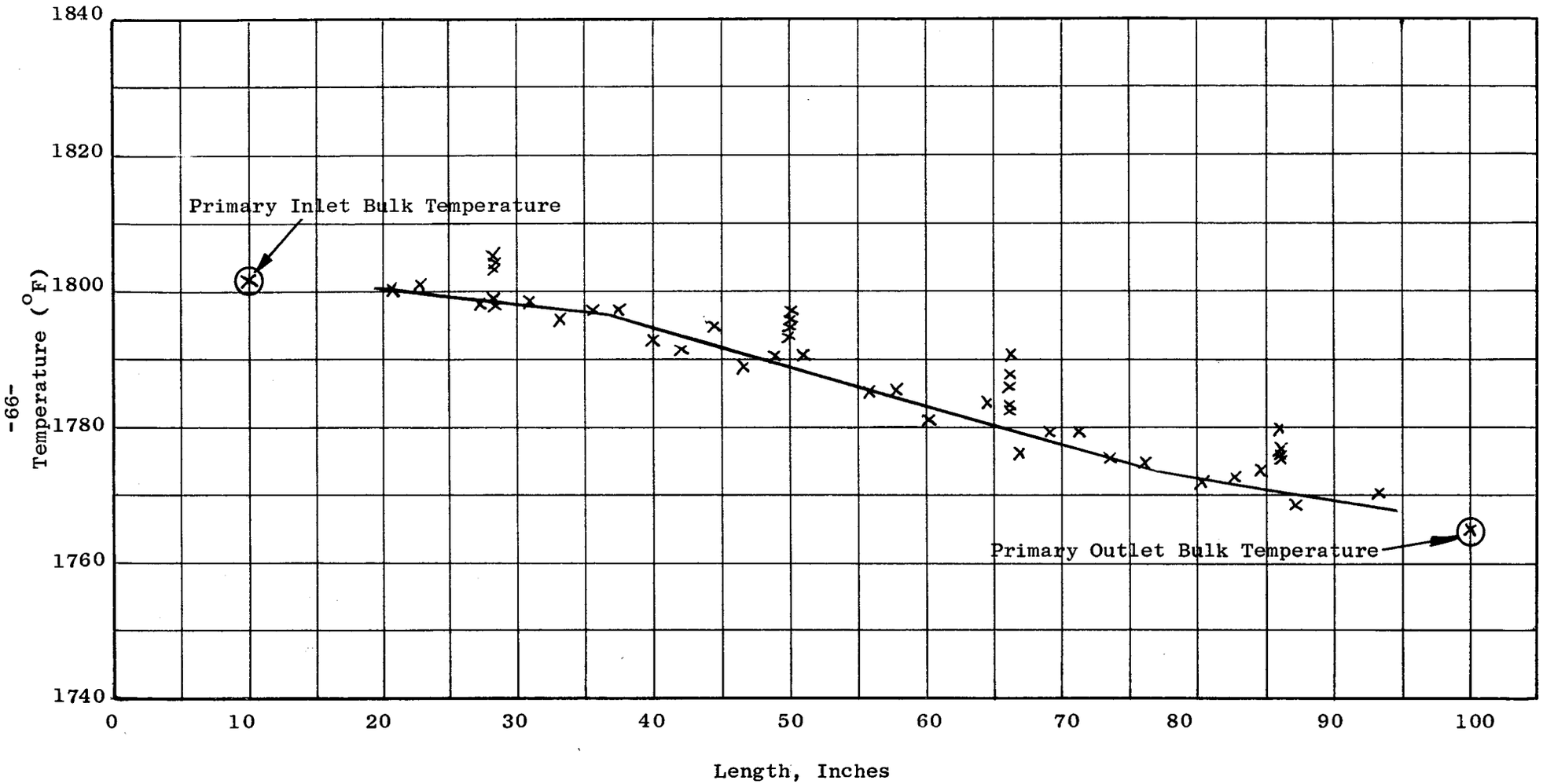

Figure 25. Primary Shell Wall Temperature vs Length - 300 KW System
Film Boiling Run 6/28 0202

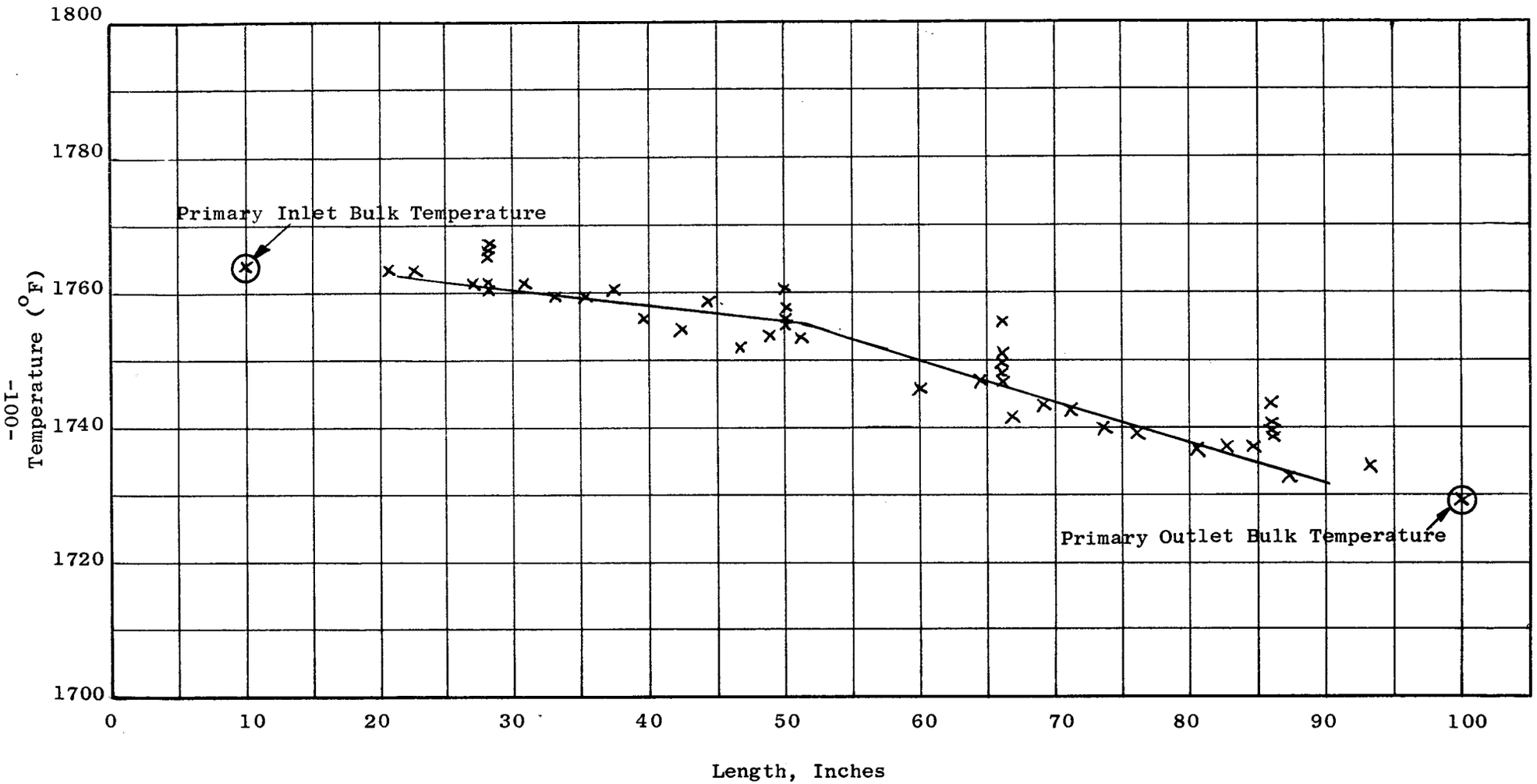

Figure 26. Primary Shell Wall Temperature vs Length - 300 KW System
Film Boiling Run 6/28 0300

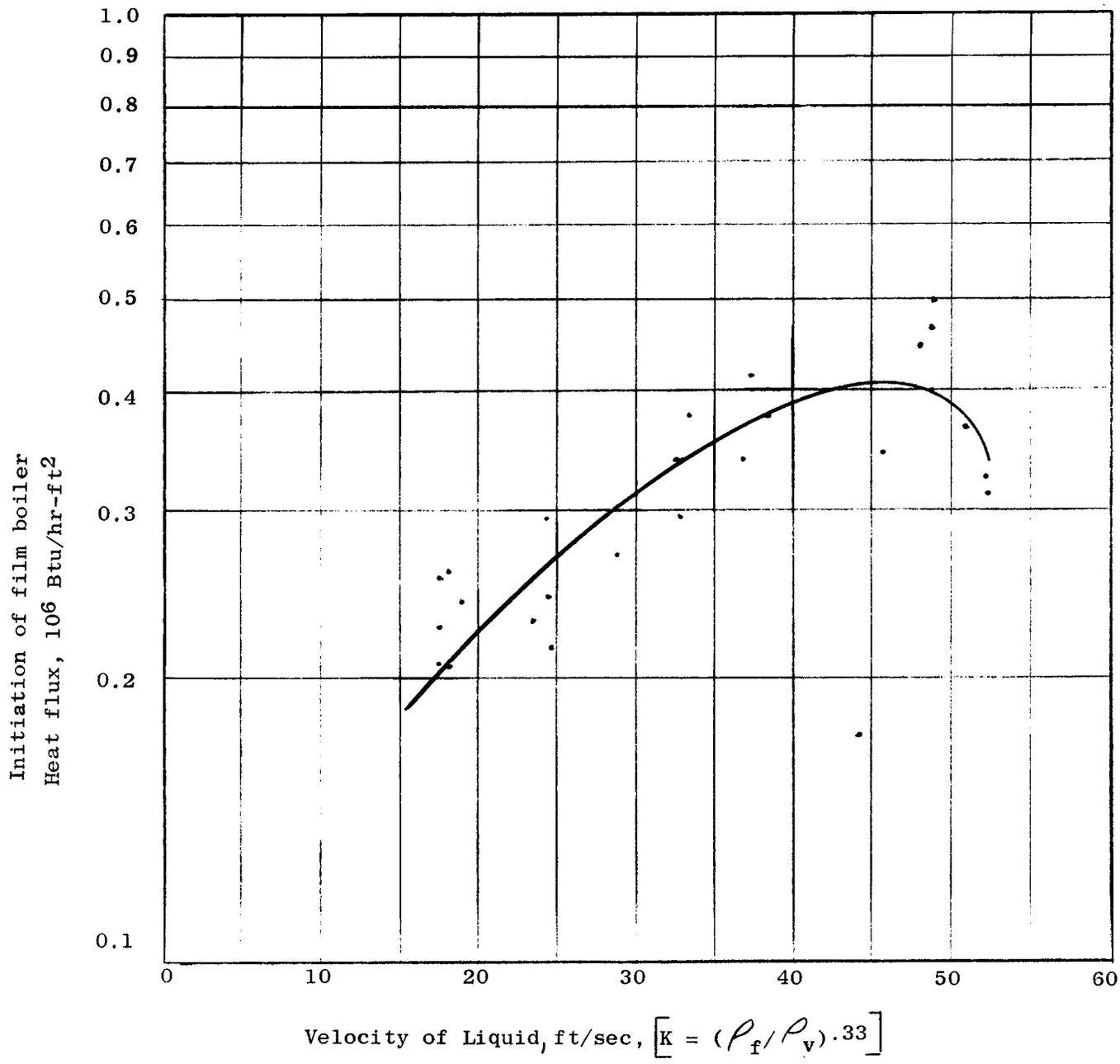

Figure 27. Film Boiling Heat Flux vs Liquid Velocity - 300 KW System.

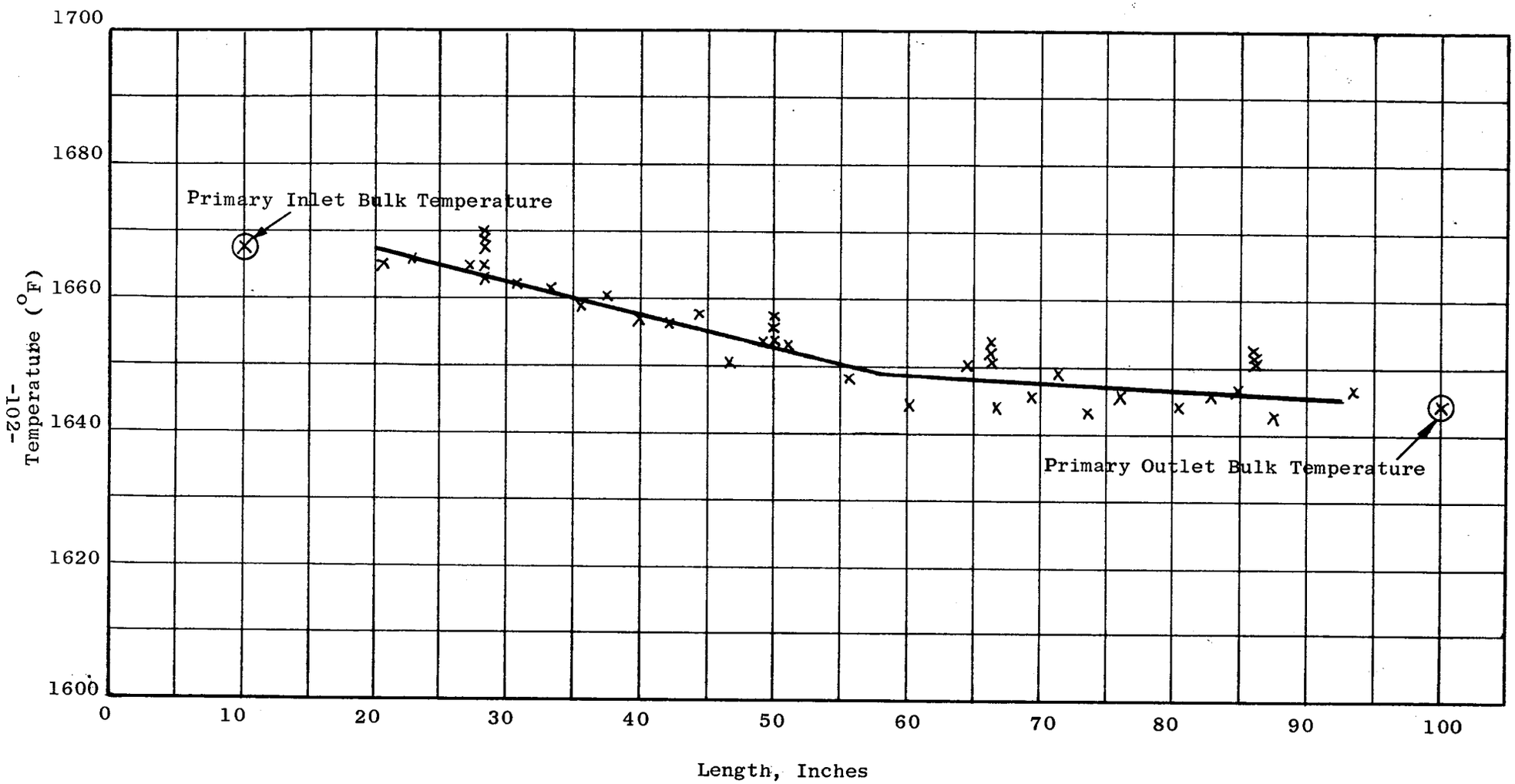

Figure 28. Primary Shell Wall Temperature vs Length - 300 KW System
Film Boiling Run 5/23 1000

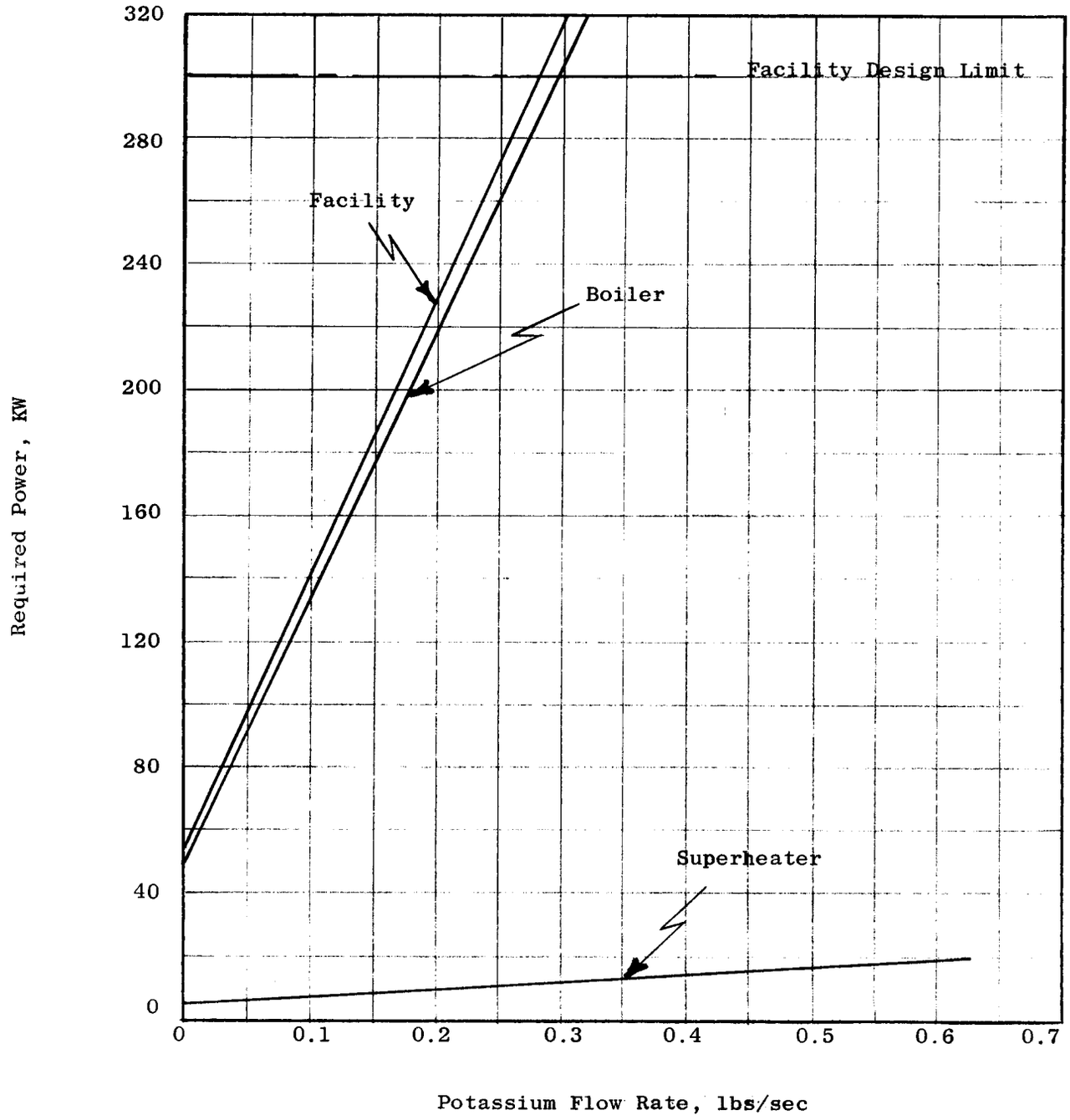

Figure 29. Required Power Vs. Potassium Flow Rate for Superheat of 50°F - 300 KW System

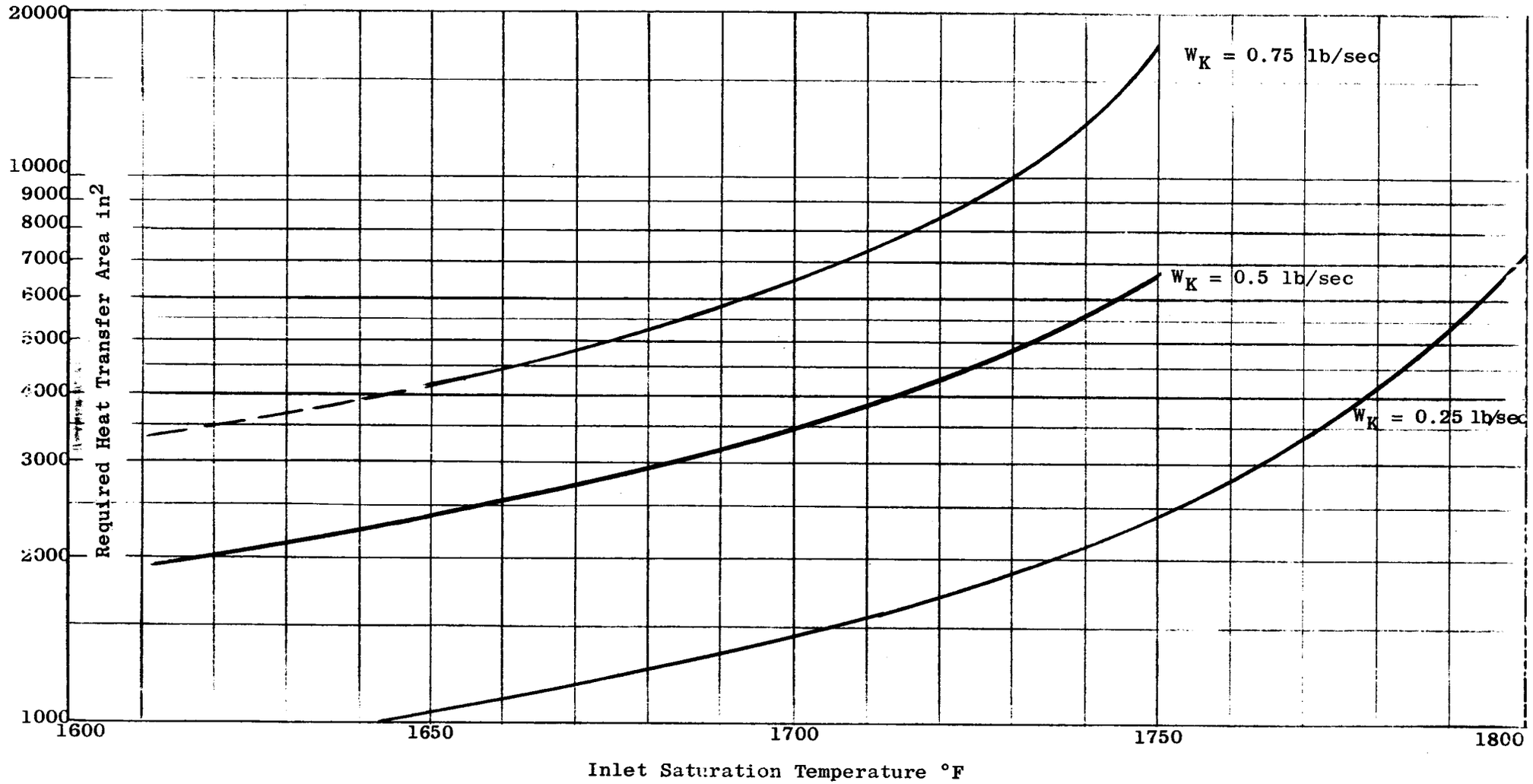

Figure 30. Required Heat Transfer Area Vs. Potassium Inlet Saturation Temperature and Flow Rate For 100% Quality at Boiler Exit - 300 KW System

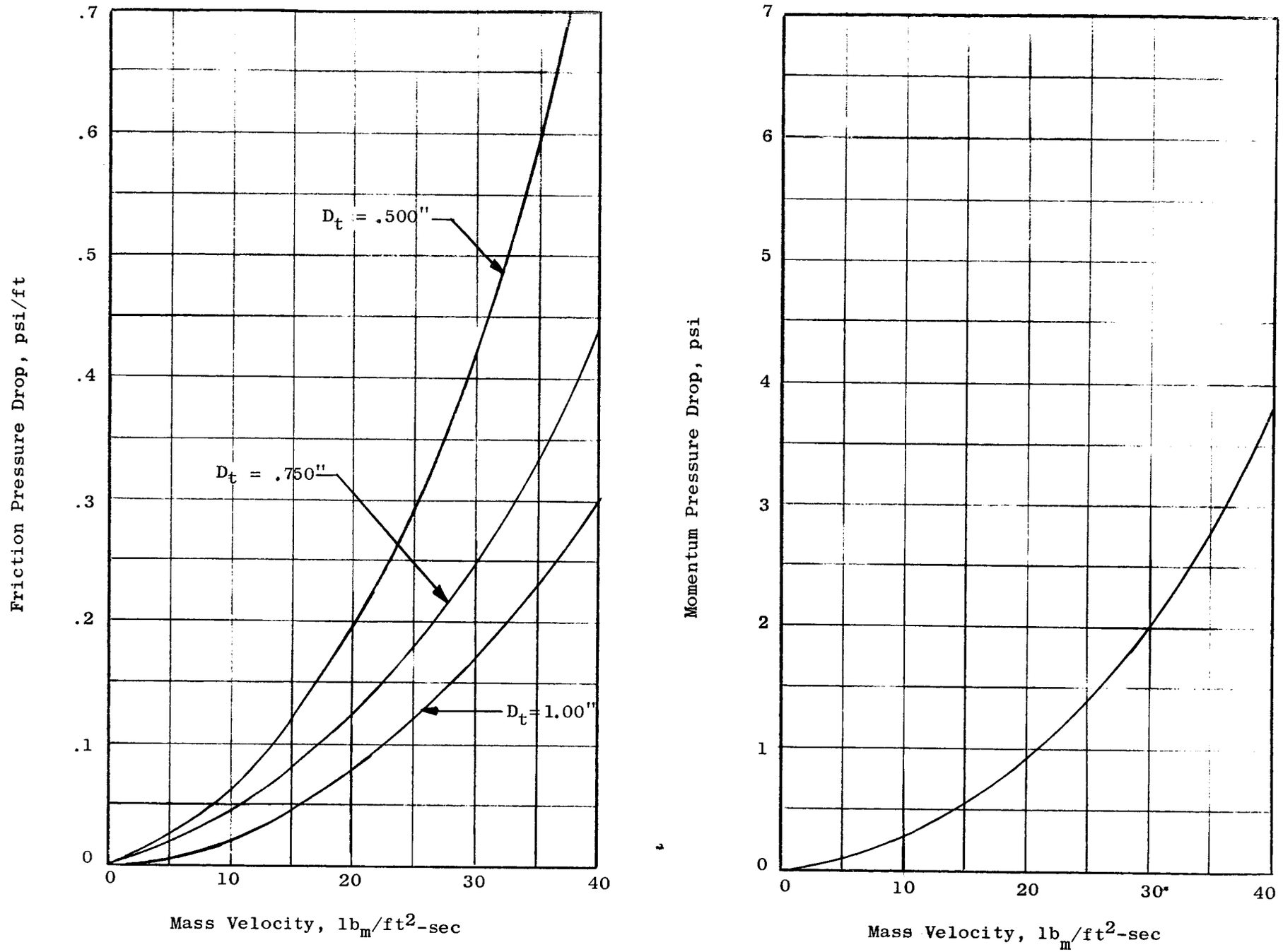

Figure 31. Two-Phase Friction and Momentum Pressure Drop Vs. Mass Velocity and Tube Diameter

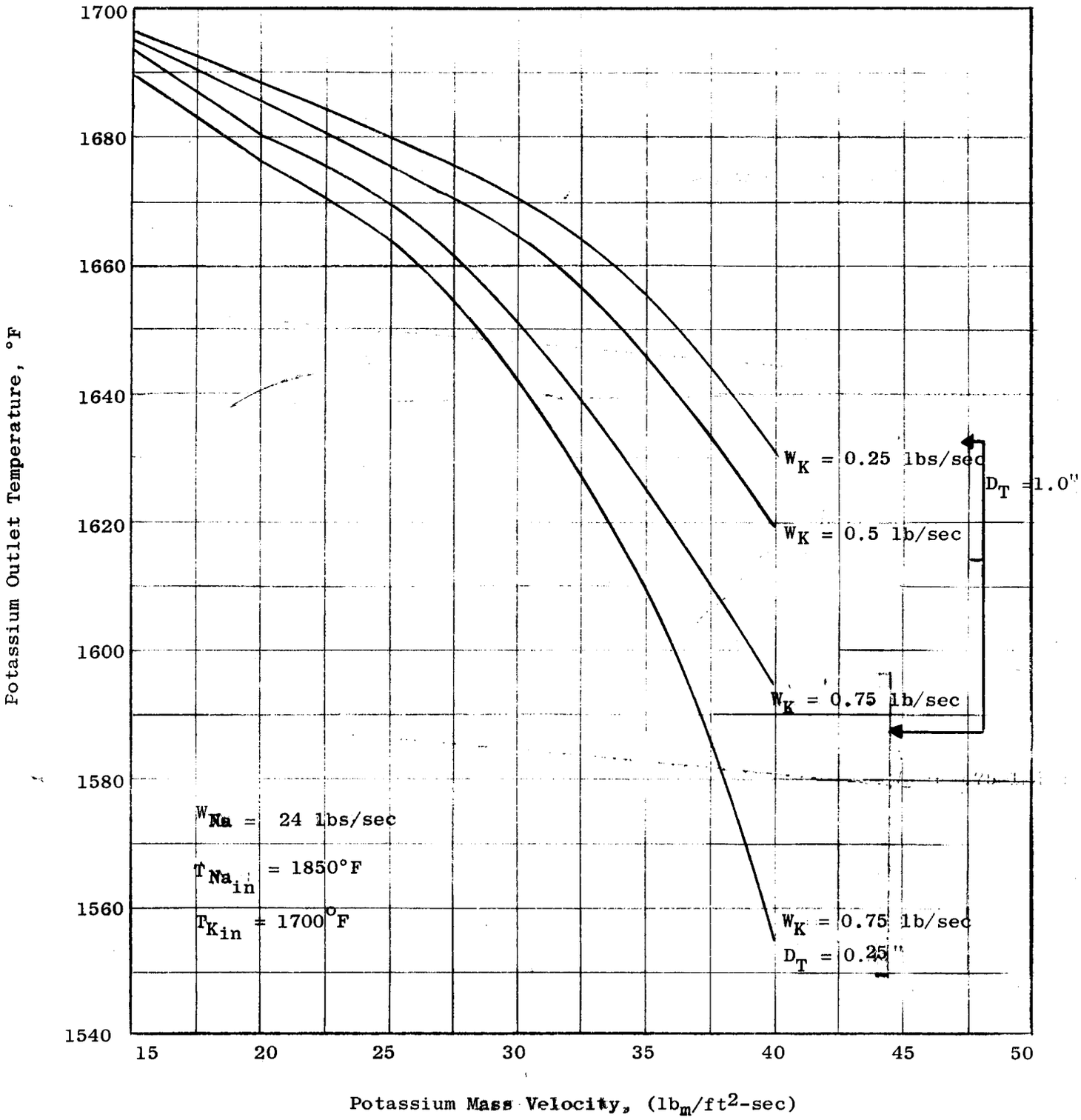

Figure 32. Potassium Outlet Temperature at 100% Quality Vs Tube Diameter, Potassium Mass Velocity Flow Rate and Tube Diameter.

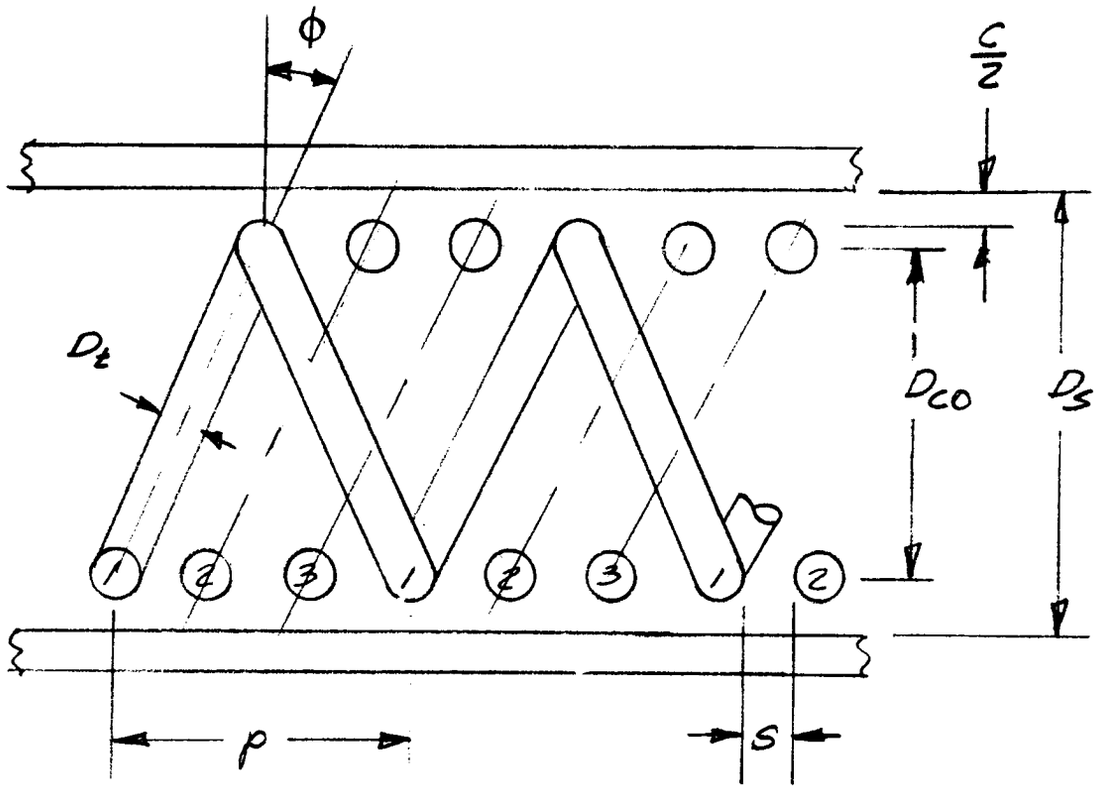

Figure 33. Coiled Tube Configuration - 300 KW System

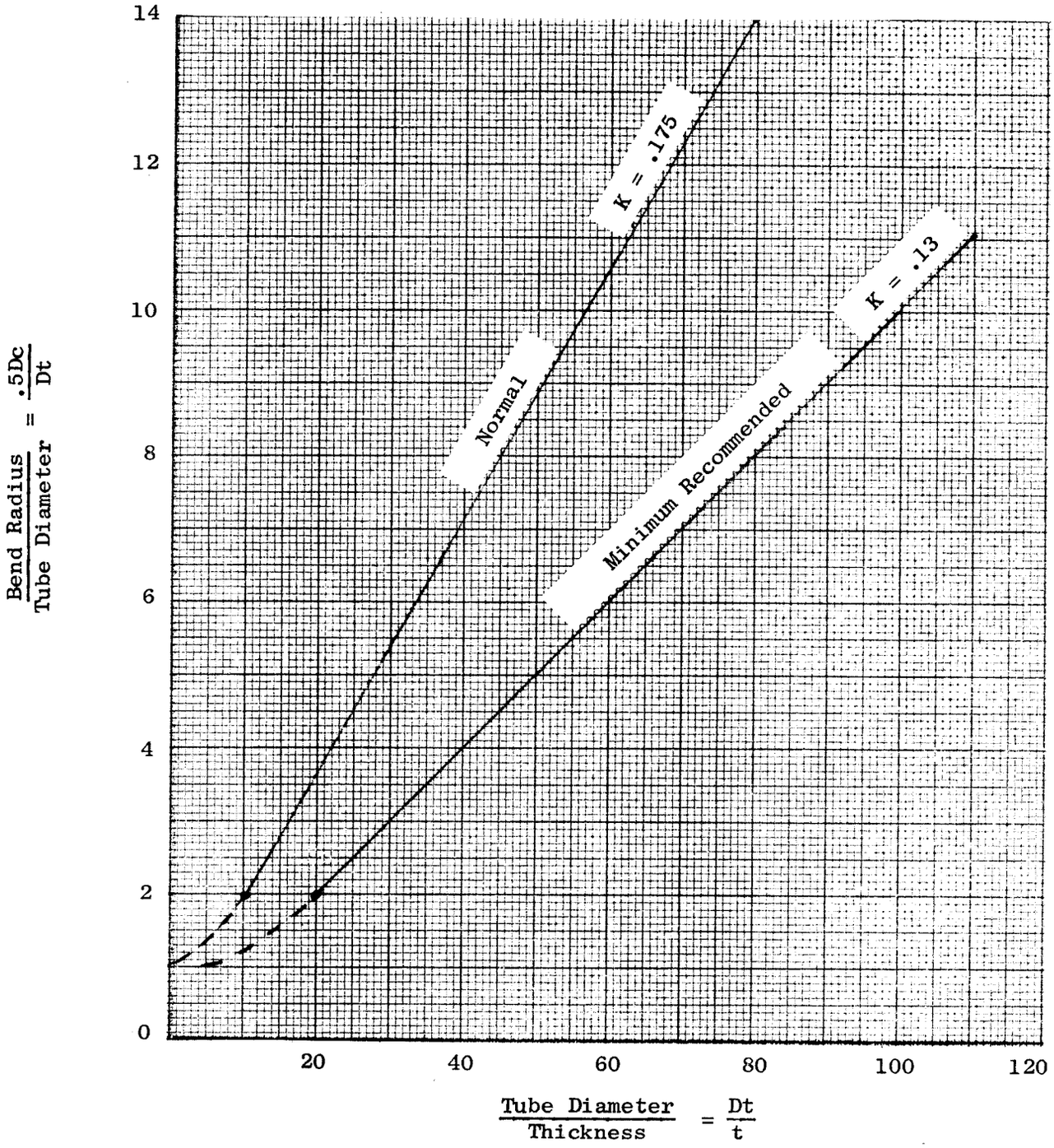

Figure 34. Tubing Bend Radius Relationship

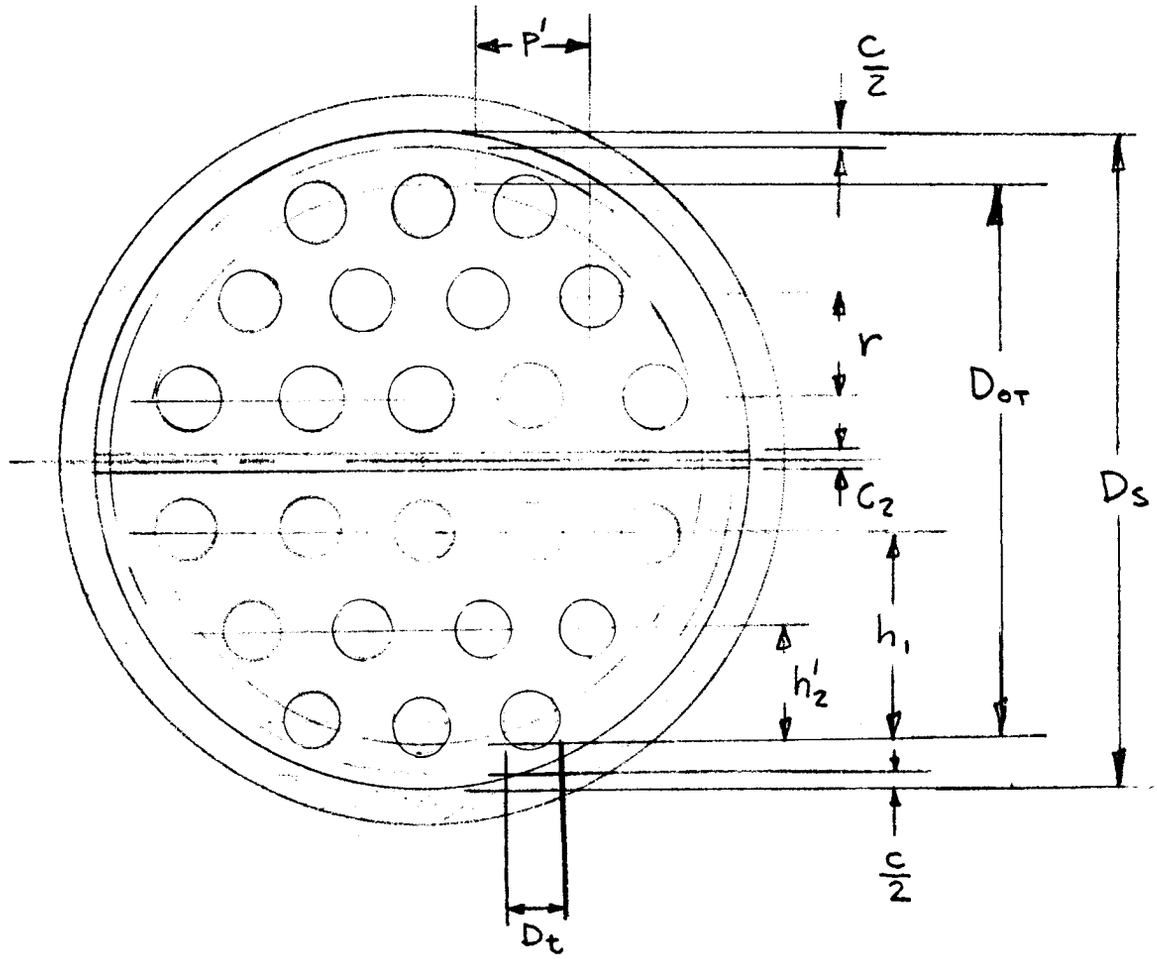

Figure 35. Straight Tube Configuration - 300 KW System

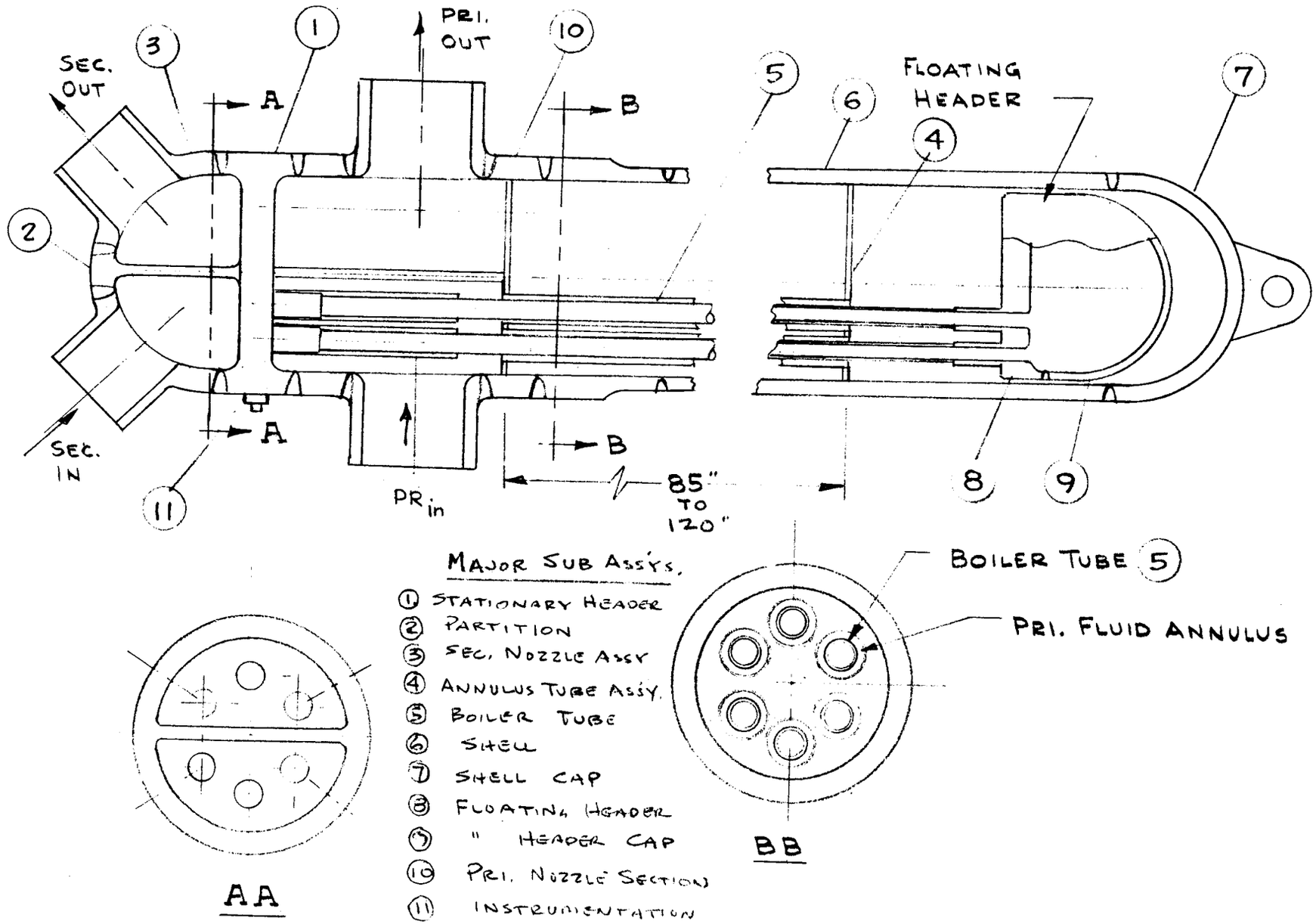

Figure 36. Straight Tube, Floating Heater Multitube Boiler - 300 KW System

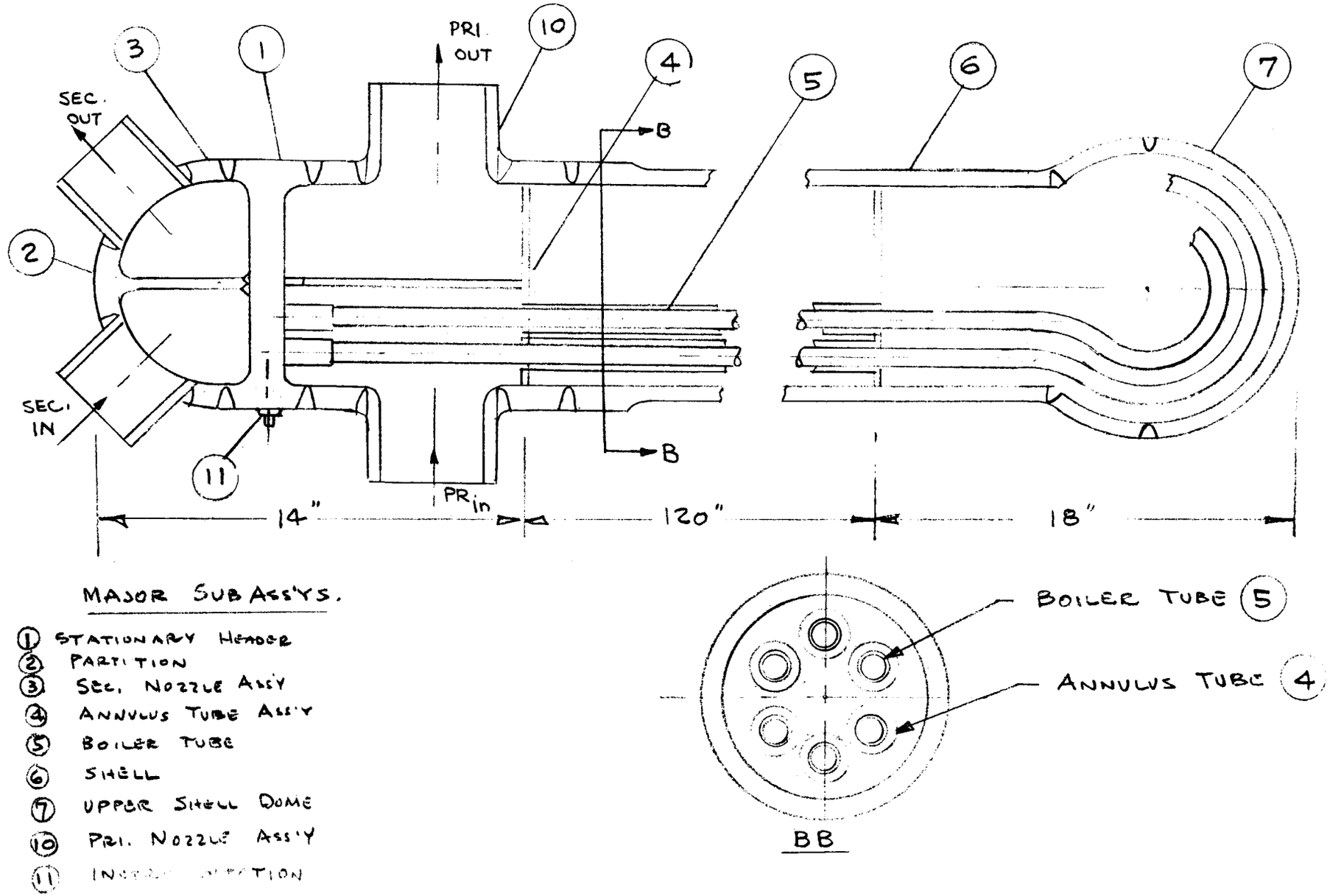

Figure 37. "U" Tube Test Boiler - 300 KW System

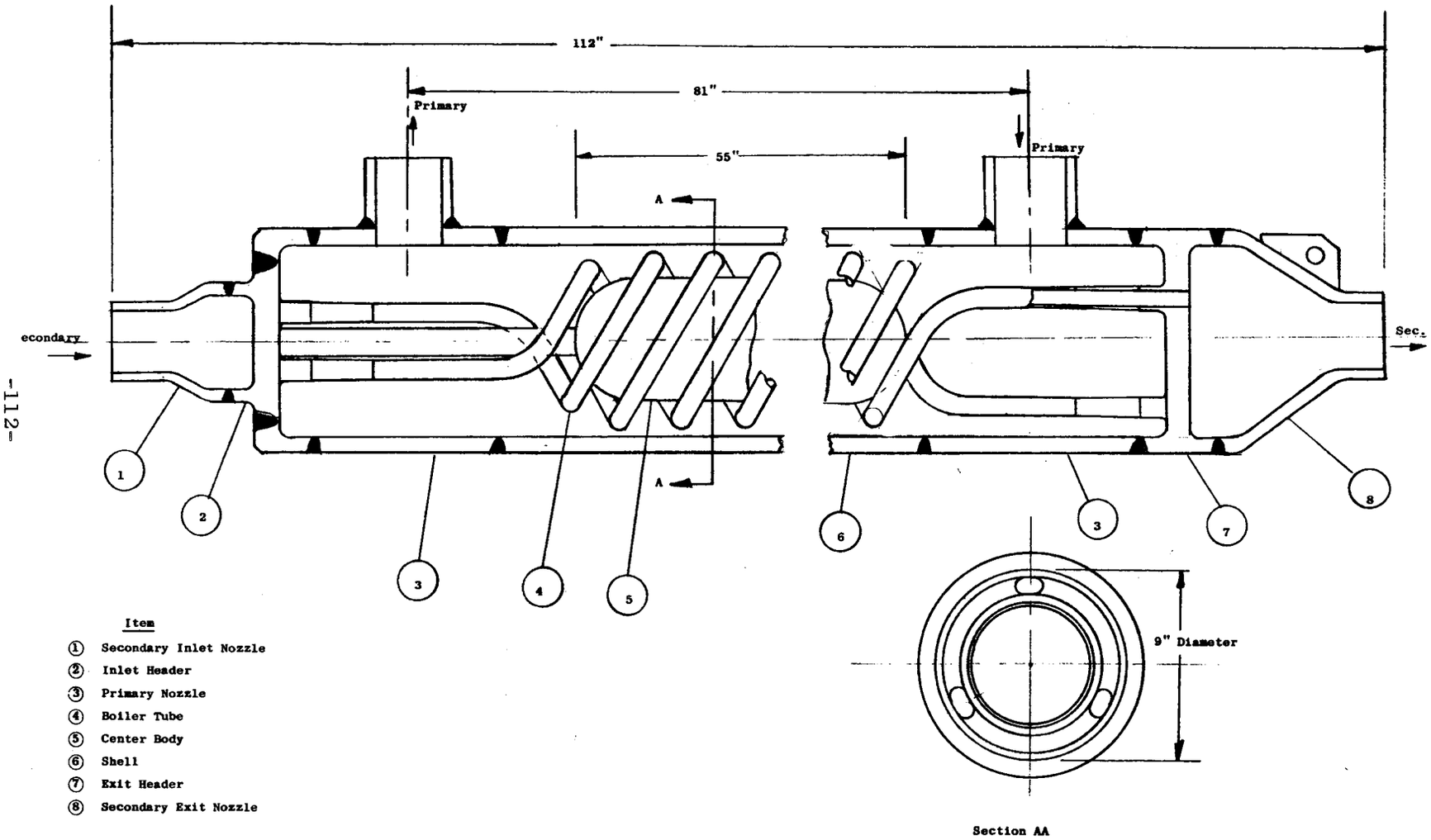

Figure 38. **Multiple Coil Tube Test Boiler** - 300 KW System

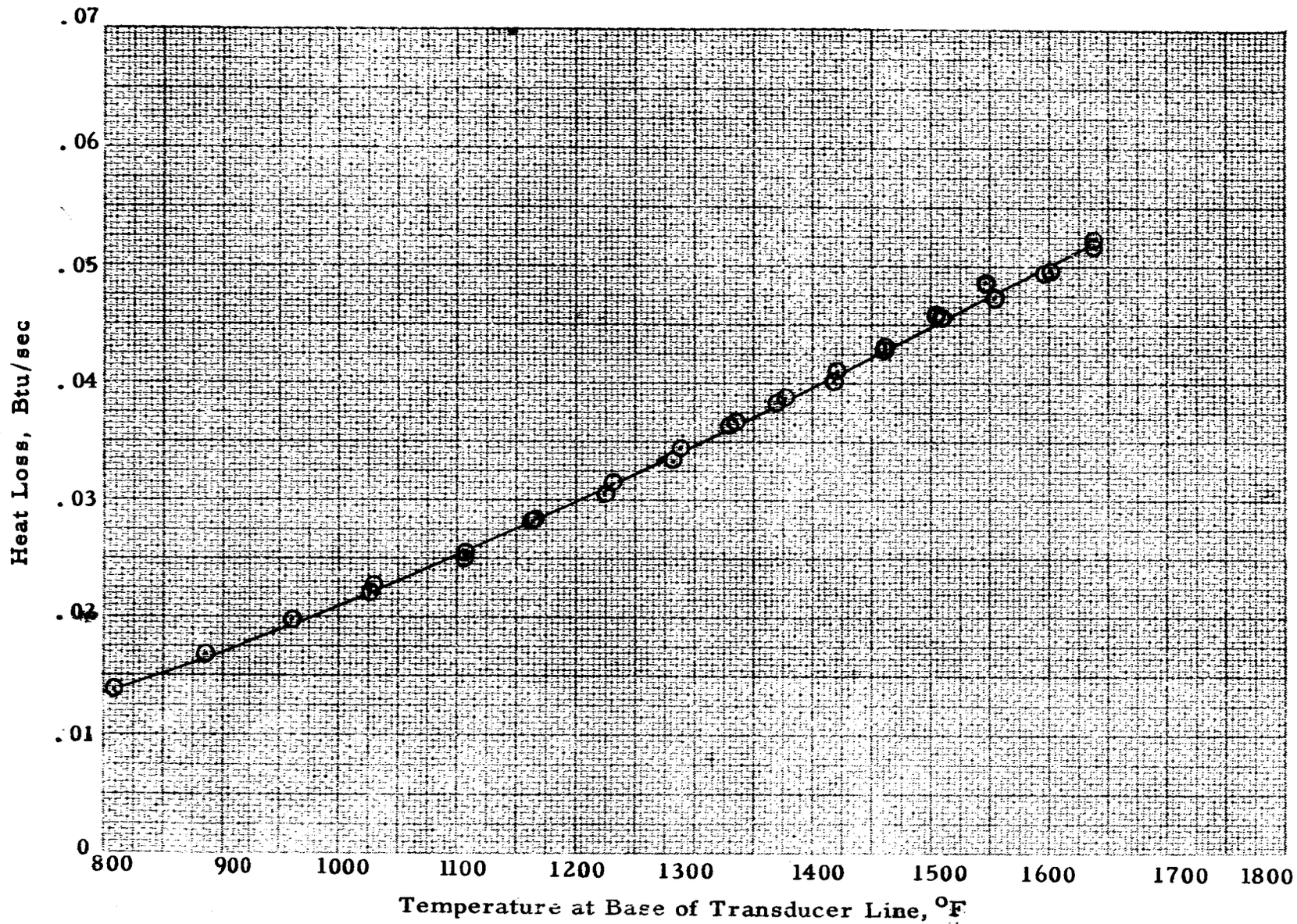

Figure 39. Heat Loss From the Transducer Line at the Boiler Exit of the 100 KW Loop

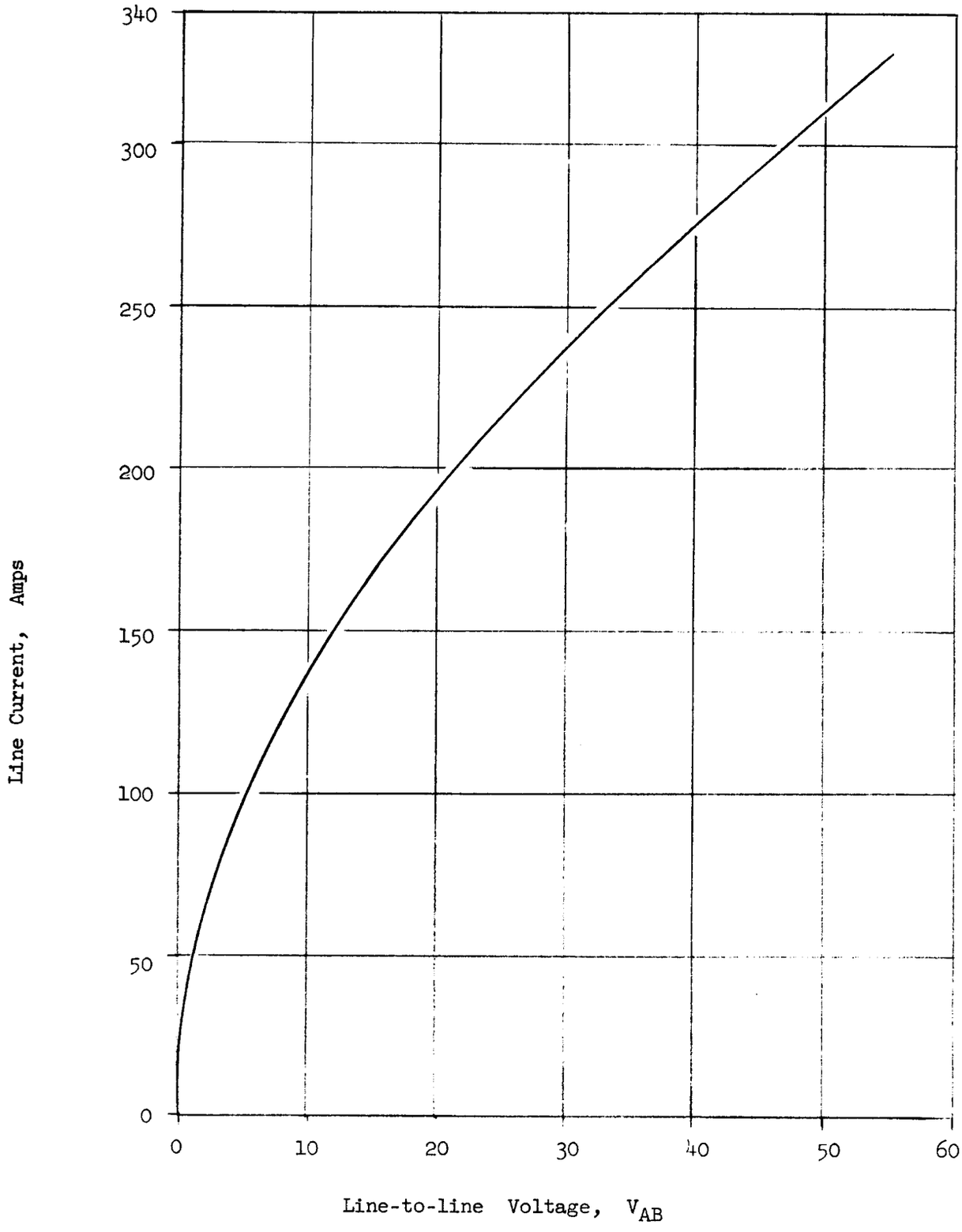

Figure 40. Operating Characteristics of 100 KW System.
a) Boiler Test Section Heater Current vs Voltage.

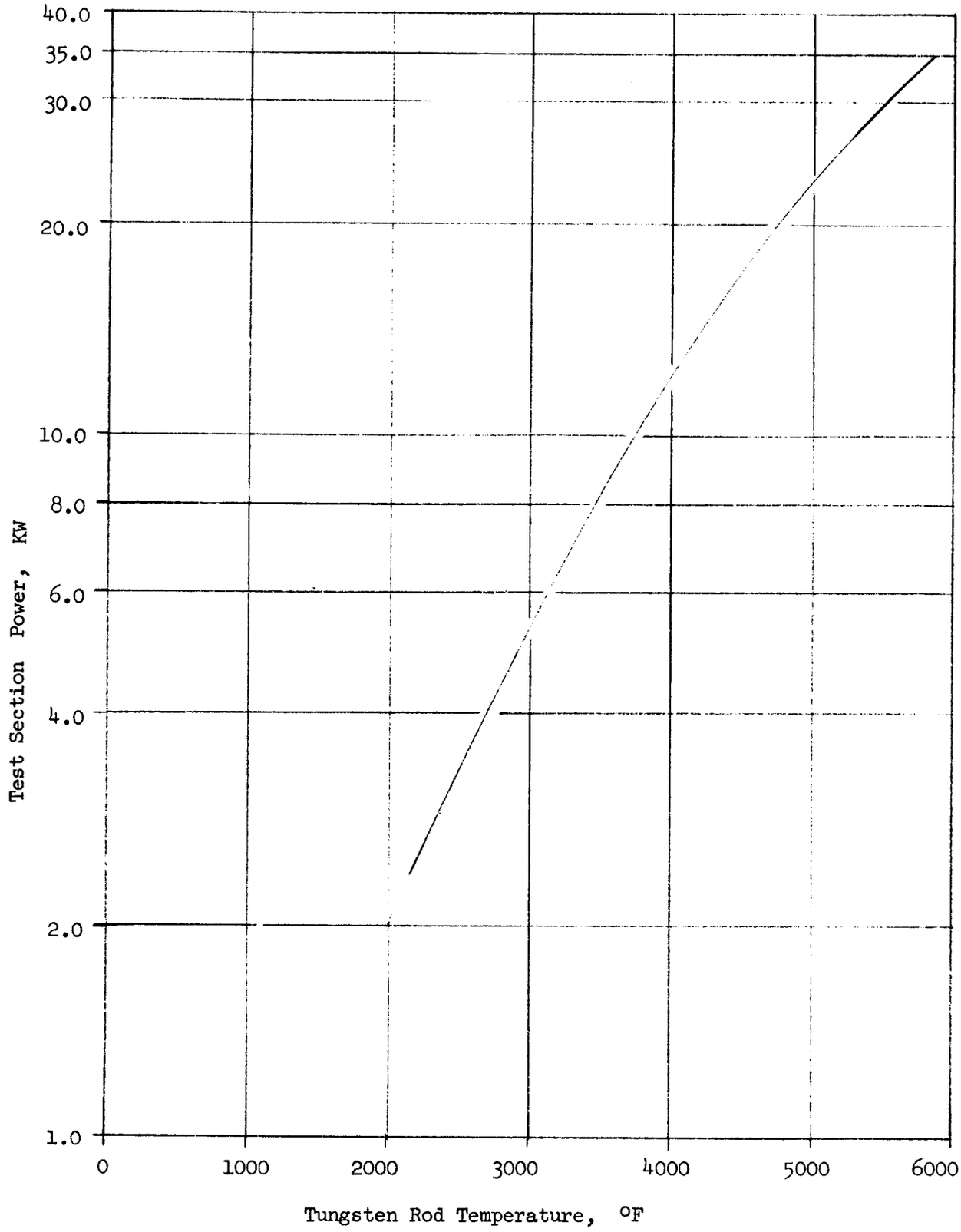

Figure 40. Operating Characteristics of 100 KW System.
b) Boiler Test Section Heater Power as a Function of Rod Temperature.

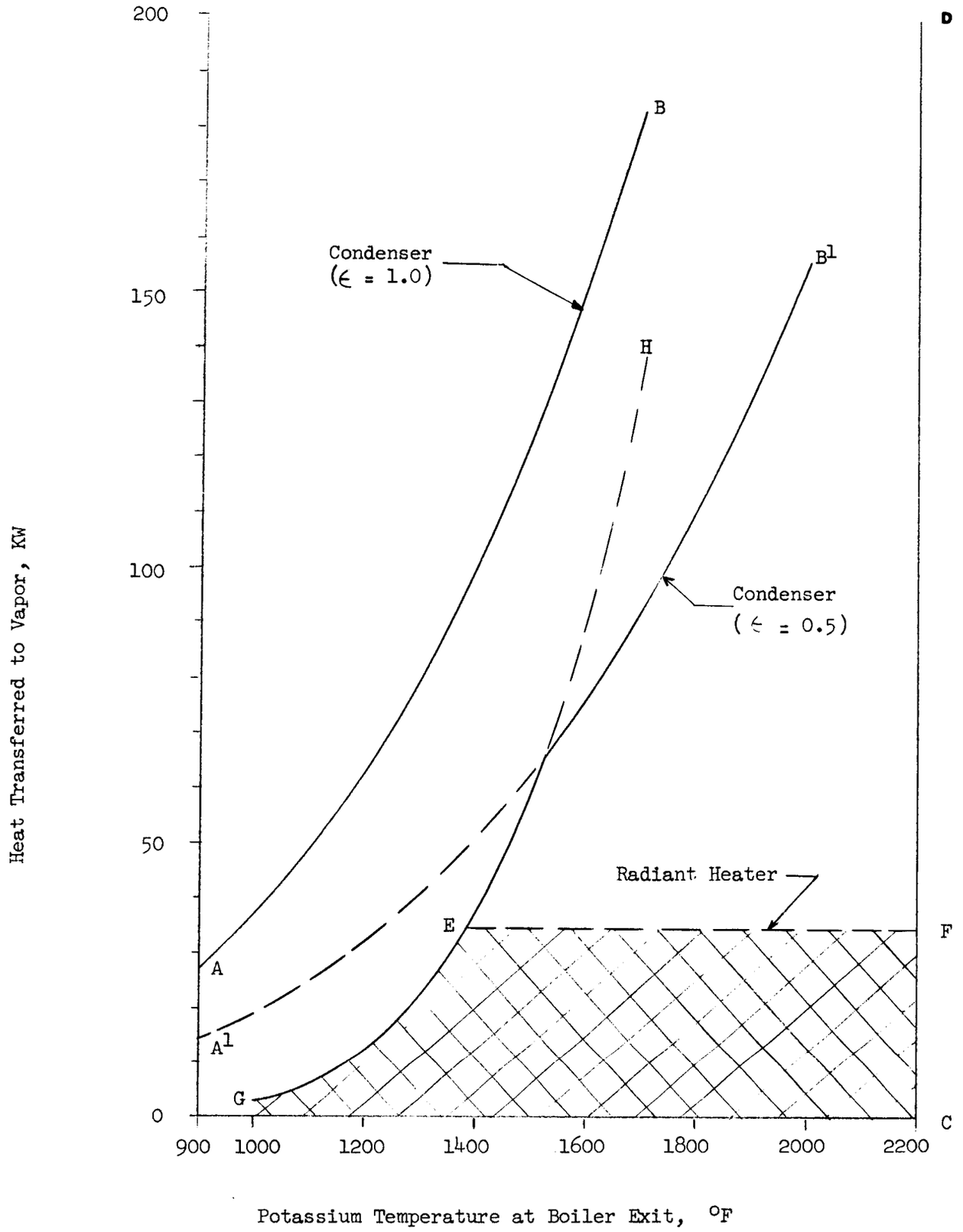

Figure 40. Operating Characteristics of 100 KW System.
c) Operating Envelope based on Thermodynamic and Heat Transfer Considerations.

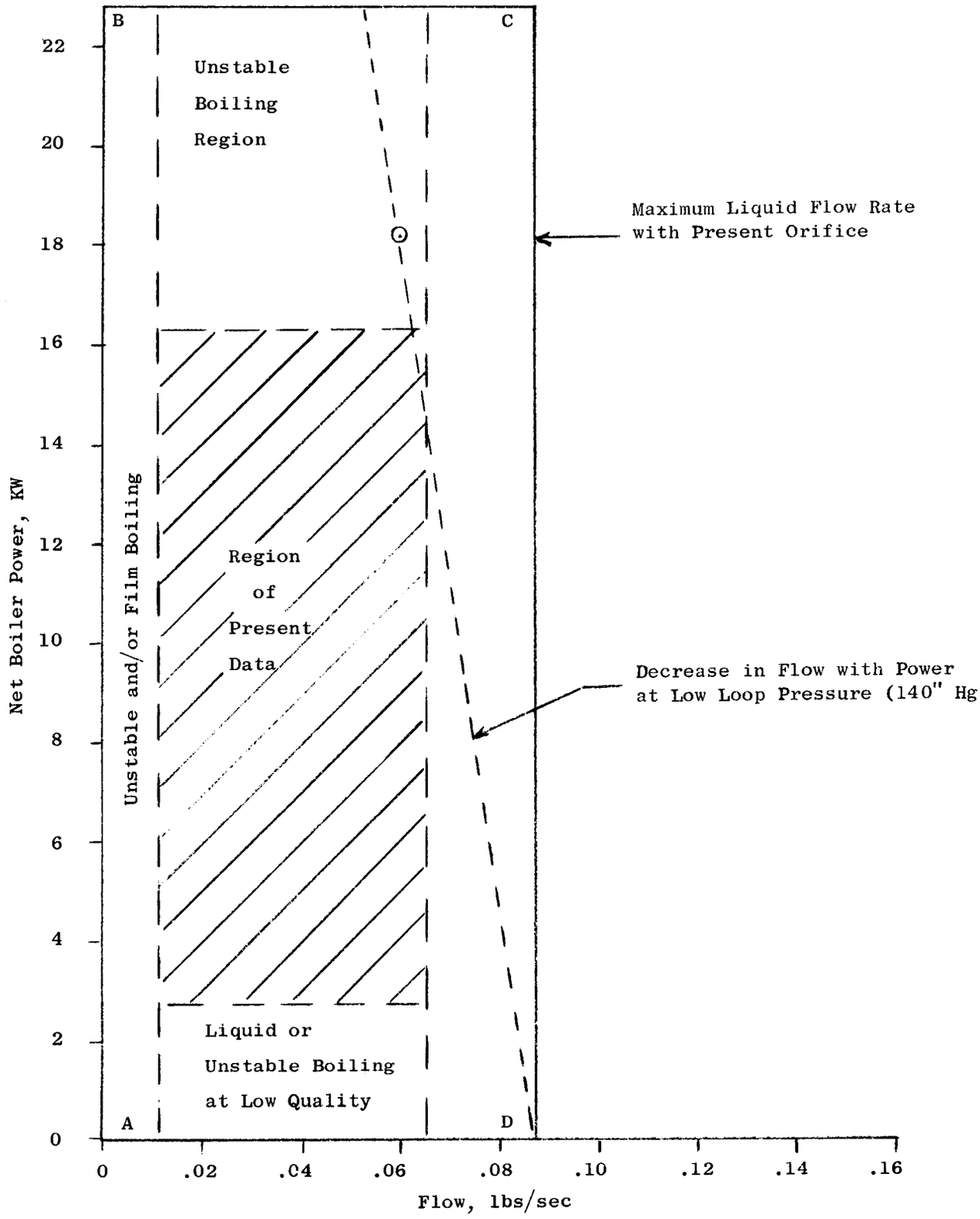

Figure 40. Operating Characteristics of 100 KW System.
d) Operating Envelope based on Stability Considerations.

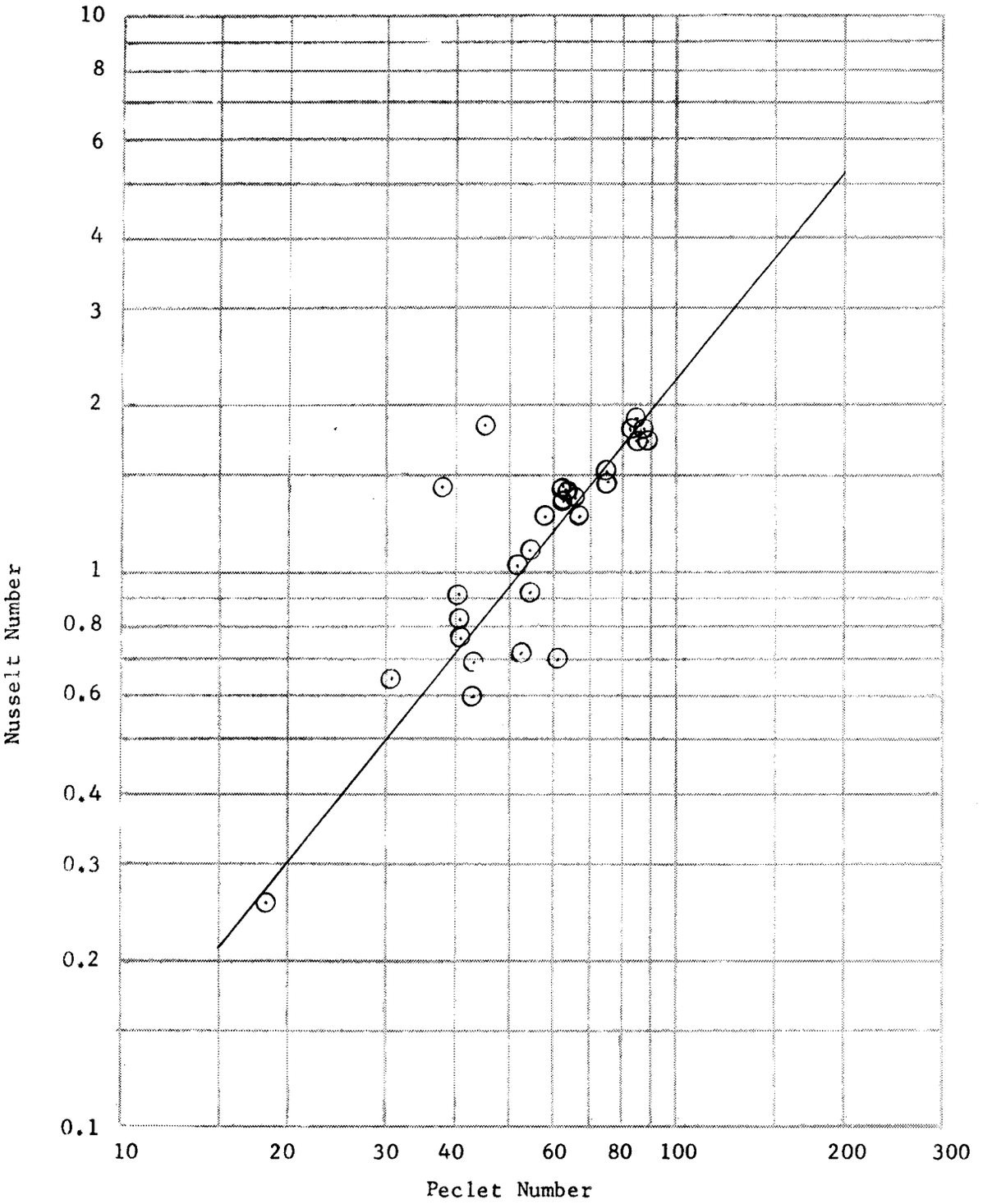

Figure 41. 100 KW Liquid Potassium Data (Thermocouple 13)

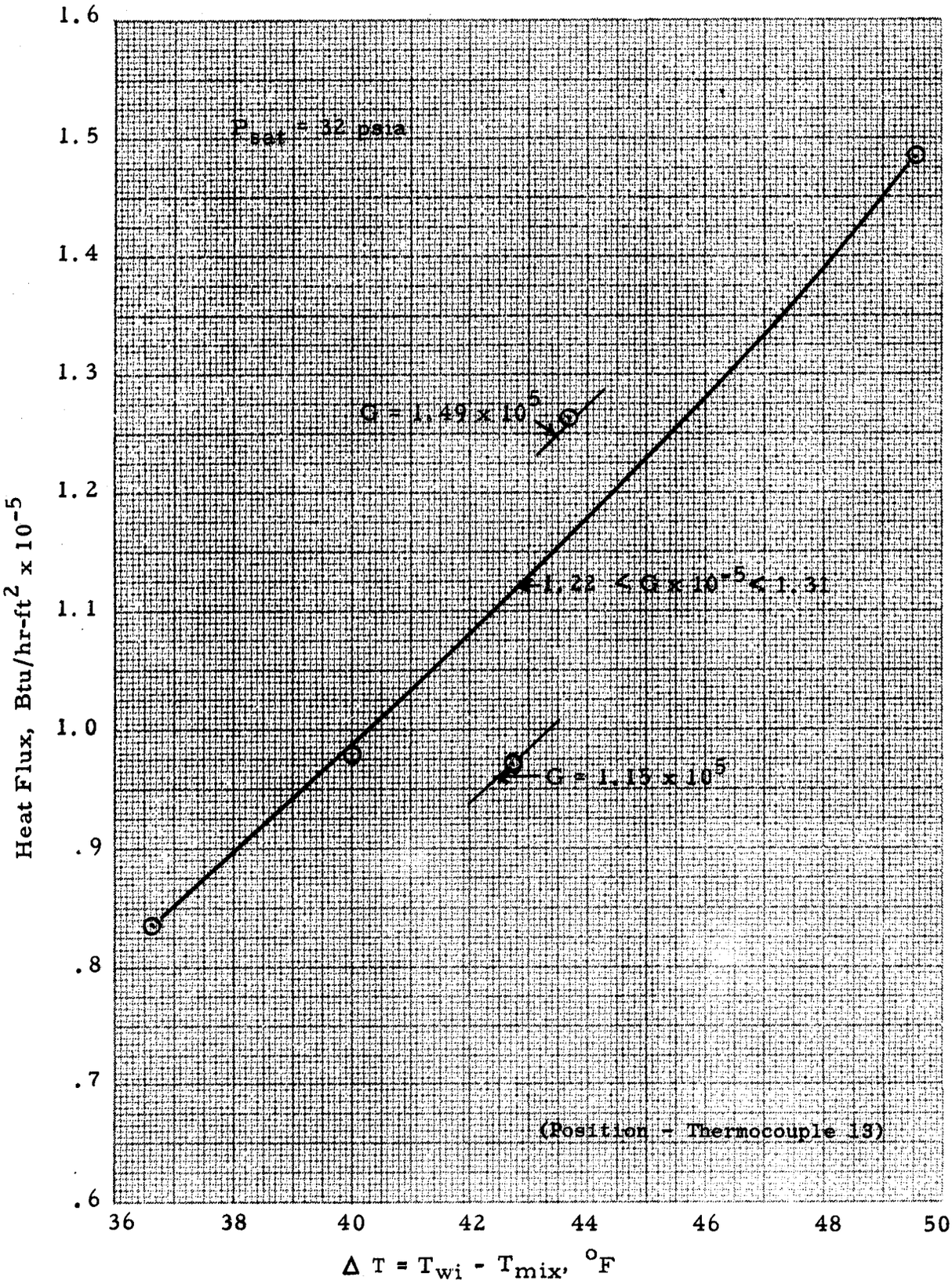

Figure 42. Heat Flux versus ΔT for Boiling Potassium in the 100 KW System.

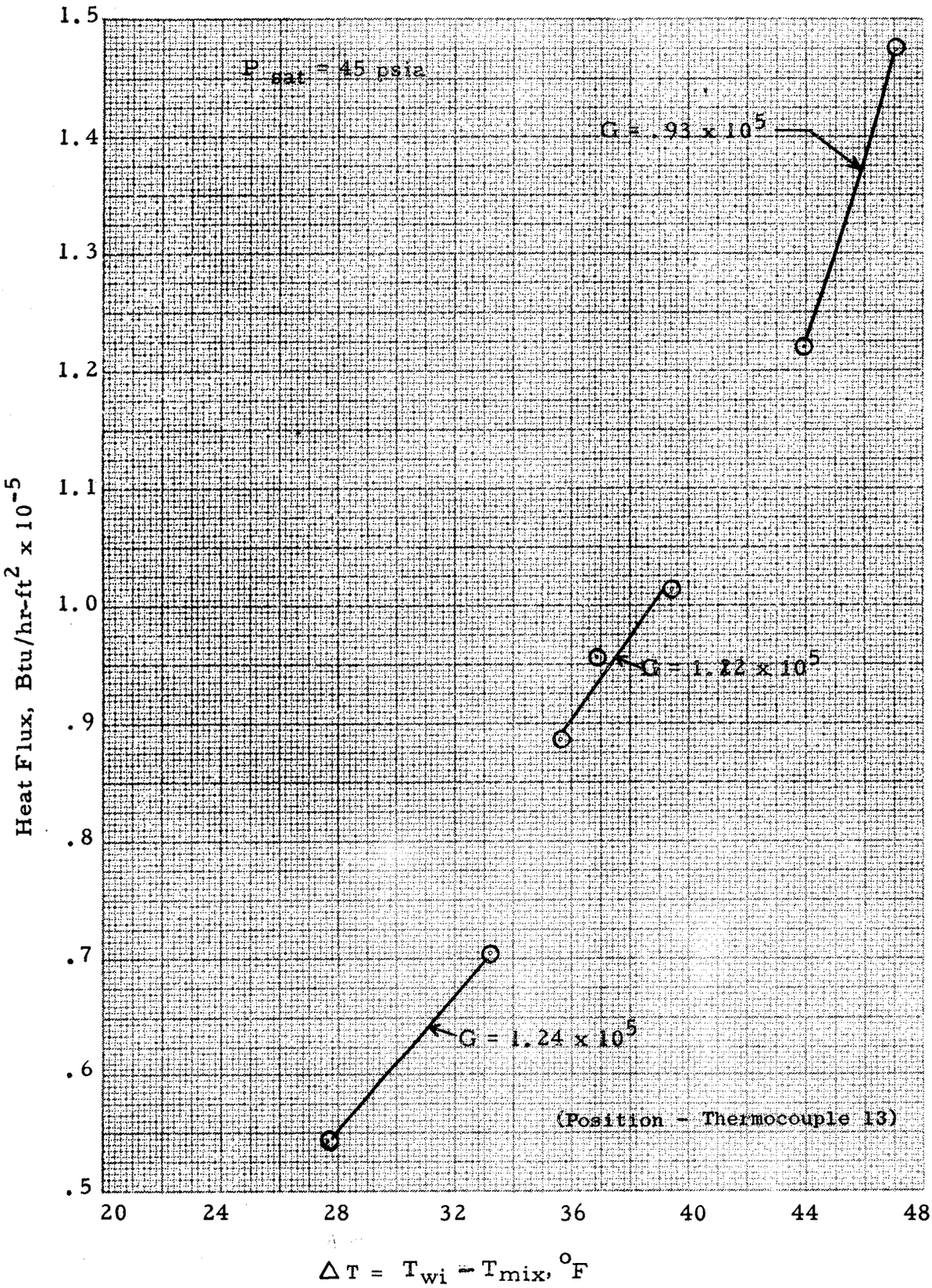

Figure 43. Heat Flux versus ΔT for Boiling Potassium in the 100 KW System.

Figure 43. Heat Flux versus ΔT for Boiling Potassium in the 100 KW System.

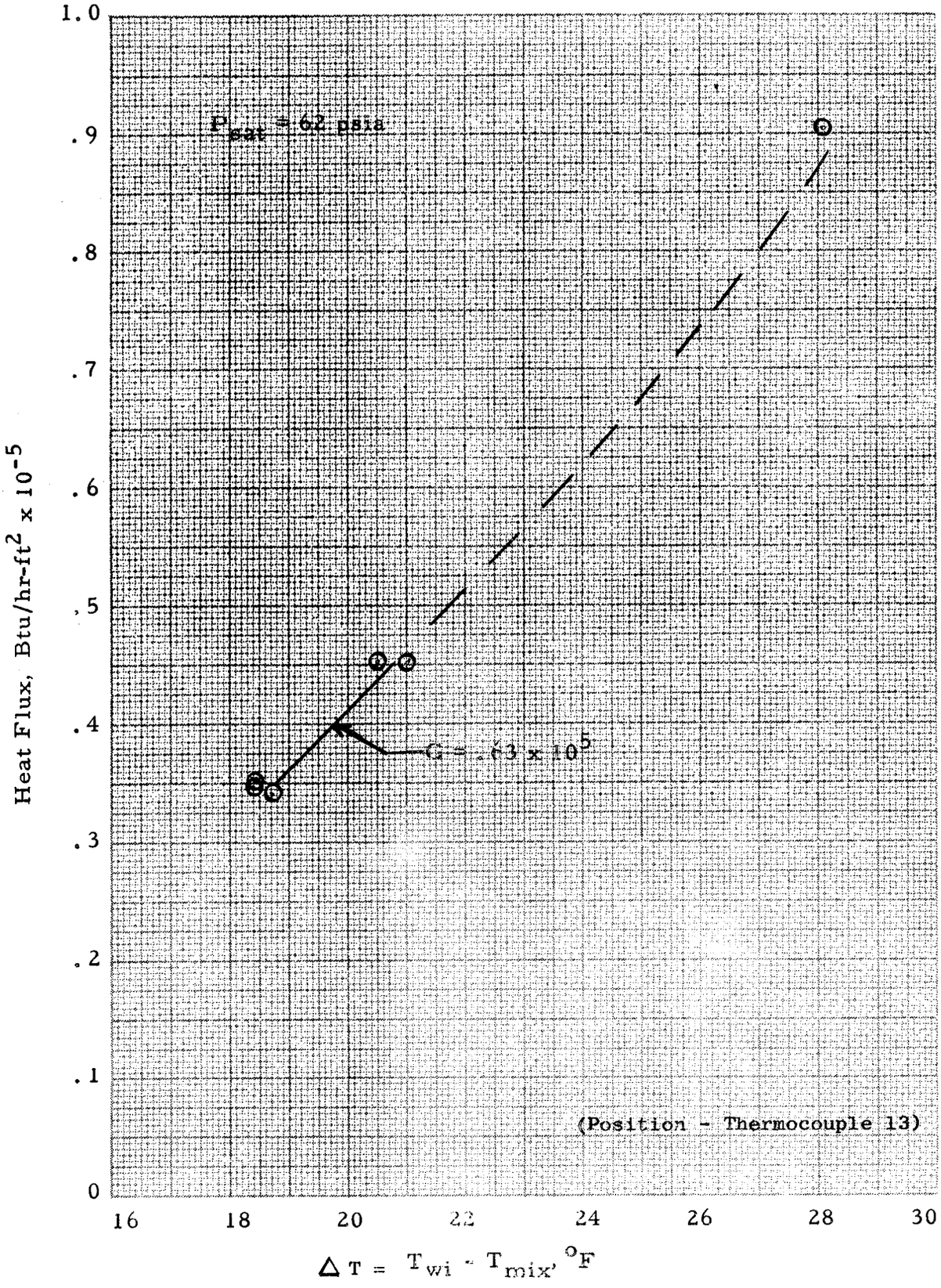

Figure 44. Heat Flux versus ΔT for Boiling Potassium in the 100 KW System

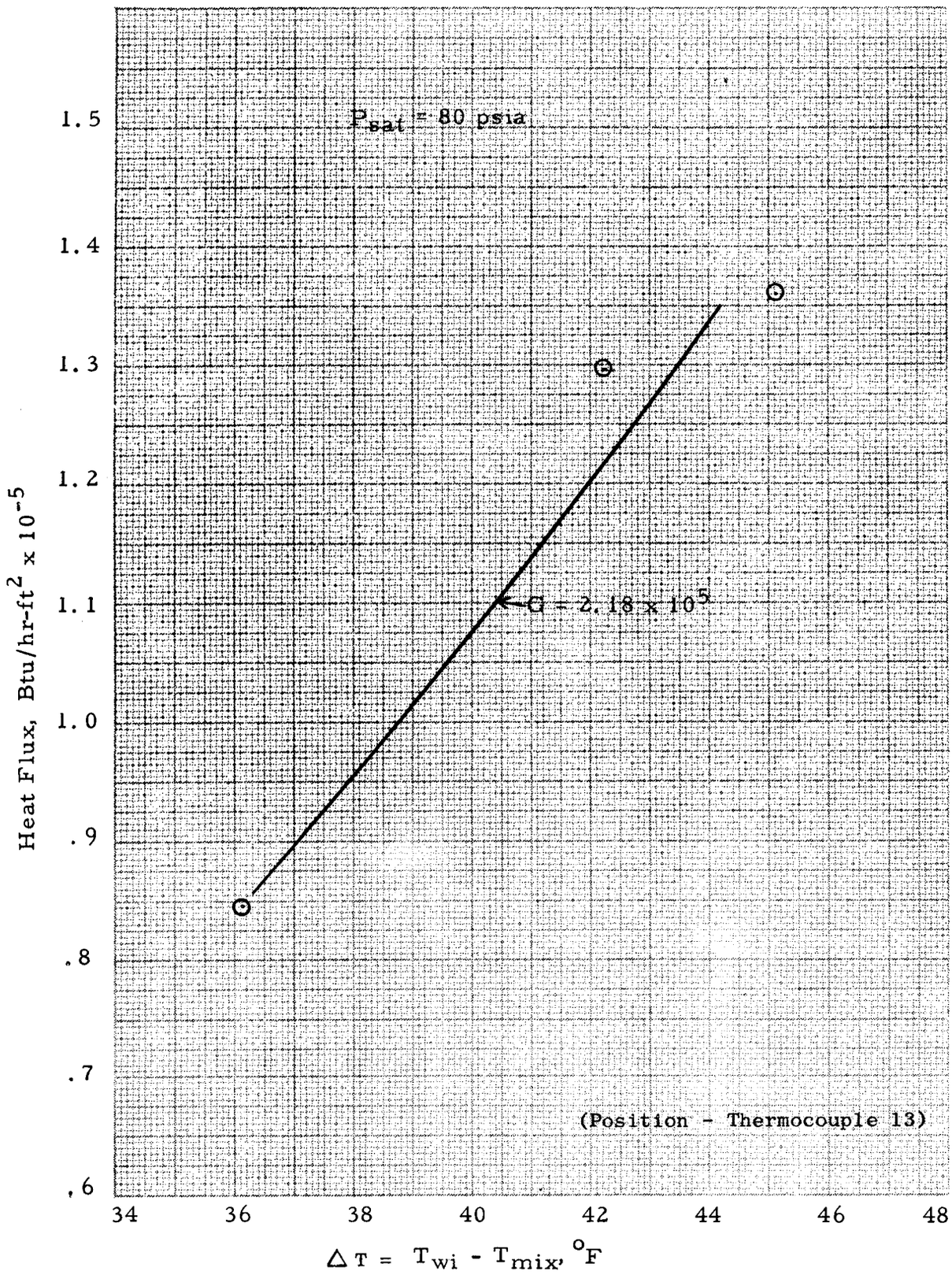

Figure 45. Heat Flux versus Δ T for Boiling Potassium in the 100 KW System.

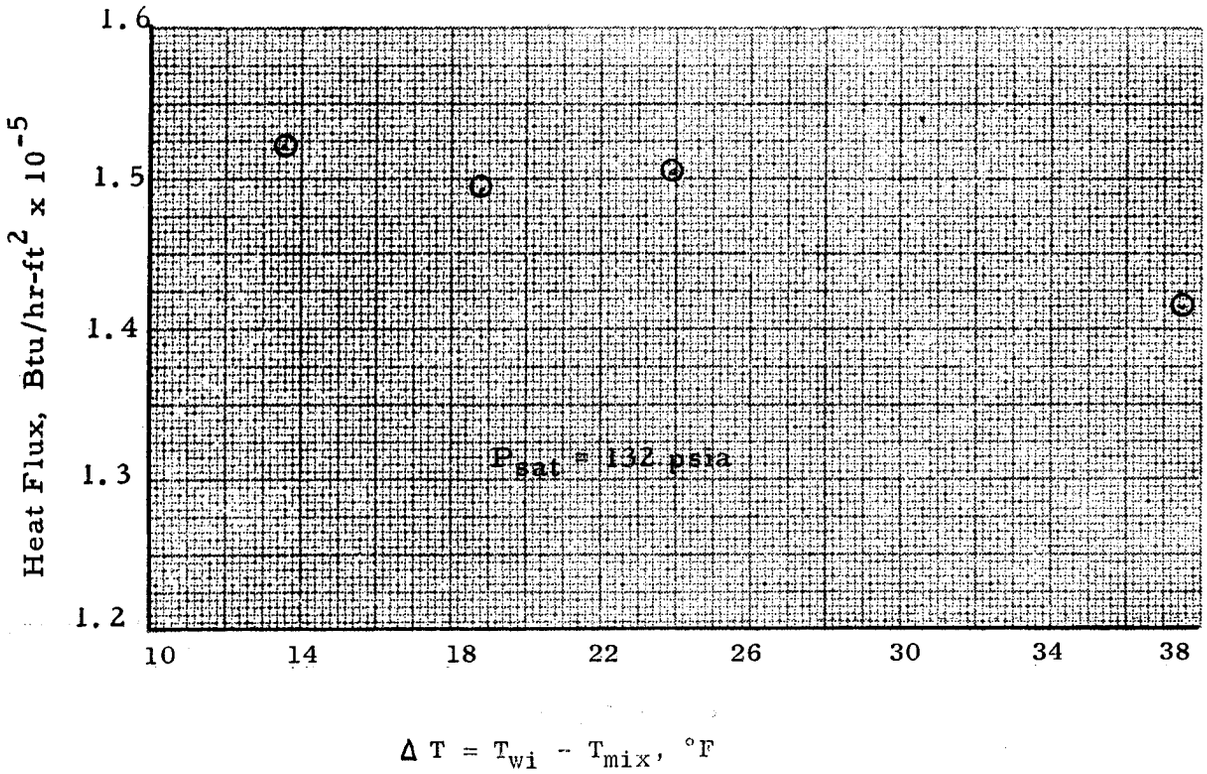

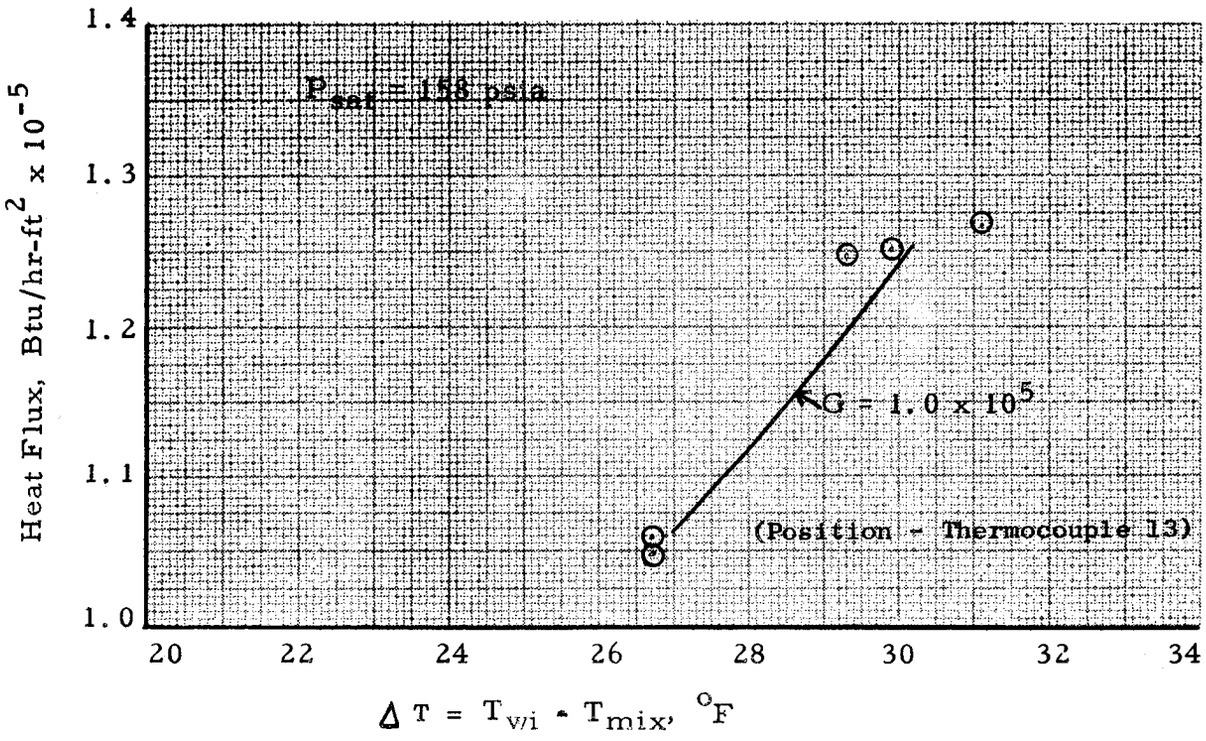

Figure 46. Heat Flux versus ΔT for Boiling Potassium in the 100 KW System.

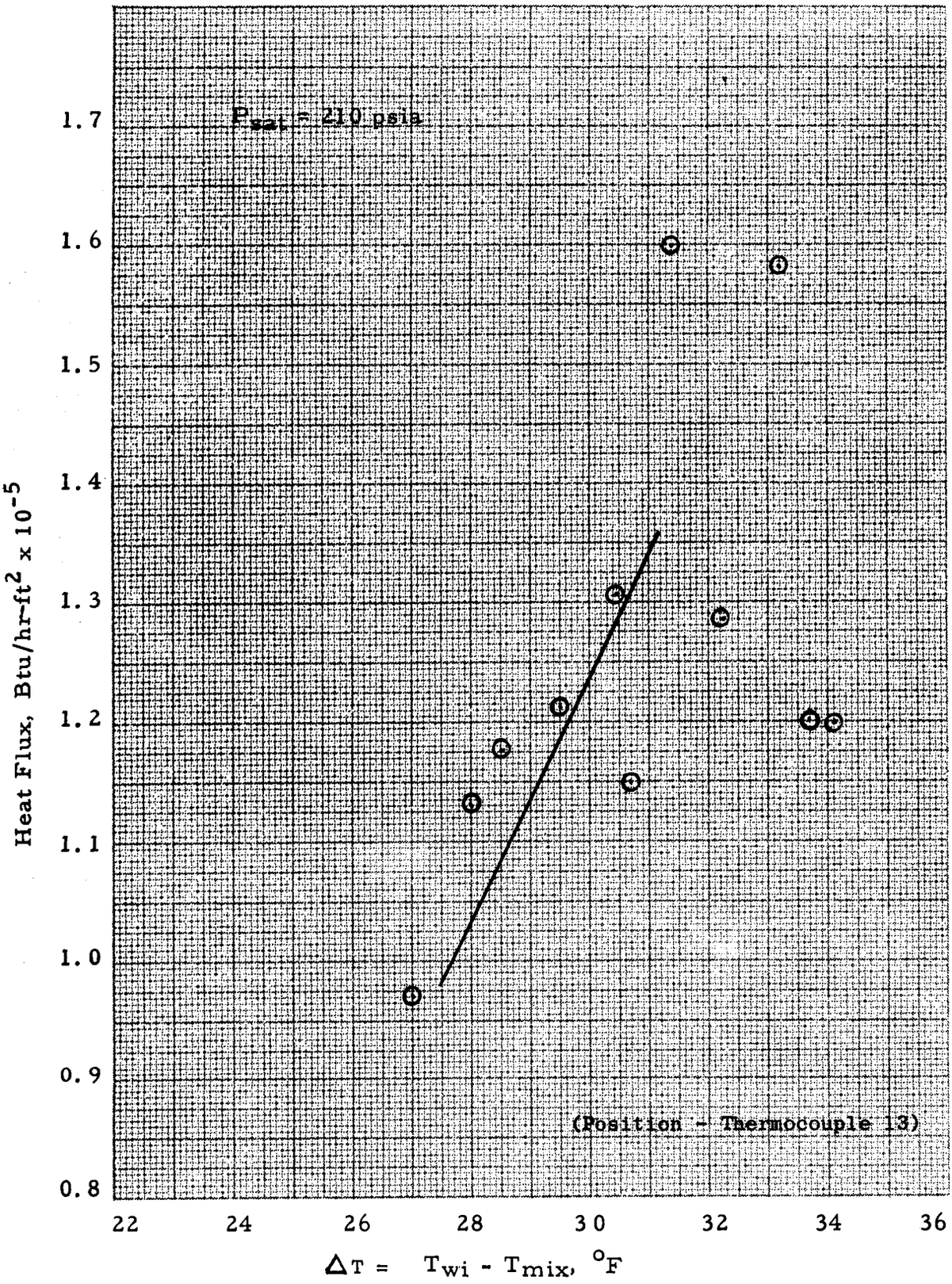

Figure 47. Heat Flux versus ΔT for Boiling Potassium in the 100 KW System (Thermocouple 13)

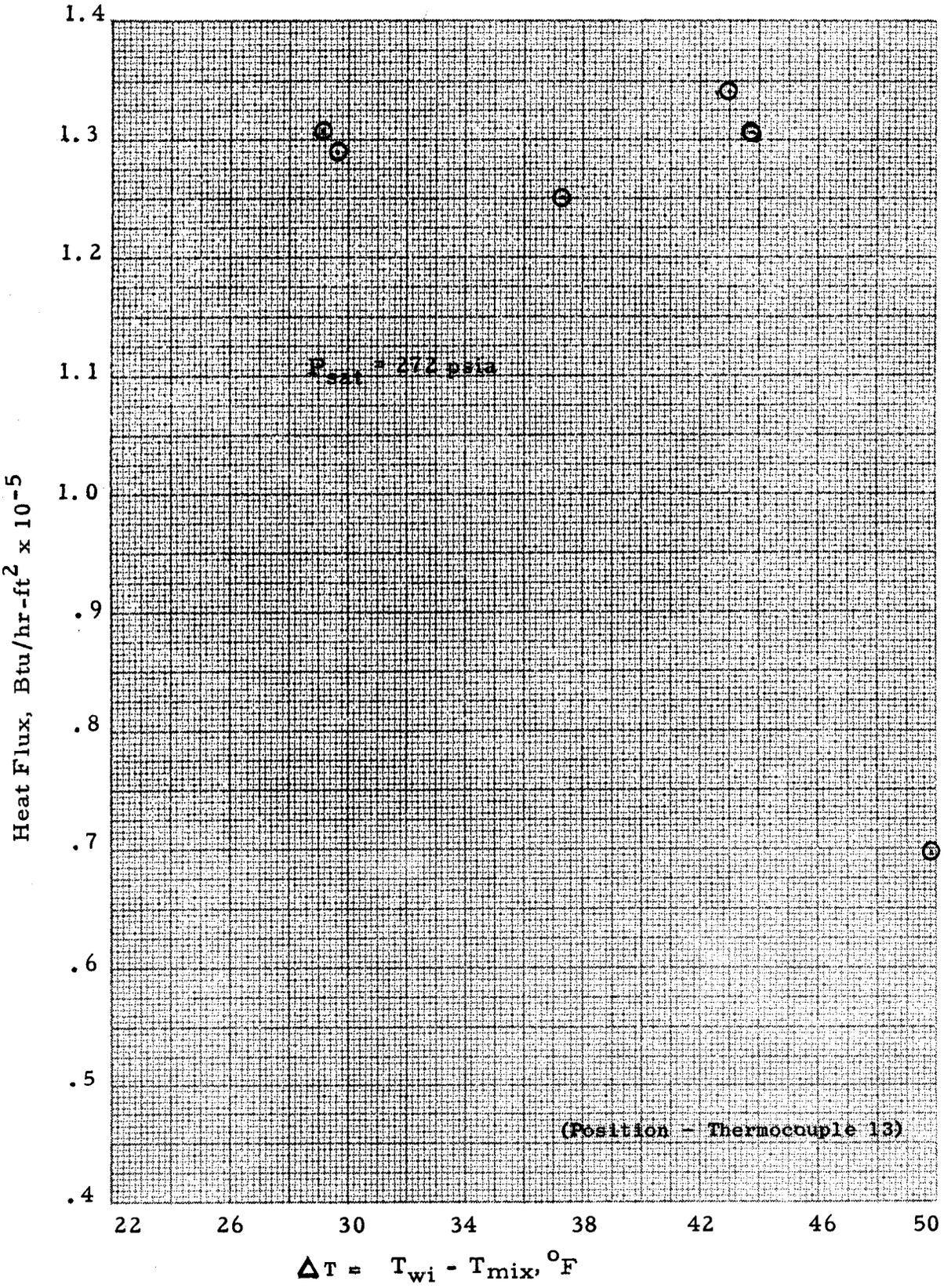

Figure 48. Heat Flux versus ΔT for Boiling Potassium in the 100 KW System.

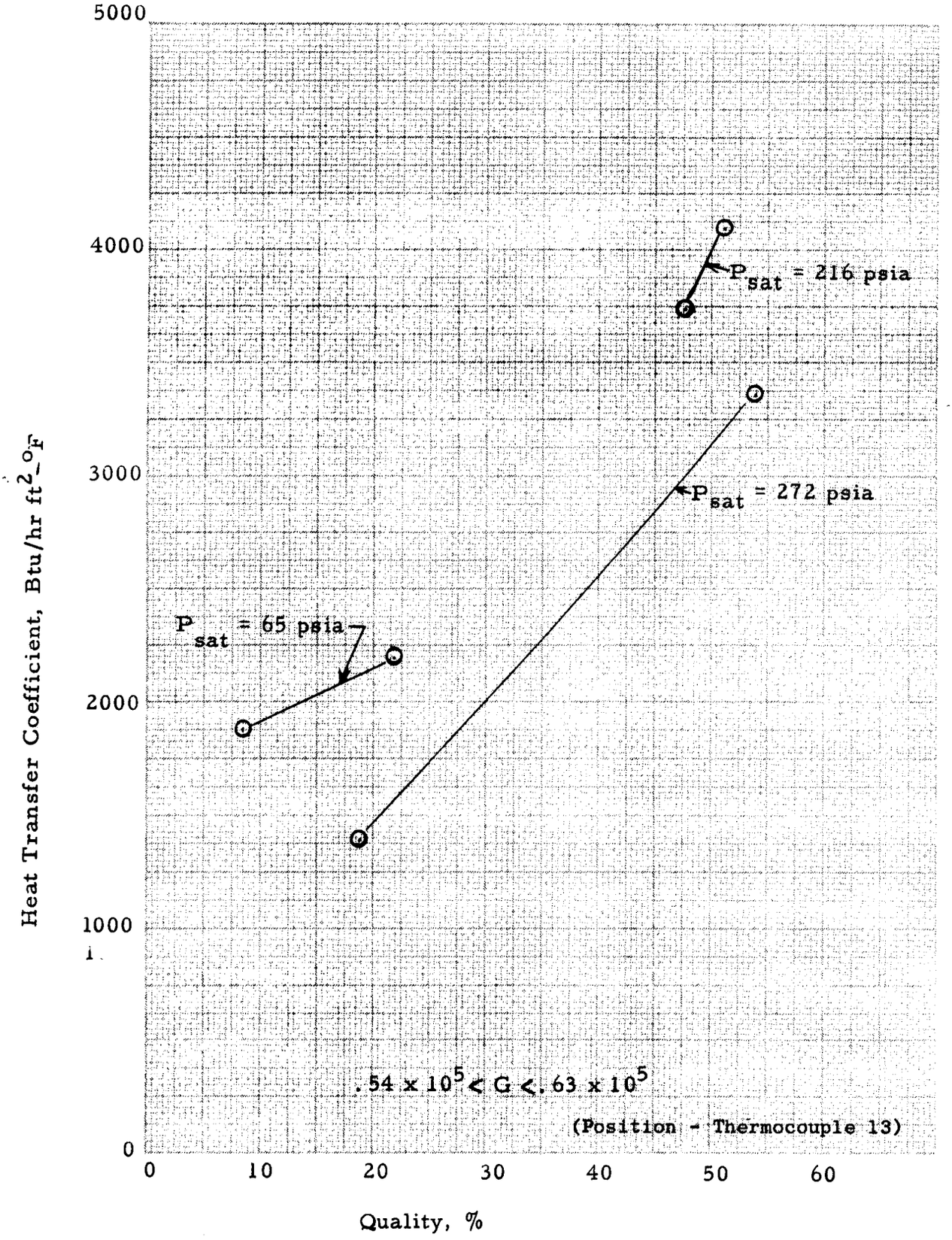

Figure 49. Heat Transfer Coefficients for Boiling Potassium in the 100 KW System.

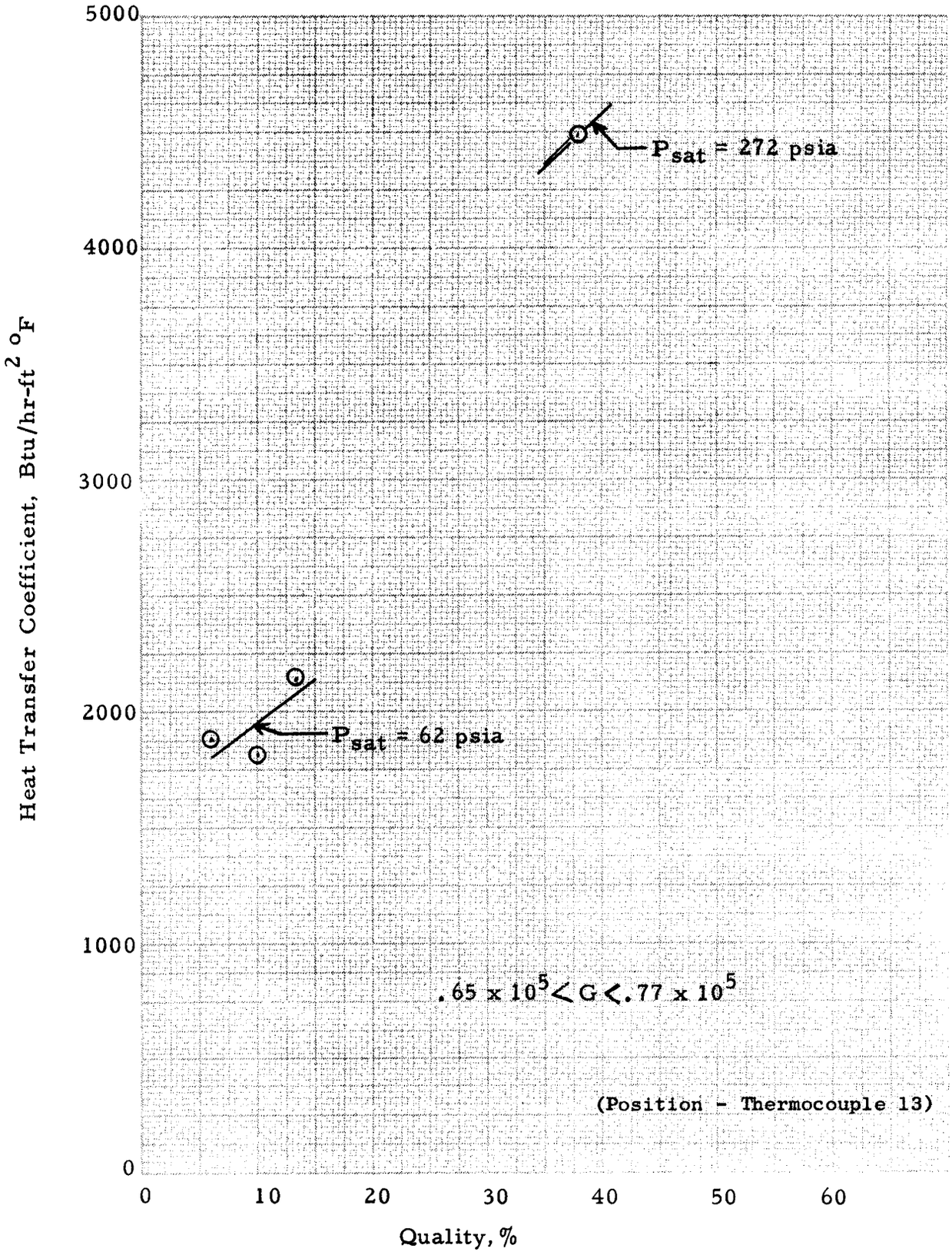

Figure 50. Heat Transfer Coefficients for Boiling Potassium in the 100 KW System.

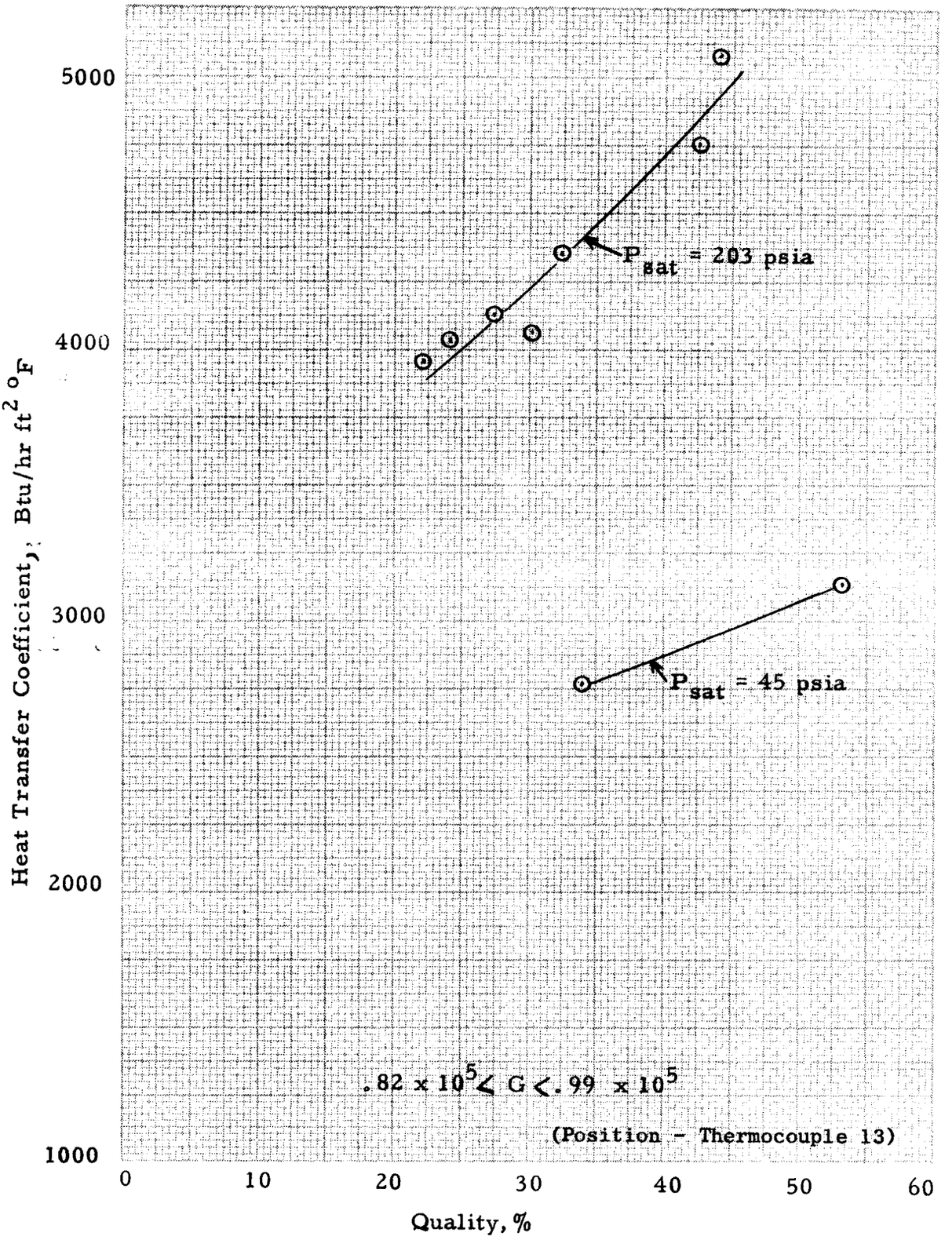

Figure 51. Heat Transfer Coefficients for Boiling Potassium in the 100 KW System.

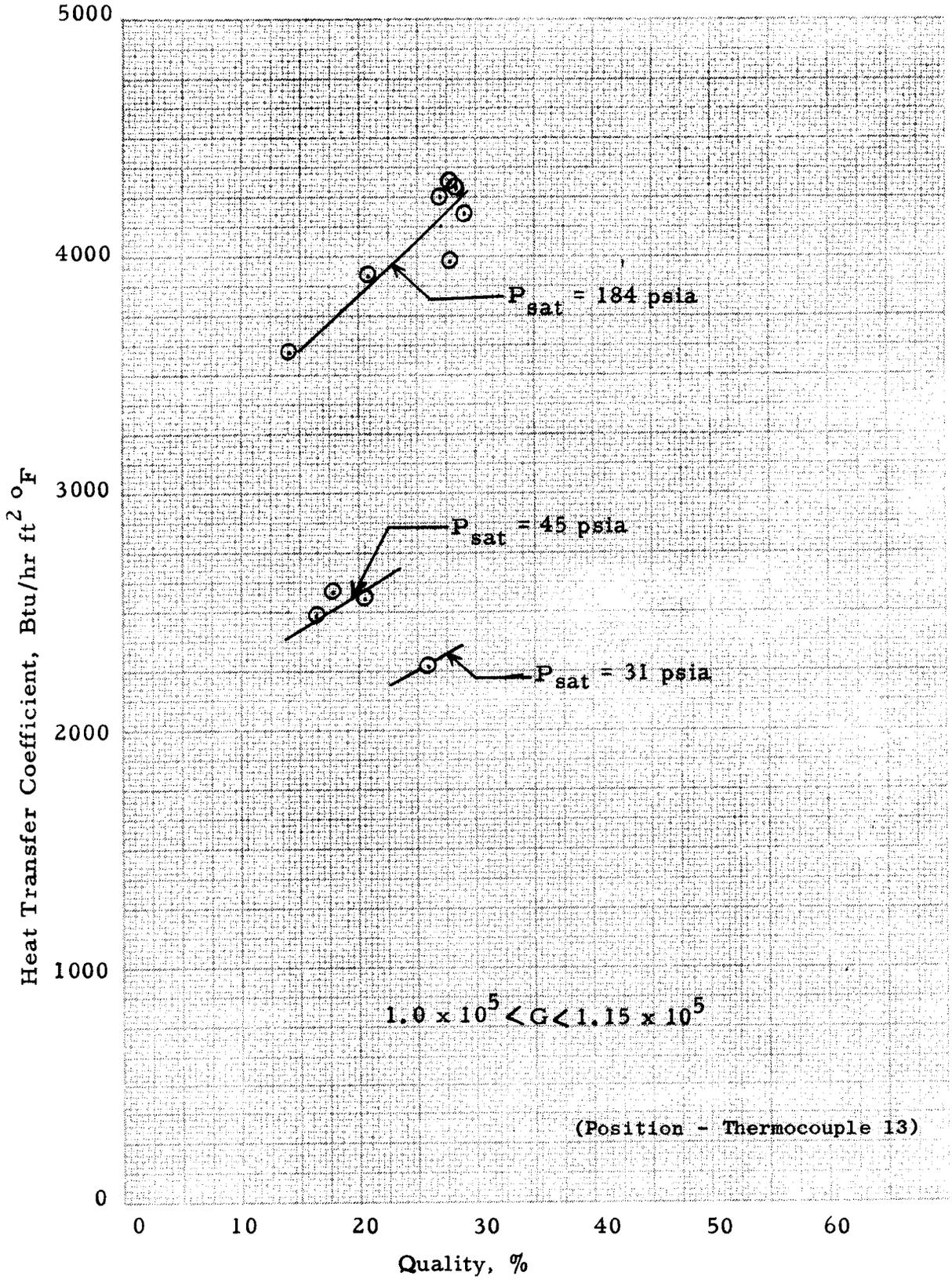

Figure 52. Heat Transfer Coefficients for Boiling Potassium in the 100 KW System.

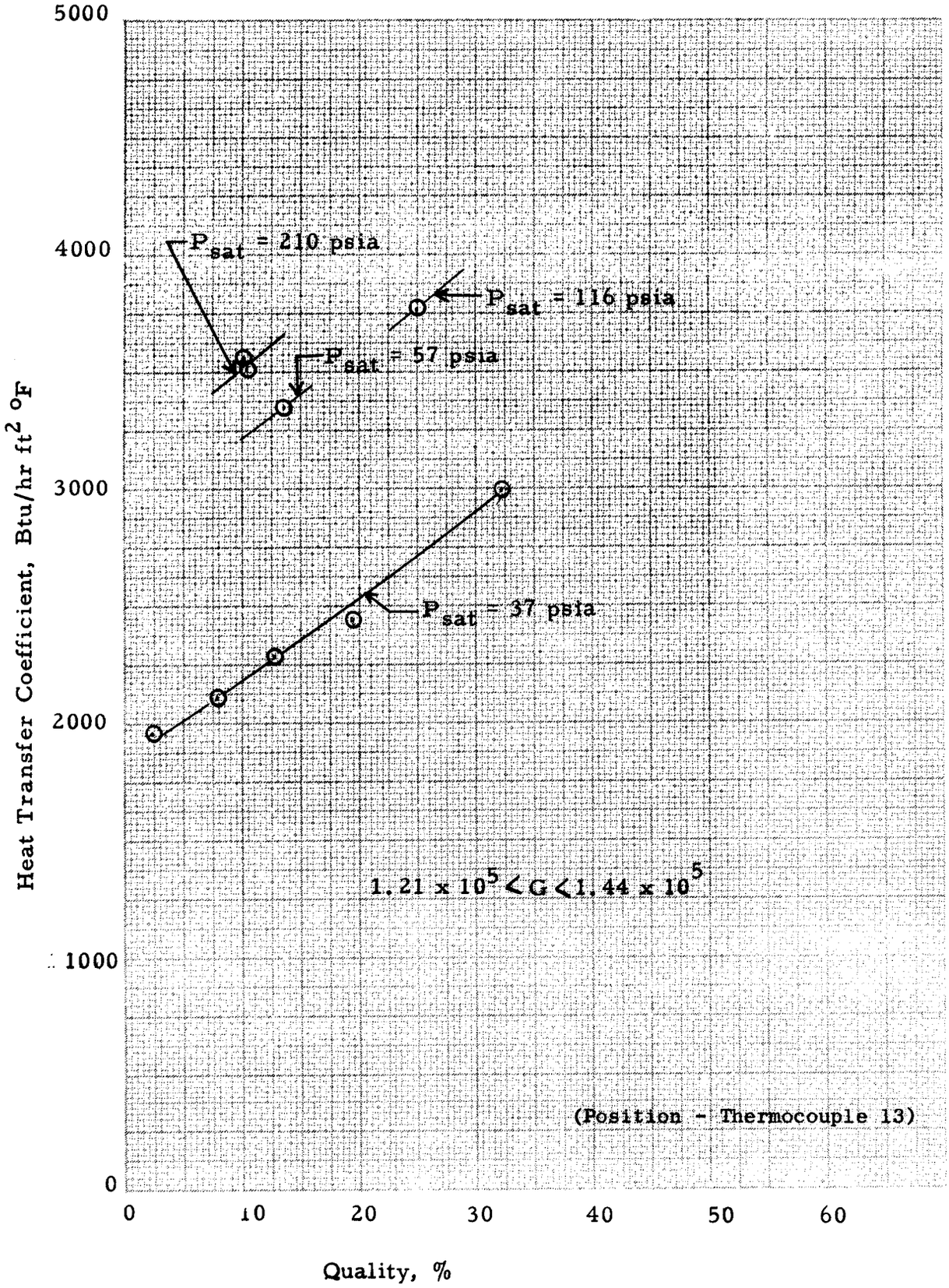

Figure 53. Heat Transfer Coefficients for Boiling Potassium in the 100 KW System.

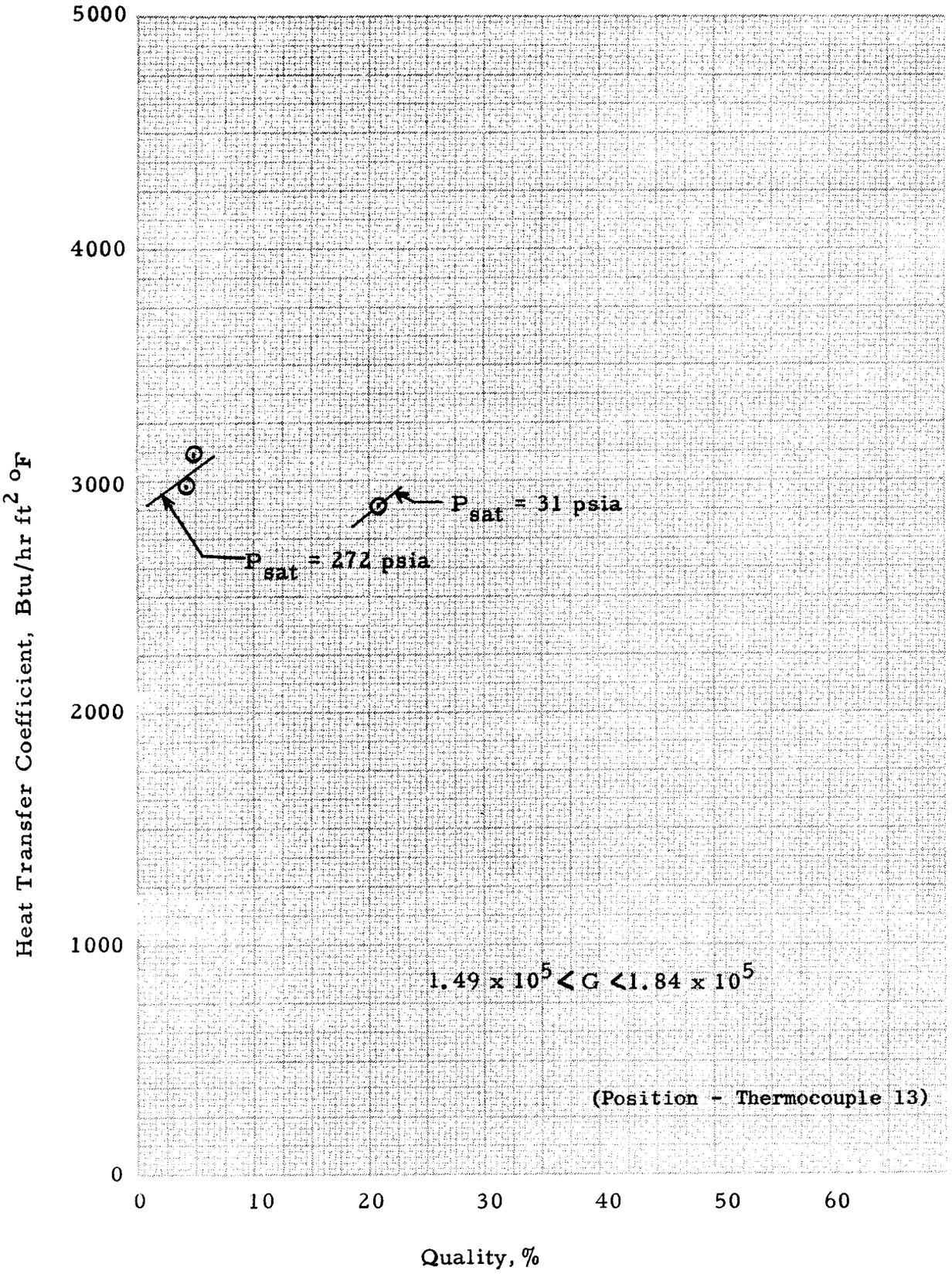

Figure 54. Heat Transfer Coefficients for Boiling Potassium in the 100 KW System.

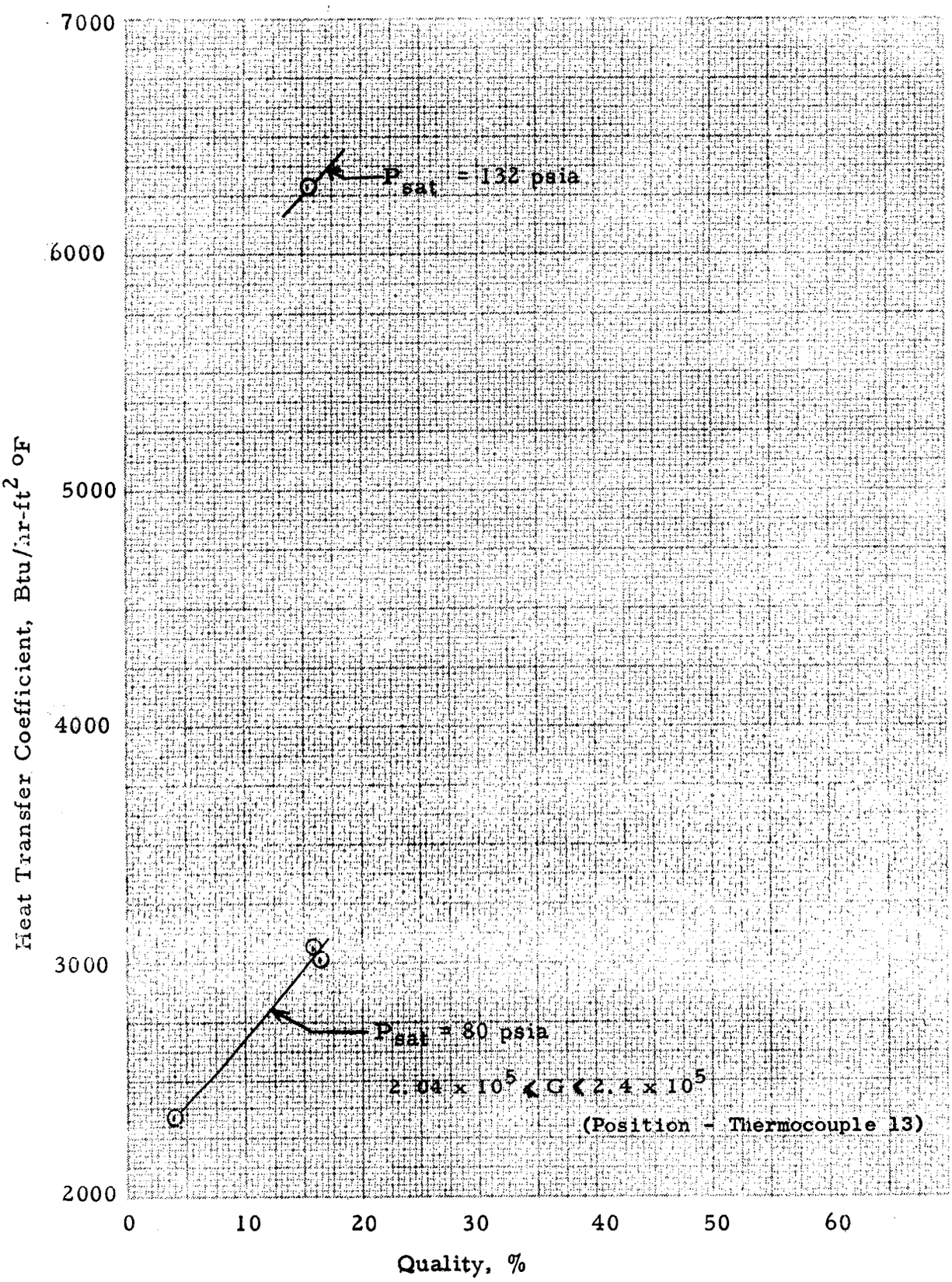

Figure 55. Heat Transfer Coefficients for Boiling Potassium in in the 100 KW System

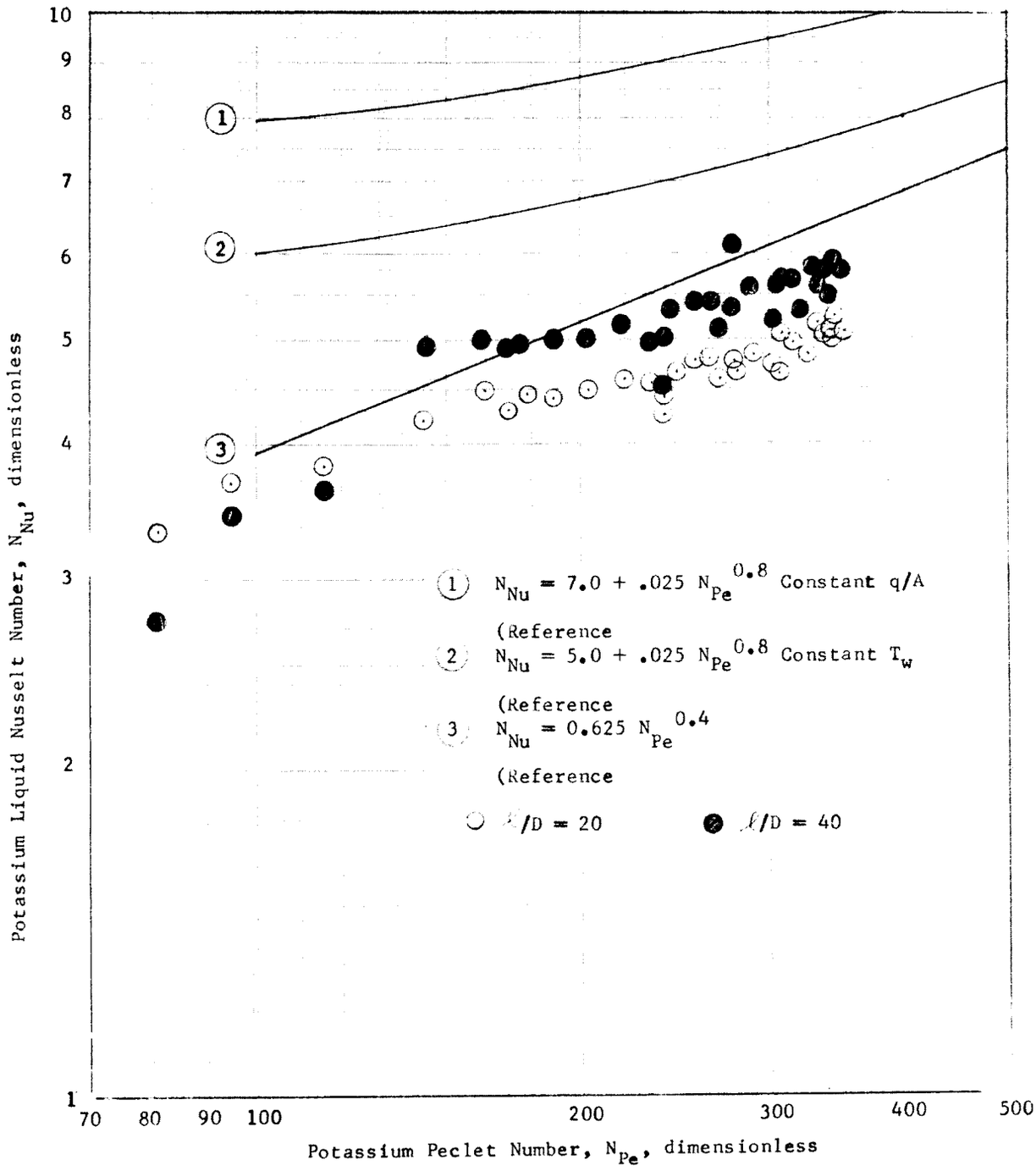

Figure 56. Liquid Heat Transfer Results for Potassium in a 5/8" Diameter Vertical Tube - 50 KW System

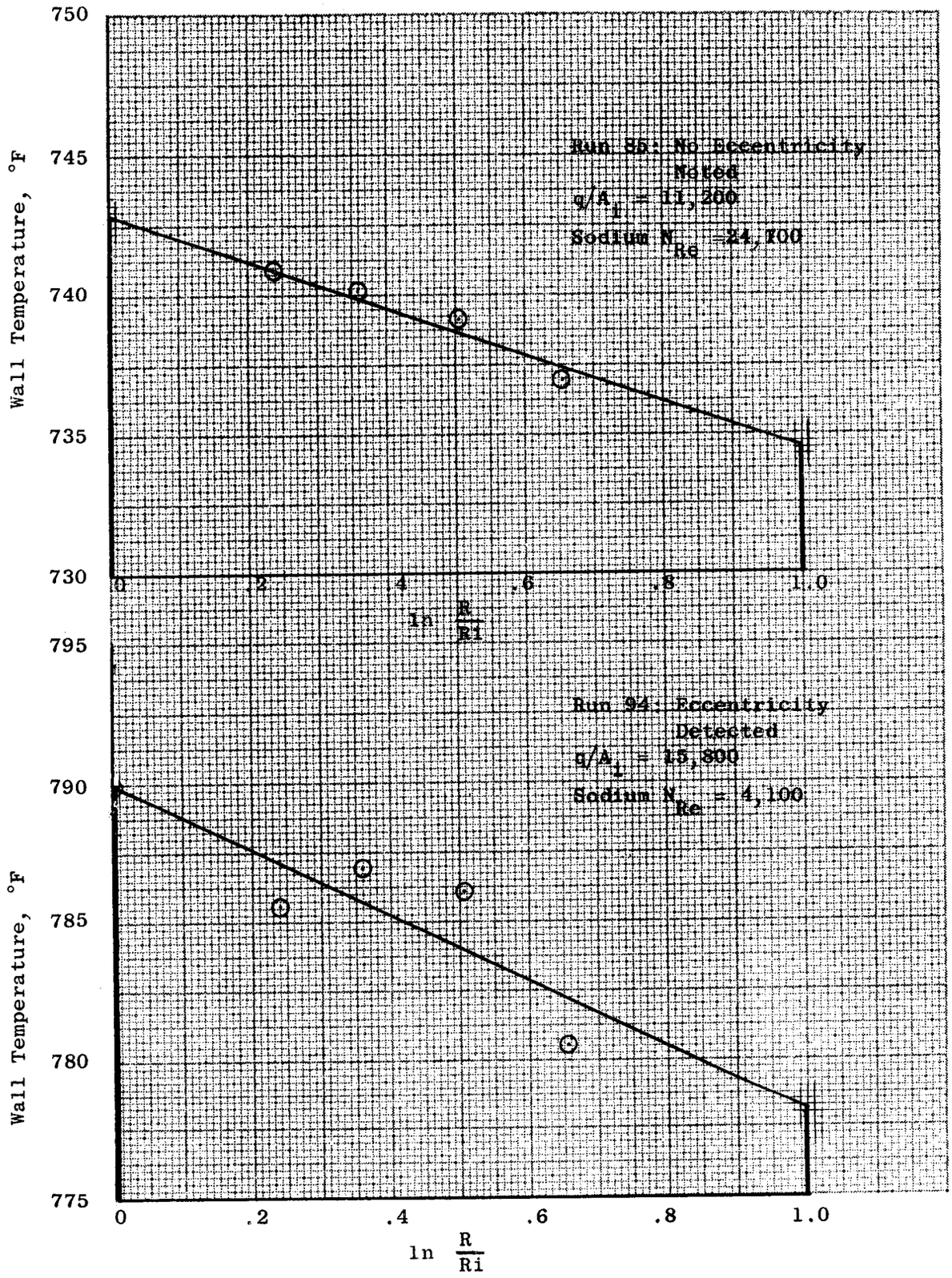

Figure 57. Comparison of Wall Radial Temperature Profile with Varying Sodium Reynolds Number - 50 KW System

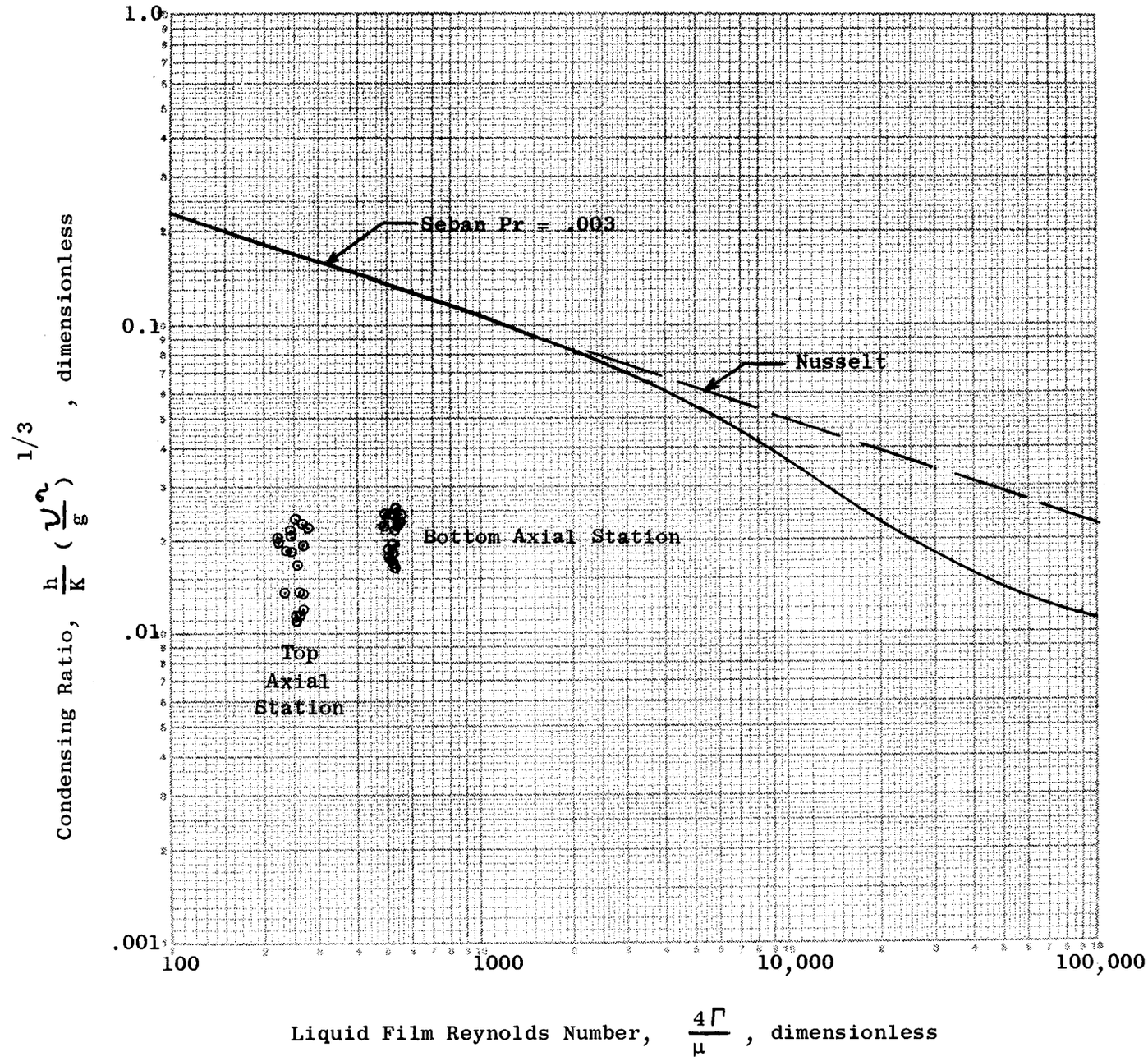

Figure 58. Local Condensing Heat Transfer Results for Potassium Vapor - 50 KW System

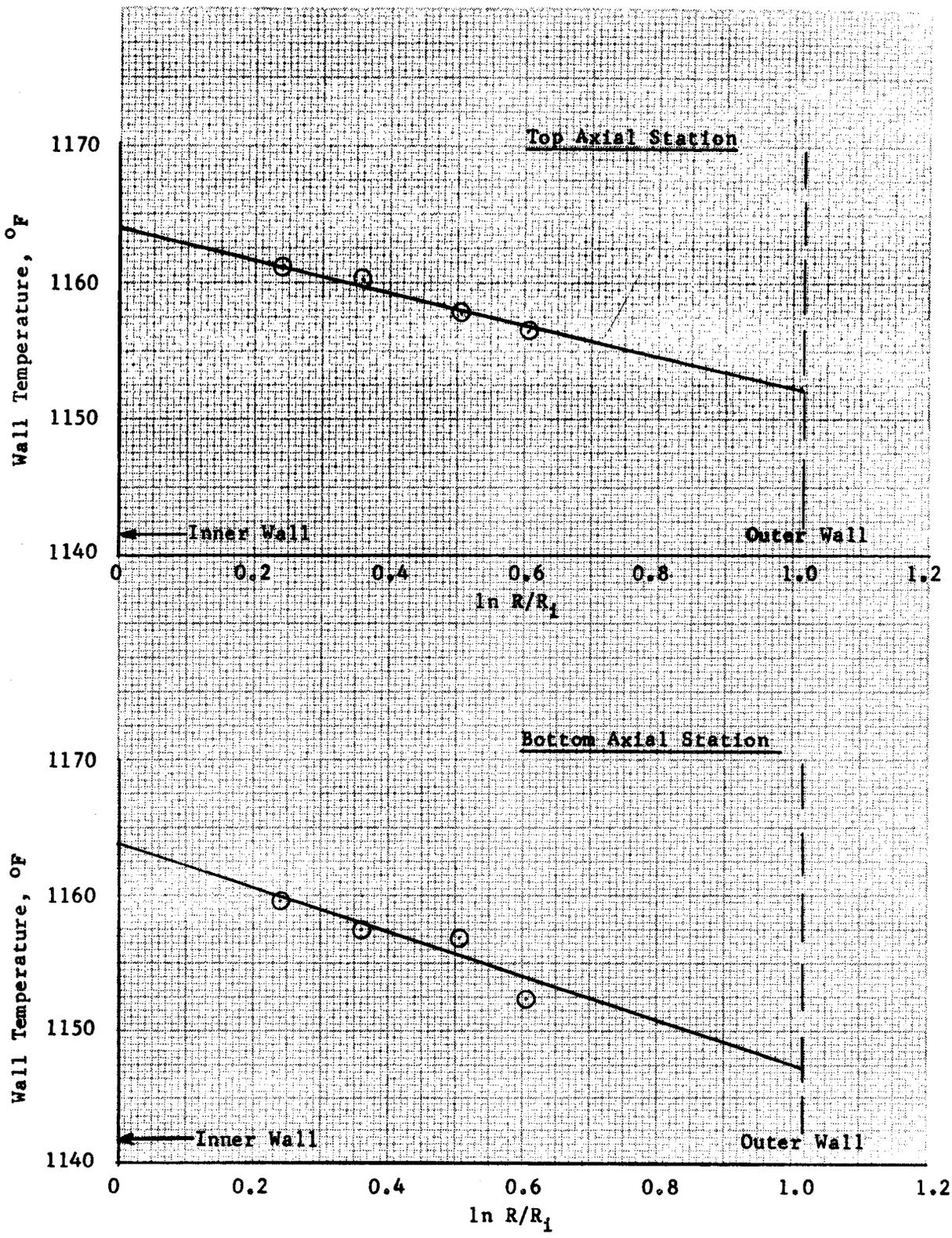

Figure 59. Comparison of Radial Temperature Profiles at Top and Bottom Axial Stations - 50 KW System

Figure 60. Condensing Heat Transfer Results- 50 KW Systems

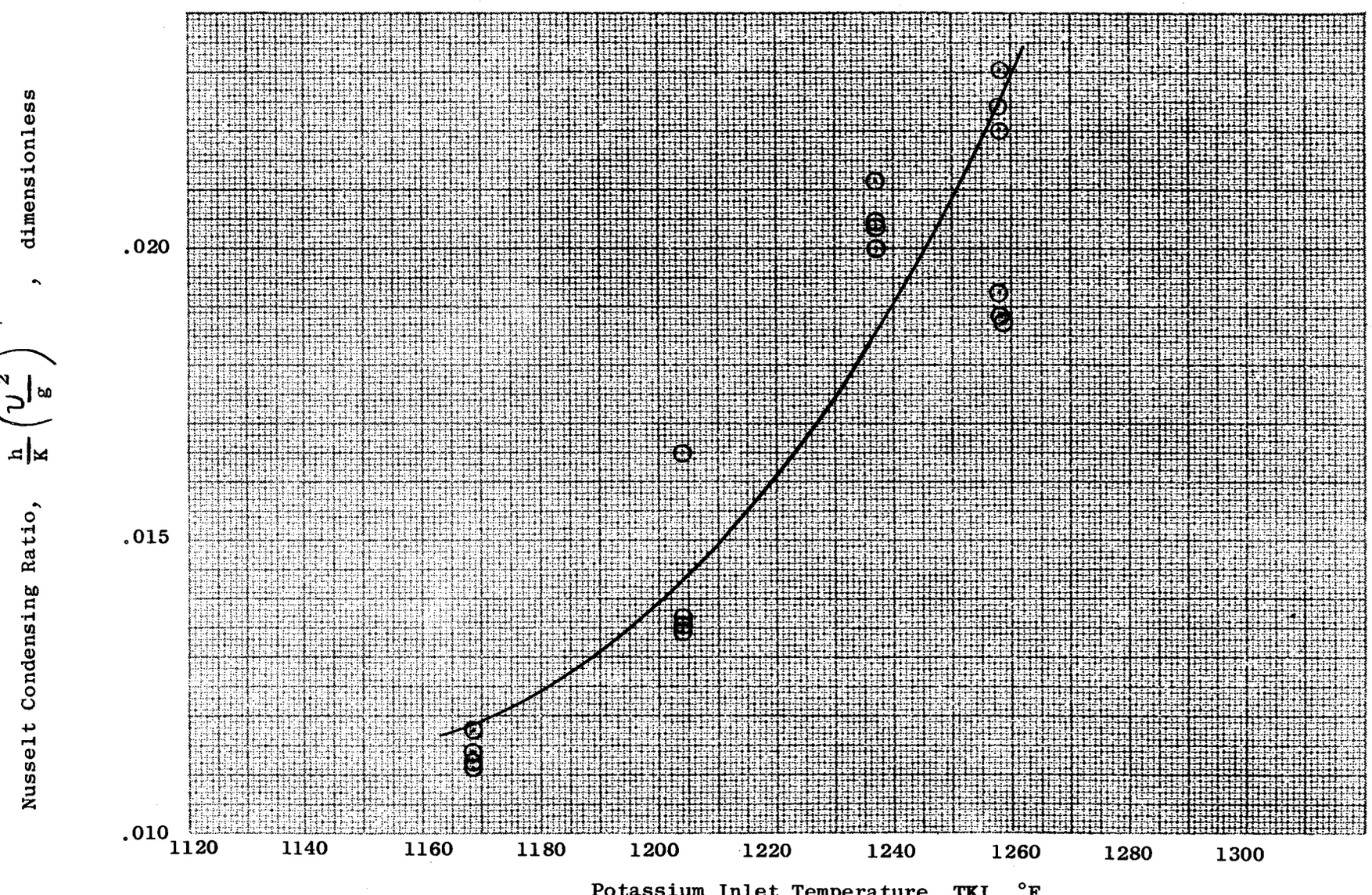

Figure 61. Hypothetical Liquid Vapor Distribution Over a Cross Section

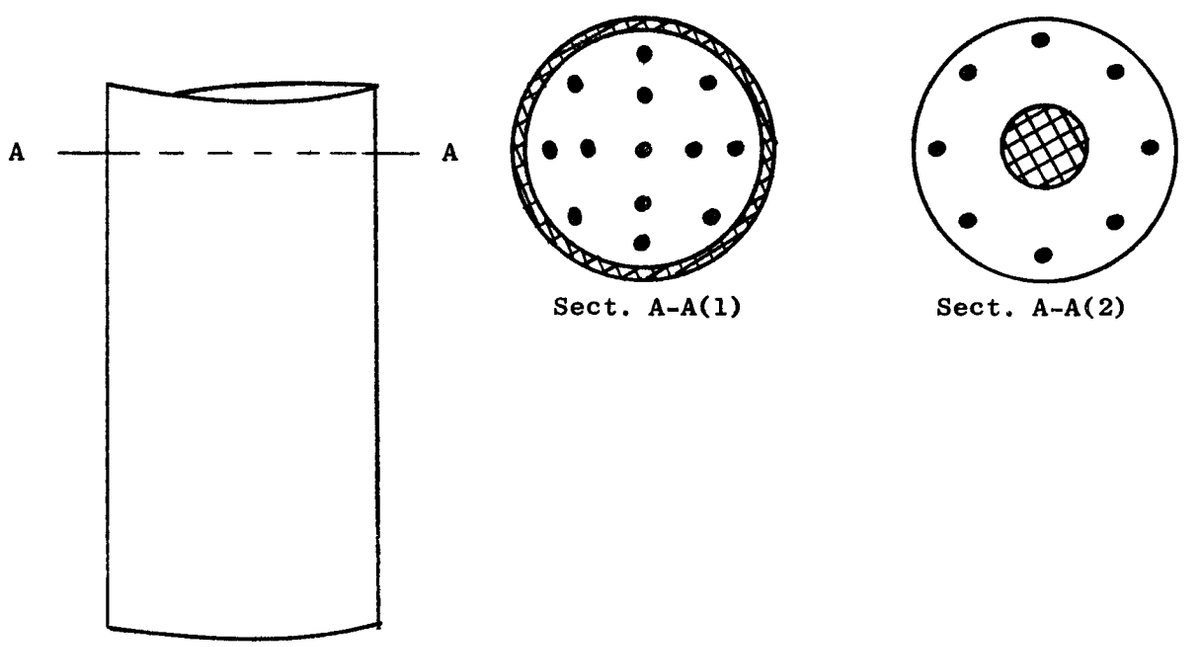

Legend

Vapor (Velocity, V_g)

Liquid (Velocity, V_g)

Liquid (Velocity, $V_{f(a)}$)

Note: The distribution of the two phases over the cross section is immaterial so long as the angular momentum equation is not violated (this implies radial symmetry for the horizontal cross sections shown).

Figure 62. The System Under Investigation

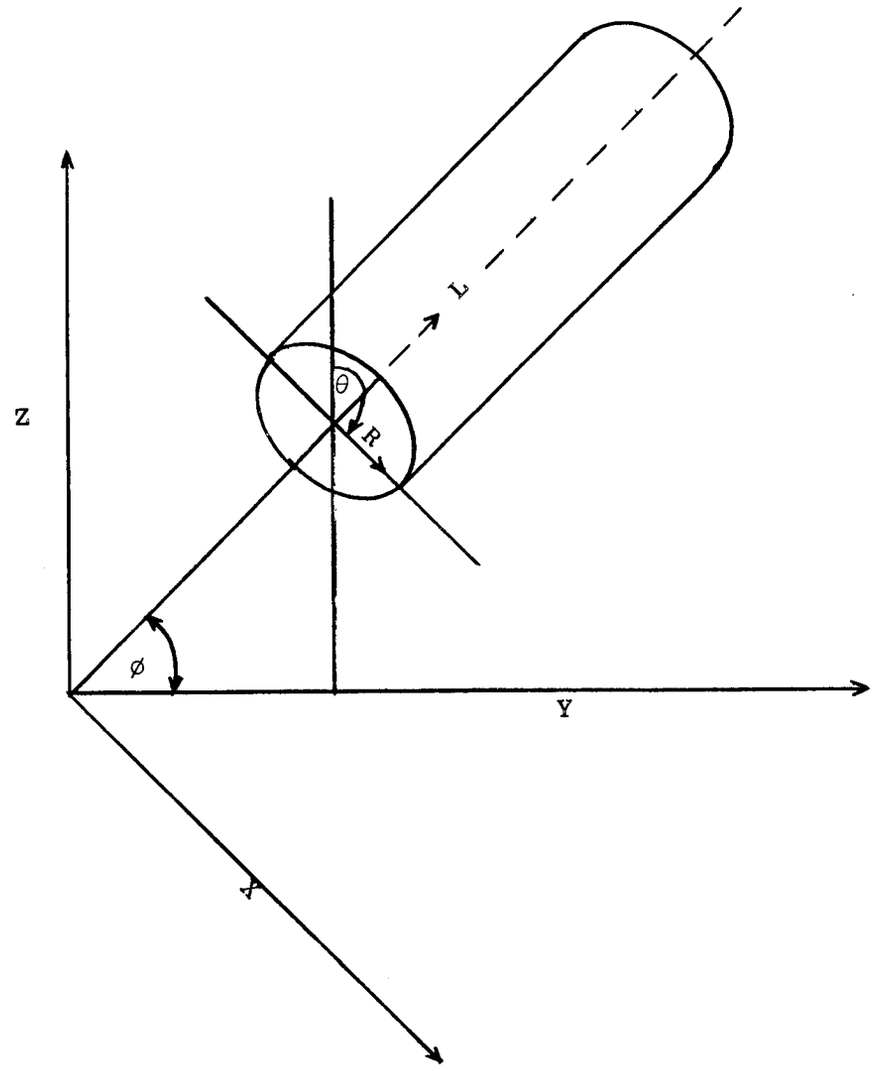

Assumptions:

1. The velocity and density of each phase are functions only of the axial distance L, i.e., they are independent of R and θ.

2. The system is in steady state operation.

3. The pressure is a function only of the axial distance L, i.e., it is independent of R and θ.

4. The wall shear stress (T_w) is a function only of L, i.e., it is independent of θ.

Geometry Conditions: 1. Constant area duct A_T = Constant

2. $A_f + A_g = A_T$

Figure 63. $\left(\frac{\rho_f}{\rho_g}\right)^m$ vs. Saturation Temperature (m = 1, 1/2, 1/3, 0)

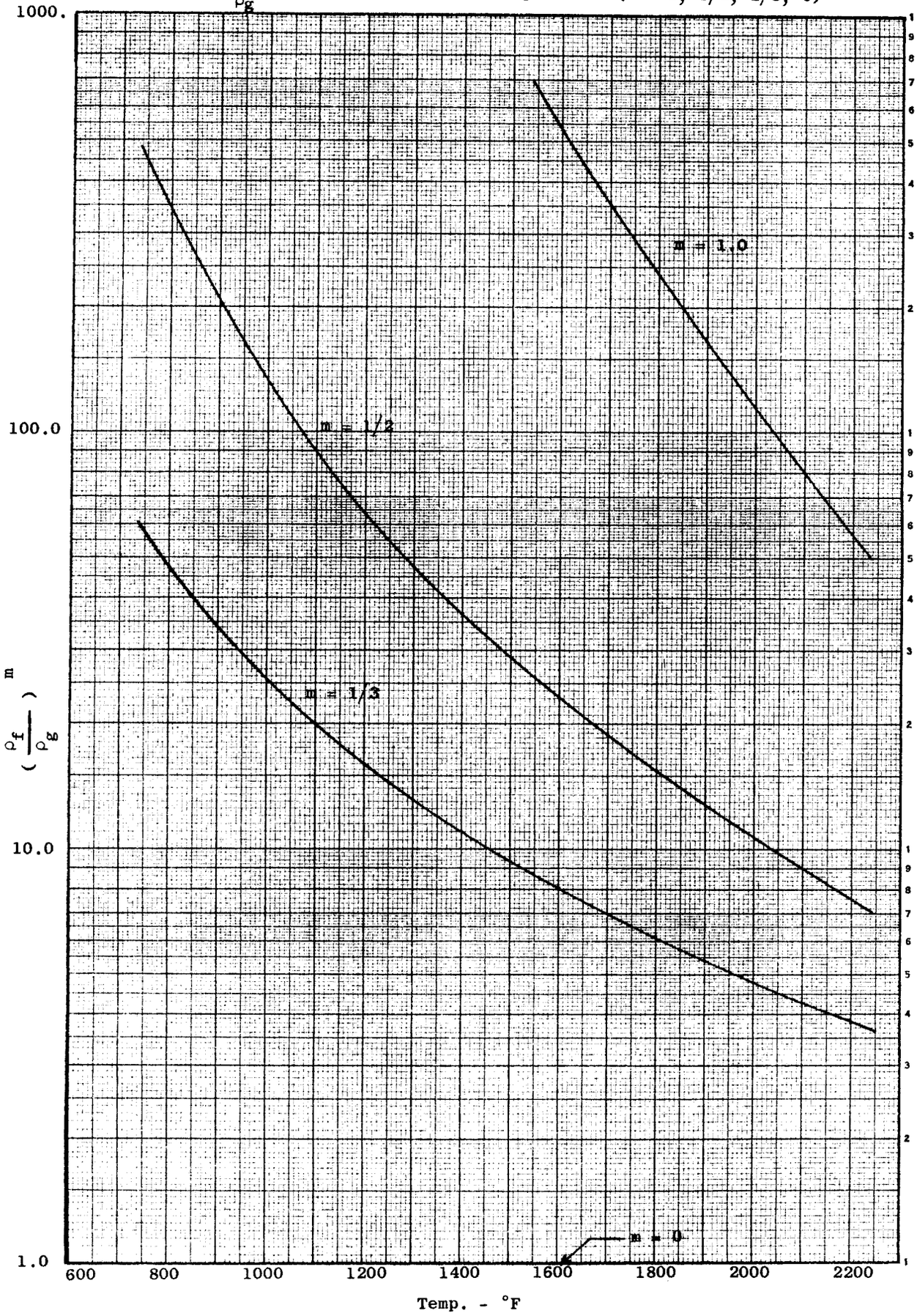

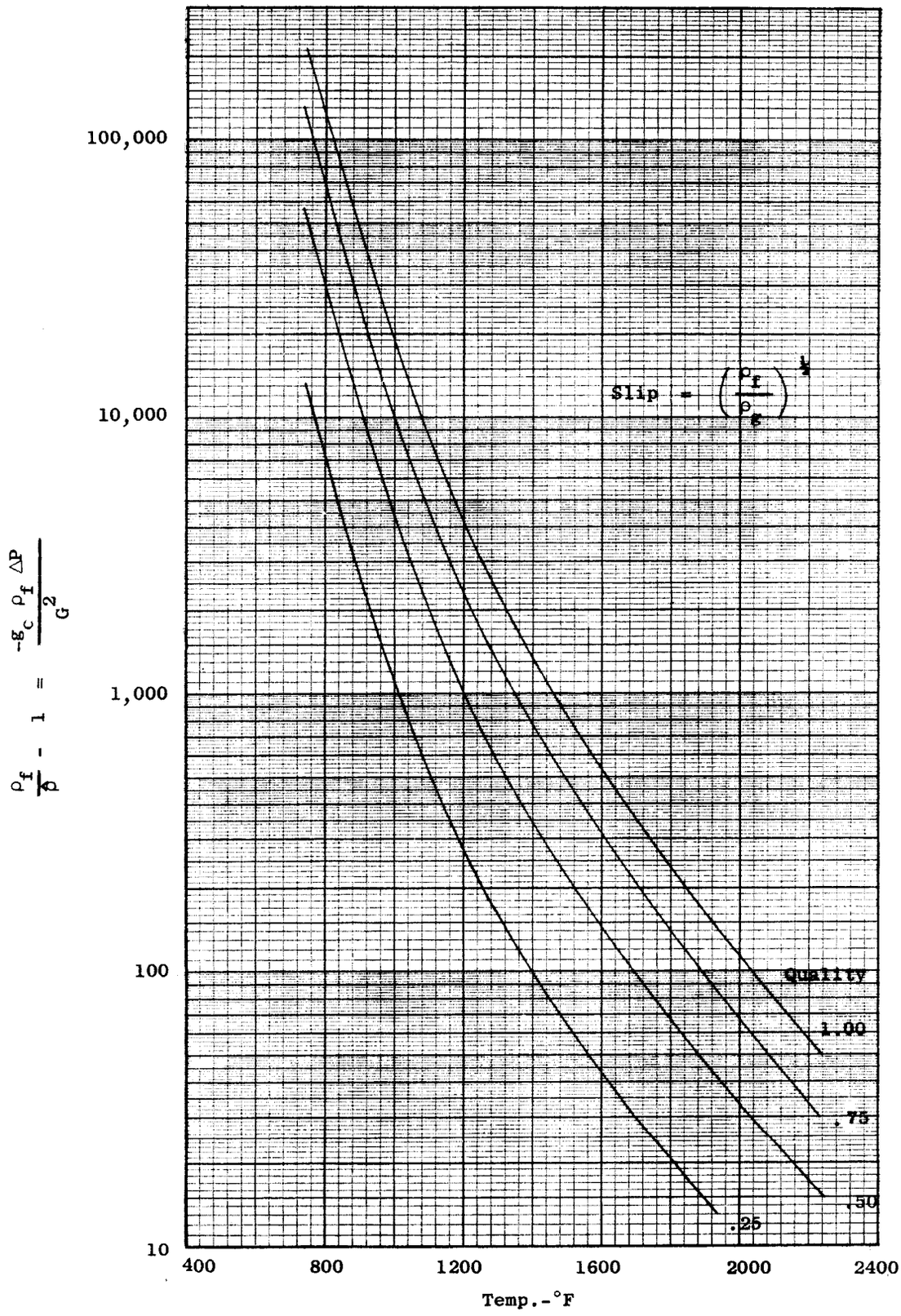

Figure 64.. Minimum Value of the Acceleration Pressure Drop with Quality as a Parameter.

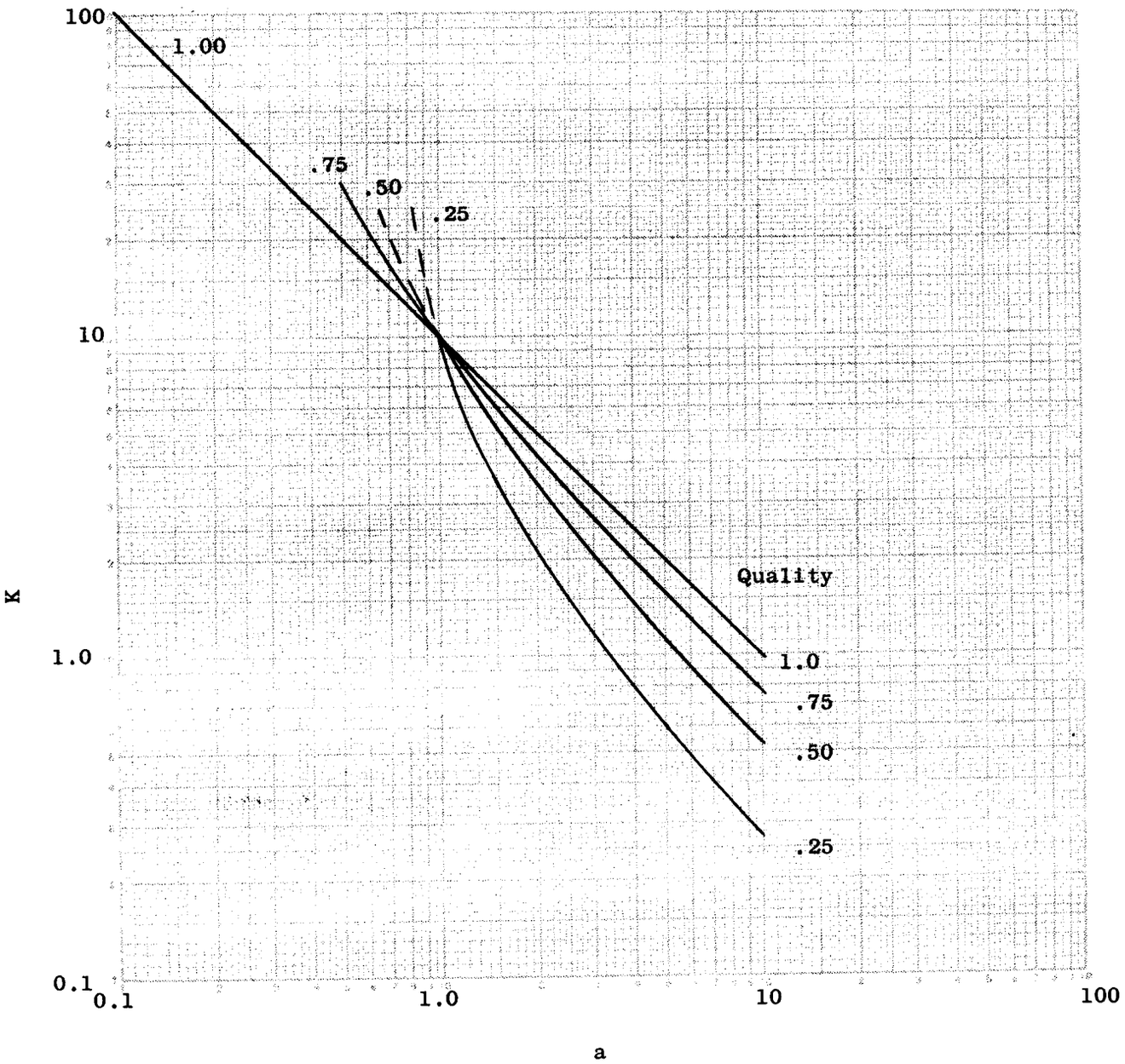

Figure 65. Slip Ratio vs. Acceleration Factor for a Density Ratio of Ten.

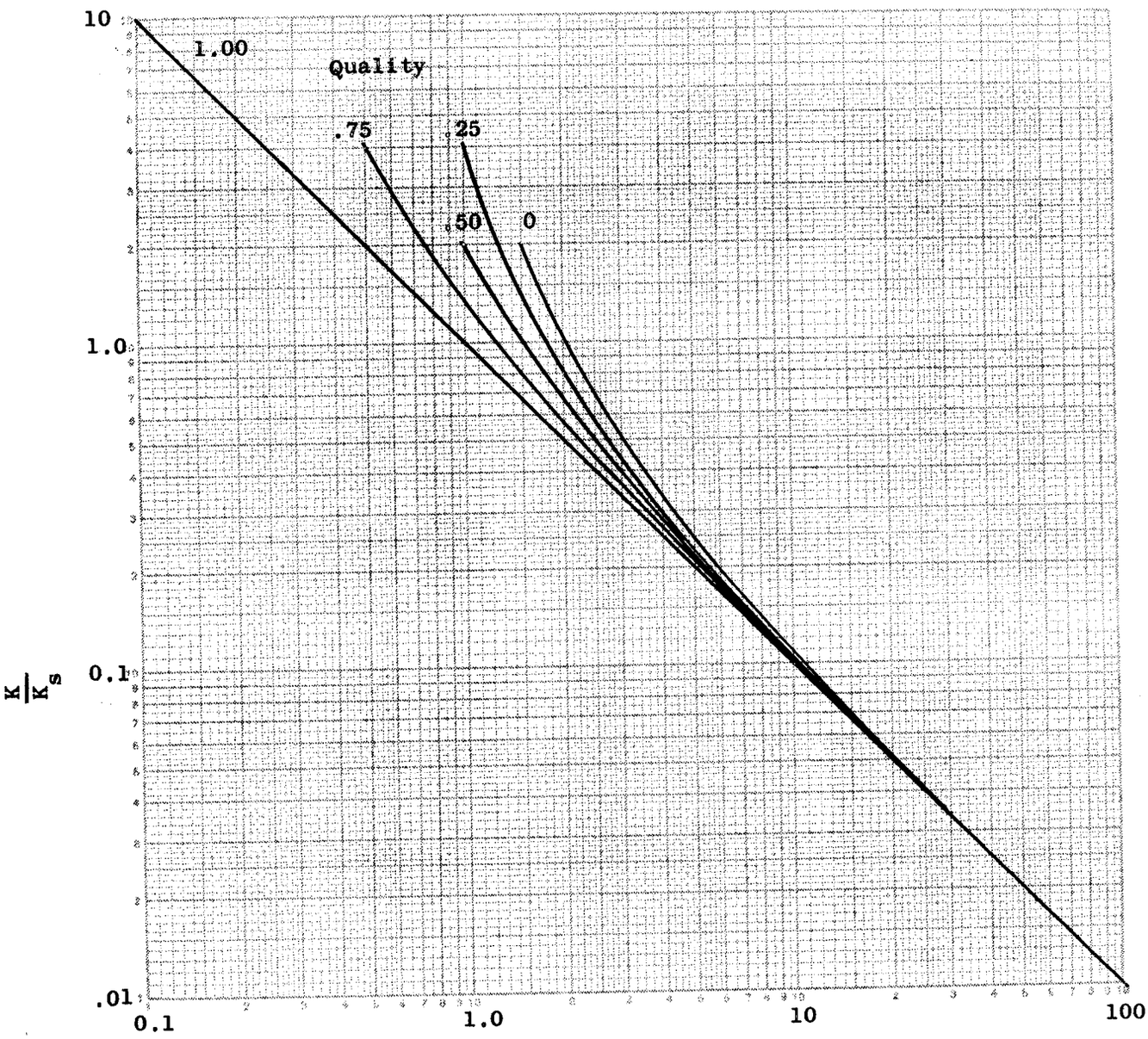

Figure 66. Ratio of Slip to the Superficial Slip vs. the Acceleration Factor (any fluid).

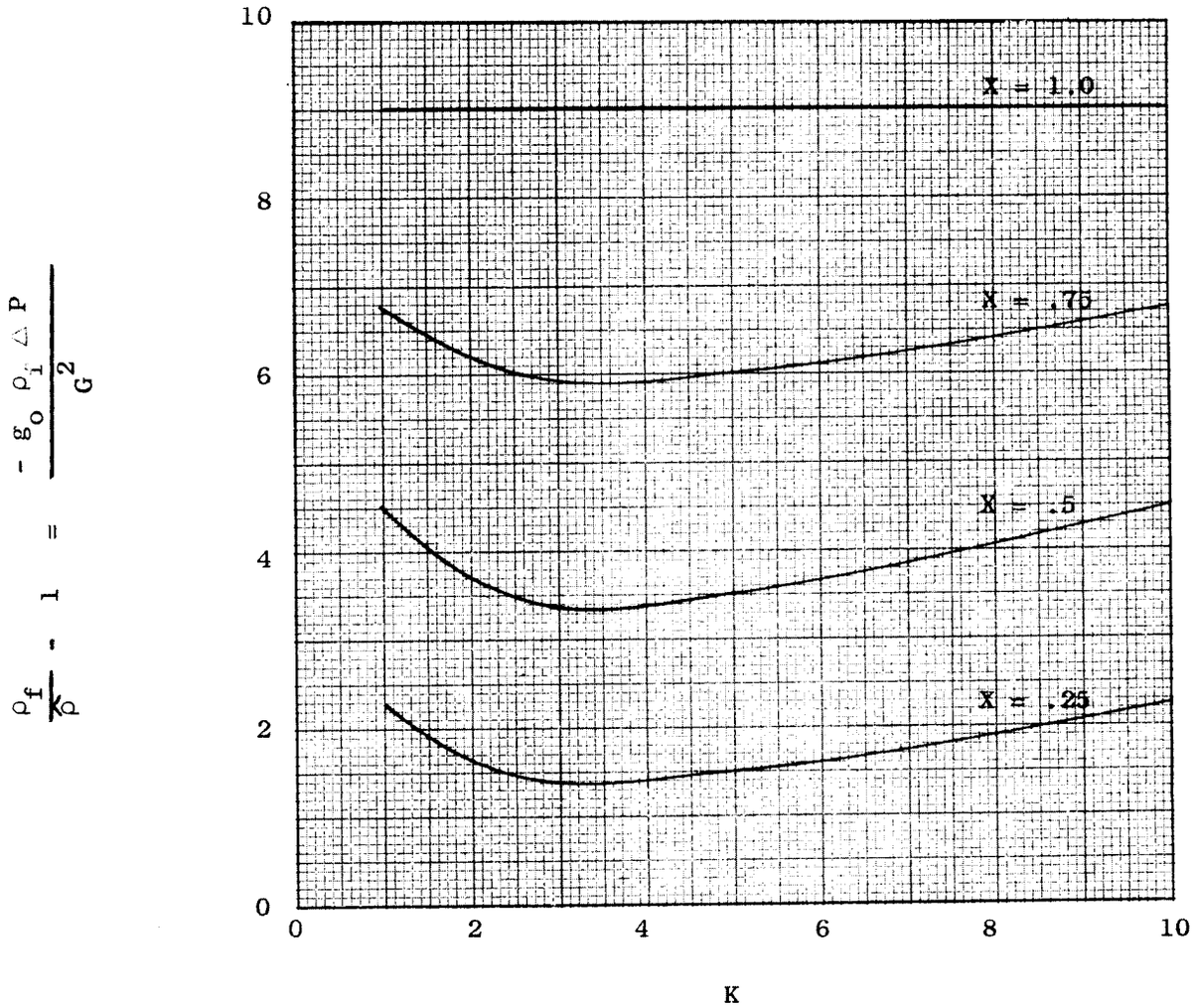

Figure 67. Dimensionless Acceleration Pressure Drop vs. Slip for a Density Ratio of 10.

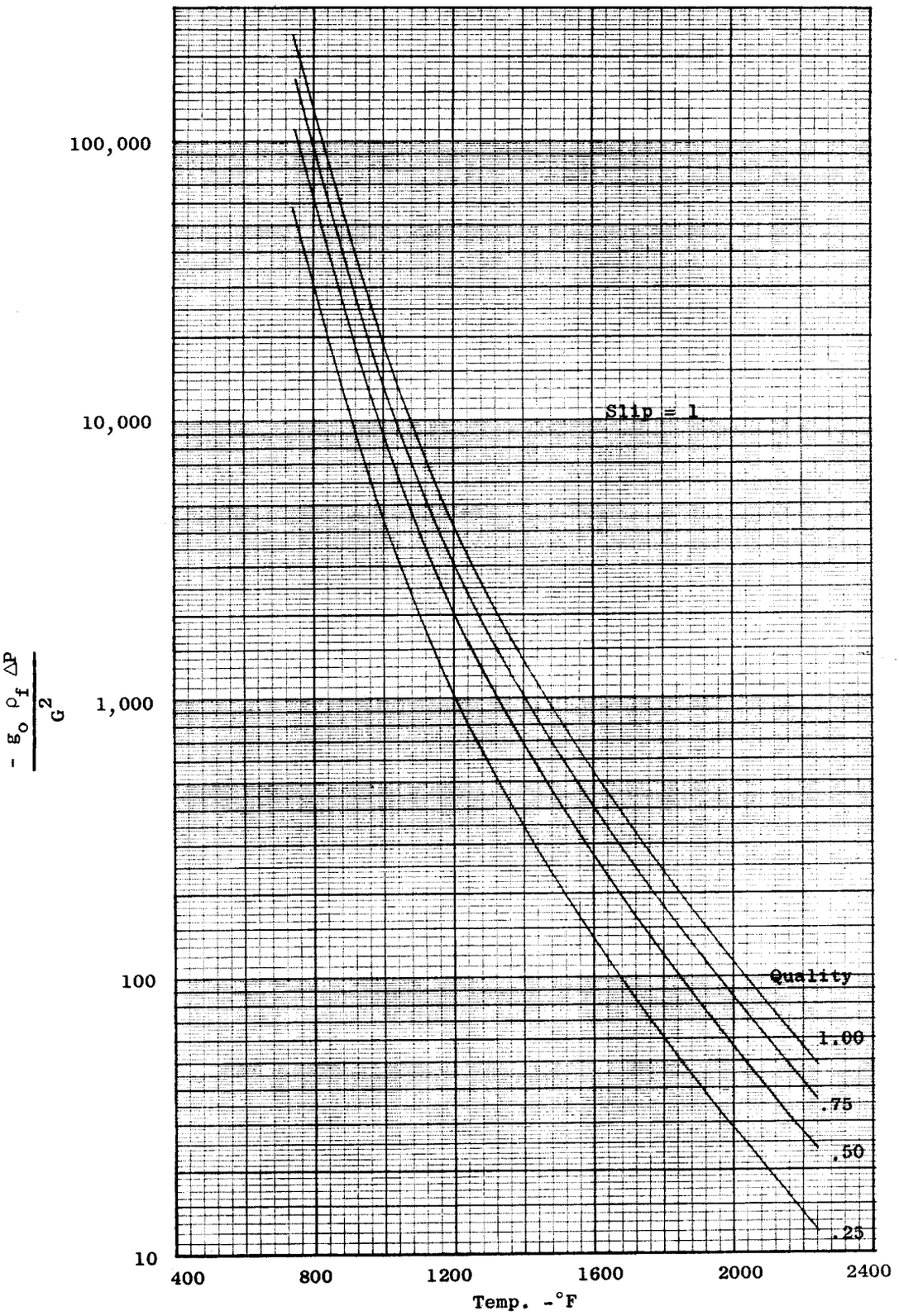

Figure 68. Dimensionless Acceleration Pressure Drop for a Slip of One with Quality as a Parameter

Figure 69. Comparison of Dimensionless Acceleration Pressure Drops for $K = 1$ and $K = \left(\frac{\rho_f}{\rho_g}\right)^{1/2}$

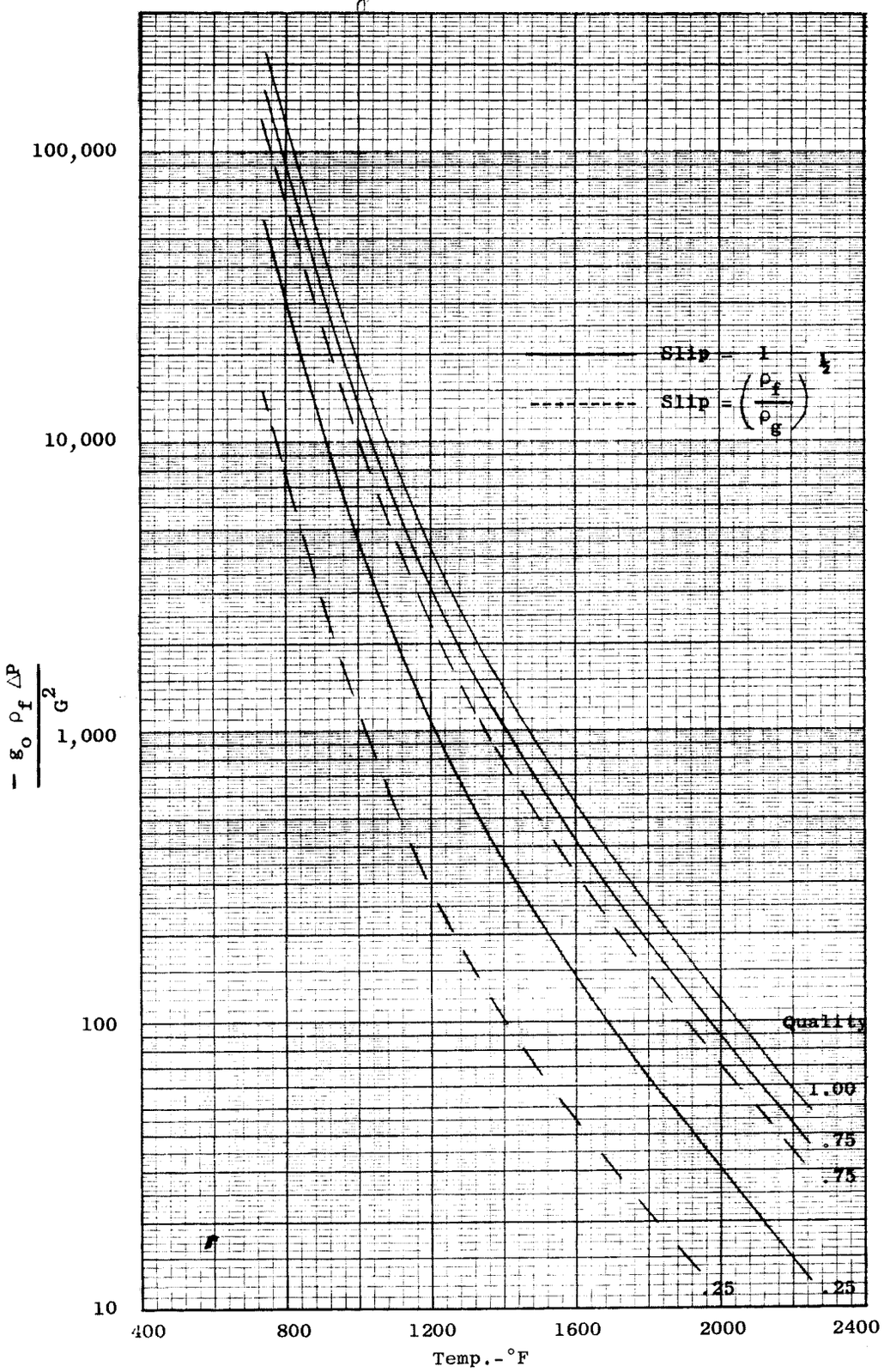

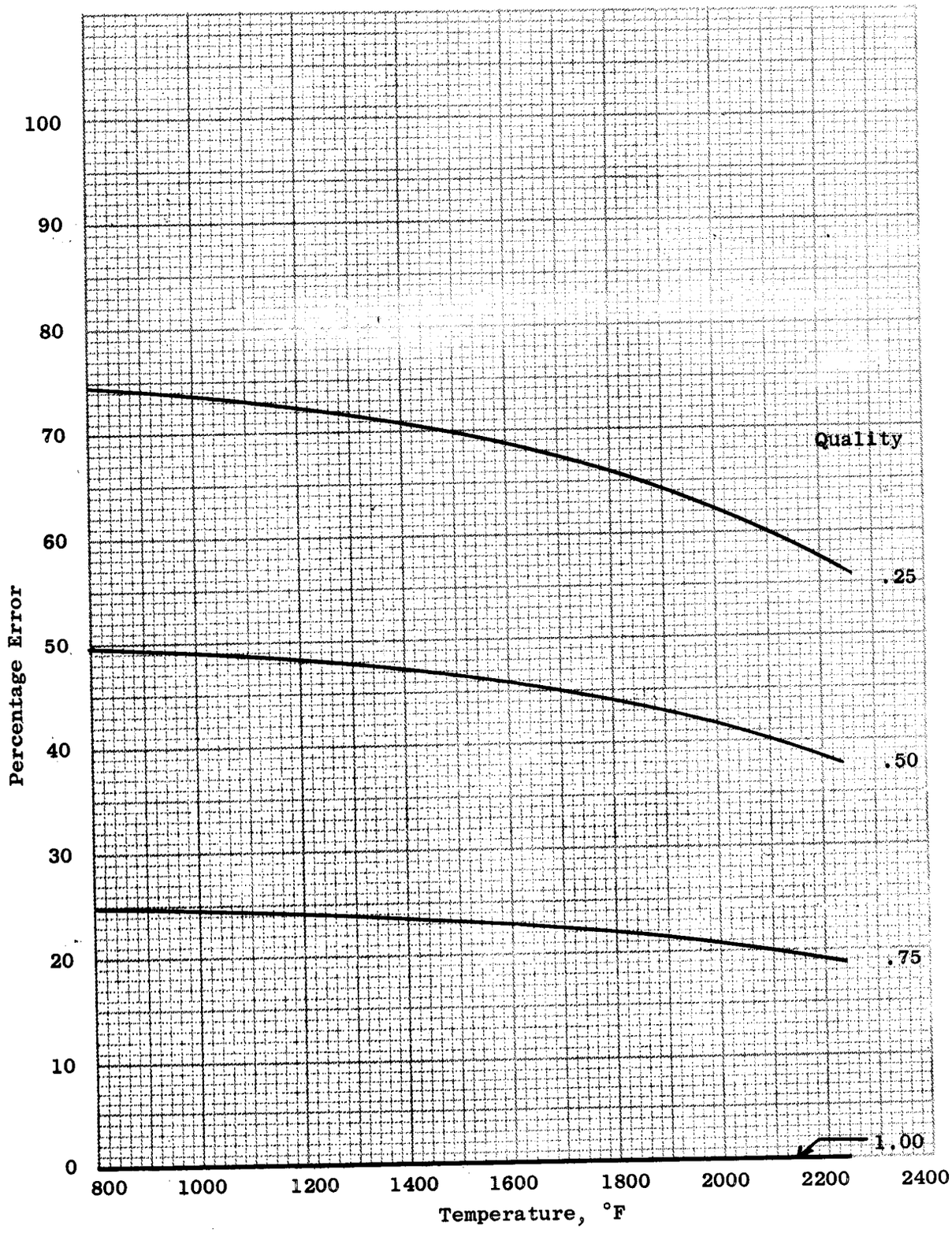

Figure 70. Percentage Error in the Acceleration Pressure Drop Due to the Uncertainty in the Slip Ratio (Quality Parameter)

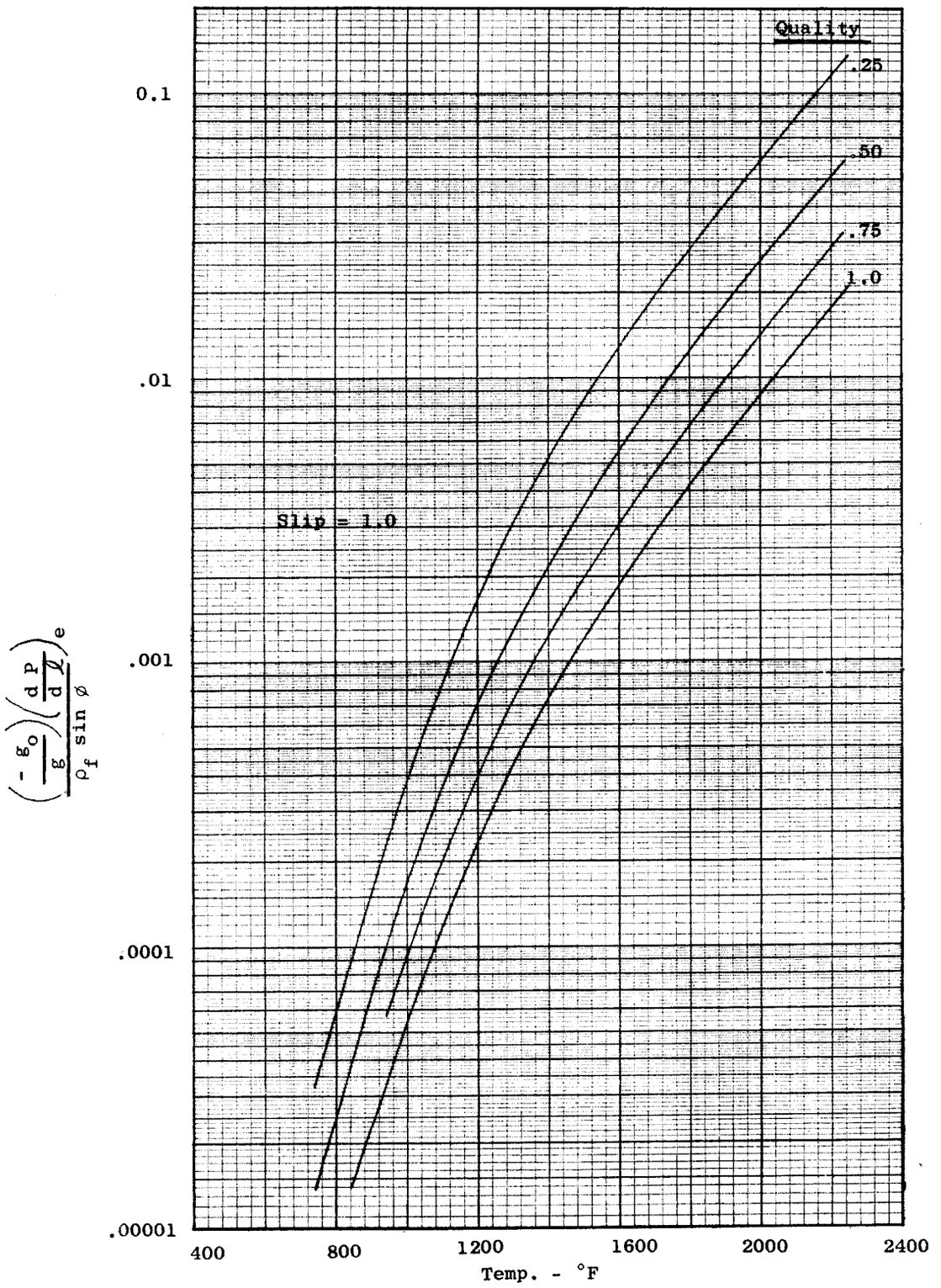

Figure 71. Dimensionless Elevation Pressure Drop for K = 1.

Figure 72. Dimensionless Elevation Pressure Drop for $K = \left(\frac{\rho_f}{\rho_g}\right)^{1/2}$

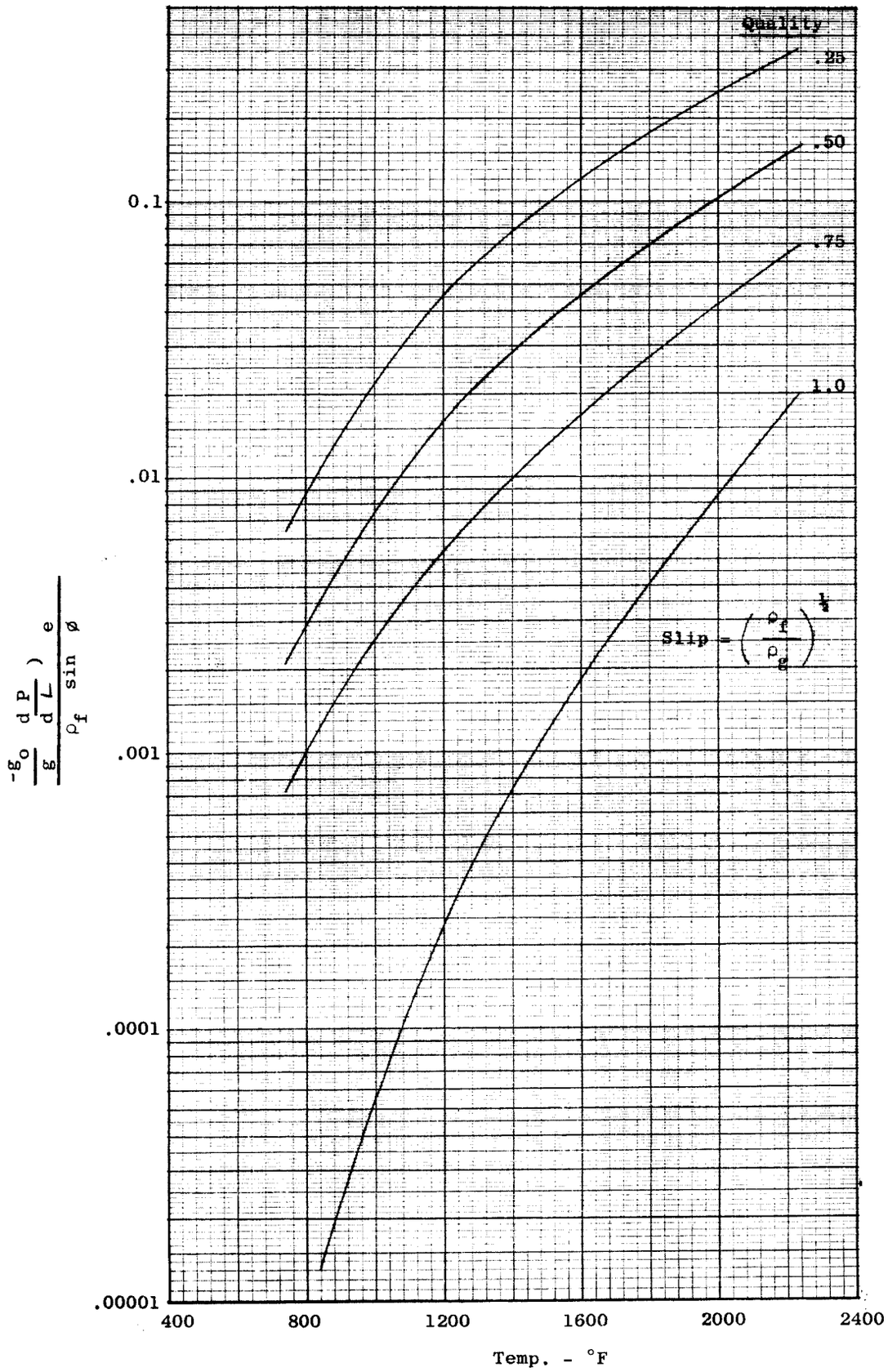

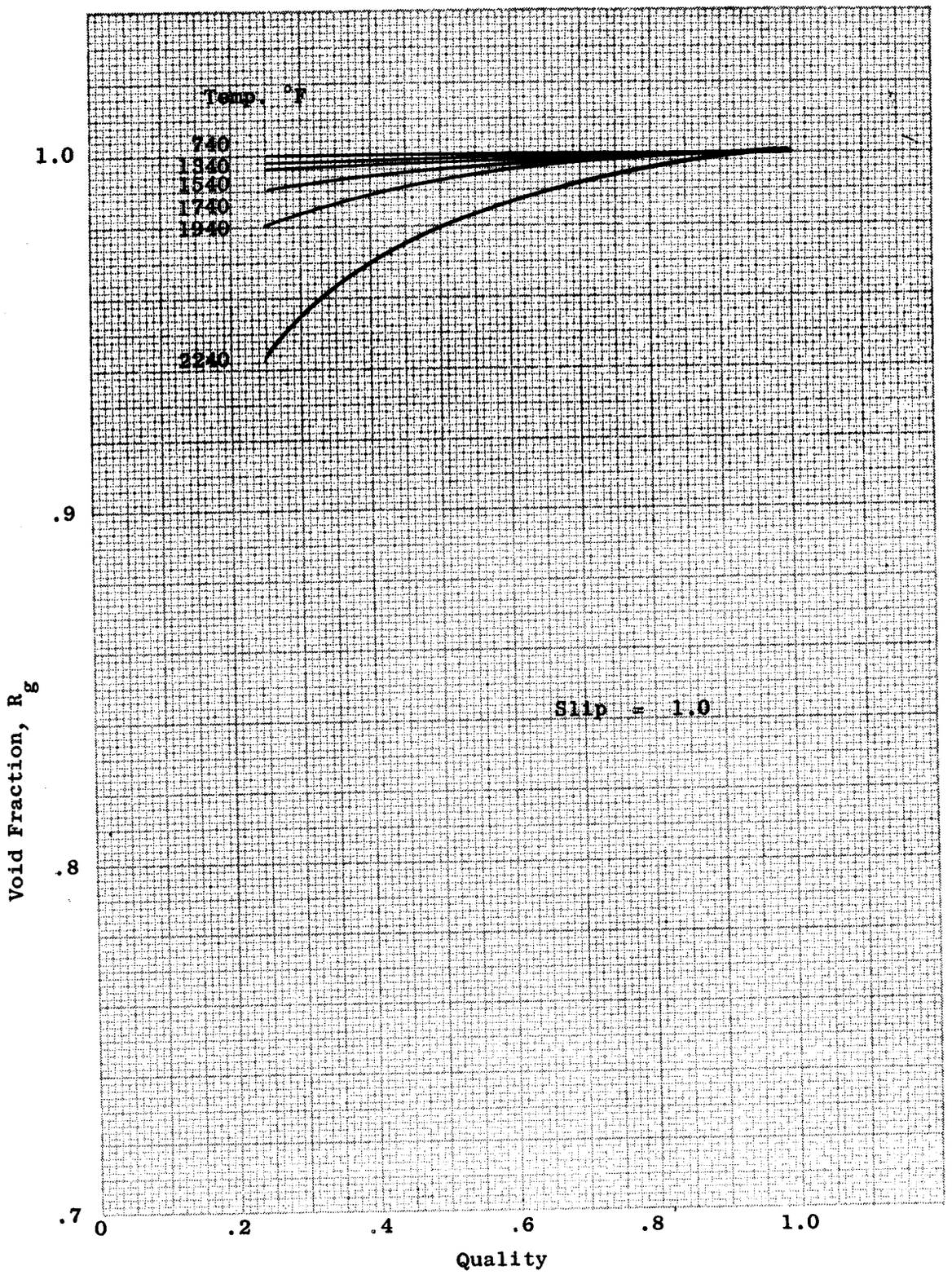

Figure 73. Void Fraction vs. Quality for Potassium (K = 1.0)

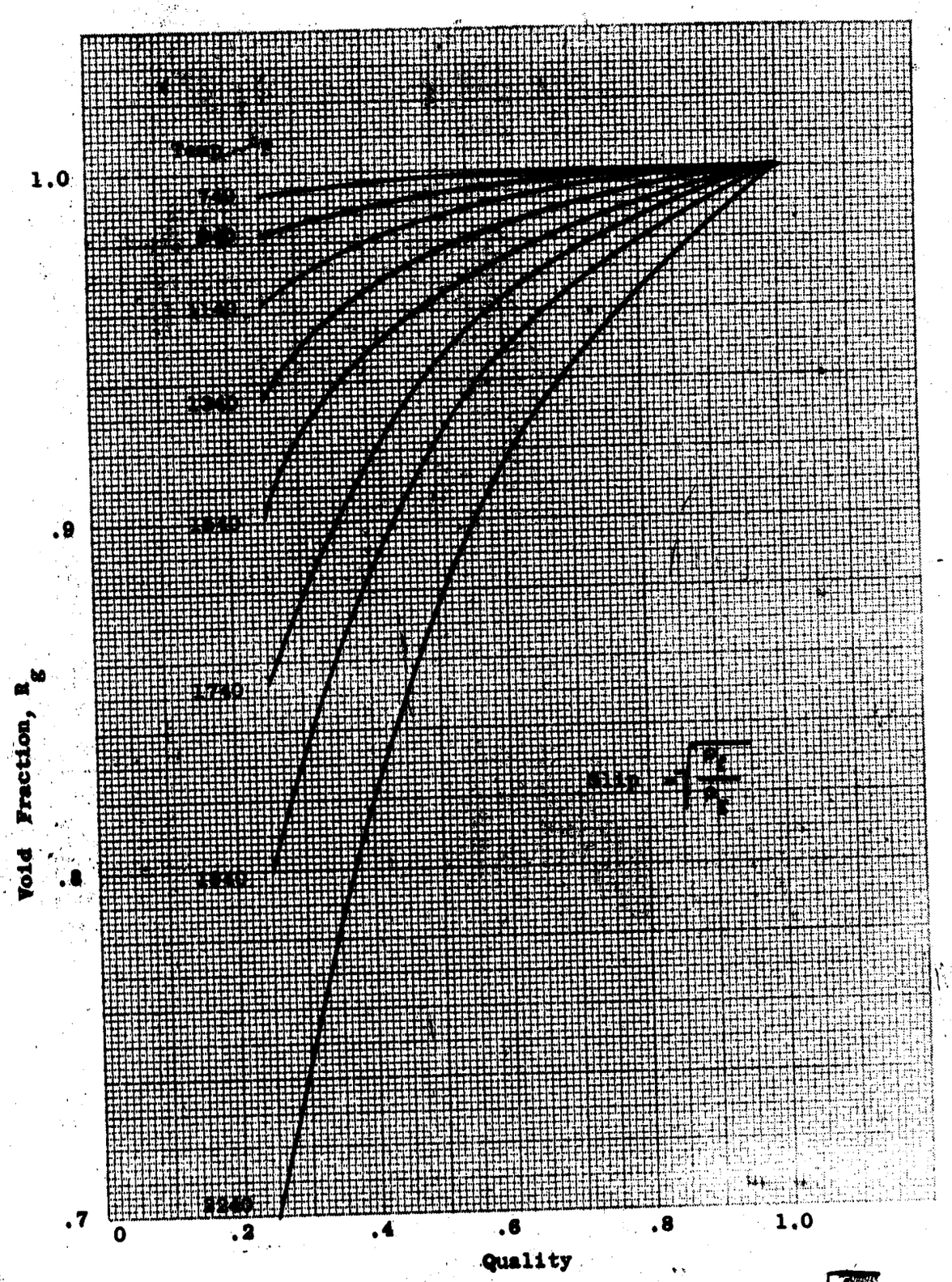

Figure 74. Void Fraction vs. Quality for Potassium ($K = \sqrt{\frac{\rho_f}{\rho_g}}$)

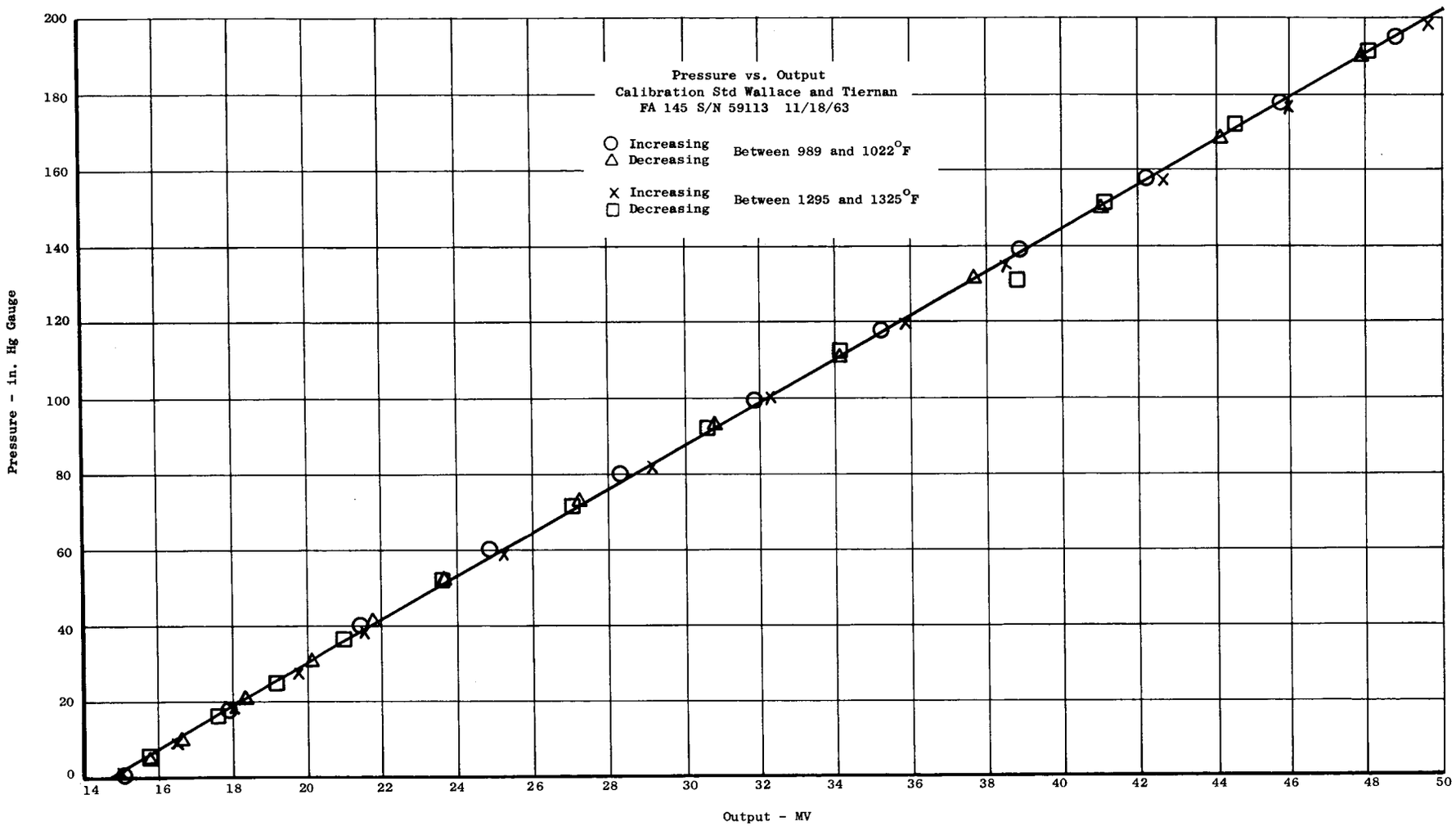

Figure 75. Boiler Inlet Pressure Gage Calibration - 300 KW System

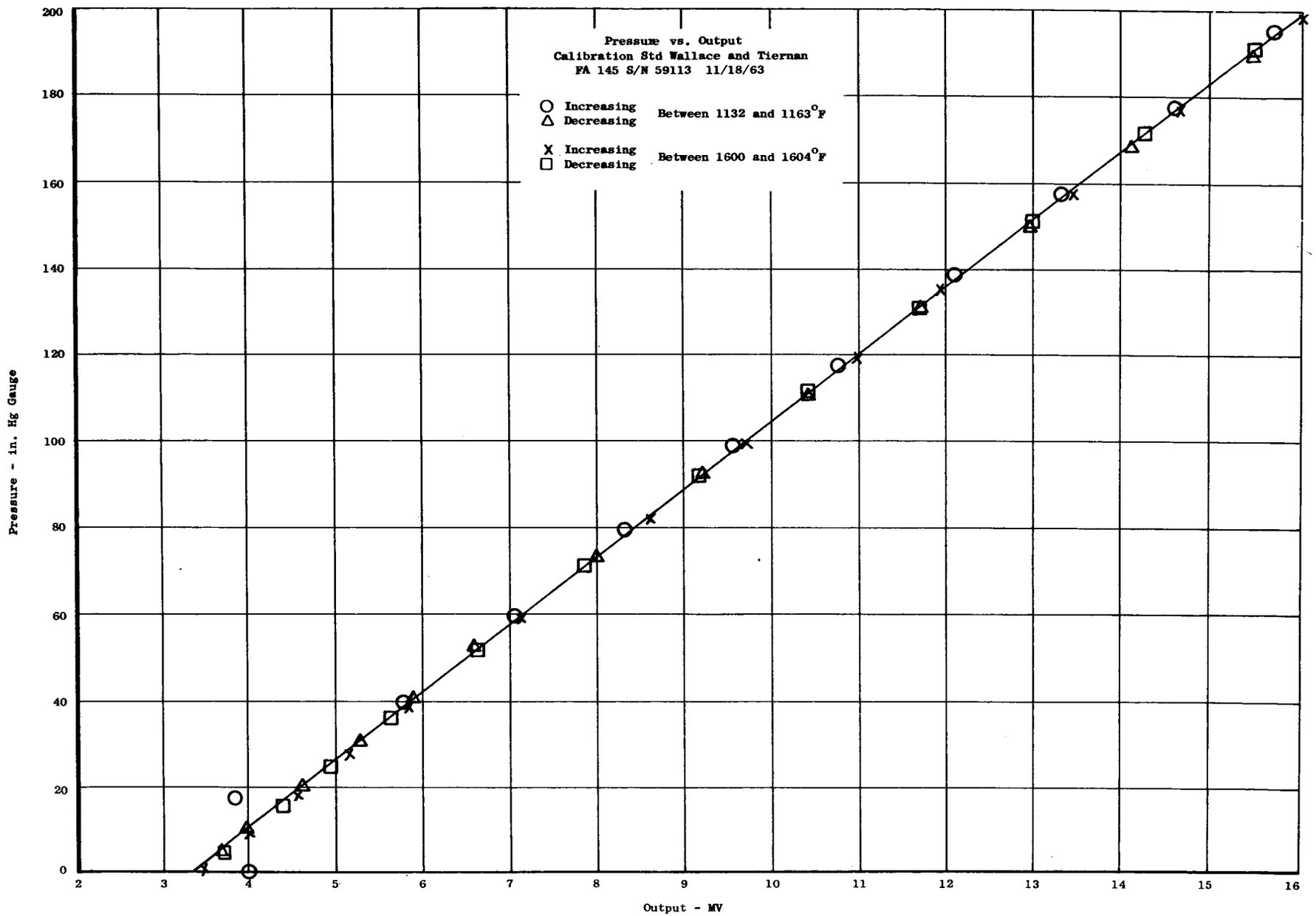

Figure 76. Boiler Exit Pressure Gage Calibration - 300 KW System

REFERENCES

1 "Alkali Metals Boiling and Condensing Investigation," Quarterly Rept. 3, Ctr. NAS 5-681, SPPS, MSD, General Electric Company, October, 1961.

2 "Alkali Metals Boiling and Condensing Investigations," Quarterly Rept. 5, Volumes I and II, Ctr. NAS 3-2528, SPPS, MSD, General Electric Company, January, 1964.

3 "Alkali Metals Boiling and Condensing Investigations," Quarterly Rept. 4, Ctr. NAS 3-2528, SPPS, MSD, General Electric Company, August, 1963.

4 Silvestri, M, "Two Phase (Steam and Water) Flow and Heat Transfer," Paper 39 International Heat Transfer Conference, 1961, University of Colorado, Boulder, Colorado.

5 Tippets, F. E., "Analyses of the Critical Heat Flux Condition in High Pressure Boiling Water Flows," Paper 62 -WA - 161, ASME November, 1962.

6 Waters, E. D., et al., "Experimental Observations of Upstream Boiling Burnout," Preprint 7, AIChE, August, 1963.

7 Lowdermilk, W. H., et al., "Investigation of Boiling Burnout and Flow Stability for Water Flowing in Tubes," Technical Note 4382, NACA, September, 1958.

8 "Alkali Metals Boiling and Condensing Investigations," Quarterly Repts. 2 and 3, Ctr. NAS 3-2528, SPPS, MSD, General Electric Company, March, 1963.

9 "Data in the Temperature Range of 1200 to 2700°R," SPPS, MSD, General Electric Company, January 7, 1964.

10 "Haynes Alloy No. 25," Haynes Stellite Co., March 1959.

11 Semmel, J. W., et al., "Alkali Metals Boiling and Condensing Investigations, Final Report, Vol. I, Materials Support," Ctr , NAS 5-681, SPPS, MSD, General Electric Company, January, 1963.

12 Leiblein, S., "Analysis of Temperature Distribution and Radiant Heat Transfer Along A Rectangular Fin of Constant Thickness," Technical Note D-196, NASA.

13 Lyon, R. N., "Liquid Metal Heat Transfer Coefficients," Chemical Engineering Progress, 47, 75 (1951).

14 Lubarsky, B., et al., "Review of Experimental Investigations of Liquid Metal Heat Transfer," Technical Note 1270, NACA, 1956.

15 Johnson, H. A., and Hartnett, J. P., "Heat Transfer to Lead Bismuth and Mercury in Laminar and Transitum Pipe Flow," Paper 53-A-188, ASME, November, 1953.

16 Johnson, H. A., et at., "Heat Transfer to Mercury in Turbulent Pipe Flow," ASME Paper 53-A-189, November, 1953.

17 Bonilla, C. F., Personal Communication.

18 Polomik, E. E., "Vapor Voids in Flow Systems from a Total Energy Balance," Rept. GEAP 3214, General Electric Company, August, 1959.

19 "Investigation of Liquid Metal Boiling Heat Transfer", Technical Document Report No. RTD-TDR-63-4130, Air Force Aero Propulsion Laboratory Research and Technology Division, Air Force Systems Command, Wright-Patterson Air Force Base, Ohio, Pages 100 thru 105, November 1963.

20 "Liquid Metals Handbook, Sodium - NaK Supplement", July, 1955, Atomic Energy Commission, Department of the Navy.

21 Lemmon, A.W., (Jr.), Deem, H.W., Hall, E.H., and Walling, J.R., "The Thermodynamic and Transport Properties of Potassium", Battelle Memorial Institute.

22 Hildebrand, F.B., "Method of Applied Mathematics", Prentice Hall, Inc., Englewood Cliffs, N.J., 1952.

APPENDICES

Appendix		Page
A.	EVALUATION OF THE 300 KW FACILITY MULTITUBE BOILER CONCEPT	159
B.	100 KW FACILITY HEAT TRANSFER DATA	161
C.	50 KW FACILITY HEAT TRANSFER DATA	195
D.	A CALORIMETRIC METHOD FOR THE MEASUREMENT OF ALKALI METAL FLOW RATE	273
E.	DERIVATION OF THE EXPRESSION FOR THE TWO-PHASE GRADIENT FROM CONTINUITY AND MOMENTUM CONSIDERATIONS	279
F.	DERIVATION OF THE RELATIONSHIP BETWEEN SLIP, VOID FRACTION, AND FLOWING QUALITY	283
G.	EXPRESSIONS FOR THE SLIP AND SHAPE FACTOR IN TERMS OF THE ENTRAINMENT FRACTION FOR THE MODIFIED ANNULAR FLOW MODEL	285
H.	THE DETERMINATION OF EXPRESSIONS FOR SEVERAL OF THE DENSITIES IN TERMS OF THE SLIP RATIO	289
I.	THE DETERMINATION OF THE DERIVATIVE OF $1/\hat{\rho}$ WITH RESPECT TO THE SLIP RATIO	291
J.	THE RELATIONSHIP BETWEEN THE SLIP RATIO AND THE ACCELERATION FACTOR	293
K.	PROOF THAT THE VALUE OF $1/\hat{\rho}$ IS IDENTICAL FOR A SLIP OF ONE AND A SLIP EQUAL TO ρ_f/ρ_g.	295

APPENDIX A. EVALUATION OF THE 300 KW FACILITY MULTITUBE BOILER CONCEPT

The multitube boiler concept, which is reviewed in Section I.A. of this sixth quarterly report, is to provide a more advanced boiler geometry for testing in the 300 kw facility than the present single tube design affords. Basically, a straight and a coiled tube design configuration are being considered. Here, the advantages and disadvantages of each are enumerated.

Straight Tube Boiler

Advantages

1. A straight tube annular arrangement is thermally similar to existing 300 kw single tube boiler.

2. Structural piping loads are confined to the short squat shell section, eliminating boiler shell bending and associated problems.

3. Inserts may be installed or withdrawn with minimum rework.

4. The two-pass tube arrangement precludes a bellows expansion joint.

5. Thermal and mechanical test data from the 300 kw single tube are more applicable design information for this unit.

6. A two-pass secondary tube doubles the boiler tube length for the same shell length.

7. Secondary tube inlet and exit conditions can be instrumented readily for pressure and/or temperature.

Disadvantages

1. Leakage from the primary inlet to exit compartment, which will effect over-all performance, is of concern.

2. The secondary manifold requires complex longitudinal welding.

3. During fabrication and operation, the annulus spacing must be controlled within extremely close tolerance.

4. A significant temperature difference in the secondary manifold compartment may be a problem relative to thermal stress.

5. Servicing and inspecting the annulus boiler tubes is more difficult.

6. Fitting this design into the existing 300 kw facility requires significant repiping.

7. The hairpin bend tube requires 28'-0 lengths; the availability in seamless tube is questionable. The floating header arrangement, however, requires 14'-0 lengths.

Coiled Tube Boiler

Advantages

1. Coiled boiler tubes preclude a bellows expansion joint.

2. Coiled tube geometry provides approximately 3 times the boiler tube length for the same shell length.

3. The arrangement of the secondary and primary nozzles locations require minimum repiping for installation into the 300 kw facility.

4. Compared to the straight tube configuration, fewer special forged and shaped parts are required.

5. Less welding is required because most joints are girth welds; some noncritical joints are longitudinally welded.

6. Secondary tube inlet and exit conditions can be instrumented readily.

Disadvantages

1. The coil tube configuration requires a longer tube length (approximately 28'); the availability in seamless tube is questionable.

2. A longer fabrication time is anticipated because of the coiling operation required.

3. If a swirl insert is used within the coiled tube, some development time may also be necessary.

4. With the unit mounted in a vertical position during operation, special precautions in design must be developed to prevent coil collapse and a tensile load on upper tube header joint.

5. Correlation between present 300 kw single straight tube boiler data and information obtained from this coiled tube design is not straight forward.

APPENDIX B. 100 KW FACILITY HEAT TRANSFER DATA

The heat transfer data obtained in the 100 kw facility during this quarter include liquid potassium and stable boiling runs. Because of changes in instrumentation, the latter are reported in two groups. Presentation of each of the three sets of data comprises three parts:

1) A schematic description of the boiler test section thermocouple locations appropriate to the tabulated data.

2) A list of symbols defining the column headings employed in the specific runs.

3) The tabulated data.

Location	T/C No.	Distance, Inches
Boiler Inlet	4	9/16
	5	9/16
	18	3 21/32
Heated Zone	—	4 3/4
Boiler Wall	21	4 13/16
	6	7 7/16
	7	10 13/16
	8	13 7/16
	9	16 19/32
	30	19 7/16
	10	22 1/4
	11	25 3/16
	13	29 7/8
	14[a]	32 25/32
End Heated Zone	—	34 3/4
Mixer	15,16	

[a] T/C 14 was moved to Z = 35 3/32 inches 10/18/63.

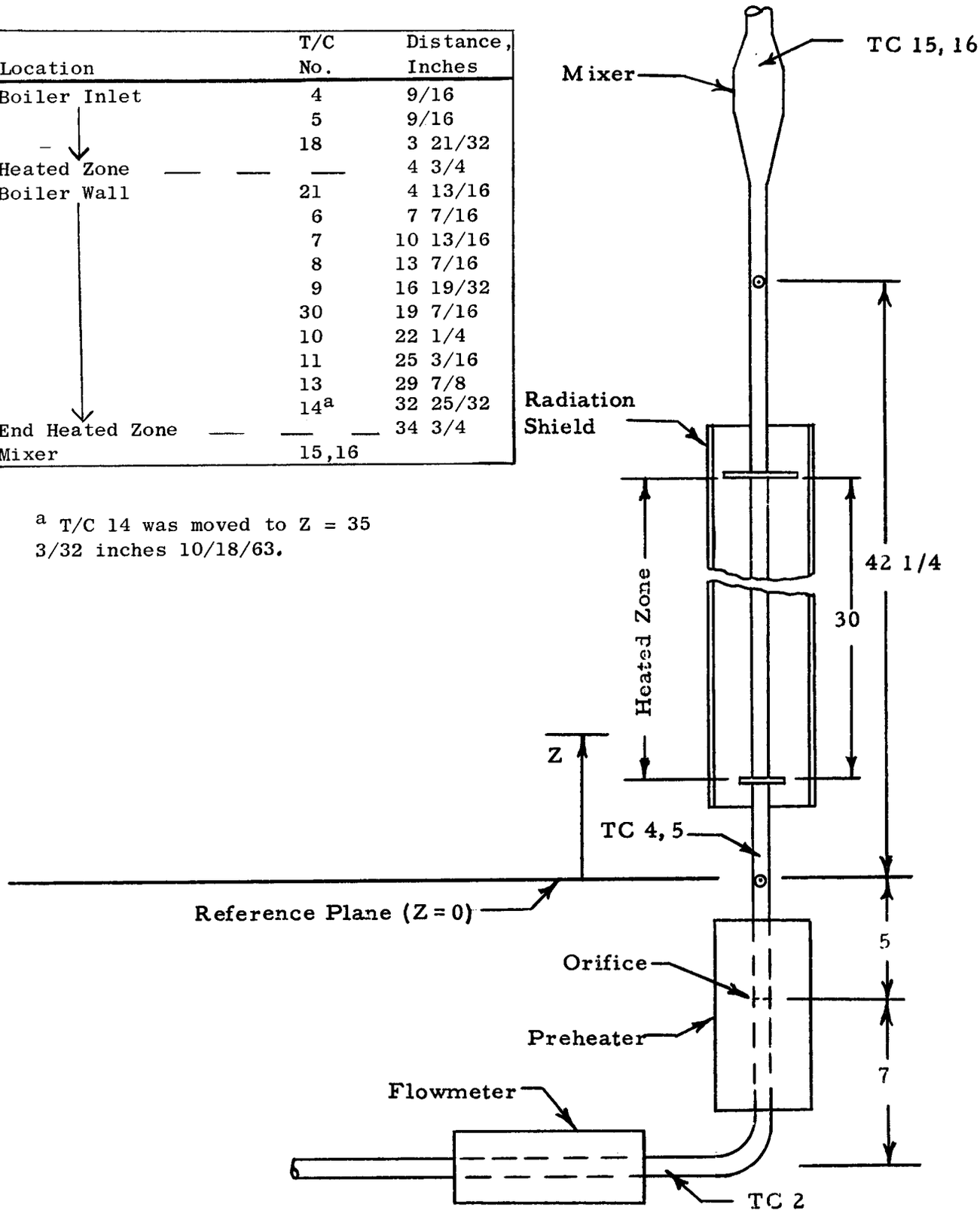

Figure B-1. Schematic of 100 KW Boiling Test Section Showing Thermocouple Locations: Effective October 7, 1963

TABLE 1: 100 KW LIQUID POTASSIUM DATA
(Part 1. List of Symbols)

Column	Symbol	Identification
240	Date	1.0143 - 10/14/63
241	Time	1216 Navy time
250, 255	TPH IN	Preheater inlet temperature, ^{o}F
260, 270	TB IN	Boiler inlet temperature, ^{o}F
275-330	TWO 18-TWO 14	Outside wall temperature, ^{o}F
350, 355	T MIX	Boiler exit temperature, ^{o}F
360	CND IN	Condenser inlet temperature, ^{o}F
370-390	CND 19-CND 23	Condenser temperature, ^{o}F
395	PUMPIN	EM pump inlet temperature, ^{o}F
410, 420	TRADSH	Temperature of radiation shield, ^{o}F
453	QN PH	Net preheater power, kw
464	QN B	Net boiler power, kw
468	Q/A	Boiler heat flux, Btu/hr-ft^2
484	FLOW	Flow rate, lb/sec
487	G	Mass velocity, lb/hr-ft^2
503	DT LOS	Temperature drop between boiler exit and mixer, ^{o}F
504	TBO C	Corrected boiler outlet temperature, ^{o}F
559-615	TWI 6-TWI 13	Inside wall temperature, ^{o}F
616	TF 13	Fluid temperature at T/C 13, ^{o}F
620	TWI-TF	Inside wall temperature-fluid temperature at T/C 13, ^{o}F
621	H 13	Heat transfer coefficient at T/C 13, Btu/hr-ft^2-^{o}F
623	NNU 13	Nusselt number at T/C 13
625	NRE 13	Reynolds number at T/C 13
627	NPE 13	Peclet number at T/C 13

TABLE 1:

100 KW LIQUID POTASSIUM DAT

(Part 2. Tabulated Data)

	240	241	250	255	265	270
	DATE	TIME	TPH IN	TPH IN	TB IN	TB IN
1	1.0143+04	1.2160+03	1.1356+03	1.1293+03	1.1325+03	1.1359+03
2	1.0143+04	1.4360+03	9.7288+02	9.6820+02	9.7170+02	9.7485+02
3	1.0163+04	1.0000+03	7.9380+02	7.8981+02	7.9459+02	7.9783+02
4	1.0163+04	1.5110+03	5.2413+02	5.2122+02	5.2848+02	5.3092+02
5	1.0283+04	1.9350+03	1.1311+03	1.1257+03	1.2402+03	1.2437+03
6	1.0283+04	2.2150+03	9.8068+02	9.7585+02	1.1327+03	1.1356+03
7	1.0293+04	1.1500+02	7.9609+02	7.9219+02	1.0424+03	1.0459+03
8	1.0293+04	4.1200+02	8.6960+02	8.6569+02	9.8555+02	9.8853+02
9	1.0293+04	5.4700+02	7.7391+02	7.6956+02	9.3140+02	9.3391+02
10	1.0293+04	8.1000+02	6.6379+02	6.6093+02	9.0519+02	9.0820+02
11	1.0293+04	9.5000+02	9.1136+02	9.0711+02	1.1388+03	1.1424+03
12	1.0293+04	1.7460+03	1.0517+03	1.0460+03	1.1790+03	1.1842+03
13	1.0293+04	2.1150+03	8.9344+02	8.8816+02	1.0846+03	1.0881+03
14	1.0303+04	5.5000+01	7.1902+02	7.1612+02	9.1028+02	9.1321+02
15	1.0303+04	3.0200+02	8.1182+02	8.1009+02	9.4920+02	9.5239+02
16	1.0303+04	1.8100+03	1.1049+03	1.1002+03	1.1527+03	1.1571+03
17	1.0303+04	2.0350+03	9.7108+02	9.6709+02	1.0389+03	1.0428+03
18	1.0313+04	5.3000+01	7.8532+02	7.8239+02	8.9339+02	8.9739+02
19	1.0313+04	2.4500+02	7.8633+02	7.8317+02	7.8746+02	7.9062+02
20	1.0313+04	5.2100+02	1.0746+03	9.6493+02	9.6843+02	9.7200+02
21	1.0313+04	6.4300+02	1.1044+03	1.0993+03	1.1021+03	1.1058+03
22	1.0313+04	1.7400+03	7.3575+02	7.3265+02	7.3778+02	7.3917+02
23	1.1013+04	2.1900+02	7.9721+02	7.9168+02	1.1650+03	1.1686+03
24	1.1013+04	4.2200+02	8.9415+02	8.9005+02	1.0775+03	1.1817+03
25	1.1013+04	6.1500+02	9.8742+02	9.8373+02	1.2132+03	1.2169+03
26	1.1013+04	8.1500+02	1.0498+03	1.0453+03	1.2473+03	1.2516+03
27	1.1063+04	1.9000+03	1.2502+03	1.1213+03	1.2923+03	1.2961+03

100 KW LIQUID POTASSIUM DATA

	275	280	285	290	295	300
	TWO 18	TWO 21	TWO 6	TWO 7	TWO 8	TWO 9
1	1.2152+03	1.2469+03	1.3201+03	1.3912+03	1.4531+03	1.5315+03
2	1.0576+03	1.0895+03	1.1803+03	1.2759+03	1.3562+03	1.4544+03
3	8.8373+02	9.1574+02	1.0233+03	1.1496+03	1.2553+03	1.3782+03
4	6.1850+02	6.5519+02	7.9923+02	9.8286+02	1.1337+03	1.3029+03
5	1.3130+03	1.3499+03	1.4109+03	1.4792+03	1.5322+03	1.5999+03
6	1.2070+03	1.2436+03	1.3196+03	1.4068+03	1.4744+03	1.5516+03
7	1.1150+03	1.1529+03	1.2467+03	1.3595+03	1.4457+03	1.5403+03
8	1.0021+03	1.0082+03	1.0199+03	1.0311+03	1.0440+03	1.0550+03
9	9.4831+02	9.5528+02	9.7134+02	9.8896+02	1.0061+03	1.0209+03
10	9.2475+02	9.3419+02	9.5780+02	9.8525+02	1.0102+03	1.0332+03
11	1.1985+03	1.2282+03	1.2945+03	1.3711+03	1.4317+03	1.4992+03
12	1.2540+03	1.2928+03	1.3635+03	1.4409+03	1.5007+03	1.5748+03
13	1.1568+03	1.1948+03	1.2788+03	1.3762+03	1.4509+03	1.5352+03
14	9.3051+02	9.3905+02	9.5970+02	9.8056+02	1.0014+03	1.0199+03
15	9.6836+02	9.7492+02	9.8964+02	1.0035+03	1.0189+03	1.0321+03
16	1.2226+03	1.2601+03	1.3282+03	1.3888+03	1.4373+03	1.5073+03
17	1.1114+03	1.1485+03	1.2333+03	1.3126+03	1.3769+03	1.4591+03
18	9.6507+02	1.0012+03	1.1006+03	1.2059+03	1.2864+03	1.3871+03
19	8.6414+02	9.0382+02	1.0122+03	1.1292+03	1.2167+03	1.3311+03
20	1.0457+03	1.0845+03	1.1712+03	1.2589+03	1.3244+03	1.4174+03
21	1.1753+03	1.2139+03	1.2840+03	1.3503+03	1.4013+03	1.4761+03
22	7.5403+02	7.5808+02	7.6794+02	7.7694+02	7.8742+02	7.9847+02
23	1.2218+03	1.2532+03	1.3370+03	1.4185+03	1.4864+03	1.5675+03
24	1.2376+03	1.1736+03	1.3473+03	1.4186+03	1.4796+03	1.5564+03
25	1.2769+03	1.3091+03	1.3803+03	1.4468+03	1.5042+03	1.5780+03
26	1.3117+03	1.3425+03	1.4081+03	1.4670+03	1.5177+03	1.5886+03
27	1.3547+03	1.3855+03	1.4459+03	1.4946+03	1.5399+03	1.6048+03

100 KW LIQUID POTASSIUM DATA

	305	310	315	325	330	350
	TWO 30	TWO 10	TWO 11	TWO 13	TWO 14	T MIX
1	1.5985+03	1.6704+03	1.7088+03	1.7960+03		1.7674+03
2	1.5417+03	1.6275+03	1.6832+03	1.7831+03		1.7625+03
3	1.4873+03	1.5889+03	1.6661+03	1.7874+03		1.7590+03
4	1.4521+03	1.5749+03	1.6775+03	1.8169+03		1.6868+03
5	1.6341+03	1.7003+03	1.7486+03	1.8303+03	1.8751+03	1.7996+03
6	1.6070+03	1.6791+03	1.7365+03	1.8288+03	1.8820+03	1.8007+03
7	1.6079+03	1.6855+03	1.7523+03	1.8565+03	1.9135+03	1.8081+03
8	1.0578+03	1.0688+03	1.0757+03	1.0907+03	1.0987+03	1.0666+03
9	1.0264+03	1.0415+03	1.0528+03	1.0723+03	1.0838+03	1.1030+03
10	1.0469+03	1.0662+03	1.0844+03	1.1126+03	1.1301+03	1.1148+03
11	1.5435+03	1.6038+03	1.6526+03	1.7322+03	1.7784+03	1.6998+03
12	1.6211+03	1.6983+03	1.7427+03	1.8296+03	1.8771+03	1.7984+03
13	1.5961+03	1.6739+03	1.7343+03	1.8303+03	1.8851+03	1.7959+03
14	1.0309+03	1.0474+03	1.0618+03	1.0861+03	1.1014+03	1.1169+03
15	1.0370+03	1.0506+03	1.0600+03	1.0769+03	1.0874+03	1.0542+03
16	1.5621+03	1.6310+03	6.3042+02	1.7801+03	1.8223+03	1.7526+03
17	1.5315+03	1.6080+03	1.6137+03	1.7914+03	1.8450+03	1.7671+03
18	1.4770+03	1.5617+03	1.5604+03	1.7751+03	1.8396+03	1.7422+03
19	1.4315+03	1.5287+03	1.5283+03	1.7647+03	1.8395+03	1.7418+03
20	1.4969+03	1.5772+03	1.5814+03	1.7673+03	1.8269+03	1.7498+03
21	1.5390+03	1.6088+03	1.6074+03	1.7635+03	1.7213+03	1.7378+03
22	8.1378+02	8.2208+02	8.2863+02	8.3792+02	8.5516+02	8.3127+02
23		1.7053+03	1.7110+03	1.8700+03	1.9347+03	1.8097+03
24	8.8786+02	1.6830+03		1.8416+03	1.8858+03	1.8023+03
25	9.1680+02	1.6993+03		1.8483+03	1.8904+03	1.8126+03
26	9.2056+02	1.7006+03		1.8382+03	1.8763+03	1.8026+03
27		1.7038+03		1.8335+03	1.8755+03	1.8022+03

100 KW LIQUID POTASSIUM DATA

	355	360	370	375	385	390
	T MIX	CND IN	CND 19	CND 20	CND 22	CND 23
1	1.7674+03	1.7129+03	1.4714+03	1.3626+03	1.2203+03	1.1627+03
2	1.7625+03	1.6802+03	1.3766+03	1.2554+03	1.1035+03	1.0450+03
3	1.7590+03	1.6249+03	1.2372+03	1.1056+03	9.4823+02	8.9293+02
4	1.6868+03	1.4230+03	9.2198+02	7.9492+02	6.6384+02	6.2206+02
5	1.7996+03	1.7415+03	1.4803+03	1.3717+03	1.2264+03	1.1656+03
6	1.8007+03	1.7124+03	1.3928+03	1.2729+03	1.1156+03	1.0544+03
7	1.8081+03	1.6643+03	1.2500+03	1.1160+03	9.5593+02	8.9749+02
8	1.0666+03	1.0663+03	9.9557+02	9.5708+02	8.9248+02	8.6216+02
9	1.0490+03	1.0418+03	9.5141+02	9.0435+02	8.3122+02	7.9856+02
10	1.0868+03	1.0594+03	9.1810+02	8.5192+02	7.5890+02	7.2106+02
11	1.6998+03	1.6136+03	1.3056+03	1.1887+03	1.0364+03	9.7999+02
12	1.7984+03	1.7277+03	1.4373+03	1.3257+03	1.1720+03	1.1105+03
13	1.7959+03	1.6867+03	1.3270+03	1.2008+03	1.0417+03	9.8203+02
14	1.0639+03	1.0482+03	9.3658+02	8.8041+02	7.9590+02	7.6057+02
15	1.0542+03	1.0506+03	9.7000+02	9.2691+02	8.5700+02	8.2518+02
16	1.7526+03	1.6960+03	1.4435+03	1.3386+03	1.1984+03	1.1402+03
17	1.7671+03	1.6842+03	1.3722+03	1.2535+03	1.1027+03	1.0427+03
18	1.7422+03	1.6092+03	1.2192+03	1.0880+03	9.3780+02	8.8154+02
19	1.7418+03	1.6108+03	1.2221+03	1.0914+03	9.3995+02	8.8340+02
20	1.7498+03	1.6694+03	1.3683+03	1.2505+03	1.0998+03	1.0387+03
21	1.7378+03	1.6837+03	1.4387+03	1.3358+03	1.1976+03	1.1388+03
22	8.3127+02	8.3843+02	7.9765+02	7.7511+02	7.3665+02	7.1708+02
23	1.8097+03	1.6618+03	1.2459+03	1.1092+03	9.5141+02	8.9290+02
24	1.8023+03	1.6901+03	1.3290+03	1.2020+03	1.0428+03	9.8258+02
25	1.8126+03	1.7254+03	1.4014+03	1.2799+03	1.1228+03	1.0606+03
26	1.8026+03	1.7295+03	1.4352+03	1.3214+03	1.1696+03	1.1078+03
27	1.8005+03	1.7389+03	1.4763+03	1.3657+03	1.2227+03	1.1620+03

100 KW LIQUID POTASSIUM DATA

	395	410	420	453	464	468
	PUMPIN	TRADSH	TRADSH	QN PH	QN B	Q/A
1	1.0730+03	8.9292+02	9.1908+02	0.	7.1632+00	8.8290+04
2	9.5623+02	8.5399+02	8.8644+02	0.	6.4121+00	7.9033+04
3	8.0842+02	8.0115+02	8.3773+02	0.	4.9455+00	6.0956+04
4	5.5666+02	6.8725+02	7.4336+02	0.	2.9464+00	3.6315+04
5	1.0749+03	8.7627+02	8.9330+02	7.8820-01	6.2309+00	7.6799+04
6	9.6496+02	8.4240+02	8.6780+02	7.8820-01	5.5957+00	6.8970+04
7	8.1275+02	7.8481+02	9.3735+02	7.7560-01	3.2572+00	4.0146+04
8	8.1437+02	5.8082+02	5.8749+02	8.6560-01	1.0462+00	1.2895+04
9	7.4851+02	5.7125+02	5.7961+02	8.2600-01	1.1405+00	1.4057+04
10	6.6671+02	5.6171+02	5.7374+02	8.5270-01	1.0779+00	1.3285+04
11	8.9689+02	7.8465+02	8.1207+02	1.1342+00	3.9448+00	4.8622+04
12	1.0201+03	8.6385+02	8.9041+02	7.6240-01	5.7122+00	7.0406+04
13	8.9425+02	8.1587+02	8.4765+02	8.2690-01	4.8678+00	5.9998+04
14	7.0955+02	5.6736+02	5.7902+02	8.9140-01	1.1693+00	1.4413+04
15	7.7656+02	5.7371+02	5.8312+02	8.6560-01	1.1401+00	1.4052+04
16	1.0539+03	8.6884+02	8.7388+02	2.7580-01	6.3448+00	7.8202+04
17	9.5706+02	8.3945+02	8.5175+02	2.6890-01	5.9005+00	7.2727+04
18	8.0102+02	7.7617+02	7.9785+02	2.6692-01	4.2619+00	5.2530+04
19	8.0213+02	7.8510+02	8.0859+02	0.	5.2435+00	6.4629+04
20	9.5344+02	8.4219+02	8.5436+02	0.	6.2362+00	7.6864+04
21	1.0519+03	8.6960+02	8.7661+02	0.	6.7954+00	8.3756+04
22	6.8376+02	5.2885+02	5.2931+02	0.	1.1160+00	1.3755+04
23	8.1021+02	7.6328+02	7.8849+02	1.4181+00	3.5932+00	4.4288+04
24	8.9588+02	7.9560+02	8.1459+02	1.4181+00	4.2489+00	5.2370+04
25	9.7217+02	8.2766+02	8.4304+02	1.4181+00	5.0279+00	6.1971+04
26	1.0186+03	8.4150+02	8.5400+02	1.4518+00	5.5311+00	6.8174+04
27	1.0730+03	8.4726+02	8.5888+02	1.3893+00	5.6962+00	7.0208+04

100 KW LIQUID POTASSIUM DATA

	484	487	503	504	559	566
	FLOW	G	DT LOS	TBO C	TWI 6	TWI 7
1	5.4600-02	2.0141+05	5.4329+00	1.7729+03	1.2977+03	1.3689+03
2	3.9886-02	1.4714+05	7.4081+00	1.7699+03	1.1600+03	1.2558+03
3	2.6374-02	9.7291+04	1.1173+01	1.7701+03	1.0075+03	1.1340+03
4	1.2337-02	4.5509+04	2.2509+01	1.7093+03	7.8968+02	9.7343+02
5	5.3671-02	1.9799+05	5.6658+00	1.8053+03	1.3915+03	1.4599+03
6	4.0007-02	1.4758+05	7.6074+00	1.8083+03	1.3021+03	1.3894+03
7	2.6464-02	9.7624+04	1.1573+01	1.8197+03	1.2365+03	1.3493+03
8	5.2523-02	1.9375+05	2.5205+00	1.0691+03	1.0165+03	1.0277+03
9	3.9260-02	1.4483+05	3.4235+00	1.0794+03	9.6769+02	9.8531+02
10	2.6382-02	9.7320+04	5.2975+00	1.1061+03	9.5435+02	9.8180+02
11	3.3462-02	1.2344+05	8.3882+00	1.7082+03	1.2822+03	1.3588+03
12	4.6810-02	1.7268+05	6.4903+00	1.8049+03	1.3456+03	1.4232+03
13	3.3297-02	1.2283+05	9.1069+00	1.8050+03	1.2636+03	1.3610+03
14	3.3077-02	1.2202+05	4.1571+00	1.0945+03	9.5595+02	9.7682+02
15	4.5711-02	1.6863+05	2.8375+00	1.0570+03	9.8599+02	9.9984+02
16	5.3499-02	1.9735+05	5.4798+00	1.7580+03	1.3084+03	1.3690+03
17	3.9923-02	1.4727+05	7.4282+00	1.7745+03	1.2147+03	1.2941+03
18	2.6409-02	9.7419+04	1.1009+01	1.7532+03	1.0871+03	1.1924+03
19	2.6363-02	9.7251+04	1.1024+01	1.7528+03	9.9541+02	1.1125+03
20	4.0096-02	1.4791+05	7.2954+00	1.7571+03	1.1515+03	1.2393+03
21	5.3337-02	1.9675+05	5.4317+00	1.7433+03	1.2627+03	1.3291+03
22	5.4704-02	2.0180+05	1.4754+00	8.3275+02	7.6431+02	7.7331+02
23	2.6484-02	9.7699+04	1.1579+01	1.8213+03	1.3258+03	1.4074+03
24	3.3298-02	1.2283+05	9.1530+00	1.8115+03	1.3340+03	1.4054+03
25	4.0283-02	1.4860+05	7.6318+00	1.8202+03	1.3646+03	1.4312+03
26	4.6012-02	1.6973+05	6.6255+00	1.8093+03	1.3909+03	1.4499+03
27	5.3872-02	1.9873+05	5.6529+00	1.8070+03	1.4282+03	1.4770+03

100 KW LIQUID POTASSIUM DATA

	573	580	587	594	601	615
	TWI 8	TWI 9	TWI 30	TWI 10	TWI 11	TWI 13
1	1.4309+03	1.5094+03	1.5765+03	1.6485+03	1.6869+03	1.7743+03
2	1.3361+03	1.4345+03	1.5219+03	1.6079+03	1.6636+03	1.7636+03
3	1.2398+03	1.3628+03	1.4720+03	1.5737+03	1.6510+03	1.7724+03
4	1.1243+03	1.2936+03	1.4429+03	1.5658+03	1.6685+03	1.8080+03
5	1.5130+03	1.5807+03	1.6150+03	1.6813+03	1.7297+03	1.8115+03
6	1.4571+03	1.5343+03	1.5899+03	1.6620+03	1.7195+03	1.8119+03
7	1.4356+03	1.5303+03	1.5979+03	1.6756+03	1.7424+03	1.8467+03
8	1.0407+03	1.0516+03	1.0545+03	1.0655+03	1.0724+03	1.0874+03
9	1.0024+03	1.0173+03	1.0228+03	1.0379+03	1.0492+03	1.0687+03
10	1.0068+03	1.0298+03	1.0435+03	1.0628+03	1.0810+03	1.1091+03
11	1.4195+03	1.4870+03	1.5313+03	1.5917+03	1.6406+03	1.7202+03
12	1.4831+03	1.5573+03	1.6036+03	1.6809+03	1.7253+03	1.8123+03
13	1.4358+03	1.5202+03	1.5811+03	1.6590+03	1.7195+03	1.8156+03
14	9.9766+02	1.0162+03	1.0272+03	1.0437+03	1.0581+03	1.0824+03
15	1.0152+03	1.0284+03	1.0334+03	1.0470+03	1.0564+03	1.0733+03
16	1.4176+03	1.4877+03	1.5426+03	1.6116+03	6.0960+02	1.7608+03
17	1.3585+03	1.4409+03	1.5133+03	1.5899+03	1.5956+03	1.7735+03
18	1.2731+03	1.3738+03	1.4638+03	1.5486+03	1.5473+03	1.7621+03
19	1.2002+03	1.3147+03	1.4152+03	1.5125+03	1.5122+03	1.7488+03
20	1.3049+03	1.3980+03	1.4776+03	1.5580+03	1.5622+03	1.7484+03
21	1.3802+03	1.4551+03	1.5181+03	1.5879+03	1.5865+03	1.7429+03
22	7.8380+02	7.9485+02	8.1017+02	8.1847+02	8.2502+02	8.3431+02
23	1.4753+03	1.5565+03		1.6944+03	1.7001+03	1.8592+03
24	1.4665+03	1.5433+03	8.7417+02	1.6700+03		1.8287+03
25	1.4887+03	1.5625+03	9.0064+02	1.6840+03		1.8331+03
26	1.5006+03	1.5716+03	9.0278+02	1.6838+03		1.8215+03
27	1.5223+03	1.5873+03		1.6864+03		1.8163+03

100 KW LIQUID POTASSIUM DATA

	616	620	621	623	625	627
	TF 13	TWI-TF	H 13	NNU 13	NRE 13	NPE 13
1	1.6691+03	1.0525+02	8.3886+02	1.8639+00	2.6005+04	8.6916+01
2	1.6404+03	1.2316+02	6.4168+02	1.4058+00	1.8742+04	6.2306+01
3	1.6119+03	1.6056+02	3.7964+02	8.2018-01	1.2228+04	4.0436+01
4	1.5176+03	2.9038+02	1.2506+02	2.5839-01	5.4651+03	1.7837+01
5	1.7138+03	9.7747+01	7.8570+02	1.7855+00	2.6091+04	8.8056+01
6	1.6987+03	1.1315+02	6.0955+02	1.3747+00	1.9328+04	6.4957+01
7	1.6936+03	1.5304+02	2.6232+02	5.9009-01	1.2754+04	4.2822+01
8	1.0558+03	3.1567+01	4.0849+02	6.9669-01	1.7319+04	6.0301+01
9	1.0556+03	1.3102+01	1.0729+03	1.8297+00	1.2943+04	4.5069+01
10	1.0737+03	3.5476+01	3.7449+02	6.4322-01	8.8474+03	3.0517+01
11	1.6159+03	1.0427+02	4.6633+02	1.0095+00	1.5544+04	5.1440+01
12	1.7036+03	1.0865+02	6.4798+02	1.4650+00	2.2662+04	7.6259+01
13	1.6882+03	1.2731+02	4.7127+02	1.0572+00	1.6005+04	5.3685+01
14	1.0648+03	1.7555+01	8.2102+02	1.4052+00	1.1000+04	3.8120+01
15	1.0398+03	3.3514+01	4.1928+02	7.1063-01	1.4849+04	5.2130+01
16	1.6600+03	1.0080+02	7.7582+02	1.7161+00	2.5371+04	8.4656+01
17	1.6553+03	1.1825+02	6.1502+02	1.3573+00	1.8891+04	6.2976+01
18	1.6138+03	1.4833+02	3.5414+02	7.6580-01	1.2255+04	4.0541+01
19	1.5962+03	1.5263+02	4.2345+02	9.0794-01	1.2133+04	4.0014+01
20	1.6292+03	1.1918+02	6.4495+02	1.4052+00	1.8741+04	6.2175+01
21	1.6394+03	1.0349+02	8.0931+02	1.7721+00	2.5049+04	8.3259+01
22	8.1743+02	1.6877+01	8.1505+02	1.2709+00	1.4119+04	5.7402+01
23	1.7149+03	1.4426+02	3.0701+02	6.9809-01	1.2881+04	4.3487+01
24	1.7007+03	1.2807+02	4.0891+02	9.2310-01	1.6100+04	5.4134+01
25	1.7219+03	1.1122+02	5.5718+02	1.2715+00	1.9649+04	6.6468+01
26	1.7183+03	1.0325+02	6.6027+02	1.5039+00	2.2410+04	7.5730+01
27	1.7237+03	9.2616+01	7.5806+02	1.7315+00	2.6296+04	8.9003+01

Location	T/C No.	Distance, Inches
Boiler Inlet	4	9/16
	5	9/16
	18	3 21/32
Heated Zone		4 3/4
Boiler Wall	21	4 13/16
	6	7 7/16
	7	10 13/16
	8	13 7/16
	9	16 19/32
	30	19 7/16
	10	22 1/4
	11	25 3/16
	12	28 3/16
	13	29 7/8
End Heated Zone		34 3/4
Pipe Wall at Boiler Exit	14	35 3/32
Mixer	15,16	

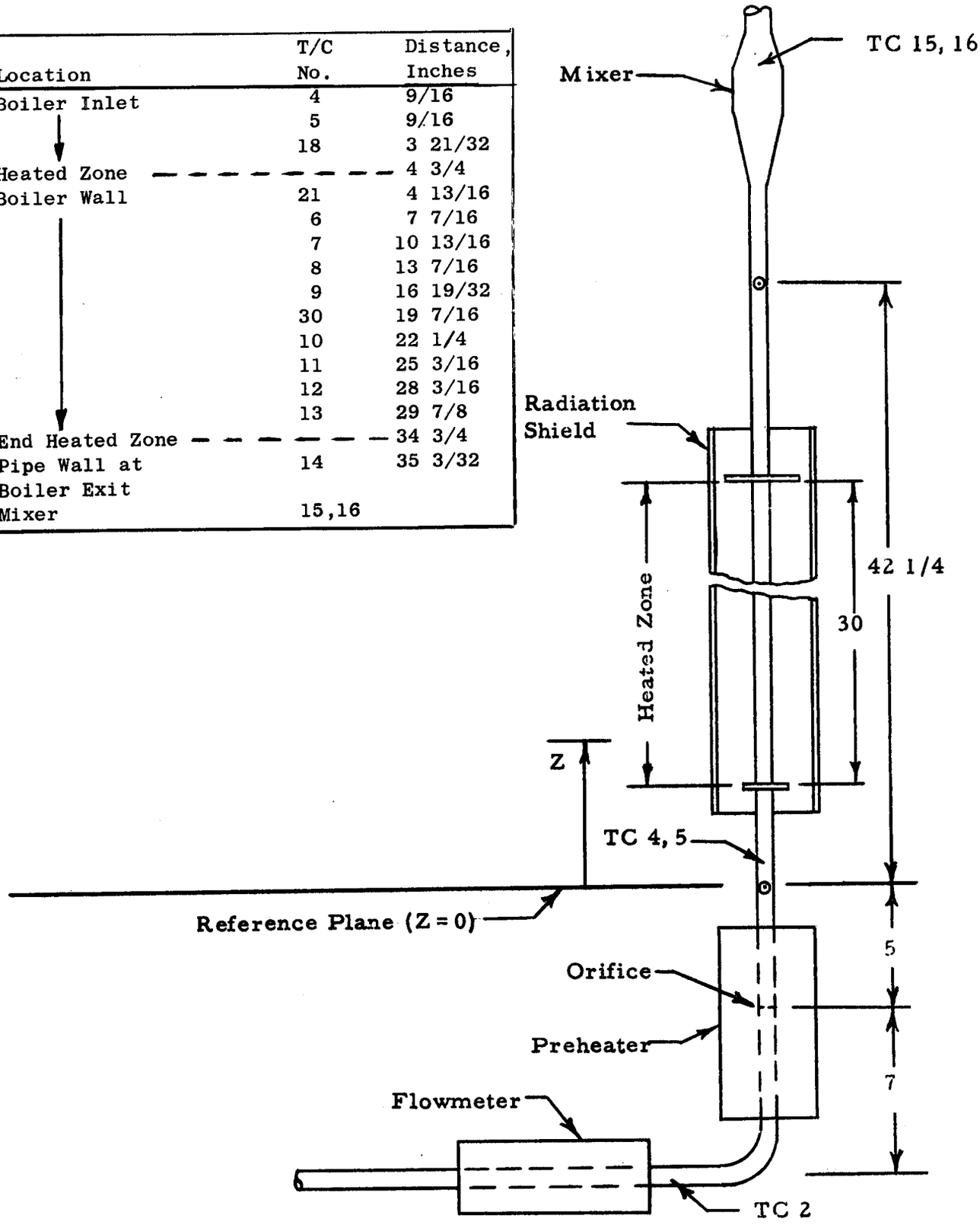

Figure B-2. Schematic of 100 KW Boiling Test Section Showing Thermocouple Locations: Effective October 25, 1963

TABLE 2: 100 KW BOILING POTASSIUM DATA
(Part 1. List of Symbols)

Column	Symbol	Identification
240	Date	1.0283 - 10/28/63
241	Time	1029 Navy time
250, 255	TPH IN	Preheater inlet temperature, ^{o}F
265, 270	TB IN	Boiler inlet temperature, ^{o}F
275-330	TWO 18-TWO 14	Outside wall temperature, ^{o}F
350, 355	T MIX	Boiler exit temperature, ^{o}F
360	CND IN	Condenser inlet temperature, ^{o}F
370-390	CND 19-CND 23	Condenser temperature, ^{o}F
395	PUMPIN	EM pump inlet temperature, ^{o}F
410, 420	TRADSH	Temperature of radiation shield, ^{o}F
453	QN PH	Net preheater power, kw
464	QN B	Net boiler power, kw
468	Q/A	Boiler heat flux, Btu/hr-ft^2
484	FLOW	Flow rate, lb/sec
487	G	Mass velocity, lb/hr-ft^2
497	X MIX	Quality at mixer, lb vapor/lb mixture
499	EB OUT	Enthalpy of mixture at mixer, Btu/lb
502	VELOUT	Vapor velocity at boiler exit, ft/sec
559-594	TWI 6-TWI 10	Inside wall temperature, ^{o}F
595	DT 10	$T_{wi} - T_{mix}$ at 10, ^{o}F
596	H 10	$\frac{q/A}{T_{wi} - T_{mix} \text{ at } 10}$, Btu/hr-ft^2-$^{o}F$
601	TWI 11	Inside wall temperature at 11, ^{o}F
602	DT 11	$T_{wi} - T_{mix}$ at 11, ^{o}F
603	H 11	$\frac{q/A}{T_{wi} - T_{mix} \text{ at } 11}$, Btu/hr-ft^2-$^{o}F$
615	TWI 13	Inside wall temperature at 13, ^{o}F
616	DT 13	$T_{wi} - T_{mix}$ at 13, ^{o}F
617	H 13	$\frac{q/A}{T_{wi} - T_{mix} \text{ at } 13}$, Btu/hr-ft^2-$^{o}F$
654	STBPAR	$\frac{q/A}{v H_{fg} V_{in}}$, dimensionless

TABLE 2:

100 KW BOILING POTASSIUM DATA

(Part 2. Tabulated Data)

	240	241	250	255	265	270
	DATE	TIME	TPH IN	TPH IN	TB IN	TB IN
1	1.0283+04	1.0290+03	9.6718+02	1.0679+03	1.2052+03	1.2085+03
2	1.0283+04	1.3070+03	1.0758+03	1.0695+03	1.3427+03	1.3482+03
3	1.0283+04	1.4360+03	1.1795+03	1.1709+03	1.4604+03	1.4656+03
4	1.0293+04	1.1310+03	9.0667+02	9.0227+02	1.1350+03	1.1386+03
5	1.0293+04	1.2510+03	9.3989+02	9.3495+02	1.1695+03	1.1734+03
6	1.0293+04	1.3470+03	9.9587+02	9.9037+02	1.2156+03	1.2195+03
7	1.0293+04	1.4560+03	1.0251+03	1.0188+03	1.2599+03	1.2646+03
8	1.0303+04	9.2600+02	1.1233+03	1.1159+03	1.4835+03	1.4898+03
9	1.0303+04	1.0490+03	1.0298+03	1.0209+03	1.6425+03	1.6468+03
10	1.0303+04	1.2210+03	1.3262+03	1.3164+03	1.5983+03	1.6042+03
11	1.0303+04	1.3300+03	1.4761+03	1.4663+03	1.6713+03	1.6773+03
12	1.0313+04	1.0150+03	1.0260+03	1.0212+03	1.2049+03	1.2098+03
13	1.0313+04	1.2300+03	1.0636+03	1.0578+03	1.2600+03	1.2649+03
14	1.0313+04	1.4300+03	1.1166+03	1.1101+03	1.5113+03	1.5162+03
15	1.1043+04	1.2180+03	1.2682+03	1.2606+03	1.2527+03	1.2576+03
16	1.1043+04	1.4110+03	1.1925+03	1.1858+03	1.1836+03	1.1781+03
17	1.1063+04	1.1420+03	1.3452+03	1.3364+03	1.5401+03	1.5472+03
18	1.1063+04	1.3450+03	1.4697+03	1.4603+03	1.6368+03	1.6429+03
19	1.1063+04	1.4470+03	1.2428+03	1.2357+03	1.4325+03	1.4371+03
20	1.1073+04	9.1000+02	1.1528+03	1.1447+03	1.4346+03	1.4392+03

100 Kw BOILING POTASSIUM DATA

	275	280	285	290	295	300
	TWO 18	TWO 21	TWO 6	TWO 7	TWO 8	TWO 9
1	1.3080+03	1.3726+03	1.4912+03	1.6333+03	1.7430+03	1.7193+03
2	1.4783+03	1.5728+03	1.7533+03	1.7301+03	1.7252+03	1.7340+03
3	1.6283+03	1.7566+03	1.7491+03	1.7483+03	1.7280+03	1.7364+03
4	1.2000+03	1.2350+03	1.3057+03	1.3904+03	1.4559+03	1.5304+03
5	1.2521+03	1.2968+03	1.3886+03	1.4962+03	1.5813+03	1.6749+03
6	1.3245+03	1.3939+03	1.5272+03	1.6857+03	1.7965+03	1.7132+03
7	1.3755+03	1.4491+03	1.5961+03	1.7632+03	1.7176+03	1.7212+03
8	1.6261+03	1.7326+03	1.9199+03	2.0434+03	1.9777+03	2.0025+03
9	1.8112+03	1.9398+03	2.0115+03	1.9933+03	1.9616+03	1.9867+03
10	1.7286+03	1.8163+03	1.9554+03	2.0379+03	1.9786+03	2.0017+03
11	1.7894+03	1.8654+03	1.9729+03	2.0424+03	1.9857+03	2.0044+03
12	1.2917+03	1.3400+03	1.4424+03	1.5414+03	1.6214+03	1.6802+03
13	1.3600+03	1.4209+03	1.5473+03	1.6745+03	1.6487+03	1.6343+03
14	1.6079+03	1.6711+03	1.6404+03	1.6335+03	1.6342+03	1.6352+03
15	1.3942+03	1.4836+03	1.6533+03	1.6705+03	1.6649+03	1.6686+03
16	1.2988+03	1.3629+03	1.4879+03	1.6147+03	1.6564+03	1.6382+03
17	1.6529+03	1.7189+03	1.8187+03	1.9092+03	1.9047+03	1.8909+03
18	1.7464+03	1.8117+03	1.9118+03	1.9300+03	1.8850+03	1.8945+03
19	1.5066+03	1.5419+03	1.6114+03	1.6688+03	1.7123+03	1.7879+03
20	1.5731+03	1.6586+03	1.8315+03	1.9862+03	1.9970+03	

100 KW BOILING POTASSIUM DATA

	305	310	315	320	325	330
	TWO 30	TWO 10	TWO 11	TWO 12	TWO 13	TWO 14
1	1.6998+03	1.7158+03	1.7068+03	1.5567+03	1.7049+03	1.6962+03
2	1.7169+03	1.7811+03	1.7649+03	1.6346+03	1.7219+03	1.7009+03
3	1.7152+03	1.7774+03	1.7787+03	1.6487+03	1.7324+03	1.7092+03
4	1.5817+03	1.6475+03	1.7024+03	1.4280+03	1.6849+03	1.6741+03
5	1.7293+03	1.6925+03	1.6919+03	1.4764+03	1.6957+03	1.6797+03
6	1.6990+03	1.7146+03	1.7128+03	1.5581+03	1.7057+03	1.6879+03
7	1.7005+03	1.7168+03	1.7202+03	1.5815+03	1.7093+03	1.6902+03
8	1.9663+03	1.9835+03		1.7547+03	1.9742+03	1.9558+03
9	1.9620+03	1.9708+03		1.7589+03	1.9753+03	1.9531+03
10	1.9611+03	1.9854+03		1.7667+03	1.9841+03	1.9554+03
11	1.9614+03	1.9924+03		1.7571+03	1.9877+03	1.9602+03
12	1.6014+03	1.6115+03	1.6058+03	1.4450+03	1.6180+03	1.5986+03
13	1.6130+03	1.6281+03	1.6279+03	1.4898+03	1.6278+03	1.6060+03
14	1.6069+03	1.6284+03	1.6275+03	1.4934+03	1.6270+03	1.6048+03
15		1.6739+03		1.5980+03	1.6602+03	1.6265+03
16		1.6469+03		1.5376+03	1.6343+03	1.6055+03
17		1.8769+03			1.8762+03	1.8468+03
18		1.8835+03		1.6793+03	1.8820+03	1.8513+03
19		1.8510+03		1.5794+03	1.8573+03	1.8338+03
20		1.9740+03			1.9786+03	1.9497+03

100 KW BOILING POTASSIUM DATA

	350	355	360	370	375	385
	T MIX	T MIX	CND IN	CND 19	CND 20	CND 22
1	1.6475+03	1.6475+03	1.6714+03	1.6672+03	1.4708+03	1.1966+03
2	1.6478+03	1.6478+03	1.6726+03	1.6689+03	1.6637+03	1.5438+03
3	1.6490+03	1.6490+03	1.6737+03	1.6639+03	1.6619+03	1.6748+03
4	1.6439+03	1.6439+03	1.6641+03	1.3347+03	1.2104+03	1.0516+03
5	1.6452+03	1.6452+03	1.6680+03	1.4659+03	1.3024+03	1.1152+03
6	1.6453+03	1.6453+03	1.6692+03	1.6593+03	1.5535+03	1.2347+03
7	1.6449+03	1.6449+03	1.6694+03	1.6600+03	1.6574+03	1.2976+03
8	1.9684+03	1.9036+03	1.9287+03	1.9117+03	1.9113+03	1.4249+03
9	1.9397+03	1.9007+03	1.9260+03	1.9091+03	1.9093+03	1.4534+03
10	1.9670+03	1.9004+03	1.9273+03	1.9107+03	1.9102+03	1.5866+03
11	1.9533+03	1.9053+03	1.9295+03	1.9122+03	1.9118+03	1.6381+03
12	1.5607+03	1.5607+03	1.5826+03	1.5724+03	1.4814+03	1.2260+03
13	1.5634+03	1.5634+03	1.5862+03	1.5763+03	1.5752+03	1.3339+03
14	1.5602+03	1.5602+03	1.5831+03	1.5736+03	1.5729+03	1.5289+03
15	1.5742+03	1.5735+03	1.5942+03	1.5862+03	1.5818+03	1.5965+03
16	1.5595+03	1.5591+03	1.5797+03	1.5746+03	1.5672+03	1.4771+03
17	1.8029+03	1.8016+03	1.8233+03	1.8105+03	1.8078+03	1.5275+03
18	1.8045+03	1.8027+03	1.8242+03	1.8117+03	1.8098+03	1.6512+03
19	1.8011+03	1.8000+03	1.8195+03	1.6341+03	1.5000+03	1.3361+03
20	1.9074+03	1.9061+03	1.9267+03	1.9122+03	1.7855+03	1.4118+03

100 KW BOILING POTASSIUM DATA

	390	395	410	420	453	464
	CND 23	PUMPIN	TRADSH	TRADSH	QN PH	QN B
1	1.1094+03	9.8627+02	9.2232+02	9.3017+02	1.0951+00	7.1728+00
2	1.3243+03	1.1115+03	1.0040+03	9.9968+02	1.0816+00	9.8863+00
3	1.6650+03	1.2442+03	1.0433+03	1.0168+03	1.0129+00	1.1950+01
4	1.9109+02	9.0224+02	8.0166+02	8.2214+02	1.1105+00	4.3796+00
5	1.0443+03	9.4132+02	8.5529+02	8.7187+02	1.1414+00	5.6849+00
6	1.1392+03	1.0115+03	9.2802+02	9.4121+02	1.0006+00	7.7237+00
7	1.1359+03	1.0408+03	9.5163+02	9.6114+02	1.0546+00	8.1862+00
8	1.3018+03	1.1335+03	1.0642+03	1.0592+03	1.9823+00	1.1860+01
9	1.2842+03	1.0760+03	1.0781+03	1.0674+03	2.3494+00	1.2118+01
10	1.4520+03	1.2866+03	1.0906+03	1.0739+03	2.3494+00	1.2341+01
11	1.5192+03	1.3711+03	1.0932+03	1.0737+03	2.3093+00	1.2193+01
12	1.1400+03	1.0235+03	8.8524+02	8.7577+02	9.4300-01	6.7772+00
13	1.2157+03	1.0671+03	9.2455+02	9.1036+02	9.7180-01	7.9301+00
14	1.3355+03	1.1337+03	9.4374+02	9.2043+02	1.9195+00	7.8710+00
15	1.5754+03	1.2638+03	1.0000+03	9.7521+02	0.	1.2035+01
16	1.3465+03	1.1713+03	9.4930+02	9.3169+02	0.	1.0242+01
17	1.4207+03	1.2802+03	1.0181+03	1.0012+03	1.9690+00	1.0511+01
18	1.5234+03	1.3669+03	1.0480+03	1.0219+03	1.9119+00	1.1038+01
19	1.2691+03	1.1656+03	9.1553+02	9.1269+02	1.8382+00	6.8413+00
20	1.3044+03	1.1520+03	1.0299+03	1.0263+03	1.7458+00	1.1480+01

100 KW BOILING POTASSIUM DATA

	468	484	487	497	499	502
	Q/A	FLOW	G	X MIX	EB CUT	VELOUT
1	8.8409+04	2.9939-02	1.1044+05	1.6396-01	5.3145+02	5.9226+01
2	1.2185+05	2.6894-02	9.9210+04	3.3923-01	6.7605+02	1.0994+02
3	1.4729+05	2.3311-02	8.5992+04	5.3246-01	8.3555+02	1.4884+02
4	5.3978+04	3.3568-02	1.2383+05	2.1983-02	4.1369+02	9.0324+00
5	7.0069+04	3.3139-02	1.2225+05	7.7794-02	4.5997+02	3.1398+01
6	9.5198+04	3.0856-02	1.1382+05	1.7831-01	5.4291+02	6.6965+01
7	1.0090+05	3.0770-02	1.1351+05	2.0503-01	5.6489+02	7.6907+01
8	1.4618+05	3.2864-02	1.2123+05	3.0694-01	6.9739+02	4.9061+01
9	1.4936+05	2.3348-02	8.6130+04	5.2524-01	8.6843+02	6.2114+01
10	1.5211+05	4.8700-02	1.7965+05	2.1178-01	6.2140+02	5.0453+01
11	1.5029+05	6.5079-02	2.4007+05	1.5411-01	5.7477+02	4.9614+01
12	8.3533+04	3.5629-02	1.3143+05	1.2736-01	4.8579+02	7.5620+01
13	9.7742+04	3.3163-02	1.2233+05	1.9382-01	5.4169+02	1.0585+02
14	9.7015+04	3.1195-02	1.1508+05	2.5772-01	5.9443+02	1.3427+02
15	1.4833+05	3.5180-02	1.2977+05	3.2060-01	6.4903+02	1.7792+02
16	1.2624+05	4.0270-02	1.4855+05	2.0695-01	5.5193+02	1.3969+02
17	1.2955+05	5.5269-02	2.0388+05	1.5638-01	5.5304+02	6.1726+01
18	1.3604+05	6.2470-02	2.3045+05	1.6322-01	5.5881+02	7.2516+01
19	8.4322+04	5.9985-02	2.2128+05	3.8259-02	4.5723+02	1.6474+01
20	1.4150+05	3.6595-02	1.3499+05	2.4893-01	6.4614+02	4.7828+01

100 KW BOILING POTASSIUM DATA

	559	566	573	580	587	594
	TWI 6	TWI 7	TWI 8	TWI 9	TWI 30	TWI 10
1	1.4690+03	1.6113+03	1.7212+03	1.6975+03	1.6779+03	1.6940+03
2	1.7232+03	1.7000+03	1.6951+03	1.7040+03	1.6868+03	1.7511+03
3	1.7128+03	1.7119+03	1.6917+03	1.7020+03	1.6788+03	1.7411+03
4	1.2920+03	1.3767+03	1.4423+03	1.5169+03	1.5683+03	1.6341+03
5	1.3709+03	1.4787+03	1.5638+03	1.6575+03	1.7120+03	1.6752+03
6	1.5033+03	1.6622+03	1.7731+03	1.6897+03	1.6754+03	1.6910+03
7	1.5710+03	1.7384+03	1.6927+03	1.6962+03	1.6755+03	1.6919+03
8	1.8842+03	2.0080+03	1.9422+03	1.9670+03	1.9307+03	1.9479+03
9	1.9753+03	1.9571+03	1.9253+03	1.9505+03	1.9257+03	1.9345+03
10	1.9184+03	2.0011+03	1.9416+03	1.9648+03	1.9241+03	1.9494+03
11	1.9364+03	2.0060+03	1.9492+03	1.9679+03	1.9249+03	1.9559+03
12	1.4213+03	1.5205+03	1.6006+03	1.6595+03	1.5006+03	1.5907+03
13	1.5229+03	1.6503+03	1.6244+03	1.6100+03	1.5887+03	1.6038+03
14	1.6163+03	1.6093+03	1.6100+03	1.6111+03	1.5828+03	1.6043+03
15	1.6165+03	1.6337+03	1.6281+03	1.6318+03		1.6372+03
16	1.4562+03	1.5833+03	1.6250+03	1.6068+03		1.6156+03
17	1.7869+03	1.8776+03	1.8730+03	1.8593+03		1.8452+03
18	1.8786+03	1.8968+03	1.8527+03	1.8613+03		1.8502+03
19	1.5905+03	1.6479+03	1.6915+03	1.7671+03		1.8303+03
20	1.7968+03	1.9518+03	1.9626+03			1.9396+03

100 KW BOILING POTASSIUM DATA

	595	596	601	602	603	615
	DT 10	H 10	TWI 11	DT 11	H 11	TWI 13
1	4.6531+01	1.9000+03	1.6849+03	3.7427+01	2.3621+03	1.6831+03
2	1.0332+02	1.1793+03	1.7348+03	8.7057+01	1.3997+03	1.6918+03
3	9.2101+01	1.5992+03	1.7425+03	9.3475+01	1.5757+03	1.6961+03
4	-9.7787+00	-5.5200+03	1.6890+03	4.5096+01	1.1969+03	1.6715+03
5	2.9998+01	2.3358+03	1.6745+03	2.9392+01	2.3840+03	1.6784+03
6	4.5724+01	2.0820+03	1.6893+03	4.3989+01	2.1641+03	1.6822+03
7	4.6981+01	2.1477+03	1.6953+03	5.0362+01	2.0035+03	1.6844+03
8	1.1934+01	1.2249+04				1.9387+03
9	1.4302+01	1.0443+04				1.9390+03
10	1.4712+01	1.0339+04				1.9472+03
11	2.6978+01	5.6557+03				1.9533+03
12	3.0006+01	2.7838+03	1.5851+03	2.4385+01	3.4256+03	1.5973+03
13	4.0330+01	2.4206+03	1.6036+03	4.0117+01	2.4364+03	1.6035+03
14	4.4109+01	2.1995+03	1.6034+03	4.3234+01	2.2440+03	1.6029+03
15	6.3337+01	2.3420+03				1.6234+03
16	5.6278+01	2.2432+03				1.6030+03
17	4.3001+01	3.0126+03				1.8445+03
18	4.6634+01	2.9172+03				1.8487+03
19	2.9786+01	2.8309+03				1.8366+03
20	3.2914+01	4.2991+03				1.9443+03

100 KW BOILING POTASSIUM DATA

	616	617	654
	DT 13	H 13	STBPAR
1	3.5607+01	2.4829+03	4.8938-01
2	4.3996+01	2.7696+03	7.3258-01
3	4.7060+01	3.1298+03	9.9715-01
4	2.7592+01	1.9563+03	2.7350-01
5	3.3205+01	2.1102+03	3.5576-01
6	3.6879+01	2.5814+03	5.1466-01
7	3.9436+01	2.5585+03	5.4369-01
8	2.6804+00	5.4537+04	2.9442-01
9	1.8757+01	7.9627+03	4.2899-01
10	1.3469+01	1.1293+04	2.0406-01
11	2.3922+01	6.2825+03	1.5072-01
12	3.6594+01	2.2827+03	5.3058-01
13	4.0030+01	2.4417+03	6.5323-01
14	4.2709+01	2.2715+03	6.7011-01
15	4.9564+01	2.9928+03	8.9743-01
16	4.3675+01	2.8905+03	7.1678-01
17	4.2247+01	3.0664+03	2.2179-01
18	4.5131+01	3.0144+03	2.0212-01
19	3.6097+01	2.3360+03	1.3607-01
20	3.7533+01	3.7700+03	2.7750-01

Location	T/C No.	Distance, Inches
Boiler Inlet	4	9/16
	5	9/16
	18	3 21/32
Heated Zone		4 3/4
Boiler Wall	21	4 13/16
	6	7 7/16
	7	10 13/16
	8	13 7/16
	9	16 19/32
	30	19 7/16
	11	25 3/16
	12	28 3/16
	13	29 7/8
	10	31 7/8
End Heated Zone		34 3/4
Pipe Wall at Boiler Exit	14	35 3/32
Mixer	15,16	

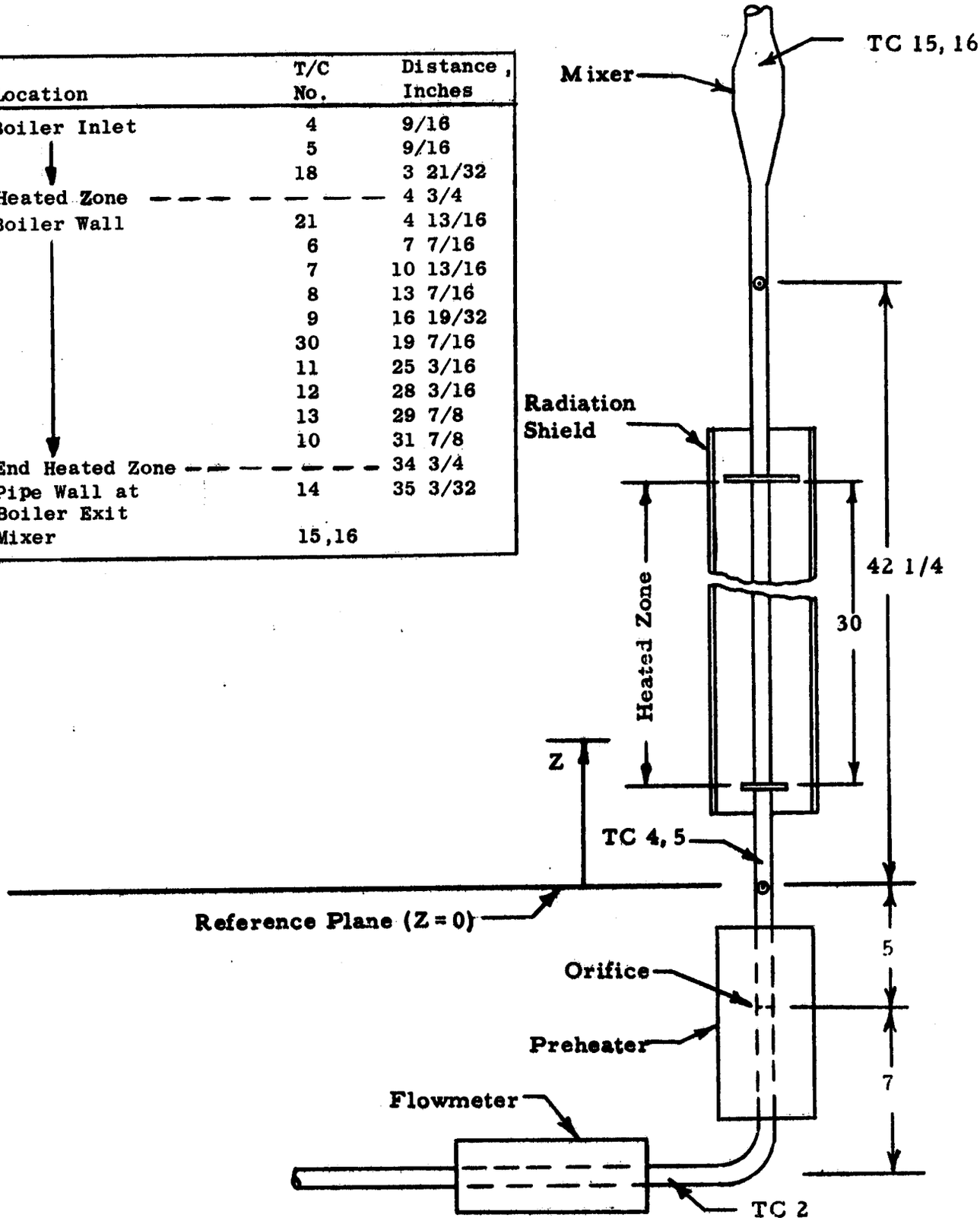

Figure B-3. Schematic of 100 KW Boiling Test Section Showing Thermocouple Locations: Effective November 14, 1963

TABLE 3: 100 KW BOILING POTASSIUM DATA
(Part 1. List of Symbols)

Column	Symbol	Identification
240	Date	1.1183 - 11/18/63
241	Time	1127 Navy time
250, 255	TPH IN	Preheater inlet temperature, ^{o}F
265, 270	TB IN	Boiler inlet temperature, ^{o}F
275-330	TWO 18-TWO 14	Outside wall temperature, ^{o}F
350, 355	T MIX	Boiler exit temperature, ^{o}F
360	CND IN	Condenser inlet temperature, ^{o}F
370-390	CND 19-CND 23	Condenser temperature, ^{o}F
395	PUMPIN	EM pump inlet temperature, ^{o}F
410, 420	TRADSH	Temperature of radiation shield, ^{o}F
453	QN PH	Net preheater power, kw
464	QN B	Net boiler power, kw
468	Q/A	Boiler heat flux, Btu/hr-ft^2
484	FLOW	Flow rate, lb/sec
487	G	Mass velocity, lb/hr-ft^2
497	X MIX	Quality at mixer, lbs vapor/lbs mixture
499	EB OUT	Enthalpy of mixture at mixer, Btu/lb
502	VELOUT	Vapor velocity at boiler exit, ft/sec
559-601	TWI 6-TWI 11	Inside wall temperature, ^{o}F
602	DT 11	$T_{wi} - T_{mix}$ at 11, ^{o}F
603	H 11	$\frac{q/A}{T_{wi} - T_{mix} \text{ at } 11}$, Btu/hr-ft^2-$^{o}F$
608	TWI 12	Inside wall temperature at 12, ^{o}F
609	DT 12	$T_{wi} - T_{mix}$ at 12, ^{o}F
610	H 12	$\frac{q/A}{T_{wi} - T_{mix} \text{ at } 12}$, Btu/hr-ft^2-$^{o}F$
615	TWI 13	Inside wall temperature at 13, ^{o}F
616	DT 13	$T_{wi} - T_{mix}$ at 13, ^{o}F
617	H 13	$\frac{q/A}{T_{wi} - T_{mix} \text{ at } 13}$, Btu/hr-ft^2-$^{o}F$
654	STBPAR	$\frac{q/A}{v H_{fg} V_{in}}$, dimensionless

TABLE 3:

100 KW BOILING POTASSIUM DATA

(Part 2. Tabulated Data)

	240	241	250	255	265	270
	DATE	TIME	TPH IN	TPH IN	TB IN	TB IN
1	1.1263+04	1.1270+03	9.9773+02	9.9253+02	1.2291+03	1.2341+03
2	1.1223+04	9.0100+02	9.2982+02	9.2425+02	1.4469+03	1.4550+03
3	1.1223+04	9.1700+02	9.3436+02	9.2857+02	1.4542+03	1.4608+03
4	1.1223+04	1.0030+03	9.5537+02	9.4941+02	1.4861+03	1.4935+03
5	1.1223+04	1.0200+03	9.6497+02	9.5763+02	1.4928+03	1.4992+03
6	1.1223+04	1.1040+03	9.6469+02	9.5782+02	1.4874+03	1.4969+03
7	1.1223+04	1.1180+03	9.6428+02	9.5718+02	1.4877+03	1.4964+03
8	1.1223+04	1.2160+03	9.6917+02	9.6196+02	1.4972+03	1.5048+03
9	1.1223+04	1.2420+03	9.7097+02	9.6371+02	1.4969+03	1.5047+03
10	1.1223+04	1.3260+03	1.0023+03	9.9409+02	1.5413+03	1.5498+03
11	1.1223+04	1.3460+03	1.0069+03	9.9851+02	1.5518+03	1.5606+03
12	1.1223+04	1.4420+03	9.4137+02	9.3476+02	1.4555+03	1.4614+03
13	1.1263+04	1.2330+03	6.5526+02	6.5188+02	1.4379+03	1.4438+03
14	1.1263+04	1.3260+03	6.4874+02	6.4479+02	1.4484+03	1.4532+03
15	1.1263+04	1.4400+03	6.7530+02	6.7163+02	1.6457+03	1.6515+03
16	1.1273+04	1.1360+03	6.8772+02	6.8391+02	1.5217+03	1.5287+03
17	1.1273+04	1.2360+03	6.6771+02	6.6353+02	1.6418+03	1.6462+03
18	1.1293+04	1.0250+03	9.1420+02	9.0836+02	1.4377+03	1.4443+03
19	1.1293+04	1.0440+03	9.1140+02	9.0312+02	1.4321+03	1.4387+03
20	1.1293+04	1.2550+03	8.0399+02	7.9760+02	1.5911+03	1.5997+03
21	1.1293+04	1.3290+03	8.0213+02	7.9573+02	1.5880+03	1.5956+03
22	1.1293+04	1.5040+03	1.0733+03	1.0668+03	1.3900+03	1.3968+03
23	1.1293+04	1.5220+03	1.0774+03	1.0710+03	1.3951+03	1.4027+03
24	1.2023+04	1.2360+03	8.9358+02	8.8708+02	1.3279+03	1.3345+03
25	1.2023+04	1.2560+03	8.9131+02	8.8495+02	1.3256+03	1.3324+03
26	1.2023+04	1.3460+03	8.2682+02	8.2003+02	1.5068+03	1.5152+03
27	1.2023+04	1.4030+03	8.1602+02	8.0936+02	1.4962+03	1.5011+03
28	1.2023+04	1.5430+03	1.1827+03	1.1758+03	1.3951+03	1.4040+03
29	1.2023+04	1.6020+03	1.1841+03	1.1776+03	1.3981+03	1.4058+03

100 KW BOILING POTASSIUM DATA

	275	280	285	290	295	300
	TWO 18	TWO 21	TWO 6	TWO 7	TWO 8	TWO 9
1	1.3194+03	9.9249+02	1.5057+03	1.6258+03	1.7265+03	1.8193+03
2	1.5588+03	1.6558+03	1.8445+03	2.0067+03	2.1172+03	2.0823+03
3	1.5656+03	1.6589+03	1.8482+03	2.0133+03	2.1172+03	2.0810+03
4	1.6227+03	1.7483+03	1.9689+03	2.1177+03	2.0905+03	2.0955+03
5	1.6328+03	1.7554+03	1.9747+03	2.1255+03	2.0890+03	2.0967+03
6	1.6286+03	1.7526+03	1.9758+03	2.1553+03	2.1347+03	2.1380+03
7	1.6287+03	1.7531+03	1.97[illegible]+03	2.1552+03	2.1381+03	2.1400+03
8	1.6[illegible]70+03	1.7740+03	2.0145+03	2.2031+03	2.1819+03	2.1929+03
9	1.6470+03	1.7741+03	2.0120+03	2.2020+03	2.1821+03	2.1931+03
10	1.7235+03	1.8841+03	2.1687+03	2.1976+03	2.1510+03	2.1978+03
11	1.7343+03	1.8932+03	2.1806+03	2.1973+03	2.1582+03	2.1954+03
12	1.5673+03	1.6567+03	1.8387+03	1.9890+03	2.0966+03	2.1725+03
13	1.4812+03	1.5210+03	1.6250+03	1.7159+03	1.7795+03	1.7688+03
14	1.4958+03	1.5356+03	1.6277+03	1.7181+03	1.7825+03	1.7630+03
15	1.6765+03	1.7123+03	1.7975+03	1.8356+03	1.7691+03	1.7677+03
16	1.5787+03	1.6339+03	1.7639+03	1.8477+03	1.7933+03	1.7917+03
17	1.6933+03	1.7515+03	1.8801+03	1.7867+03	1.7902+03	1.7898+03
18	1.5796+03	1.7091+03	1.9453+03	2.1500+03	2.1923+03	2.1902+03
19	1.5713+03	1.6958+03	1.9267+03	2.1265+03	2.1924+03	2.1916+03
20	1.7744+03	1.9340+03	2.2328+03	2.1877+03	2.1791+03	2.1866+03
21	1.7719+03	1.9320+03	2.2297+03	2.1880+03	2.1817+03	2.1891+03
22	1.5068+03	1.6071+03	1.7735+03	1.9228+03	2.0266+03	2.1710+03
23	1.5121+03	1.6115+03	1.7783+03	1.9220+03	2.0211+03	2.160[illegible]+03
24	1.5090+03	1.6714+03	1.9644+03	2.2289+03	2.2892+03	2.2878+03
25	1.5092+03	1.6703+03	1.9620+03	2.2257+03	2.2871+03	2.2841+03
26	1.7258+03	1.9152+03	2.2646+03	2.2817+03	2.277[illegible]+03	2.2843+03
27	1.7120+03	1.9003+03	2.2518+03	2.2812+03	2.2782+03	2.2817+03
28	1.5151+03	1.6128+03	1.7559+03	1.8790+03	1.9706+03	2.1111+03
29	1.5151+03	1.6137+03	1.7560+03	1.8775+03	1.9723+03	2.1150+03

100 KW BOILING POTASSIUM DATA

	305	310	315	320	325	330
	TWO 30	TWO 10	TWO 11	TWO 12	TWO 13	TWO 14
1	1.7540+03		1.7410+03	1.7361+03	1.7560+03	1.7402+03
2	2.0348+03	2.0372+03	2.0373+03	2.0392+03	2.0598+03	2.0429+03
3	2.0299+03	2.0363+03	2.0371+03	2.0376+03	2.0594+03	2.0426+03
4	2.0568+03	2.0468+03	2.0486+03	2.0535+03	2.0765+03	2.0572+03
5	2.0461+03	2.0452+03	2.0516+03	2.0540+03	2.0742+03	2.0566+03
6	2.0195+03	2.0870+03	2.0922+03	2.0907+03	2.1172+03	2.1036+03
7	2.0230+03	2.0884+03	2.0959+03	2.0908+03	2.1187+03	2.1029+03
8	2.0378+03	2.1329+03	2.1424+03	2.1418+03	2.1661+03	2.1513+03
9	2.0563+03	2.1320+03	2.1495+03	2.1438+03	2.1668+03	2.1508+03
10	2.0531+03	2.1324+03	2.1726+03	2.1385+03	2.1723+03	2.1612+03
11	2.0583+03	2.1322+03	2.1726+03	2.1423+03	2.1748+03	2.1606+03
12	2.1229+03	2.1140+03	2.1341+03	2.1308+03	2.1488+03	2.1351+03
13	1.7541+03	1.7475+03	1.7435+03	1.7427+03	1.7572+03	1.7445+03
14	1.7531+03	1.7465+03	1.7423+03	1.7418+03	1.7568+03	1.7432+03
15	1.7530+03	1.7490+03	1.7450+03	1.7438+03	1.7589+03	1.7459+03
16		1.7700+03	1.7691+03	1.7657+03	1.7823+03	1.7684+03
17		1.7697+03	1.7684+03	1.7653+03	1.7817+03	1.7677+03
18		2.1361+03	2.1527+03	2.1488+03	2.1700+03	2.1559+03
19		2.1356+03	2.1541+03	2.1482+03	2.1686+03	2.1550+03
20		2.1381+03	2.1507+03		2.1732+03	2.1625+03
21		2.1389+03	2.1535+03		2.1743+03	2.1623+03
22		2.1364+03	2.1633+03		2.1754+03	2.1605+03
23		2.1356+03	2.1643+03		2.1757+03	2.1615+03
24		2.2248+03	2.2417+03		2.2614+03	2.2495+03
25		2.2229+03	2.2413+03		2.2599+03	2.2472+03
26		2.2267+03	2.2365+03		2.2689+03	2.5668+03
27		2.2254+03	2.2382+03		2.2688+03	2.5952+03
28		2.2263+03	2.2604+03		2.2758+03	2.5806+03
29		2.2253+03	2.2641+03		2.2747+03	2.5788+03

100 KW BOILING POTASSIUM DATA

	350	355	360	370	375	385
	T MIX	T MIX	CND IN	CND 19	CND 20	CND 22
1	1.7058+03	1.7037+03	1.7233+03	1.6888+03	1.4416+03	1.2048+03
2	2.0087+03	2.0064+03	2.0245+03	1.6931+03	1.4137+03	1.1698+03
3	2.0085+03	2.0062+03	2.0242+03	1.6928+03	1.4138+03	1.1706+03
4	2.0159+03	2.0136+03	2.0319+03	2.0054+03	1.5435+03	1.2357+03
5	2.0154+03	2.0130+03	2.0312+03	1.9919+03	1.5406+03	1.2360+03
6	2.0592+03	2.0567+03	2.0748+03	1.8875+03	1.5072+03	1.2246+03
7	2.0606+03	2.0581+03	2.0761+03	1.8942+03	1.5067+03	1.2258+03
8	2.1056+03	2.1031+03	2.1205+03	1.9083+03	1.5218+03	1.2383+03
9	2.1050+03	2.1027+03	2.1200+03	1.8980+03	1.5112+03	1.2351+03
10	2.1037+03	2.1012+03	2.1182+03	2.1032+03	1.7391+03	1.3233+03
11	2.1050+03	2.1023+03	2.1195+03	2.1043+03	1.7467+03	1.3245+03
12	2.0995+03	2.0975+03	2.1125+03	1.5744+03	1.3562+03	1.1447+03
13	1.7312+03	1.7294+03	1.7455+03	1.1517+03	9.9135+02	8.3204+02
14	1.7307+03	1.7290+03	1.7445+03	1.1478+03	9.9086+02	8.2994+02
15	1.7329+03	1.7309+03	1.7471+03	1.2285+03	1.0499+03	8.7269+02
16	1.7512+03	1.7493+03	1.7656+03	1.2848+03	1.0819+03	8.9576+02
17	1.7510+03	1.7492+03	1.7650+03	1.2772+03	1.0536+03	8.7006+02
18	2.1148+03	2.1119+03	2.1275+03	1.7082+03	1.4144+03	1.1647+03
19	2.1148+03	2.1121+03	2.1275+03	1.6759+03	1.3956+03	1.1568+03
20	2.1163+03	2.1137+03	2.1288+03	1.8068+03	1.3579+03	1.0964+03
21	2.1169+03	2.1146+03	2.1294+03	1.7809+03	1.3534+03	1.0922+03
22	2.1134+03	2.1124+03	2.1246+03	1.7263+03	1.5016+03	1.2804+03
23	2.1142+03	2.1115+03	2.1251+03	1.7207+03	1.5011+03	1.2801+03
24	2.2025+03	2.1997+03	2.2132+03	1.7108+03	1.4035+03	1.1594+03
25	2.2009+03	2.1982+03	2.2114+03	1.7024+03	1.3974+03	1.1540+03
26	2.2037+03	2.2011+03	2.2142+03	1.7572+03	1.3555+03	1.1043+03
27	2.2032+03	2.2003+03	2.2134+03	1.7447+03	1.3518+03	1.1053+03
28	2.2024+03	2.1992+03	2.2106+03	1.7478+03	1.5603+03	1.3563+03
29	2.2012+03	2.1983+03	2.2095+03	1.7467+03	1.5594+03	1.3557+03

100 KW BOILING POTASSIUM DATA

	390	395	410	420	453	464
	CND 23	PUMPIN	TRADSH	TRADSH	QN PH	QN B
1	1.1212+03	1.0039+03	8.7730+02	9.0525+02	1.3814+00	7.6303+00
2	1.0876+03	9.6146+02	9.4358+02	9.7288+02	2.2109+00	8.5812+00
3	1.0896+03	9.6337+02	9.4650+02	9.7544+02	2.2180+00	8.4856+00
4	1.1428+03	9.9877+02	9.9984+02	1.0223+03	2.1791+00	1.0272+01
5	1.1435+03	9.9952+02	1.0005+03	1.0225+03	2.1721+00	1.0122+01
6	1.1356+03	9.9421+02	1.0049+03	1.0290+03	2.2109+00	1.0099+01
7	1.1375+03	9.9745+02	1.0068+03	1.0308+03	2.2180+00	1.0180+01
8	1.1480+03	1.0047+03	1.0261+03	1.0502+03	2.2679+00	1.0582+01
9	1.1465+03	1.0050+03	1.0261+03	1.0493+03	2.2393+00	1.0398+01
10	1.2161+03	1.0481+03	1.0835+03	1.0996+03	2.2322+00	1.2968+01
11	1.2169+03	1.0489+03	1.0863+03	1.1004+03	2.2180+00	1.2819+01
12	1.0727+03	9.4911+02	9.5154+02	9.8218+02	2.2180+00	7.8707+00
13	7.7951+02	8.4354+02	7.2963+02	7.5632+02	1.9090+00	2.8001+00
14	7.7519+02	8.3828+02	7.2789+02	7.5320+02	1.9894+00	2.8143+00
15	8.1299+02	8.9381+02	7.4736+02	7.6147+02	2.6692+00	2.7438+00
16	8.3382+02	9.3495+02	7.8283+02	7.9962+02	2.0815+00	3.6401+00
17	8.1327+02	9.2623+02	7.8730+02	8.0126+02	2.0710+00	3.6539+00
18	1.0832+03	9.5104+02	9.9283+02	1.0206+03	1.8886+00	9.5280+00
19	1.0863+03	9.4910+02	9.8667+02	1.0163+03	1.8496+00	9.1609+00
20	1.0162+03	8.7162+02	1.0124+03	1.0311+03	1.8524+00	9.3095+00
21	1.0144+03	8.6937+02	1.0120+03	1.0314+03	1.8496+00	9.8077+00
22	1.1976+03		9.9073+02	1.0330+03	1.8166+00	9.7304+00
23	1.1977+03	1.0772+03	9.9129+02	1.0342+03	1.8718+00	9.7136+00
24	1.0787+03		1.0226+03	1.0611+03	1.3893+00	1.0595+01
25	1.0741+03		1.0207+03	1.0600+03	1.3559+00	1.0452+01
26	1.0307+03		1.9411+03	1.0698+03	1.6324+00	5.6413+00
27	1.0273+03		1.0374+03	1.0681+03	1.5649+00	1.0142+01
28	1.2757+03		1.0108+03	1.0715+03	1.6486+00	1.0871+01
29	1.2755+03		1.0095+03	1.0711+03	1.6324+00	1.0589+01

100 KW BOILING POTASSIUM DATA

	468	484	487	497	499	502
	Q/A	FLOW	G	X MIX	EB OUT	VELOUT
1	9.4047+04	3.5171-02	1.2974+05	1.3526-01	5.1812+02	4.6634+01
2	1.0577+05	2.6931-02	9.9347+04	2.2150-01	6.4272+02	2.3906+01
3	1.0459+05	2.7535-02	1.0157+05	2.0813-01	6.3217+02	2.2976+01
4	1.2661+05	2.6860-02	9.9084+04	3.0160-01	7.0703+02	3.1892+01
5	1.2475+05	2.7170-02	1.0023+05	2.9046-01	6.9817+02	3.1110+01
6	1.2448+05	2.7739-02	1.0233+05	2.6981-01	6.8989+02	2.6472+01
7	1.2547+05	2.7472-02	1.0134+05	2.7846-01	6.9691+02	2.6958+01
8	1.3043+05	2.7766-02	1.0243+05	2.8299-01	7.0873+02	2.4823+01
9	1.2816+05	2.7514-02	1.0150+05	2.7925-01	7.0572+02	2.4300+01
10	1.5984+05	2.6002-02	9.5917+04	4.3973-01	8.3020+02	3.6275+01
11	1.5800+05	2.6308-02	9.7048+04	4.2466-01	8.1868+02	3.5350+01
12	9.7011+04	2.8779-02	1.0616+05	1.4104-01	5.9727+02	1.2996+01
13	3.4512+04	1.6610-02	6.1274+04	8.4655-02	4.8145+02	1.2720+01
14	3.4688+04	1.8218-02	6.7206+04	6.0257-02	4.6146+02	9.9437+00
15	3.3819+04	1.8476-02	6.8155+04	9.9808-02	4.9411+02	1.6599+01
16	4.4866+04	1.7691-02	6.5261+04	1.3385-01	5.2524+02	2.0045+01
17	4.5031+04	1.4513-02	5.3538+04	2.1210-01	5.8888+02	2.6075+01
18	1.1744+05	2.4434-02	9.0135+04	2.7338-01	7.0292+02	2.0673+01
19	1.1291+05	2.4969-02	9.2107+04	2.4061-01	6.7752+02	1.8588+01
20	1.1474+05	1.7062-02	5.2938+04	4.7552-01	8.6007+02	2.5018+01
21	1.2089+05	1.7055-02	6.2916+04	5.1069-01	8.8748+02	2.6812+01
22	1.1993+05	3.9112-02	1.4428+05	1.0077-01	5.6887+02	1.2210+01
23	1.1972+05	3.9140-02	1.4438+05	1.0267-01	5.7034+02	1.2450+01
24	1.3059+05	2.0914-02	7.7150+04	3.7753-01	7.9943+02	2.0039+01
25	1.2883+05	2.2276-02	8.2174+04	3.2433-01	7.5832+02	1.8397+01
26	6.9533+04	1.6777-02	6.1888+04	1.8908-01	6.5508+02	8.0288+00
27	1.2500+05	1.6270-02	6.0019+04	5.3995-01	9.2415+02	2.2267+01
28	1.3399+05	4.9942-02	1.8423+05	4.8203-02	5.4666+02	6.1138+00
29	1.3051+05	4.9976-02	1.8436+05	4.1251-02	5.4110+02	5.2474+00

100 KW BOILING POTASSIUM DATA

	559	566	573	580	587	601
	TWI 6	TWI 7	TWI 8	TWI 9	TWI 30	TWI 11
1	1.4822+03	1.6024+03	1.7032+03	1.7962+03	1.7308+03	1.7178+03
2	1.8186+03	1.9811+03	2.0917+03	2.0567+03	2.0092+03	2.0117+03
3	1.8226+03	1.9880+03	2.0920+03	2.0557+03	2.0045+03	2.0117+03
4	1.9381+03	2.0872+03	2.0599+03	2.0650+03	2.0262+03	2.0180+03
5	1.9444+03	2.0955+03	2.0589+03	2.0646+03	2.0139+03	2.0215+03
6	1.9455+03	2.1254+03	2.1047+03	2.1081+03	1.9894+03	2.0622+03
7	1.9461+03	2.1251+03	2.1079+03	2.1098+03	1.9926+03	2.0656+03
8	1.9829+03	2.1718+03	2.1506+03	2.1617+03	2.0063+03	2.1111+03
9	1.9818+03	2.1713+03	2.1514+03	2.1624+03	2.0253+03	2.1187+03
10	2.1304+03	2.1593+03	2.1126+03	2.1595+03	2.0144+03	2.1342+03
11	2.1428+03	2.1600+03	2.1203+03	2.1575+03	2.0202+03	2.1347+03
12	1.8149+03	1.9654+03	2.0732+03	2.1493+03	2.0995+03	2.1108+03
13	1.6165+03	1.7074+03	1.7710+03	1.7603+03	1.7456+03	1.7350+03
14	1.6191+03	1.7095+03	1.7740+03	1.7594+03	1.7445+03	1.7337+03
15	1.7892+03	1.8274+03	1.7608+03	1.7594+03	1.7447+03	1.7367+03
16	1.7529+03	1.8367+03	1.7823+03	1.7807+03		1.7581+03
17	1.8691+03	1.7756+03	1.7791+03	1.7788+03		1.7573+03
18	1.9167+03	2.1217+03	2.1642+03	2.1621+03		2.1244+03
19	1.8992+03	2.0993+03	2.1654+03	2.1645+03		2.1270+03
20	2.2053+03	2.1601+03	2.1516+03	2.1591+03		2.1231+03
21	2.2008+03	2.1591+03	2.1527+03	2.1602+03		2.1244+03
22	1.7440+03	1.8935+03	1.9976+03	2.1422+03		2.1345+03
23	1.7488+03	1.8928+03	1.9921+03	2.1317+03		2.1356+03
24	1.9327+03	2.1977+03	2.2581+03	2.2567+03		2.2105+03
25	1.9307+03	2.1949+03	2.2564+03	2.2534+03		2.2106+03
26	2.2480+03	2.2651+03	2.2609+03	2.2677+03		2.2199+03
27	2.2219+03	2.2514+03	2.2484+03	2.2519+03		2.2083+03
28	1.7229+03	1.8463+03	1.9380+03	2.0788+03		2.2284+03
29	1.7239+03	1.8456+03	1.9406+03	2.0835+03		2.2329+03

100 KW BOILING POTASSIUM DATA

	602	603	608	609	610	615
	DT 11	H 11	TWI 12	DT 12	H 12	TWI 13
1	1.3078+01	7.1912+03	1.7129+03	8.1613+00	1.1524+04	1.7329+03
2	4.1480+00	2.5498+04	2.0136+03	6.0520+00	1.7477+04	2.0342+03
3	4.3719+00	2.3923+04	2.0123+03	4.9513+00	2.1124+04	2.0341+03
4	3.1840+00	3.9763+04	2.0229+03	8.0900+00	1.5650+04	2.0459+03
5	7.2431+00	1.7224+04	2.0238+03	9.5713+00	1.3034+04	2.0441+03
6	4.2508+00	2.9284+04	2.0607+03	2.7479+00	4.5301+04	2.0872+03
7	6.2494+00	2.0077+04	2.0605+03	1.1562+00	1.0852+05	2.0885+03
8	6.7410+00	1.9349+04	2.1104+03	6.0645+00	2.1507+04	2.1348+03
9	1.4858+01	8.6256+03	2.1130+03	9.1926+00	1.3941+04	2.1361+03
10	3.1714+01	5.0399+03	2.1001+03	-2.4245+00	-6.5925+04	2.1339+03
11	3.1042+01	5.0898+03	2.1044+03	7.0386-01	2.2447+05	2.1369+03
12	1.2238+01	7.9267+03	2.1075+03	8.9563+00	1.0832+04	2.1255+03
13	4.6856+00	7.3656+03	1.7342+03	3.9127+00	8.8207+03	1.7487+03
14	3.8461+00	9.0190+03	1.7333+03	3.4167+00	1.0153+04	1.7483+03
15	4.7531+00	7.1152+03	1.7355+03	3.5507+00	9.5246+03	1.7506+03
16	7.7896+00	5.7597+03	1.7547+03	4.3683+00	1.0271+04	1.7712+03
17	7.2067+00	6.2486+03	1.7542+03	4.1275+00	1.0910+04	1.7707+03
18	1.1089+01	1.0590+04	2.1206+03	7.2002+00	1.6310+04	2.1418+03
19	1.3499+01	8.3648+03	2.1211+03	7.5812+00	1.4894+04	2.1415+03
20	8.1672+00	1.4049+04				2.1457+03
21	8.6698+00	1.3943+04				2.1453+03
22	2.1646+01	5.5407+03				2.1466+03
23	2.2720+01	5.2695+03				2.1470+03
24	9.3861+00	1.3913+04				2.2302+03
25	1.0981+01	1.1732+04				2.2292+03
26	1.7477+01	3.9784+03				2.2523+03
27	6.5662+00	1.9037+04				2.2390+03
28	2.7620+01	4.8513+03				2.2438+03
29	3.3190+01	3.9323+03				2.2436+03

100 KW BOILING POTASSIUM DATA

	616	617	654
	H 13	H 13	STBPAR
1	2.8123+01	3.3442+03	3.6118-01
2	2.6664+01	3.9668+03	2.1747-01
3	2.6720+01	3.9143+03	2.1019-01
4	3.1123+01	4.0679+03	2.5501-01
5	2.9860+01	4.1780+03	2.4848-01
6	2.9287+01	4.2504+03	2.1928-01
7	2.9122+01	4.3084+03	2.2239-01
8	3.0443+01	4.2845+03	2.0596-01
9	3.2220+01	3.9775+03	2.0444-01
10	3.1453+01	5.0907+03	2.6863-01
11	3.3250+01	4.7517+03	2.6134-01
12	2.7004+01	3.5925+03	1.5073-01
13	1.8427+01	1.8729+03	2.5089-01
14	1.8447+01	1.8805+03	2.2983-01
15	1.8666+01	1.8118+03	2.1273-01
16	2.0952+01	2.1414+03	2.8337-01
17	2.0942+01	2.1921+03	3.4037-01
18	2.8462+01	4.1261+03	2.0872-01
19	2.7990+01	4.0340+03	1.9651-01
20	3.0710+01	3.7364+03	2.8386-01
21	2.9523+01	4.0939+03	2.9884-01
22	3.3702+01	3.5586+03	1.3435-01
23	3.4097+01	3.5113+03	1.3391-01
24	2.9090+01	4.4889+03	2.2904-01
25	2.9570+01	4.3567+03	2.1288-01
26	4.9890+01	1.3937+03	1.4720-01
27	3.7300+01	3.3512+03	2.7379-01
28	4.3036+01	3.1135+03	9.7371-02
29	4.3809+01	2.9791+03	9.4937-02

APPENDIX C. 50 KW FACILITY
HEAT TRANSFER DATA

In this quarter, 128 data runs were completed. The tabulated data from the eighteen condensing runs and the liquid runs are given here. Presentation of the data comprises the following:

A. Liquid and Condensing Data Reduction Procedure

B. Liquid Liquid Data
   - Part 1) List of Symbols defining the Column headings employed in the Condensing runs
   - Part 2) Tabulated Liquid Liquid data

C. Condensing Data
   - Part 1) A list of Symbols defining the Column headings employed in the Condensing runs
   - Part 2) The tabulated Condensing runs data

A. 50 KW Liquid and Condensing Data Reduction Procedure

Reduction of the raw data for the liquid-liquid runs followed the following pattern.

Fluid and Wall Temperatures:

1. Each test section thermocouple reading was converted from millivolts to °F.

2. The inlet and outlet potassium and sodium temperatures were then determined by averaging the thermocouples at each respective station. There are three thermocouples measuring the sodium inlet temperature and three thermocouples measuring the sodium outlet temperature. The potassium inlet and outlet temperatures are measured by two thermocouples at each position.

Liquid Data Reduction

Liquid Flow Rate

The standard equation for calculation of the flow rate of a conducting fluid from the emf generated by an electromagnetic is from reference 20.

$$\left(\frac{W}{E}\right)' = \frac{60 \times 10^5 \, D_i \, \rho_t'}{3.96 \, BC_1C_2C_3} \qquad (1)$$

where

$$C_1 = \frac{2 \, D_i/D_o}{1 + \left(\frac{D_i}{D_o}\right)^2 + \frac{\rho'_f}{\rho'_w}\left[1 - \left(\frac{D_i}{D_o}\right)^2\right]}$$

C_2 = End effect correction = 0.989 (Reference 20)

C_3 = Correction for flux and dimension change with temperature (Reference 20)

The critical dimensions and flux ratings of the two magnetic flowmeters are:

Flowmeter	Fluid	Room Temperature Constants		
		D_1, in	D_o, in	B, gauss
1	K	0.618	0.841	1989
2	Na	0.610	0.843	2019

The resultant flow-emf relation as a function of temperature is given in Figure C-1. The correction factor C_3 was left as a parameter in Figure C-1 since it depends on the magnet temperature. Its value for this set of experiments was $.99<C_3<1.0$ (reference 20). The potassium flowrate calculated from the flow-emf curve of Figure C-1 was found to give a flow that was 14.5% too low and was subsequently adjusted (see Calorimetric Flowmeter). The sodium flow-emf curve is considered approximately correct since the standard deviation of the test section heat balance results was $\pm 6.7\%$ with a mean of 0.3%. Both magnets were checked for flux density at the end of the experiment and showed less than 3% change.

Test Section Heat Load, Q,

The test section heat load was calculated from the potassium heat balance.

$$q_c = q_K = W_K C_{pKM} (T_{K,\ in} - T_{K,\ out}) \tag{2}$$

This is undoubtedly the most accurate method of determining the heat load since the potassium flowrate is known within $\pm 3\%$ and the potassium temperature difference is at least 30°F for all liquid data runs. A test section heat balance was carried out to compare the results of this calculation to that of the sum of the sodium heat gain and the test section heat loss by equation (2).

$$\%\ \text{Error} = \frac{q_K - (q_L + q_{Na})}{q_K} (100) \tag{3}$$

This relation gave a standard error of $\pm 6.7\%$ with an average error of 0.3% when the relative sodium thermocouple corrections were made.

Overall Heat Transfer Coefficient, U_i, Btu/hr ft^2 °F

From the log mean temperature difference, °F, which is calculated from equation (4)

$$\Delta T_{lm} = \frac{(T_K - T_{Na})in - (T_K - T_{Na})\ out}{\ln \frac{(T_K - T_{Na})\ in}{(T_K - T_{Na})\ out}} \quad (4)$$

and the test section head load, q_c, the overall heat transfer coefficient based on the tube's inside area was calculated by equation (5)

$$U_i = q_c/(\Delta T_{lm})(A_i) \quad (5)$$

Local Potassium and Sodium Temperatures

Assuming that the controlling resistance to heat transfer in the test section is the thick walled nickel tube for the range of liquid Peclet numbers covered, (i.e. that the overall coefficient U_i is not a function of length, but is a constant) at any point along the test section, equation (5) holds:

$$q = U_i A_i (T_K - T_{Na}) \quad (6)$$

A heat balance to the axial point z gives

$$q = W_K C_{pK}(T_{K,in} - T_{K,z}) = W_{Na} C_{pNa}(T_{Na,z} - T_{Na,in}) \quad (7)$$

Letting $\beta = W_K C_{pK}/W_{Na} C_{pNa}$ (8)

from (7) $\beta (T_{K,in} - T_{K,z}) + T_{Na,in} = T_{Na,z}$ (9)

From equations (6) and (9) one obtains

$$q = U_i A_i \left[T_{K,z} - \beta (T_{K,in} - T_{K,z}) - T_{Na,in}\right] \quad (10)$$

For a differential length, equation (11) can be obtained

$$\frac{dq}{dz} = 2\pi R_i U_i \left[T_K - \beta (T_{K,in} - T_{K,z}) - T_{Na,in}\right] \quad (11)$$

From Equation (7)

$$\frac{dq}{dz} = -W_K C_{pK} \frac{dT_K}{dz} \quad (12)$$

Equating the right hand side of Equations (11) and (12) gives

$$\frac{-L\,T_K}{T_{K,z}(1+\beta) - \beta\,T_{K,in} - T_{Na,in}} = \frac{2\pi R_i U_i}{W_K C_{pK}}\,dZ \tag{13}$$

Integration of Equation (13) yields the following expression for T_K

$$T_{K,z} = T_{K,in} - \left\{ \frac{1 - \exp\left[\frac{(1+\beta)(T_{K,out} - T_{K,in})}{\Delta T_{lmn}} \frac{Z}{L}\right]}{1+\beta} \right\} \left(T_K - T_{Na} \right)_{in} \tag{14}$$

From equation (7) $T_{Na,z}$ can be calculated using the above relation for $T_{K,z}$

Local Heat Flux

From equation 6, the local heat flux based on the inside area of the tube can be calculated:

$$q/A_i = U_i\,(T_K - T_{Na})_z \tag{15}$$

Inner and Outer Wall Tube Temperatures

The radial heat flow in the tube wall is governed by Fourier's law of conduction:

$$q/z = -2\pi R k_W \frac{dT}{dR} \tag{16}$$

Integration of equation (16) from the inner wall gives

$$T = T_i - \frac{q}{2\pi z k_W} \ln R/R_i \tag{17}$$

The integration assumes that $k_W \neq f(T)$ which is a reasonable assumption for the small wall temperature drops encountered during the liquid data runs. Choosing the form of equation (17), the measured radial temperature profile is fit by a least squares process in the following manner:

1. Let $T = A' + B' \ln R/R_i$ (18)
2. Minimize $\sum_{N=1}^{N=i} (A' + B' \ln R/R_i - T_{WN})^2$ (19)
3. Since the local heat flow is known, the value of B' is set in equation (19) and

$$B' = \frac{-q}{2\pi z k_W} \tag{20}$$

4. The value of (A') required to minimize equation (19) is now calculated by differentiating equation (19) with respect to (A') and equating it to zero which yields

$$d/dA' \sum (A' + B' \ln \frac{R}{R_i} - T_{W_N})^2 = 0 \tag{21}$$

$$\sum_1^N A' + \sum_1^N B' \ln \frac{R}{R_i} - \sum_1^N T_{W_N} = 0 \tag{22}$$

and

$$A' = \frac{\sum_1^N T_{W_N} - \frac{q}{2\pi z k_W} \sum_1^N \ln \frac{R}{R_i}}{N} \tag{23}$$

The value of (A') is the desired inner wall temperature T_{W_i} as can be seen by comparing equations (17) and (18). The outer wall temperature is then calculated from the relation obtained by integrating equation (16) over the tube wall and

$$T_{W_O} = T_{W_i} - \frac{q}{2\pi z k_W} \ln \frac{R_o}{R_i} \tag{24}$$

Liquid Heat Transfer Coefficient and Nusselt Number

From the local heat flux q/Ai, the potassium fluid temperature, and the inner wall temperature, the local liquid heat transfer coefficient can be calculated from equation (25)

$$h_K = \frac{(q/A)_i}{T_K - T_{W_i}} \tag{25}$$

The potassium Nusselt number can be calculated from equation (26)

$$N_{Nu\,K} = \frac{h_K D_i}{k_K} \tag{26}$$

For these calculations, the potassium thermal conductivity was evaluated at the bulk stream potassium temperature. In the same manner, the sodium side heat transfer coefficient and Nusselt number were calculated from equations (27) and (28) respectively.

$$h_{Na} = \frac{(q/A)_o}{T_{W_o} - T_{Na}} \tag{27}$$

$$N_{Nu\,Na} = \frac{h_{Na} D_A}{k_{Na}} \tag{28}$$

Sodium and Potassium Peclet Numbers

The sodium and potassium Peclet numbers are defined by equations (29) and (30) respectively.

$$N_{Pe\,Na} = \left[\frac{4\,W\,C_p}{\pi\,k\,(D_i + D_o)}\right]_{Na} \tag{29}$$

$$N_{Pe\,K} = \left[\frac{4\,W\,C_p}{\pi\,D_i\,k}\right]_{K} \tag{30}$$

Condensing Data Reduction

Potassium Flow Rate

For the condensing runs reported in this quarterly, the potassium flowrate was calculated by a test section heat balance. This procedure was necessary since the line heaters were maintained at low power to minimize the chance of plugging in the return line from the condenser to the boiler due to excessive subcooling. The line heater has subsequently been routed away from the calorimeter so that in future testing, if line heat is required, it will not affect the calorimeter heat input. Normally the calorimeter measurement will be taken as a primary flow standard since the error analysis of Appendix A indicates a standard error of less than 3%.

The test section heat balance gives:

$$q_K = q_{Na} + q_L \tag{1}$$

Neglecting subcooling in the condensed film and velocity effects, q_K is given by

$$q_K = W_K\, X_{in}\, H_{fg,K} \tag{2}$$

or from equation (1) and (2)

$$q_{Na} + q_L = W_K\, X_{in}\, H_{fg,K} \tag{3}$$

Assuming that $X_{in} \sim 1.0$* the potassium flowrate can be obtained from equation (3) as

$$W_K = \frac{q_{Na} + q_L}{H_{fg,K}} \tag{4}$$

Local Nickel Inner Wall Tube Temperature and Heat Flux

A least squares procedure was used to fit the temperature profile in the tube wall to the theoretical Fourier conduction relation of equation (5)

$$T = T_{wi} - \frac{q}{2\pi\, z k_w} \ln \frac{R}{R_i} \tag{5}$$

* The assumption of 100% inlet quality will not be necessary when the potassium flowrate is determined from the calorimeter measurements.

The following relations were obtained:

$$T_{Wi} = \begin{vmatrix} \sum_1^N T_{WN} & \sum_1^N \ln \frac{R}{R_i} \\ \sum_1^N T_{WN} \ln R/R_i & \sum_1^N \left(\ln \frac{R}{R_i}\right)^2 \end{vmatrix} \left(\frac{1}{\bar{A}}\right) \tag{6}$$

$$q/2\pi k_W z = \begin{vmatrix} N & \sum_1^N T_{WN} \\ \sum_1^N \ln \frac{R}{R_i} & \sum_1^N T_{WN} \ln R/R_i \end{vmatrix} \left(\frac{1}{\bar{A}}\right) \tag{7}$$

$$\text{where } \bar{A} = \begin{vmatrix} 4 & \sum_1^N \ln R/R_i \\ \sum_1^N \ln R/R_i & \sum_1^N (\ln R/R_i)^2 \end{vmatrix} \tag{8}$$

The local inner wall heat flux is given by equation (9).

$$q/A_i = \left[q/2\pi z k_w\right]\left[k_w/R_i\right] \tag{9}$$

Local Potassium Temperature

The local potassium temperature was calculated by linear interpolation between measured inlet and outlet potassium bulk fluid temperatures.

Condensing Heat Transfer Coefficient

The condensing coefficient was calculated from equation (10)

Nusselts Condensing Ratio

$$h_c = \frac{q/A_i}{T_K - T_{wi}} \tag{10}$$

Nusselts condensing ratio is defined by equation (11)

$$N_{Nu\,c} = \frac{h_c}{k_K}\left(\frac{\nu_K^2}{g}\right)^{1/3} \tag{11}$$

All properties were evaluated at the potassium vapor temperature.

Condensing Pressure Drop

The potassium pressure drop was calculated by subtracting the outlet from the inlet pressure which corresponded to the respective measured saturation temperatures.

Sodium Heat Gain

The sodium heat gain was calculated from Equation 12.

$$q_{Na} = W_{Na}\, C_{p_{Na}}\, (T_{Na,\ out} - T_{Na,\ in}) \tag{12}$$

where Cp_{Na} was evaluated at the average sodium temperature from reference 20.

Film Reynolds Number

The local potassium liquid flowrate was calculated from a sodium heat balance up to the local station and the total calculated potassium flowrate. The local sodium temperature was calculated from the standard countercurrent heat exchanger equations similar to those used for the liquid reduction. The film Reynolds number is defined by Equation (13).

$$\frac{4\Gamma}{\mu_K} = \frac{4\, W_{K\,f}}{\pi\, D_i\, \mu_K} \tag{13}$$

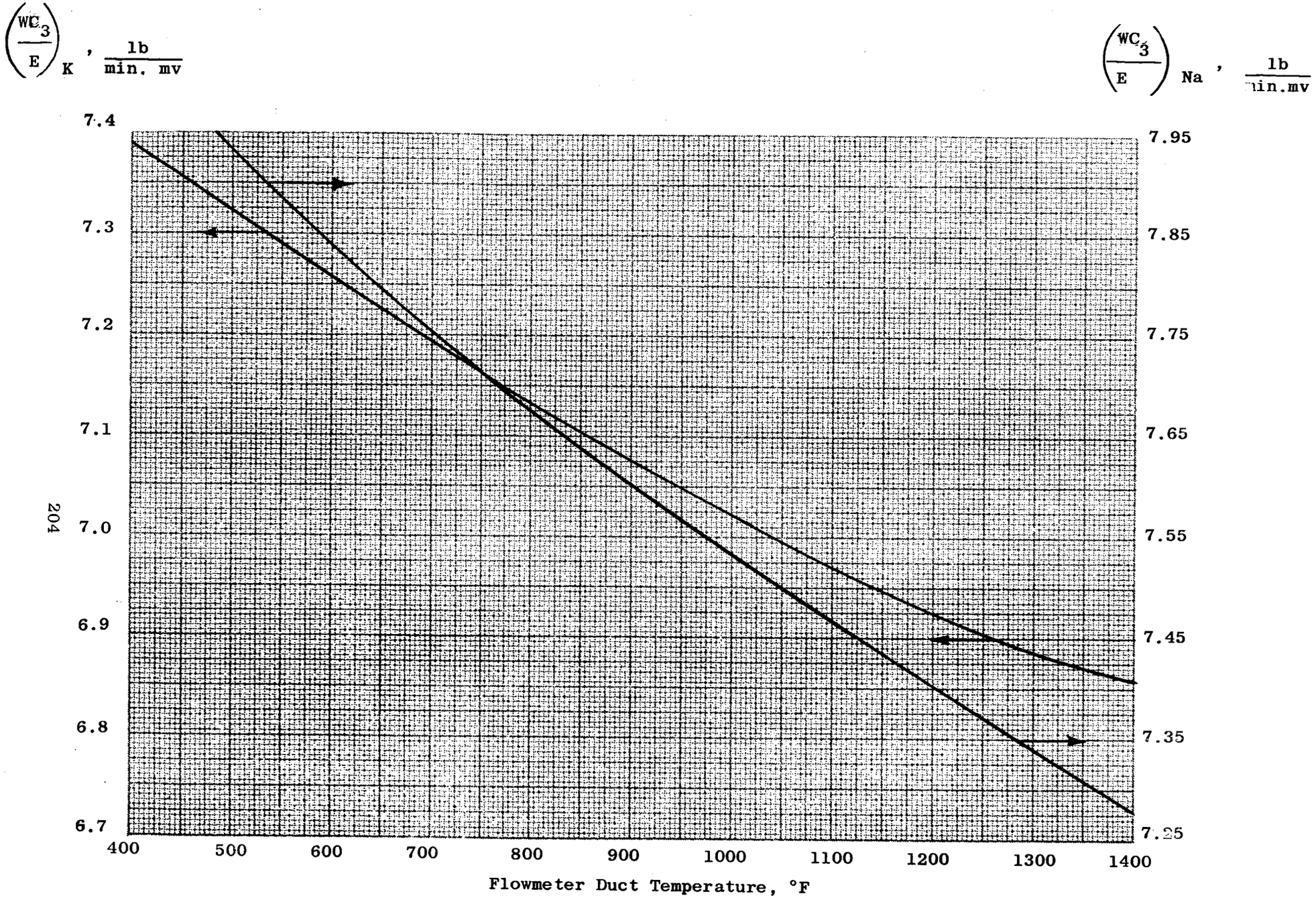

Figure C-1. 50 KW Flowmeter Relations.

TABLE 1: LIQUID-LIQUID RUNS CORRECTED K FLOW
(Part 1. List of Symbols)

Column	Symbol	Identification
251-306	TCN	Temperature of thermocouple N, ^{o}F
311	TKO	Outlet potassium temperature, ^{o}F
313	TKI	Inlet potassium temperature, ^{o}F
316	TNA O	Outlet sodium temperature, ^{o}F
319	TNAI	Inlet sodium temperature, ^{o}F
325	WK	Potassium flowrate, lb/hr
330	WNA	Sodium flow rate, lb/hr
332	TKM	A verage potassium temperature, ^{o}F
334	TNAM	Average sodium temperature, ^{o}F
345	DTLM	Log mean T, ^{o}F
354	TKI	Local potassium temperature at first axial station, ^{o}F
359	TK2	Local potassium temperature at second axial station, ^{o}F
361	TNA 1	Local sodium temperature at fi rst axial station, ^{o}F
363	TNA 2	Local sodium temperature at second axial station, ^{o}F
364	QK	Heat transferred from potassium in test section, Btu/hr
366	UI	Over-all heat transfer coefficient based on inside area, Btu/hr ft^2 ^{o}F
369	Q/AI1	Local heat flux based on inside area at first axial station, Btu/hr-ft^2
370	Q/AI2	Local heat flux based on inside area at second axial station, Btu/hr-ft^2
379	NRENA	Sodium Reynolds number at first axial location, dimensionless
381	NREK 1	Potassium Reynolds number at first axial location, dimensionless
385	NPRNA	Sodium Prandtl number at first axial station, dimensionless
387	NPRK 1	Potassium Prandtl number at first axial station, dimensionless
388	NPENA 1	Sodium Peclet number at first axial station, dimensionless
389	NPEK 1	Potassium Peclet number at first axial station, dimensionless
398	NRENA 2	Sodium Reynolds number at second axial location, dimensionless
400	NREK 2	Potassium Reynolds number at second axial location, dimensionless

TABLE 1: LIQUID-LIQUID RUNS CORRECTED K FLOW
(Part 1. List of Symbols)

Column	Symbol	Identification
405	DTW 1	Wall temperature drop at first axial station, ^{o}F
406	DTW 2	Wall temperature drop at second axial station, ^{o}F
408	QNA	Heat gained by sodium in test section, Btu/hr
418	QL	Heat loss from test section, Btu/hr
422	DQ PCT	QK - (QL + QNA)/QK, error in heat balance, %
442	TWI 1	Inside wall temperature at first axial station, ^{o}F
443	TWO 1	Outside wall temperature at first axial station, ^{o}F
444	DTW-W 1	Local temperature difference from potassium to inside wall at first axial station, ^{o}F
445	DTW-N 1	Local temperature difference from outside wall to sodium atfirst axial station, ^{o}F
446	HK 1	Potassium heat transfer coefficient at first axial station, Btu/hr - ft^2 - ^{o}F
449	HNA 1	Sodium heat transfer coefficient at first axial station, Btu/hr - ft^2 - ^{o}F
448	Q/AO 1	O uter wall heat flux at first axial station, Btu/hr - ft^2
453	NUK 1	Potassium Nusselt number at first axial station, dimensionless
455	NUNA 1	Sodium Nusselt number at first axial station, dimensionless
464	TWI 2	Local temperature difference from potassium to inside wall at second axial station, ^{o}F
465	TWO 2	Local temperature difference from outside wall to sodium at second axial station, ^{o}F
466	DTK-W2	Local temperature difference from potassium to inside wall at second axial station, ^{o}F
467	DTW-N 2	Local temperature difference from outside wall to sodium at second axial station, ^{o}F

TABLE 1: LIQUID-LIQUID RUNS CORRECTED K FLOW
(Part 1. List of Symbols)

Column	Symbol	Identification
468	HK 2	Potassium heat transfer coefficient at second axial station, Btu/hr-ft^2 - °F
469	Q/AO 2	Outer wall heat flux at second axial station, Btu/hr-ft^2
470	HNA 2	Sodium heat transfer coefficient at second axial station, Btu/hr-ft^2 - °F
472	NUK 2	Potassium Nusselt number at second axial station, dimensionless
474	NUNA 2	Sodium Nusselt number at second axial station, dimensionless
487	HKOMIN	Minimum potassium average heat transfer coefficient neglecting sodium resistance, Btu/hr-ft^2-°F
490	NUKMIN	Minimum potassium average Nusselt number based on HKOMIN
703	NPRNA 2	Sodium Prandtl number at second axial location, dimensionless
705	NPRK 2	Potassium Prandtl number at second axial location, dimensionless
706	NPENA 2	Sodium Peclet number at second axial location, dimensionless
707	NPEK 2	Potassium Peclet number at second axial location, dimensionless

TABLE I

LIQUID-LIQUID RUNS CORRECTED K FLOW
(Part 2. Tabulated Data)

	800	801	251	254	257	260
	DATE	TIME	TC1	TC2	TC3	TC4
1	1.0033+04	1.2100+03	7.3124+02	7.3158+02	7.6835+02	7.6881+02
2	1.0033+04	1.2100+03	7.3120+02	7.3145+02	7.6818+02	7.6894+02
3	1.0033+04	1.2100+03	7.3115+02	7.3150+02	7.6818+02	7.6860+02
4	1.0033+04	1.2250+03	7.2953+02	7.2974+02	7.6644+02	7.6699+02
5	1.0033+04	1.2250+03	7.2949+02	7.2974+02	7.6606+02	7.6657+02
6	1.0033+04	1.2250+03	7.2940+02	7.2966+02	7.6589+02	7.6674+02
7	1.0033+04	1.3100+03	7.1825+02	7.1850+02	7.5576+02	7.5631+02
8	1.0033+04	1.3100+03	7.1816+02	7.1842+02	7.5564+02	7.5631+02
9	1.0033+04	1.3100+03	7.1799+02	7.1825+02	7.5597+02	7.5648+02
10	1.0033+04	1.3400+03	7.1017+02	7.1034+02	7.5004+02	7.5072+02
11	1.0033+04	1.3400+03	7.1009+02	7.1038+02	7.5013+02	7.5073+02
12	1.0033+04	1.3400+03	7.0996+02	7.1026+02	7.5025+02	7.5081+02
13	1.0033+04	1.4500+03	7.1154+02	7.1171+02	7.4893+02	7.4949+02
14	1.0033+04	1.4500+03	7.1137+02	7.1179+02	7.4915+02	7.4949+02
15	1.0033+04	1.4500+03	7.1132+02	7.1175+02	7.4919+02	7.4953+02
16	1.0033+04	1.5050+03	7.1013+02	7.1043+02	7.5025+02	7.5055+02
17	1.0033+04	1.5050+03	7.1009+02	7.1043+02	7.5051+02	7.5089+02
18	1.0033+04	1.5050+03	7.1021+02	7.1051+02	7.5021+02	7.5068+02
19	1.0033+04	1.5200+03	7.0748+02	7.0769+02	7.5191+02	7.5258+02
20	1.0033+04	1.5200+03	7.0752+02	7.0774+02	7.5178+02	7.5237+02
21	1.0033+04	1.5200+03	7.0756+02	7.0774+02	7.5182+02	7.5258+02
22	1.0033+04	1.5400+03	7.0410+02	7.0427+02	7.5398+02	7.5466+02
23	1.0033+04	1.5400+03	7.0402+02	7.0419+02	7.5398+02	7.5458+02
24	1.0033+04	1.5400+03	7.0402+02	7.0415+02	7.5403+02	7.5470+02
25	1.0033+04	1.6000+03	7.0085+02	7.0098+02	7.5559+02	7.5614+02
26	1.0033+04	1.6000+03	7.0085+02	7.0103+02	7.5559+02	7.5610+02
27	1.0033+04	1.6000+03	7.0073+02	7.0085+02	7.5581+02	7.5636+02
28	1.0033+04	1.6190+03	6.9487+02	6.9496+02	7.5864+02	7.5890+02
29	1.0033+04	1.6190+03	6.9483+02	6.9500+02	7.5864+02	7.5894+02
30	1.0033+04	1.6190+03	6.9496+02	6.9500+02	7.5839+02	7.5886+02

LIQUID-LIQUID RUNS CORRECTED K FLOW

	800	801	251	254	257	260
	DATE	TIME	TC1	TC2	TC3	TC4
31	1.0033+04	1.7050+03	7.0449+02	7.0462+02	7.5903+02	7.5936+02
32	1.0033+04	1.7050+03	7.0470+02	7.0479+02	7.5890+02	7.5945+02
33	1.0033+04	1.7050+03	7.0453+02	7.0470+02	7.5919+02	7.5949+02
34	1.0033+04	1.7270+03	7.0919+02	7.0919+02	7.5928+02	7.5975+02
35	1.0033+04	1.7270+03	7.0915+02	7.0949+02	7.5903+02	7.5945+02
36	1.0033+04	1.7270+03	7.0927+02	7.0940+02	7.5877+02	7.5932+02
37	1.0033+04	1.7500+03	7.1419+02	7.1436+02	7.5775+02	7.5805+02
38	1.0033+04	1.7500+03	7.1440+02	7.1457+02	7.5746+02	7.5792+02
39	1.0033+04	1.7500+03	7.1444+02	7.1440+02	7.5754+02	7.5805+02
40	1.0033+04	1.8300+03	7.2171+02	7.2188+02	7.5966+02	7.6008+02
41	1.0033+04	1.8300+03	7.2188+02	7.2192+02	7.5975+02	7.6030+02
42	1.0033+04	1.8300+03	7.2192+02	7.2179+02	7.6000+02	7.6047+02
43	1.0033+04	1.9300+03	7.3265+02	7.3286+02	7.6797+02	7.6835+02
44	1.0033+04	1.9300+03	7.3282+02	7.3312+02	7.6805+02	7.6839+02
45	1.0033+04	1.9300+03	7.3278+02	7.3299+02	7.6809+02	7.6856+02
46	1.0033+04	2.0250+03	7.4526+02	7.4534+02	7.7767+02	7.7809+02
47	1.0033+04	2.0250+03	7.4513+02	7.4526+02	7.7767+02	7.7814+02
48	1.0033+04	2.0250+03	7.4513+02	7.4538+02	7.7754+02	7.7814+02
49	1.0033+04	2.1100+03	7.5161+02	7.5174+02	7.8305+02	7.8356+02
50	1.0033+04	2.1100+03	7.5153+02	7.5174+02	7.8309+02	7.8347+02
51	1.0033+04	2.1100+03	7.5165+02	7.5191+02	7.8314+02	7.8356+02
52	1.0033+04	2.2100+03	7.6161+02	7.6186+02	7.9148+02	7.9203+02
53	1.0033+04	2.2100+03	7.6169+02	7.6195+02	7.9165+02	7.9237+02
54	1.0033+04	2.2100+03	7.6174+02	7.6199+02	7.9165+02	7.9237+02
55	1.0033+04	2.3450+03	7.7195+02	7.7212+02	8.0107+02	8.0162+02
56	1.0033+04	2.3450+03	7.7195+02	7.7220+02	8.0085+02	8.0158+02
57	1.0033+04	2.3450+03	7.7195+02	7.7220+02	8.0090+02	8.0158+02
58	1.0043+04	6.0400+02	7.8424+02	7.8445+02	8.2632+02	8.2692+02
59	1.0043+04	6.0400+02	7.8428+02	7.8449+02	8.2628+02	8.2697+02
60	1.0043+04	6.0400+02	7.8403+02	7.8432+02	8.2615+02	8.2671+02

LIQUID-LIQUID RUNS CORRECTED K FLOW

	800	801	251	254	257	260
	DATE	TIME	TC1	TC2	TC3	TC4
61	1.0043+04	6.3500+02	7.8225+02	7.8263+02	8.2530+02	8.2611+02
62	1.0043+04	6.3500+02	7.8225+02	7.8246+02	8.2530+02	8.2603+02
63	1.0043+04	6.3500+02	7.8225+02	7.8233+02	8.2534+02	8.2607+02
64	1.0043+04	7.3000+02	7.7669+02	7.7674+02	8.2214+02	8.2286+02
65	1.0043+04	7.3000+02	7.7669+02	7.7708+02	8.2209+02	8.2286+02
66	1.0043+04	7.3000+02	7.7674+02	7.7691+02	8.2222+02	8.2291+02
67	1.0043+04	9.0500+02	7.6326+02	7.6369+02	8.1389+02	8.1470+02
68	1.0043+04	9.0500+02	7.6318+02	7.6356+02	8.1368+02	8.1449+02
69	1.0043+04	9.0500+02	7.6314+02	7.6326+02	8.1368+02	8.1427+02
70	1.0043+04	1.2350+03	7.3410+02	7.3436+02	7.8784+02	7.8822+02
71	1.0043+04	1.2350+03	7.3427+02	7.3453+02	7.8763+02	7.8852+02
72	1.0043+04	1.2350+03	7.3423+02	7.3432+02	7.8797+02	7.8847+02
73	1.0043+04	1.4100+03	7.2355+02	7.2363+02	7.7818+02	7.7877+02
74	1.0043+04	1.4100+03	7.2363+02	7.2368+02	7.7792+02	7.7873+02
75	1.0043+04	1.4100+03	7.2350+02	7.2368+02	7.7784+02	7.7869+02
76	1.0043+04	1.4400+03	7.2637+02	7.2679+02	7.7419+02	7.7458+02
77	1.0043+04	1.4400+03	7.2662+02	7.2679+02	7.7390+02	7.7466+02
78	1.0043+04	1.4400+03	7.2662+02	7.2675+02	7.7394+02	7.7470+02
79	1.0043+04	1.5150+03	7.3162+02	7.3179+02	7.7564+02	7.7636+02
80	1.0043+04	1.5150+03	7.3158+02	7.3197+02	7.7568+02	7.7640+02
81	1.0043+04	1.5150+03	7.3167+02	7.3188+02	7.7597+02	7.7644+02
82	1.0043+04	1.6100+03	7.4231+02	7.4239+02	7.8453+02	7.8555+02
83	1.0043+04	1.6100+03	7.4201+02	7.4235+02	7.8466+02	7.8551+02
84	1.0043+04	1.6100+03	7.4209+02	7.4265+02	7.8508+02	7.8555+02
85	1.0043+04	1.7550+03	7.3440+02	7.3453+02	7.7983+02	7.8068+02
86	1.0043+04	1.7550+03	7.3432+02	7.3466+02	7.8017+02	7.8059+02
87	1.0043+04	1.7550+03	7.3436+02	7.3466+02	7.8000+02	7.8047+02
88	1.0043+04	1.8350+03	7.3346+02	7.3363+02	7.8538+02	7.8627+02
89	1.0043+04	1.8350+03	7.3350+02	7.3368+02	7.8538+02	7.8610+02
90	1.0043+04	1.8350+03	7.3355+02	7.3376+02	7.8547+02	7.8606+02

LIQUID-LIQUID RUNS CORRECTED K FLOW

	800	801	251	254	257	260
	DATE	TIME	TC1	TC2	TC3	TC4
91	1.0043+04	1.9550+03	7.3825+02	7.3846+02	7.9936+02	8.0021+02
92	1.0043+04	1.9550+03	7.3825+02	7.3846+02	7.9941+02	8.0026+02
93	1.0043+04	1.9550+03	7.3825+02	7.3859+02	7.9962+02	8.0000+02
94	1.0033+04	5.0000+01	7.8458+02	7.8432+02	8.3312+02	8.3355+02
95	1.0033+04	5.0000+01	7.8475+02	7.8462+02	8.3329+02	8.3342+02
96	1.0033+04	5.0000+01	7.8470+02	7.8449+02	8.3325+02	8.3355+02
97	1.0033+04	2.4100+02	7.9521+02	7.9504+02	8.4026+02	8.4111+02
98	1.0033+04	3.2000+02	8.0145+02	8.0141+02	8.4043+02	8.4103+02
99	1.0033+04	5.0200+02	8.1094+02	8.1081+02	8.4615+02	8.4684+02
100	1.0033+04	5.0200+02	8.1098+02	8.1098+02	8.4624+02	8.4671+02
101	1.0033+04	5.0200+02	8.1107+02	8.1094+02	8.4607+02	8.4658+02
102	1.0033+04	5.4400+02	8.1573+02	8.1556+02	8.4714+02	8.4778+02
103	1.0033+04	5.4400+02	8.1573+02	8.1560+02	8.4726+02	8.4799+02
104	1.0033+04	5.4400+02	8.1573+02	8.1560+02	8.4731+02	8.4791+02
105	1.0033+04	7.3500+02	8.2607+02	8.2594+02	8.5525+02	8.5588+02
106	1.0033+04	7.3500+02	8.2624+02	8.2603+02	8.5529+02	8.5618+02
107	1.0033+04	7.3500+02	8.2611+02	8.2598+02	8.5555+02	8.5622+02
108	1.0033+04	9.3000+02	8.3513+02	8.3538+02	8.6223+02	8.6290+02
109	1.0033+04	9.3000+02	8.3513+02	8.3534+02	8.6239+02	8.6303+02
110	1.0033+04	9.3000+02	8.3526+02	8.3547+02	8.6231+02	8.6286+02

LIQUID-LIQUID RUNS CORRECTED K FLOW

	263	266	269	273	276	279
	TC5	TC6	TC7	TC8	TC9	TC10
1	7.1701+02	7.1526+02	7.1654+02	7.0987+02	7.0799+02	7.1291+02
2	7.1726+02	7.1521+02	7.1641+02	7.1021+02	7.0829+02	7.1410+02
3	7.1709+02	7.1530+02	7.1662+02	7.1017+02	7.0799+02	7.1303+02
4	7.1650+02	7.1436+02	7.1573+02	7.0966+02	7.0769+02	7.1333+02
5	7.1624+02	7.1449+02	7.1573+02	7.0949+02	7.0748+02	7.1231+02
6	7.1645+02	7.1436+02	7.1547+02	7.0944+02	7.0774+02	7.1299+02
7	7.0628+02	7.0449+02	7.0560+02	6.9961+02	6.9780+02	7.0222+02
8	7.0624+02	7.0436+02	7.0543+02	6.9957+02	6.9789+02	7.0231+02
9	7.0607+02	7.0402+02	7.0543+02	6.9970+02	6.9759+02	7.0303+02
10	6.9914+02	6.9733+02	6.9841+02	6.9263+02	6.9086+02	6.9530+02
11	6.9901+02	6.9707+02	6.9832+02	6.9267+02	6.9082+02	6.9573+02
12	6.9892+02	6.9690+02	6.9832+02	6.9267+02	6.9052+02	6.9582+02
13	7.0286+02	7.0111+02	7.0218+02	6.9776+02	6.9608+02	6.9966+02
14	7.0278+02	7.0094+02	7.0222+02	6.9802+02	6.9595+02	7.0009+02
15	7.0274+02	7.0085+02	7.0222+02	6.9802+02	6.9595+02	7.0013+02
16	7.0205+02	7.0043+02	7.0158+02	6.9711+02	6.9543+02	6.9905+02
17	7.0222+02	7.0030+02	7.0162+02	6.9733+02	6.9552+02	6.9974+02
18	7.0231+02	7.0051+02	7.0154+02	6.9711+02	6.9543+02	6.9892+02
19	7.0056+02	6.9853+02	6.9966+02	6.9556+02	6.9405+02	6.9772+02
20	7.0051+02	6.9871+02	6.9966+02	6.9530+02	6.9384+02	6.9707+02
21	7.0051+02	6.9862+02	6.9961+02	6.9534+02	6.9397+02	6.9750+02
22	6.9832+02	6.9647+02	6.9737+02	6.9310+02	6.9177+02	6.9496+02
23	6.9823+02	6.9638+02	6.9733+02	6.9302+02	6.9164+02	6.9474+02
24	6.9832+02	6.9642+02	6.9733+02	6.9306+02	6.9168+02	6.9487+02
25	6.9586+02	6.9405+02	6.9500+02	6.9082+02	6.8927+02	6.9004+02
26	6.9582+02	6.9405+02	6.9509+02	6.9086+02	6.8909+02	6.8944+02
27	6.9582+02	6.9388+02	6.9487+02	6.9108+02	6.8931+02	6.8909+02
28	6.9129+02	6.8948+02	6.9060+02	6.8672+02	6.8470+02	6.8789+02
29	6.9125+02	6.8944+02	6.9065+02	6.8677+02	6.8466+02	6.8802+02
30	6.9138+02	6.8957+02	6.9060+02	6.8659+02	6.8461+02	6.8754+02

LIQUID-LIQUID RUNS CORRECTED K FLOW

	263	266	269	273	276	279
	TC5	TC6	TC7	TC8	TC9	TC10
31	7.0051+02	6.9871+02	6.9983+02	6.9815+02	6.9616+02	6.9871+02
32	7.0056+02	6.9897+02	6.9987+02	6.9797+02	6.9625+02	6.9888+02
33	7.0060+02	6.9871+02	6.9987+02	6.9819+02	6.9621+02	6.9871+02
34	7.0432+02	7.0235+02	7.0359+02	7.0184+02	6.9991+02	7.0329+02
35	7.0419+02	7.0261+02	7.0363+02	7.0179+02	6.9978+02	7.0197+02
36	7.0436+02	7.0269+02	7.0368+02	7.0175+02	7.0009+02	7.0278+02
37	7.0825+02	7.0641+02	7.0761+02	7.0590+02	7.0397+02	7.0684+02
38	7.0825+02	7.0671+02	7.0769+02	7.0577+02	7.0410+02	7.0679+02
39	7.0842+02	7.0662+02	7.0756+02	7.0594+02	7.0415+02	7.0774+02
40	7.1436+02	7.1274+02	7.1376+02	7.1192+02	7.1004+02	7.1265+02
41	7.1444+02	7.1274+02	7.1372+02	7.1192+02	7.1013+02	7.1359+02
42	7.1457+02	7.1278+02	7.1368+02	7.1209+02	7.1021+02	7.1402+02
43	7.2487+02	7.2303+02	7.2419+02	7.2252+02	7.2051+02	7.2419+02
44	7.2483+02	7.2333+02	7.2432+02	7.2252+02	7.2047+02	7.2299+02
45	7.2491+02	7.2321+02	7.2427+02	7.2265+02	7.2060+02	7.2402+02
46	7.3658+02	7.3479+02	7.3598+02	7.3432+02	7.3226+02	7.3573+02
47	7.3654+02	7.3474+02	7.3594+02	7.3427+02	7.3226+02	7.3564+02
48	7.3658+02	7.3483+02	7.3585+02	7.3410+02	7.3231+02	7.3620+02
49	7.4192+02	7.4000+02	7.4128+02	7.3932+02	7.3731+02	7.4026+02
50	7.4184+02	7.4021+02	7.4141+02	7.3932+02	7.3744+02	7.4034+02
51	7.4192+02	7.4030+02	7.4141+02	7.3927+02	7.3752+02	7.4111+02
52	7.5144+02	7.4970+02	7.5064+02	7.4846+02	7.4675+02	7.5089+02
53	7.5153+02	7.4970+02	7.5064+02	7.4872+02	7.4671+02	7.5059+02
54	7.5161+02	7.4970+02	7.5064+02	7.4872+02	7.4675+02	7.5076+02
55	7.6153+02	7.5958+02	7.6051+02	7.5843+02	7.5627+02	7.5932+02
56	7.6161+02	7.5966+02	7.6051+02	7.5852+02	7.5640+02	7.5983+02
57	7.6169+02	7.5970+02	7.6051+02	7.5852+02	7.5636+02	7.6008+02
58	7.6763+02	7.6665+02	7.6771+02	7.6237+02	7.6000+02	7.6483+02
59	7.6763+02	7.6653+02	7.6763+02	7.6233+02	7.5996+02	7.6496+02
60	7.6754+02	7.6653+02	7.6767+02	7.6225+02	7.5996+02	7.6513+02

LIQUID-LIQUID RUNS CORRECTED K FLOW

	263	266	269	273	276	279
	TC5	TC6	TC7	TC8	TC9	TC10
61	7.6636+02	7.6534+02	7.6623+02	7.6119+02	7.5903+02	7.6551+02
62	7.6644+02	7.6525+02	7.6627+02	7.6127+02	7.5903+02	7.6534+02
63	7.6636+02	7.6508+02	7.6627+02	7.6123+02	7.5898+02	7.6398+02
64	7.6161+02	7.6025+02	7.6144+02	7.5631+02	7.5432+02	7.5915+02
65	7.6161+02	7.6038+02	7.6140+02	7.5640+02	7.5441+02	7.6072+02
66	7.6165+02	7.6025+02	7.6148+02	7.5640+02	7.5436+02	7.5966+02
67	7.4940+02	7.4829+02	7.4919+02	7.4380+02	7.4184+02	7.4812+02
68	7.4932+02	7.4816+02	7.4919+02	7.4376+02	7.4179+02	7.4803+02
69	7.4923+02	7.4791+02	7.4910+02	7.4372+02	7.4158+02	7.4667+02
70	7.2184+02	7.2103+02	7.2188+02	7.1662+02	7.1662+02	7.1662+02
71	7.2197+02	7.2085+02	7.2145+02	7.1671+02	7.1671+02	7.1671+02
72	7.2192+02	7.2081+02	7.2171+02	7.1662+02	7.1662+02	7.1662+02
73	7.1171+02	7.1056+02	7.1124+02	7.0462+02	7.0256+02	7.0248+02
74	7.1175+02	7.1064+02	7.1115+02	7.0462+02	7.0269+02	7.0248+02
75	7.1171+02	7.1068+02	7.1128+02	7.0440+02	7.0269+02	7.0261+02
76	7.1286+02	7.1192+02	7.1274+02	7.0590+02	7.0355+02	7.0368+02
77	7.1303+02	7.1197+02	7.1252+02	7.0590+02	7.0393+02	7.0389+02
78	7.1312+02	7.1197+02	7.1252+02	7.0577+02	7.0389+02	7.0389+02
79	7.1701+02	7.1577+02	7.1632+02	7.1026+02	7.0778+02	7.0744+02
80	7.1667+02	7.1568+02	7.1654+02	7.1009+02	7.0756+02	7.0765+02
81	7.1679+02	7.1564+02	7.1654+02	7.1034+02	7.0756+02	7.0756+02
82	7.2615+02	7.2504+02	7.2581+02	7.1846+02	7.1671+02	7.1679+02
83	7.2620+02	7.2487+02	7.2573+02	7.1855+02	7.1667+02	7.1679+02
84	7.2603+02	7.2491+02	7.2611+02	7.1889+02	7.1650+02	7.1641+02
85	7.3295+02	7.3175+02	7.3265+02	7.3197+02	7.2996+02	7.3026+02
86	7.3282+02	7.3162+02	7.3282+02	7.3239+02	7.2991+02	7.2991+02
87	7.3282+02	7.3171+02	7.3286+02	7.3239+02	7.2983+02	7.2996+02
88	7.3291+02	7.3158+02	7.3252+02	7.3209+02	7.2996+02	7.3034+02
89	7.3278+02	7.3162+02	7.3265+02	7.3222+02	7.2983+02	7.3013+02
90	7.3282+02	7.3167+02	7.3274+02	7.3231+02	7.2983+02	7.3017+02

LIQUID-LIQUID RUNS CORRECTED K FLOW

	263	266	269	273	276	279
	TC5	TC6	TC7	TC8	TC9	TC10
91	7.3808+02	7.3658+02	7.3786+02	7.3791+02	7.3534+02	7.3534+02
92	7.3808+02	7.3658+02	7.3786+02	7.3791+02	7.3526+02	7.3530+02
93	7.3799+02	7.3679+02	7.3803+02	7.3769+02	7.3521+02	7.3560+02
94	7.8148+02	7.7932+02	7.8008+02	7.5648+02	7.5411+02	7.6322+02
95	7.8131+02	7.7949+02	7.8038+02	7.5631+02	7.5394+02	7.6305+02
96	7.8144+02	7.7936+02	7.8034+02	7.5648+02	7.5403+02	7.6309+02
97	7.9157+02	7.8953+02	7.9042+02	7.6682+02	7.6470+02	7.7356+02
98	7.9708+02	7.9508+02	7.9640+02	7.7254+02	7.7008+02	7.7924+02
99	8.0585+02	8.0376+02	8.0496+02	7.8064+02	7.7839+02	7.8746+02
100	8.0577+02	8.0380+02	8.0521+02	7.8076+02	7.7822+02	7.8746+02
101	8.0577+02	8.0402+02	8.0521+02	7.8051+02	7.7814+02	7.8729+02
102	8.1026+02	8.0825+02	8.0957+02	7.8462+02	7.8237+02	7.9169+02
103	8.1021+02	8.0829+02	8.0966+02	7.8479+02	7.8237+02	7.9169+02
104	8.1013+02	8.0829+02	8.0974+02	7.8466+02	7.8229+02	7.9153+02
105	8.2047+02	8.1872+02	8.1974+02	7.9458+02	7.9212+02	8.0162+02
106	8.2051+02	8.1868+02	8.1991+02	7.9445+02	7.9199+02	8.0145+02
107	8.2034+02	8.1872+02	8.2009+02	7.9432+02	7.9191+02	8.0141+02
108	8.2987+02	8.2799+02	8.2915+02	8.0269+02	8.0047+02	8.1026+02
109	8.2974+02	8.2795+02	8.2932+02	8.0278+02	8.0043+02	8.1034+02
110	8.2987+02	8.2812+02	8.2932+02	8.0261+02	8.0030+02	8.1009+02

LIQUID-LIQUID RUNS CORRECTED K FLOW

	282	285	288	291	297	300
	TC11	TC12	TC13	TC14	TC16	TC17
1	7.1346+02	7.2838+02	7.2500+02	7.2359+02	7.3162+02	7.3081+02
2	7.1359+02	7.2833+02	7.2530+02	7.2359+02	7.3162+02	7.3115+02
3	7.1312+02	7.2838+02	7.2504+02	7.2346+02	7.3179+02	7.3068+02
4	7.1248+02	7.2709+02	7.2410+02	7.2252+02	7.3056+02	7.2983+02
5	7.1239+02	7.2701+02	7.2385+02	7.2235+02	7.3047+02	7.2949+02
6	7.1329+02	7.2671+02	7.2380+02	7.2248+02	7.3009+02	7.2953+02
7	7.0286+02	7.1624+02	7.1325+02	7.1201+02	7.1979+02	7.1876+02
8	7.0303+02	7.1611+02	7.1316+02	7.1197+02	7.1949+02	7.1880+02
9	7.0222+02	7.1607+02	7.1333+02	7.1179+02	7.1957+02	7.1906+02
10	6.9599+02	7.0863+02	7.0585+02	7.0474+02	7.1235+02	7.1158+02
11	6.9599+02	7.0846+02	7.0603+02	7.0462+02	7.1218+02	7.1175+02
12	6.9509+02	7.0859+02	7.0598+02	7.0440+02	7.1226+02	7.1179+02
13	7.0021+02	7.1094+02	7.0859+02	7.0765+02	7.1453+02	7.1380+02
14	6.9961+02	7.1103+02	7.0885+02	7.0752+02	7.1466+02	7.1415+02
15	6.9966+02	7.1098+02	7.0880+02	7.0752+02	7.1457+02	7.1410+02
16	6.9888+02	7.1017+02	7.0791+02	7.0667+02	7.1402+02	7.1342+02
17	6.9905+02	7.1009+02	7.0803+02	7.0684+02	7.1389+02	7.1350+02
18	6.9918+02	7.1009+02	7.0786+02	7.0671+02	7.1397+02	7.1338+02
19	6.9784+02	7.0778+02	7.0598+02	7.0496+02	7.1184+02	7.1175+02
20	6.9763+02	7.0799+02	7.0577+02	7.0496+02	7.1205+02	7.1171+02
21	6.9789+02	7.0791+02	7.0581+02	7.0496+02	7.1188+02	7.1162+02
22	6.9543+02	7.0513+02	7.0316+02	7.0244+02	7.0970+02	7.0932+02
23	6.9530+02	7.0509+02	7.0308+02	7.0235+02	7.0966+02	7.0932+02
24	6.9534+02	7.0509+02	7.0308+02	7.0239+02	7.0962+02	7.0932+02
25	4.7500+02	7.0248+02	7.0051+02	6.9983+02	7.0735+02	7.0697+02
26	6.8940+02	7.0235+02	7.0051+02	6.9966+02	7.0735+02	7.0692+02
27	6.8901+02	7.0222+02	7.0068+02	6.9983+02	7.0714+02	7.0718+02
28	6.8763+02	6.9720+02	6.9569+02	6.9474+02	7.0286+02	7.0256+02
29	6.8763+02	6.9720+02	6.9573+02	6.9474+02	7.0286+02	7.0274+02
30	6.8797+02	6.9716+02	6.9552+02	6.9470+02	7.0278+02	7.0239+02

LIQUID-LIQUID RUNS CORRECTED K FLOW

	282	285	288	291	297	300
	TC11	TC12	TC13	TC14	TC16	TC17
31	6.9819+02	7.0650+02	7.0504+02	7.0427+02	7.1175+02	7.1154+02
32	6.9961+02	7.0641+02	7.0487+02	7.0423+02	7.1158+02	7.1132+02
33	6.9819+02	7.0654+02	7.0504+02	7.0432+02	7.1179+02	7.1150+02
34	7.0222+02	7.1060+02	7.0915+02	7.0829+02	7.1568+02	7.1543+02
35	7.0295+02	7.1077+02	7.0897+02	7.0821+02	7.1556+02	7.1521+02
36	7.0350+02	7.1064+02	7.0893+02	7.0825+02	7.1551+02	7.1509+02
37	7.0620+02	7.1513+02	7.1350+02	7.1261+02	7.1962+02	7.1927+02
38	7.0765+02	7.1513+02	7.1321+02	7.1248+02	7.1949+02	7.1915+02
39	7.0709+02	7.1509+02	7.1338+02	7.1269+02	7.1936+02	7.1936+02
40	7.1363+02	7.2184+02	7.1970+02	7.1897+02	7.2577+02	7.2517+02
41	7.1397+02	7.2167+02	7.1979+02	7.1906+02	7.2577+02	7.2526+02
42	7.1355+02	7.2171+02	7.1987+02	7.1923+02	7.2581+02	7.2547+02
43	7.2312+02	7.3244+02	7.3064+02	7.2979+02	7.3620+02	7.3585+02
44	7.2389+02	7.3274+02	7.3060+02	7.2966+02	7.3650+02	7.3564+02
45	7.2312+02	7.3261+02	7.3081+02	7.2996+02	7.3650+02	7.3585+02
46	7.3479+02	7.4453+02	7.4256+02	7.4154+02	7.4808+02	7.4744+02
47	7.3474+02	7.4453+02	7.4252+02	7.4154+02	7.4803+02	7.4744+02
48	7.3581+02	7.4436+02	7.4239+02	7.4162+02	7.4791+02	7.4752+02
49	7.4009+02	7.5055+02	7.4821+02	7.4722+02	7.5369+02	7.5314+02
50	7.4158+02	7.5047+02	7.4816+02	7.4735+02	7.5360+02	7.5343+02
51	7.4179+02	7.5038+02	7.4821+02	7.4748+02	7.5386+02	7.5343+02
52	7.5064+02	7.6008+02	7.5788+02	7.5695+02	7.6343+02	7.6280+02
53	7.4957+02	7.6025+02	7.5784+02	7.5686+02	7.6347+02	7.6263+02
54	7.4970+02	7.6030+02	7.5792+02	7.5695+02	7.6343+02	7.6271+02
55	7.5987+02	7.7017+02	7.6746+02	7.6708+02	7.7314+02	7.7271+02
56	7.5924+02	7.7021+02	7.6767+02	7.6708+02	7.7314+02	7.7267+02
57	7.5919+02	7.7021+02	7.6767+02	7.6703+02	7.7322+02	7.7271+02
58	7.6585+02	7.8042+02	7.7636+02	7.7606+02	7.8530+02	7.8411+02
59	7.6521+02	7.8034+02	7.7648+02	7.7593+02	7.8525+02	7.8415+02
60	7.6644+02	7.8030+02	7.7623+02	7.7597+02	7.8517+02	7.8424+02

LIQUID-LIQUID RUNS CORRECTED K FLOW

	282	285	288	291	297	300
	TC11	TC12	TC13	TC14	TC16	TC17
61	7.6462+02	7.7856+02	7.7492+02	7.7470+02	7.8381+02	7.8288+02
62	7.6381+02	7.7860+02	7.7496+02	7.7475+02	7.8377+02	7.8280+02
63	7.6356+02	7.7869+02	7.7496+02	7.7449+02	7.8390+02	7.8267+02
64	7.5869+02	7.7360+02	7.6996+02	7.6941+02	7.7886+02	7.7792+02
65	7.5941+02	7.7343+02	7.6992+02	7.6975+02	7.7915+02	7.7805+02
66	7.5873+02	7.7360+02	7.7000+02	7.6953+02	7.7903+02	7.7805+02
67	7.4709+02	7.6089+02	7.5733+02	7.5725+02	7.6682+02	7.6597+02
68	7.4705+02	7.6076+02	7.5720+02	7.5716+02	7.6678+02	7.6581+02
69	7.4598+02	7.6068+02	7.5720+02	7.5678+02	7.6661+02	7.6555+02
70	4.7500+02	7.3256+02	7.2910+02	7.2923+02	7.3868+02	7.3821+02
71	4.7500+02	7.3269+02	7.2923+02	7.2906+02	7.3859+02	7.3774+02
72	4.7500+02	7.3265+02	7.2893+02	7.2923+02	7.3859+02	7.3786+02
73	7.0256+02	7.2201+02	7.1846+02	7.1850+02	7.2778+02	7.2735+02
74	7.0244+02	7.2192+02	7.1842+02	7.1855+02	7.2778+02	7.2722+02
75	7.0244+02	7.2184+02	7.1842+02	7.1859+02	7.2769+02	7.2722+02
76	7.0393+02	7.2397+02	7.2004+02	7.2004+02	7.2932+02	7.2825+02
77	7.0363+02	7.3184+02	7.2013+02	7.2026+02	7.2906+02	7.2833+02
78	7.0363+02	7.2397+02	7.2009+02	7.2026+02	7.2885+02	7.2833+02
79	4.7500+02	7.2838+02	7.2372+02	7.2453+02	7.3274+02	7.3222+02
80	4.7500+02	7.3419+02	7.2419+02	7.2423+02	7.3316+02	7.3218+02
81	4.7500+02	7.2850+02	7.2444+02	7.2440+02	7.3321+02	7.3239+02
82	7.3752+02	7.3829+02	7.3410+02	7.3432+02	7.4303+02	7.4188+02
83	7.3735+02	7.3829+02	7.3406+02	7.3423+02	7.4286+02	7.4197+02
84	7.3744+02	7.3859+02	7.3432+02	7.3410+02	7.4291+02	7.4239+02
85	7.3632+02	7.3620+02	7.3543+02	7.3568+02	7.4090+02	7.4013+02
86	7.3628+02	7.3628+02	7.3560+02	7.3564+02	7.4068+02	7.4047+02
87	7.3637+02	7.3637+02	7.3560+02	7.3564+02	7.4085+02	7.4064+02
88	7.3573+02	7.3543+02	7.3491+02	7.3517+02	7.4030+02	7.3962+02
89	7.3568+02	7.3551+02	7.3500+02	7.3513+02	7.4026+02	7.3983+02
90	7.3573+02	7.3556+02	7.3500+02	7.3517+02	7.4026+02	7.3991+02

LIQUID-LIQUID RUNS CORRECTED K FLOW

	282	285	288	291	297	300
	TC11	TC12	TC13	TC14	TC16	TC17
91	7.4064+02	7.4038+02	7.4004+02	7.4009+02	7.4513+02	7.4440+02
92	7.4064+02	7.4038+02	7.4000+02	7.4013+02	7.4513+02	7.4444+02
93	7.4073+02	7.4030+02	7.4000+02	7.4030+02	7.4487+02	7.4432+02
94	7.6305+02	7.8572+02	7.8508+02	7.8458+02	7.8559+02	7.8699+02
95	7.6309+02	7.8572+02	7.8496+02	7.8462+02	7.8559+02	7.8678+02
96	7.6309+02	7.8585+02	7.8500+02	7.8458+02	7.8564+02	7.8691+02
97	7.7364+02	7.9581+02	7.9538+02	7.9458+02	7.9581+02	7.9653+02
98	7.7903+02	8.0171+02	8.0124+02	8.0017+02	8.0111+02	8.0201+02
99	7.8746+02	8.1051+02	8.1013+02	8.0889+02	8.0979+02	8.1068+02
100	7.8733+02	8.1060+02	8.1009+02	8.0880+02	8.0991+02	8.1077+02
101	7.8729+02	8.1056+02	8.1000+02	8.0872+02	8.0987+02	8.1051+02
102	7.9174+02	8.1487+02	8.1457+02	8.1325+02	8.1410+02	8.1466+02
103	7.9153+02	8.1500+02	8.1453+02	8.1325+02	8.1415+02	8.1466+02
104	7.9157+02	8.1496+02	8.1444+02	8.1333+02	8.1410+02	8.1453+02
105	8.0137+02	8.2521+02	8.2462+02	8.2329+02	8.2419+02	8.2423+02
106	8.0145+02	8.2526+02	8.2462+02	8.2333+02	8.2410+02	8.2436+02
107	8.0167+02	8.2513+02	8.2474+02	8.2359+02	8.2410+02	8.2453+02
108	8.1030+02	8.3440+02	8.3402+02	8.3278+02	8.3312+02	8.3329+02
109	8.1009+02	8.3457+02	8.3410+02	8.3278+02	8.3316+02	8.3342+02
110	8.1030+02	8.3453+02	8.3389+02	8.3286+02	8.3321+02	8.3329+02

LIQUID-LIQUID RUNS CORRECTED K FLOW

	303 TC18	306 TC19	311 TKO	313 TKI	316 TNAO	319 TNAI
1	7.2932+02	7.2150+02	7.3141+02	7.6858+02	7.1627+02	7.0893+02
2	7.2949+02	7.2115+02	7.3132+02	7.6856+02	7.1630+02	7.0925+02
3	7.2919+02	7.2150+02	7.3132+02	7.6839+02	7.1634+02	7.0908+02
4	7.2808+02	7.2026+02	7.2964+02	7.6672+02	7.1553+02	7.0868+02
5	7.2795+02	7.2038+02	7.2962+02	7.6631+02	7.1548+02	7.0848+02
6	7.2821+02	7.2026+02	7.2953+02	7.6631+02	7.1543+02	7.0859+02
7	7.1744+02	7.1030+02	7.1838+02	7.5604+02	7.0546+02	6.9871+02
8	7.1761+02	7.1017+02	7.1829+02	7.5597+02	7.0534+02	6.9873+02
9	7.1744+02	7.0983+02	7.1812+02	7.5623+02	7.0517+02	6.9864+02
10	7.1043+02	7.0316+02	7.1026+02	7.5038+02	6.9829+02	6.9175+02
11	7.1051+02	7.0299+02	7.1024+02	7.5053+02	6.9813+02	6.9175+02
12	7.1026+02	7.0261+02	7.1011+02	7.5053+02	6.9805+02	6.9159+02
13	7.1261+02	7.0667+02	7.1162+02	7.4921+02	7.0205+02	6.9692+02
14	7.1274+02	7.0637+02	7.1158+02	7.4932+02	7.0198+02	6.9698+02
15	7.1274+02	7.0641+02	7.1154+02	7.4936+02	7.0194+02	6.9698+02
16	7.1197+02	7.0581+02	7.1028+02	7.5040+02	7.0135+02	6.9627+02
17	7.1222+02	7.0581+02	7.1026+02	7.5070+02	7.0138+02	6.9642+02
18	7.1201+02	7.0585+02	7.1036+02	7.5044+02	7.0145+02	6.9627+02
19	7.1064+02	7.0436+02	7.0759+02	7.5225+02	6.9958+02	6.9481+02
20	7.1038+02	7.0449+02	7.0763+02	7.5208+02	6.9962+02	6.9457+02
21	7.1051+02	7.0453+02	7.0765+02	7.5220+02	6.9958+02	6.9466+02
22	7.0812+02	7.0239+02	7.0419+02	7.5432+02	6.9739+02	6.9244+02
23	7.0812+02	7.0235+02	7.0410+02	7.5428+02	6.9731+02	6.9233+02
24	7.0812+02	7.0226+02	7.0408+02	7.5436+02	6.9736+02	6.9237+02
25	7.0560+02	7.0000+02	7.0092+02	7.5587+02	6.9497+02	6.9004+02
26	7.0564+02	6.9991+02	7.0094+02	7.5585+02	6.9499+02	6.8998+02
27	7.0585+02	6.9983+02	7.0079+02	7.5608+02	6.9486+02	6.9019+02
28	7.0090+02	6.9517+02	6.9491+02	7.5877+02	6.9046+02	6.8571+02
29	7.0103+02	6.9522+02	6.9491+02	7.5879+02	6.9045+02	6.8571+02
30	7.0094+02	6.9547+02	6.9498+02	7.5862+02	6.9052+02	6.8560+02

LIQUID-LIQUID RUNS CORRECTED K FLOW

	303 TC18	306 TC19	311 TKO	313 TKI	316 TNAO	319 TNAI
31	7.0996+02	7.0479+02	7.0455+02	7.5919+02	6.9968+02	6.9716+02
32	7.1013+02	7.0500+02	7.0474+02	7.5917+02	6.9980+02	6.9711+02
33	7.1013+02	7.0479+02	7.0462+02	7.5934+02	6.9973+02	6.9720+02
34	7.1393+02	7.0846+02	7.0919+02	7.5951+02	7.0342+02	7.0088+02
35	7.1389+02	7.0880+02	7.0932+02	7.5924+02	7.0348+02	7.0079+02
36	7.1393+02	7.0880+02	7.0934+02	7.5905+02	7.0358+02	7.0092+02
37	7.1782+02	7.1244+02	7.1427+02	7.5790+02	7.0742+02	7.0494+02
38	7.1795+02	7.1269+02	7.1449+02	7.5769+02	7.0755+02	7.0494+02
39	7.1795+02	7.1248+02	7.1442+02	7.5780+02	7.0754+02	7.0504+02
40	7.2393+02	7.1880+02	7.2179+02	7.5987+02	7.1362+02	7.1098+02
41	7.2410+02	7.1880+02	7.2190+02	7.6002+02	7.1363+02	7.1103+02
42	7.2419+02	7.1872+02	7.2186+02	7.6023+02	7.1368+02	7.1115+02
43	7.3444+02	7.2897+02	7.3276+02	7.6816+02	7.2403+02	7.2152+02
44	7.3440+02	7.2932+02	7.3297+02	7.6822+02	7.2416+02	7.2150+02
45	7.3462+02	7.2910+02	7.3288+02	7.6833+02	7.2413+02	7.2162+02
46	7.4607+02	7.4081+02	7.4530+02	7.7788+02	7.3578+02	7.3329+02
47	7.4607+02	7.4094+02	7.4519+02	7.7790+02	7.3574+02	7.3327+02
48	7.4615+02	7.4073+02	7.4526+02	7.7784+02	7.3575+02	7.3321+02
49	7.5186+02	7.4645+02	7.5167+02	7.8331+02	7.4107+02	7.3831+02
50	7.5203+02	7.4620+02	7.5163+02	7.8328+02	7.4115+02	7.3838+02
51	7.5199+02	7.4628+02	7.5178+02	7.8335+02	7.4121+02	7.3840+02
52	7.6127+02	7.5572+02	7.6174+02	7.9176+02	7.5059+02	7.4761+02
53	7.6127+02	7.5597+02	7.6182+02	7.9201+02	7.5062+02	7.4771+02
54	7.6131+02	7.5606+02	7.6186+02	7.9201+02	7.5065+02	7.4774+02
55	7.7127+02	7.6572+02	7.7203+02	8.0135+02	7.6054+02	7.5735+02
56	7.7123+02	7.6585+02	7.7208+02	8.0122+02	7.6059+02	7.5746+02
57	7.7123+02	7.6589+02	7.7208+02	8.0124+02	7.6064+02	7.5744+02
58	7.8203+02	7.7449+02	7.8434+02	8.2662+02	7.6733+02	7.6119+02
59	7.8195+02	7.7462+02	7.8439+02	8.2662+02	7.6726+02	7.6114+02
60	7.8195+02	7.7436+02	7.8417+02	8.2643+02	7.6725+02	7.6110+02

LIQUID-LIQUID RUNS CORRECTED K FLOW

	303	306	311	313	316	319
	TC18	TC19	TKO	TKI	TNAO	TNAI
61	7.8059+02	7.7301+02	7.8244+02	8.2571+02	7.6597+02	7.6011+02
62	7.8055+02	7.7309+02	7.8235+02	8.2566+02	7.6599+02	7.6015+02
63	7.8042+02	7.7326+02	7.8229+02	8.2571+02	7.6590+02	7.6011+02
64	7.7564+02	7.6843+02	7.7672+02	8.2250+02	7.6110+02	7.5532+02
65	7.7572+02	7.6831+02	7.7689+02	8.2248+02	7.6113+02	7.5540+02
66	7.7572+02	7.6852+02	7.7682+02	8.2256+02	7.6113+02	7.5538+02
67	7.6356+02	7.5606+02	7.6347+02	8.1429+02	7.4896+02	7.4282+02
68	7.6347+02	7.5593+02	7.6337+02	8.1408+02	7.4889+02	7.4278+02
69	7.6326+02	7.5597+02	7.6320+02	8.1397+02	7.4875+02	7.4265+02
70	7.3581+02	7.2821+02	7.3423+02	7.8803+02	7.2158+02	7.1662+02
71	7.3573+02	7.2846+02	7.3440+02	7.8807+02	7.2142+02	7.1671+02
72	7.3585+02	7.2812+02	7.3427+02	7.8822+02	7.2148+02	7.1662+02
73	7.2491+02	7.1714+02	7.2359+02	7.7847+02	7.1117+02	7.0359+02
74	7.2487+02	7.1709+02	7.2365+02	7.7833+02	7.1118+02	7.0365+02
75	7.2496+02	7.1726+02	7.2359+02	7.7826+02	7.1123+02	7.0355+02
76	7.2590+02	7.1846+02	7.2658+02	7.7439+02	7.1251+02	7.0472+02
77	7.2632+02	7.1846+02	7.2671+02	7.7428+02	7.1251+02	7.0491+02
78	7.2641+02	7.1850+02	7.2669+02	7.7432+02	7.1254+02	7.0483+02
79	7.3009+02	7.2248+02	7.3171+02	7.7600+02	7.1637+02	7.0902+02
80	7.3004+02	7.2248+02	7.3177+02	7.7604+02	7.1630+02	7.0882+02
81	7.3013+02	7.2235+02	7.3177+02	7.7621+02	7.1632+02	7.0895+02
82	7.3966+02	7.3214+02	7.4235+02	7.8504+02	7.2567+02	7.1759+02
83	7.3979+02	7.3214+02	7.4218+02	7.8508+02	7.2560+02	7.1761+02
84	7.4009+02	7.3188+02	7.4237+02	7.8532+02	7.2568+02	7.1769+02
85	7.3915+02	7.3697+02	7.3447+02	7.8025+02	7.3245+02	7.3096+02
86	7.3953+02	7.3688+02	7.3449+02	7.8038+02	7.3242+02	7.3115+02
87	7.3944+02	7.3675+02	7.3451+02	7.8023+02	7.3246+02	7.3111+02
88	7.3855+02	7.3641+02	7.3355+02	7.8583+02	7.3234+02	7.3103+02
89	7.3868+02	7.3628+02	7.3359+02	7.8574+02	7.3235+02	7.3103+02
90	7.3872+02	7.3637+02	7.3365+02	7.8576+02	7.3241+02	7.3107+02

LIQUID-LIQUID RUNS CORRECTED K FLOW

	303 TC18	306 TC19	311 TKO	313 TKI	316 TNAO	319 TNAI
91	7.4342+02	7.4179+02	7.3835+02	7.9979+02	7.3751+02	7.3662+02
92	7.4346+02	7.4188+02	7.3835+02	7.9983+02	7.3751+02	7.3658+02
93	7.4368+02	7.4201+02	7.3842+02	7.9981+02	7.3761+02	7.3645+02
94	7.8602+02	7.8051+02	7.8445+02	8.3333+02	7.8030+02	7.5530+02
95	7.8602+02	7.8076+02	7.8468+02	8.3335+02	7.8040+02	7.5513+02
96	7.8593+02	7.8068+02	7.8460+02	8.3340+02	7.8038+02	7.5525+02
97	7.9619+02	7.9064+02	7.9513+02	8.4068+02	7.9051+02	7.6576+02
98	8.0158+02	7.9581+02	8.0143+02	8.4073+02	7.9619+02	7.7131+02
99	8.1013+02	8.0427+02	8.1088+02	8.4650+02	8.0486+02	7.7951+02
100	8.1004+02	8.0419+02	8.1098+02	8.4647+02	8.0493+02	7.7949+02
101	8.0996+02	8.0423+02	8.1100+02	8.4632+02	8.0500+02	7.7932+02
102	8.1423+02	8.0795+02	8.1564+02	8.4746+02	8.0936+02	7.8350+02
103	8.1415+02	8.0821+02	8.1566+02	8.4763+02	8.0939+02	7.8358+02
104	8.1427+02	8.0829+02	8.1566+02	8.4761+02	8.0939+02	7.8347+02
105	8.2385+02	8.1808+02	8.2600+02	8.5557+02	8.1964+02	7.9335+02
106	8.2423+02	8.1808+02	8.2613+02	8.5574+02	8.1970+02	7.9322+02
107	8.2419+02	8.1799+02	8.2605+02	8.5588+02	8.1972+02	7.9311+02
108	8.3316+02	8.2697+02	8.3526+02	8.6256+02	8.2900+02	8.0158+02
109	8.3312+02	8.2692+02	8.3524+02	8.6271+02	8.2900+02	8.0160+02
110	8.3312+02	8.2701+02	8.3536+02	8.6258+02	8.2910+02	8.0145+02

LIQUID-LIQUID RUNS CORRECTED K FLOW

	325	330	332	334	345	354
	WK	WNA	TKM	TNAM	DTLM	TK1
1	1.8253+03	4.2512+03	7.5000+02	7.1260+02	3.2463+01	7.5049+02
2	1.8253+03	4.2512+03	7.4994+02	7.1277+02	3.2255+01	7.5046+02
3	1.8253+03	4.2512+03	7.4986+02	7.1271+02	3.2219+01	7.5034+02
4	1.7682+03	4.2587+03	7.4818+02	7.1210+02	3.1062+01	7.4851+02
5	1.7682+03	4.2587+03	7.4796+02	7.1198+02	3.1011+01	7.4829+02
6	1.7682+03	4.2587+03	7.4792+02	7.1201+02	3.0952+01	7.4827+02
7	1.6443+03	4.2349+03	7.3721+02	7.0208+02	2.9805+01	7.3719+02
8	1.6443+03	4.2349+03	7.3713+02	7.0204+02	2.9803+01	7.3715+02
9	1.6443+03	4.2349+03	7.3717+02	7.0191+02	2.9912+01	7.3718+02
10	1.5129+03	4.2380+03	7.3032+02	6.9502+02	2.9366+01	7.2986+02
11	1.5129+03	4.2380+03	7.3038+02	6.9494+02	2.9537+01	7.2998+02
12	1.5129+03	4.2380+03	7.3032+02	6.9482+02	2.9546+01	7.2988+02
13	1.3806+03	4.2351+03	7.3042+02	6.9948+02	2.5159+01	7.2958+02
14	1.3806+03	4.2351+03	7.3045+02	6.9948+02	2.5200+01	7.2963+02
15	1.3806+03	4.2351+03	7.3045+02	6.9946+02	2.5213+01	7.2964+02
16	1.2742+03	4.2210+03	7.3034+02	6.9881+02	2.5078+01	7.2897+02
17	1.2742+03	4.2210+03	7.3048+02	6.9890+02	2.5072+01	7.2909+02
18	1.2742+03	4.2210+03	7.3040+02	6.9886+02	2.5077+01	7.2901+02
19	1.1447+03	4.2444+03	7.2992+02	6.9719+02	2.5084+01	7.2760+02
20	1.1447+03	4.2444+03	7.2985+02	6.9710+02	2.5103+01	7.2750+02
21	1.1447+03	4.2444+03	7.2993+02	6.9712+02	2.5184+01	7.2762+02
22	9.8700+02	4.2092+03	7.2926+02	6.9491+02	2.4948+01	7.2532+02
23	9.8700+02	4.2092+03	7.2919+02	6.9482+02	2.4949+01	7.2523+02
24	9.8700+02	4.2092+03	7.2922+02	6.9486+02	2.4882+01	7.2521+02
25	8.9436+02	4.2026+03	7.2839+02	6.9251+02	2.4907+01	7.2295+02
26	8.9436+02	4.2026+03	7.2839+02	6.9248+02	2.4928+01	7.2294+02
27	8.9436+02	4.2026+03	7.2844+02	6.9253+02	2.4906+01	7.2300+02
28	7.5099+02	4.2457+03	7.2684+02	6.8809+02	2.4524+01	7.1799+02
29	7.5099+02	4.2457+03	7.2685+02	6.8808+02	2.4552+01	7.1802+02
30	7.5099+02	4.2457+03	7.2680+02	6.8806+02	2.4526+01	7.1795+02

LIQUID-LIQUID RUNS CORRECTED K FLOW

	325	330	332	334	345	354
	WK	WNA	TKM	TNAM	DTLM	TK1
31	8.4948+02	5.7212+03	7.3187+02	6.9842+02	2.2465+01	7.2577+02
32	8.4948+02	5.7212+03	7.3196+02	6.9845+02	2.2580+01	7.2593+02
33	8.4948+02	5.7212+03	7.3198+02	6.9846+02	2.2521+01	7.2589+02
34	9.2342+02	5.7294+03	7.3435+02	7.0215+02	2.2799+01	7.2989+02
35	9.2342+02	5.7294+03	7.3428+02	7.0213+02	2.2840+01	7.2990+02
36	9.2342+02	5.7294+03	7.3419+02	7.0225+02	2.2656+01	7.2980+02
37	1.0567+03	5.7346+03	7.3609+02	7.0618+02	2.2548+01	7.3350+02
38	1.0567+03	5.7346+03	7.3609+02	7.0624+02	2.2584+01	7.3358+02
39	1.0567+03	5.7346+03	7.3611+02	7.0629+02	2.2528+01	7.3358+02
40	1.2141+03	5.7095+03	7.4083+02	7.1230+02	2.2767+01	7.3963+02
41	1.2141+03	5.7095+03	7.4096+02	7.1233+02	2.2890+01	7.3980+02
42	1.2141+03	5.7095+03	7.4105+02	7.1241+02	2.2830+01	7.3984+02
43	1.3315+03	5.7106+03	7.5046+02	7.2277+02	2.2619+01	7.4981+02
44	1.3315+03	5.7106+03	7.5060+02	7.2283+02	2.2726+01	7.4996+02
45	1.3315+03	5.7106+03	7.5061+02	7.2288+02	2.2665+01	7.4997+02
46	1.4386+03	5.7227+03	7.6159+02	7.3454+02	2.2708+01	7.6148+02
47	1.4386+03	5.7227+03	7.6155+02	7.3450+02	2.2664+01	7.6141+02
48	1.4386+03	5.7227+03	7.6155+02	7.3448+02	2.2709+01	7.6142+02
49	1.5904+03	5.7464+03	7.6749+02	7.3969+02	2.3795+01	7.6773+02
50	1.5904+03	5.7464+03	7.6746+02	7.3976+02	2.3657+01	7.6766+02
51	1.5904+03	5.7464+03	7.6756+02	7.3980+02	2.3750+01	7.6779+02
52	1.7073+03	5.7405+03	7.7675+02	7.4910+02	2.3976+01	7.7720+02
53	1.7073+03	5.7405+03	7.7692+02	7.4917+02	2.4072+01	7.7739+02
54	1.7073+03	5.7405+03	7.7694+02	7.4919+02	2.4077+01	7.7741+02
55	1.7733+03	5.6794+03	7.8669+02	7.5894+02	2.4216+01	7.8724+02
56	1.7733+03	5.6794+03	7.8665+02	7.5903+02	2.4126+01	7.8721+02
57	1.7733+03	5.6794+03	7.8666+02	7.5904+02	2.4105+01	7.8720+02
58	1.7458+03	5.6438+03	8.0548+02	7.6426+02	3.5947+01	8.0610+02
59	1.7458+03	5.6438+03	8.0550+02	7.6420+02	3.6054+01	8.0615+02
60	1.7458+03	5.6438+03	8.0530+02	7.6417+02	3.5840+01	8.0590+02

LIQUID-LIQUID RUNS CORRECTED K FLOW

	325	330	332	334	345	354
	WK	WNA	TKM	TNAM	DTLM	TK1
61	1.6578+03	5.6399+03	8.0407+02	7.6304+02	3.5542+01	8.0453+02
62	1.6578+03	5.6399+03	8.0401+02	7.6307+02	3.5431+01	8.0445+02
63	1.6578+03	5.6399+03	8.0400+02	7.6300+02	3.5477+01	8.0445+02
64	1.5465+03	5.6991+03	7.9961+02	7.5821+02	3.5339+01	7.9969+02
65	1.5465+03	5.6991+03	7.9968+02	7.5827+02	3.5427+01	7.9982+02
66	1.5465+03	5.6991+03	7.9969+02	7.5826+02	3.5407+01	7.9980+02
67	1.3877+03	5.6478+03	7.8888+02	7.4589+02	3.5730+01	7.8815+02
68	1.3877+03	5.6478+03	7.8872+02	7.4583+02	3.5644+01	7.8799+02
69	1.3877+03	5.6478+03	7.8859+02	7.4570+02	3.5626+01	7.8785+02
70	1.2384+03	5.6459+03	7.6113+02	7.1910+02	3.3948+01	7.5963+02
71	1.2384+03	5.6459+03	7.6124+02	7.1907+02	3.4252+01	7.5992+02
72	1.2384+03	5.6459+03	7.6125+02	7.1905+02	3.4144+01	7.5980+02
73	1.2396+03	4.6411+03	7.5103+02	7.0738+02	3.4769+01	7.4897+02
74	1.2396+03	4.6411+03	7.5099+02	7.0742+02	3.4756+01	7.4898+02
75	1.2396+03	4.6411+03	7.5093+02	7.0739+02	3.4662+01	7.4884+02
76	1.4518+03	4.6617+03	7.5048+02	7.0861+02	3.4758+01	7.4974+02
77	1.4518+03	4.6617+03	7.5049+02	7.0871+02	3.4782+01	7.4985+02
78	1.4518+03	4.6617+03	7.5051+02	7.0868+02	3.4776+01	7.4982+02
79	1.5826+03	4.6666+03	7.5385+02	7.1269+02	3.5037+01	7.5385+02
80	1.5826+03	4.6666+03	7.5391+02	7.1256+02	3.5231+01	7.5392+02
81	1.5826+03	4.6666+03	7.5399+02	7.1264+02	3.5219+01	7.5400+02
82	1.7392+03	4.7108+03	7.6370+02	7.2163+02	3.6341+01	7.6404+02
83	1.7392+03	4.7108+03	7.6363+02	7.2160+02	3.6263+01	7.6396+02
84	1.7397+03	4.7108+03	7.6384+02	7.2169+02	3.6402+01	7.6419+02
85	5.9972+02	4.7370+03	7.5736+02	7.3171+02	1.4789+01	7.4952+02
86	5.9972+02	4.7370+03	7.5743+02	7.3179+02	1.4873+01	7.4975+02
87	5.9972+02	4.7370+03	7.5737+02	7.3179+02	1.4808+01	7.4965+02
88	4.8999+02	4.7137+03	7.5969+02	7.3168+02	1.4057+01	7.4805+02
89	4.8999+02	4.7137+03	7.5967+02	7.3169+02	1.4119+01	7.4815+02
90	4.8999+02	4.7137+03	7.5971+02	7.3174+02	1.4134+01	7.4822+02

LIQUID-LIQUID RUNS CORRECTED K FLOW

	325	330	332	334	345	354
	WK	WNA	TKM	TNAM	DTLM	TK1
91	4.1916+02	4.7919+03	7.6907+02	7.3707+02	1.4455+01	7.5327+02
92	4.1916+02	4.7919+03	7.6909+02	7.3704+02	1.4470+01	7.5326+02
93	4.1916+02	4.7919+03	7.6911+02	7.3703+02	1.4355+01	7.5303+02
94	8.1047+02	7.5918+02	8.0889+02	7.6780+02	2.5187+01	8.0219+02
95	8.1047+02	7.5918+02	8.0902+02	7.6776+02	2.5461+01	8.0240+02
96	8.1047+02	7.5918+02	8.0900+02	7.6782+02	2.5321+01	8.0233+02
97	8.5966+02	7.5990+02	8.1791+02	7.7814+02	2.5231+01	8.1227+02
98	9.8318+02	7.5354+02	8.2108+02	7.8375+02	2.4845+01	8.1698+02
99	1.0890+03	7.5538+02	8.2869+02	7.9219+02	2.5301+01	8.2553+02
100	1.0890+03	7.5538+02	8.2873+02	7.9221+02	2.5348+01	8.2558+02
101	1.0890+03	7.5538+02	8.2866+02	7.9216+02	2.5287+01	8.2546+02
102	1.2352+03	7.5638+02	8.3155+02	7.9643+02	2.4856+01	8.2902+02
103	1.2352+03	7.5638+02	8.3165+02	7.9648+02	2.4869+01	8.2911+02
104	1.2352+03	7.5638+02	8.3163+02	7.9643+02	2.4891+01	8.2909+02
105	1.3156+03	7.0473+02	8.4079+02	8.0650+02	2.4493+01	8.3871+02
106	1.3156+03	7.0473+02	8.4093+02	8.0646+02	2.4661+01	8.3886+02
107	1.3156+03	7.0473+02	8.4096+02	8.0641+02	2.4603+01	8.3883+02
108	1.4816+03	6.9429+02	8.4891+02	8.1529+02	2.4031+01	8.4708+02
109	1.4816+03	6.9429+02	8.4897+02	8.1530+02	2.4037+01	8.4714+02
110	1.4816+03	6.9429+02	8.4897+02	8.1528+02	2.4079+01	8.4712+02

LIQUID-LIQUID RUNS CORRECTED K FLOW

	359	361	363	364	366	369
	TK2	TNA1	TNA2	QK	UI	Q/AI1
1	7.3929+02	7.1354+02	7.1640+02	1.2382+04	7.7696+02	2.8708+04
2	7.3929+02	7.1386+02	7.1671+02	1.2403+04	7.8334+02	2.8665+04
3	7.3918+02	7.1368+02	7.1652+02	1.2347+04	7.8063+02	2.8615+04
4	7.3742+02	7.1316+02	7.1589+02	1.1967+04	7.8478+02	2.7739+04
5	7.3727+02	7.1292+02	7.1564+02	1.1844+04	7.7800+02	2.7517+04
6	7.3725+02	7.1304+02	7.1575+02	1.1871+04	7.8131+02	2.7526+04
7	7.2597+02	7.0305+02	7.0563+02	1.1309+04	7.7296+02	2.6394+04
8	7.2594+02	7.0306+02	7.0565+02	1.1316+04	7.7348+02	2.6363+04
9	7.2588+02	7.0303+02	7.0563+02	1.1444+04	7.7934+02	2.6616+04
10	7.1804+02	6.9609+02	6.9859+02	1.1091+04	7.6937+02	2.5980+04
11	7.1813+02	6.9609+02	6.9860+02	1.1138+04	7.6813+02	2.6026+04
12	7.1800+02	6.9596+02	6.9848+02	1.1173+04	7.7034+02	2.6127+04
13	7.1874+02	7.0071+02	7.0281+02	9.4802+03	7.6758+02	2.2155+04
14	7.1879+02	7.0079+02	7.0289+02	9.5179+03	7.6940+02	2.2194+04
15	7.1878+02	7.0080+02	7.0290+02	9.5394+03	7.7074+02	2.2228+04
16	7.1755+02	7.0011+02	7.0215+02	9.3404+03	7.5870+02	2.1899+04
17	7.1762+02	7.0029+02	7.0234+02	9.4144+03	7.6492+02	2.2024+04
18	7.1758+02	7.0011+02	7.0216+02	9.3303+03	7.5794+02	2.1908+04
19	7.1522+02	6.9875+02	7.0073+02	9.3399+03	7.5850+02	2.1888+04
20	7.1511+02	6.9850+02	7.0048+02	9.2956+03	7.5433+02	2.1876+04
21	7.1522+02	6.9859+02	7.0057+02	9.3176+03	7.5368+02	2.1885+04
22	7.1180+02	6.9647+02	6.9835+02	9.0407+03	7.3820+02	2.1302+04
23	7.1170+02	6.9636+02	6.9825+02	9.0485+03	7.3880+02	2.1329+04
24	7.1167+02	6.9642+02	6.9831+02	9.0677+03	7.4236+02	2.1367+04
25	7.0857+02	6.9419+02	6.9601+02	8.9796+03	7.3441+02	2.1119+04
26	7.0855+02	6.9413+02	6.9594+02	8.9727+03	7.3323+02	2.1127+04
27	7.0862+02	6.9437+02	6.9618+02	9.0352+03	7.3900+02	2.1161+04
28	7.0236+02	6.8998+02	6.9162+02	8.7631+03	7.2790+02	2.0385+04
29	7.0238+02	6.8998+02	6.9162+02	8.7660+03	7.2730+02	2.0390+04
30	7.0230+02	6.8987+02	6.9150+02	8.7339+03	7.2541+02	2.0371+04

LIQUID-LIQUID RUNS CORRECTED K FLOW

	359	361	363	364	366	369
	TK2	TNA1	TNA2	QK	UI	Q/AI1
31	7.1194+02	7.0010+02	7.0132+02	8.4798+03	7.6894+02	1.9744+04
32	7.1206+02	7.0004+02	7.0126+02	8.4466+03	7.6202+02	1.9729+04
33	7.1203+02	7.0014+02	7.0136+02	8.4928+03	7.6818+02	1.9775+04
34	7.1667+02	7.0371+02	7.0497+02	8.4882+03	7.5840+02	1.9860+04
35	7.1670+02	7.0359+02	7.0486+02	8.4201+03	7.5099+02	1.9758+04
36	7.1668+02	7.0372+02	7.0497+02	8.3844+03	7.5387+02	1.9665+04
37	7.2157+02	7.0760+02	7.0891+02	8.4200+03	7.6068+02	1.9700+04
38	7.2169+02	7.0757+02	7.0887+02	8.3378+03	7.5206+02	1.9557+04
39	7.2169+02	7.0769+02	7.0899+02	8.3706+03	7.5689+02	1.9593+04
40	7.2883+02	7.1354+02	7.1490+02	8.4416+03	7.5532+02	1.9709+04
41	7.2898+02	7.1358+02	7.1495+02	8.4507+03	7.5205+02	1.9719+04
42	7.2899+02	7.1373+02	7.1510+02	8.5071+03	7.5906+02	1.9821+04
43	7.3968+02	7.2406+02	7.2546+02	8.6020+03	7.7471+02	1.9949+04
44	7.3983+02	7.2403+02	7.2543+02	8.5654+03	7.6778+02	1.9912+04
45	7.3982+02	7.2417+02	7.2557+02	8.6120+03	7.7402+02	1.9969+04
46	7.5201+02	7.3574+02	7.3716+02	8.5490+03	7.6689+02	1.9734+04
47	7.5192+02	7.3574+02	7.3715+02	8.5826+03	7.7141+02	1.9805+04
48	7.5194+02	7.3566+02	7.3708+02	8.5491+03	7.6687+02	1.9753+04
49	7.5844+02	7.4088+02	7.4241+02	9.1720+03	7.8520+02	2.1086+04
50	7.5837+02	7.4095+02	7.4248+02	9.1782+03	7.9031+02	2.1112+04
51	7.5850+02	7.4096+02	7.4249+02	9.1535+03	7.8512+02	2.1065+04
52	7.6829+02	7.5019+02	7.5176+02	9.3405+03	7.9359+02	2.1438+04
53	7.6844+02	7.5030+02	7.5189+02	9.3932+03	7.9488+02	2.1527+04
54	7.6848+02	7.5032+02	7.5190+02	9.3800+03	7.9361+02	2.1499+04
55	7.7850+02	7.5998+02	7.6160+02	9.4670+03	7.9637+02	2.1711+04
56	7.7852+02	7.6006+02	7.6168+02	9.4120+03	7.9469+02	2.1572+04
57	7.7850+02	7.6005+02	7.6167+02	9.4189+03	7.9596+02	2.1611+04
58	7.9320+02	7.6497+02	7.6735+02	1.3430+04	7.6108+02	3.1304+04
59	7.9326+02	7.6492+02	7.6729+02	1.3417+04	7.5805+02	3.1258+04
60	7.9301+02	7.6488+02	7.6726+02	1.3423+04	7.6293+02	3.1294+04

LIQUID-LIQUID RUNS CORRECTED K FLOW

	359	361	363	364	366	369
	TK2	TNA1	TNA2	QK	UI	Q/AI1
61	7.9139+02	7.6381+02	7.6611+02	1.3052+04	7.4807+02	3.0461+04
62	7.9131+02	7.6386+02	7.6616+02	1.3065+04	7.5115+02	3.0487+04
63	7.9128+02	7.6383+02	7.6613+02	1.3097+04	7.5201+02	3.0545+04
64	7.8587+02	7.5900+02	7.6124+02	1.2887+04	7.4283+02	3.0220+04
65	7.8605+02	7.5906+02	7.6129+02	1.2833+04	7.3790+02	3.0072+04
66	7.8599+02	7.5906+02	7.6129+02	1.2875+04	7.4073+02	3.0177+04
67	7.7297+02	7.4664+02	7.4886+02	1.2843+04	7.3223+02	3.0395+04
68	7.7285+02	7.4659+02	7.4880+02	1.2816+04	7.3243+02	3.0326+04
69	7.7269+02	7.4647+02	7.4868+02	1.2832+04	7.3372+02	3.0359+04
70	7.4399+02	7.2032+02	7.2236+02	1.2151+04	7.2914+02	2.8659+04
71	7.4432+02	7.2037+02	7.2241+02	1.2122+04	7.2094+02	2.8510+04
72	7.4414+02	7.2032+02	7.2236+02	1.2185+04	7.2694+02	2.8700+04
73	7.3293+02	7.0826+02	7.1080+02	1.2416+04	7.2743+02	2.9612+04
74	7.3299+02	7.0830+02	7.1083+02	1.2368+04	7.2489+02	2.9488+04
75	7.3284+02	7.0821+02	7.1074+02	1.2368+04	7.2687+02	2.9536+04
76	7.3543+02	7.0927+02	7.1192+02	1.2666+04	7.4231+02	3.0040+04
77	7.3561+02	7.0943+02	7.1206+02	1.2604+04	7.3817+02	2.9835+04
78	7.3555+02	7.0936+02	7.1199+02	1.2621+04	7.3927+02	2.9911+04
79	7.4050+02	7.1347+02	7.1616+02	1.2788+04	7.4350+02	3.0020+04
80	7.4054+02	7.1328+02	7.1597+02	1.2782+04	7.3905+02	3.0036+04
81	7.4060+02	7.1342+02	7.1612+02	1.2830+04	7.4212+02	3.0116+04
82	7.5101+02	7.2219+02	7.2505+02	1.3541+04	7.5901+02	3.1764+04
83	7.5090+02	7.2224+02	7.2510+02	1.3608+04	7.6444+02	3.1892+04
84	7.5111+02	7.2232+02	7.2519+02	1.3625+04	7.6245+02	3.1921+04
85	7.3939+02	7.3328+02	7.3404+02	5.0095+03	6.9003+02	1.1212+04
86	7.3961+02	7.3346+02	7.3422+02	5.0210+03	6.8772+02	1.1201+04
87	7.3954+02	7.3341+02	7.3417+02	5.0025+03	6.8819+02	1.1176+04
88	7.3793+02	7.3336+02	7.3399+02	4.6725+03	6.7713+02	9.9489+03
89	7.3798+02	7.3335+02	7.3398+02	4.6611+03	6.7251+02	9.9547+03
90	7.3804+02	7.3339+02	7.3402+02	4.6573+03	6.7123+02	9.9566+03

LIQUID-LIQUID RUNS CORRECTED K FLOW

	359	361	363	364	366	369
	TK2	TNA1	TNA2	QK	UI	Q/AI1
91	7.4280+02	7.3904+02	7.3959+02	4.6946+03	6.6159+02	9.4146+03
92	7.4276+02	7.3900+02	7.3955+02	4.6979+03	6.6135+02	9.4290+03
93	7.4259+02	7.3889+02	7.3943+02	4.6913+03	6.6574+02	9.4139+03
94	7.9138+02	7.7511+02	7.8198+02	7.2071+03	5.8290+02	1.5783+04
95	7.9148+02	7.7482+02	7.8176+02	7.1759+03	5.7413+02	1.5834+04
96	7.9147+02	7.7502+02	7.8192+02	7.1947+03	5.7882+02	1.5811+04
97	8.0191+02	7.8493+02	7.9193+02	7.1207+03	5.7490+02	1.5720+04
98	8.0768+02	7.8980+02	7.9704+02	7.0233+03	5.7586+02	1.5650+04
99	8.1678+02	7.9756+02	8.0510+02	7.0484+03	5.6750+02	1.5874+04
100	8.1682+02	7.9748+02	8.0502+02	7.0231+03	5.6440+02	1.5863+04
101	8.1668+02	7.9729+02	8.0484+02	6.9893+03	5.6305+02	1.5862+04
102	8.2108+02	8.0148+02	8.0923+02	7.1400+03	5.8517+02	1.6111+04
103	8.2117+02	8.0164+02	8.0939+02	7.1735+03	5.8759+02	1.6143+04
104	8.2113+02	8.0154+02	8.0930+02	7.1687+03	5.8668+02	1.6161+04
105	8.3152+02	8.1215+02	8.2018+02	7.0626+03	5.8738+02	1.5603+04
106	8.3162+02	8.1205+02	8.2012+02	7.0720+03	5.8417+02	1.5664+04
107	8.3158+02	8.1214+02	8.2023+02	7.1276+03	5.9014+02	1.5751+04
108	8.4054+02	8.2132+02	8.2966+02	7.3437+03	6.2252+02	1.6035+04
109	8.4060+02	8.2146+02	8.2980+02	7.3890+03	6.2618+02	1.6081+04
110	8.4055+02	8.2118+02	8.2955+02	7.3206+03	6.1931+02	1.6062+04

LIQUID-LIQUID RUNS CORRECTED K FLOW

	370 Q/AI2	379 NRENA1	381 NRE K1	385 NPRNA1	387 NPR K1	388 NPENA1
1	1.7783+04	2.1634+04	8.2370+04	5.3050-03	4.2692-03	1.1477+02
2	1.7687+04	2.1642+04	8.2367+04	5.3035-03	4.2694-03	1.1478+02
3	1.7685+04	2.1638+04	8.2356+04	5.3044-03	4.2698-03	1.1477+02
4	1.6893+04	2.1663+04	7.9621+04	5.3069-03	4.2761-03	1.1496+02
5	1.6830+04	2.1657+04	7.9602+04	5.3081-03	4.2768-03	1.1496+02
6	1.6800+04	2.1660+04	7.9600+04	5.3075-03	4.2769-03	1.1496+02
7	1.5720+04	2.1295+04	7.3125+04	5.3561-03	4.3150-03	1.1406+02
8	1.5696+04	2.1296+04	7.3121+04	5.3560-03	4.3151-03	1.1406+02
9	1.5785+04	2.1295+04	7.3124+04	5.3562-03	4.3150-03	1.1406+02
10	1.4961+04	2.1145+04	6.6750+04	5.3899-03	4.3400-03	1.1397+02
11	1.5001+04	2.1145+04	6.6759+04	5.3899-03	4.3396-03	1.1397+02
12	1.5036+04	2.1142+04	6.6752+04	5.3905-03	4.3400-03	1.1396+02
13	1.2229+04	2.1240+04	6.0893+04	5.3675-03	4.3410-03	1.1401+02
14	1.2233+04	2.1242+04	6.0897+04	5.3671-03	4.3408-03	1.1401+02
15	1.2239+04	2.1242+04	6.0897+04	5.3671-03	4.3408-03	1.1401+02
16	1.1677+04	2.1155+04	5.6161+04	5.3704-03	4.3431-03	1.1361+02
17	1.1684+04	2.1160+04	5.6168+04	5.3695-03	4.3427-03	1.1362+02
18	1.1690+04	2.1155+04	5.6164+04	5.3704-03	4.3429-03	1.1361+02
19	1.0996+04	2.1240+04	5.0379+04	5.3770-03	4.3477-03	1.1421+02
20	1.1032+04	2.1234+04	5.0374+04	5.3782-03	4.3481-03	1.1420+02
21	1.1043+04	2.1236+04	5.0381+04	5.3778-03	4.3477-03	1.1420+02
22	9.9329+03	2.1010+04	4.3333+04	5.3881-03	4.3555-03	1.1320+02
23	9.9392+03	2.1007+04	4.3329+04	5.3885-03	4.3558-03	1.1320+02
24	9.9205+03	2.1009+04	4.3328+04	5.3883-03	4.3559-03	1.1320+02
25	9.2261+03	2.0924+04	3.9166+04	5.3991-03	4.3636-03	1.1297+02
26	9.2419+03	2.0922+04	3.9166+04	5.3994-03	4.3636-03	1.1297+02
27	9.1966+03	2.0928+04	3.9168+04	5.3982-03	4.3634-03	1.1297+02
28	7.8139+03	2.1039+04	3.2713+04	5.4194-03	4.3804-03	1.1402+02
29	7.8220+03	2.1039+04	3.2714+04	5.4194-03	4.3803-03	1.1402+02
30	7.8340+03	2.1036+04	3.2711+04	5.4200-03	4.3805-03	1.1402+02

LIQUID-LIQUID RUNS CORRECTED K FLOW

	370 Q/AI2	379 NRENA1	381 NRE K1	385 NPRNA1	387 NPR K1	388 NPENA1
31	8.1714+03	2.8674+04	3.7313+04	5.3704-03	4.3540-03	1.5399+02
32	8.2302+03	2.8672+04	3.7320+04	5.3707-03	4.3534-03	1.5399+02
33	8.1913+03	2.8675+04	3.7318+04	5.3702-03	4.3536-03	1.5399+02
34	8.8695+03	2.8832+04	4.0742+04	5.3529-03	4.3399-03	1.5434+02
35	8.8935+03	2.8828+04	4.0743+04	5.3535-03	4.3399-03	1.5433+02
36	8.8246+03	2.8832+04	4.0738+04	5.3529-03	4.3402-03	1.5434+02
37	9.6323+03	2.8986+04	4.6805+04	5.3340-03	4.3276-03	1.5461+02
38	9.6401+03	2.8985+04	4.6808+04	5.3341-03	4.3273-03	1.5461+02
39	9.6141+03	2.8989+04	4.6808+04	5.3335-03	4.3273-03	1.5461+02
40	1.0519+04	2.9055+04	5.4140+04	5.3051-03	4.3066-03	1.5414+02
41	1.0553+04	2.9056+04	5.4150+04	5.3049-03	4.3060-03	1.5414+02
42	1.0546+04	2.9061+04	5.4153+04	5.3041-03	4.3059-03	1.5414+02
43	1.1014+04	2.9415+04	6.0042+04	5.2536-03	4.2716-03	1.5453+02
44	1.1053+04	2.9414+04	6.0052+04	5.2538-03	4.2711-03	1.5453+02
45	1.1031+04	2.9418+04	6.0053+04	5.2531-03	4.2711-03	1.5454+02
46	1.1388+04	2.9882+04	6.5721+04	5.1963-03	4.2312-03	1.5527+02
47	1.1392+04	2.9881+04	6.5716+04	5.1963-03	4.2315-03	1.5527+02
48	1.1399+04	2.9879+04	6.5717+04	5.1967-03	4.2314-03	1.5527+02
49	1.2585+04	3.0187+04	7.3167+04	5.1710-03	4.2095-03	1.5610+02
50	1.2559+04	3.0189+04	7.3162+04	5.1706-03	4.2097-03	1.5610+02
51	1.2573+04	3.0190+04	7.3172+04	5.1706-03	4.2093-03	1.5610+02
52	1.3116+04	3.0491+04	7.9397+04	5.1250-03	4.1764-03	1.5627+02
53	1.3160+04	3.0495+04	7.9414+04	5.1244-03	4.1757-03	1.5627+02
54	1.3154+04	3.0496+04	7.9416+04	5.1244-03	4.1756-03	1.5627+02
55	1.3454+04	3.0440+04	8.3420+04	5.0894-03	4.1411-03	1.5492+02
56	1.3381+04	3.0442+04	8.3417+04	5.0891-03	4.1412-03	1.5492+02
57	1.3395+04	3.0442+04	8.3416+04	5.0892-03	4.1413-03	1.5492+02
58	1.9677+04	3.0380+04	8.3825+04	5.0728-03	4.0807-03	1.5411+02
59	1.9684+04	3.0378+04	8.3829+04	5.0729-03	4.0805-03	1.5411+02
60	1.9648+04	3.0377+04	8.3810+04	5.0730-03	4.0812-03	1.5411+02

LIQUID-LIQUID RUNS CORRECTED K FLOW

	370 Q/AI2	379 NRENA1	381 NRE K1	385 NPRNA1	387 NPR K1	388 NPENA1
61	1.8908+04	3.0329+04	7.9483+04	5.0766-03	4.0846-03	1.5397+02
62	1.8887+04	3.0330+04	7.9477+04	5.0765-03	4.0848-03	1.5397+02
63	1.8913+04	3.0329+04	7.9477+04	5.0766-03	4.0848-03	1.5397+02
64	1.8299+04	3.0520+04	7.3812+04	5.0927-03	4.0971-03	1.5543+02
65	1.8270+04	3.0521+04	7.3823+04	5.0925-03	4.0966-03	1.5543+02
66	1.8300+04	3.0521+04	7.3822+04	5.0925-03	4.0967-03	1.5543+02
67	1.7652+04	2.9873+04	6.5350+04	5.1425-03	4.1379-03	1.5362+02
68	1.7610+04	2.9871+04	6.5338+04	5.1428-03	4.1385-03	1.5362+02
69	1.7612+04	2.9866+04	6.5327+04	5.1434-03	4.1390-03	1.5361+02
70	1.5775+04	2.8956+04	5.6456+04	5.2719-03	4.2376-03	1.5265+02
71	1.5799+04	2.8958+04	5.6475+04	5.2717-03	4.2366-03	1.5266+02
72	1.5826+04	2.8956+04	5.6468+04	5.2719-03	4.2370-03	1.5265+02
73	1.6097+04	2.3476+04	5.5847+04	5.3308-03	4.2745-03	1.2515+02
74	1.6064+04	2.3477+04	5.5848+04	5.3306-03	4.2745-03	1.2515+02
75	1.6064+04	2.3475+04	5.5839+04	5.3310-03	4.2749-03	1.2515+02
76	1.7451+04	2.3608+04	6.5463+04	5.3258-03	4.2718-03	1.2573+02
77	1.7384+04	2.3612+04	6.5470+04	5.3251-03	4.2715-03	1.2573+02
78	1.7414+04	2.3610+04	6.5468+04	5.3254-03	4.2716-03	1.2573+02
79	1.8097+04	2.3746+04	7.1684+04	5.3054-03	4.2576-03	1.2598+02
80	1.8162+04	2.3741+04	7.1689+04	5.3063-03	4.2574-03	1.2598+02
81	1.8172+04	2.3745+04	7.1696+04	5.3056-03	4.2571-03	1.2598+02
82	1.9705+04	2.4212+04	7.9683+04	5.2628-03	4.2223-03	1.2742+02
83	1.9717+04	2.4214+04	7.9675+04	5.2626-03	4.2226-03	1.2743+02
84	1.9763+04	2.4216+04	7.9719+04	5.2621-03	4.2218-03	1.2743+02
85	3.6959+03	2.4663+04	2.7035+04	5.2084-03	4.2726-03	1.2846+02
86	3.7061+03	2.4668+04	2.7042+04	5.2075-03	4.2718-03	1.2846+02
87	3.6951+03	2.4667+04	2.7039+04	5.2077-03	4.2721-03	1.2846+02
88	2.6674+03	2.4544+04	2.2053+04	5.2080-03	4.2777-03	1.2783+02
89	2.6931+03	2.4544+04	2.2055+04	5.2081-03	4.2773-03	1.2783+02
90	2.7003+03	2.4545+04	2.2057+04	5.2079-03	4.2771-03	1.2783+02

LIQUID-LIQUID RUNS CORRECTED K FLOW

	370 Q/AI2	379 NRENA1	381 NRE K1	385 NPRNA1	387 NPR K1	388 NPENA1
91	2.1210+03	2.5119+04	1.8974+04	5.1800-03	4.2596-03	1.3012+02
92	2.1254+03	2.5117+04	1.8974+04	5.1802-03	4.2597-03	1.3011+02
93	2.1011+03	2.5114+04	1.8969+04	5.1808-03	4.2605-03	1.3011+02
94	5.4764+03	4.1228+03	3.8774+04	5.0388-03	4.0905-03	2.0774+01
95	5.5823+03	4.1217+03	3.8782+04	5.0398-03	4.0900-03	2.0772+01
96	5.5268+03	4.1224+03	3.8780+04	5.0391-03	4.0901-03	2.0773+01
97	5.7376+03	4.1623+03	4.1513+04	5.0058-03	4.0651-03	2.0836+01
98	6.1277+03	4.1453+03	4.7686+04	4.9893-03	4.0532-03	2.0682+01
99	6.6287+03	4.1841+03	5.3242+04	4.9632-03	4.0315-03	2.0766+01
100	6.6557+03	4.1838+03	5.3245+04	4.9634-03	4.0314-03	2.0766+01
101	6.6695+03	4.1831+03	5.3238+04	4.9641-03	4.0317-03	2.0765+01
102	6.9351+03	4.2043+03	6.0589+04	4.9504-03	4.0226-03	2.0813+01
103	6.9246+03	4.2049+03	6.0595+04	4.9499-03	4.0224-03	2.0814+01
104	6.9413+03	4.2045+03	6.0593+04	4.9502-03	4.0224-03	2.0813+01
105	6.6614+03	3.9550+03	6.5128+04	4.9180-03	3.9978-03	1.9451+01
106	6.7186+03	3.9546+03	6.5137+04	4.9183-03	3.9974-03	1.9450+01
107	6.6978+03	3.9549+03	6.5135+04	4.9181-03	3.9975-03	1.9450+01
108	6.7728+03	3.9288+03	7.3938+04	4.8900-03	3.9763-03	1.9212+01
109	6.7578+03	3.9293+03	7.3943+04	4.8896-03	3.9762-03	1.9213+01
110	6.8147+03	3.9283+03	7.3941+04	4.8905-03	3.9762-03	1.9211+01

LIQUID-LIQUID RUNS CORRECTED K FLOW

	389	398	400	703	705	706
	NPE K1	NRENA2	NRE K2	NPRNA2	NPR K2	NPENA2
1	3.5166+02	2.1705+04	8.1360+04	5.2911-03	4.3078-03	1.1484+02
2	3.5165+02	2.1713+04	8.1361+04	5.2896-03	4.3078-03	1.1485+02
3	3.5164+02	2.1708+04	8.1351+04	5.2905-03	4.3082-03	1.1485+02
4	3.4047+02	2.1731+04	7.8657+04	5.2936-03	4.3142-03	1.1503+02
5	3.4045+02	2.1724+04	7.8645+04	5.2948-03	4.3147-03	1.1503+02
6	3.4044+02	2.1727+04	7.8643+04	5.2943-03	4.3148-03	1.1503+02
7	3.1553+02	2.1358+04	7.2240+04	5.3436-03	4.3533-03	1.1413+02
8	3.1553+02	2.1358+04	7.2237+04	5.3435-03	4.3534-03	1.1413+02
9	3.1553+02	2.1358+04	7.2233+04	5.3436-03	4.3536-03	1.1413+02
10	2.8970+02	2.1204+04	6.5906+04	5.3778-03	4.3802-03	1.1403+02
11	2.8971+02	2.1205+04	6.5913+04	5.3777-03	4.3799-03	1.1403+02
12	2.8970+02	2.1202+04	6.5904+04	5.3783-03	4.3804-03	1.1403+02
13	2.6434+02	2.1291+04	6.0187+04	5.3573-03	4.3778-03	1.1406+02
14	2.6434+02	2.1292+04	6.0190+04	5.3569-03	4.3777-03	1.1406+02
15	2.6434+02	2.1293+04	6.0189+04	5.3569-03	4.3777-03	1.1406+02
16	2.4391+02	2.1204+04	5.5476+04	5.3605-03	4.3819-03	1.1366+02
17	2.4392+02	2.1209+04	5.5480+04	5.3595-03	4.3817-03	1.1367+02
18	2.4392+02	2.1204+04	5.5478+04	5.3605-03	4.3818-03	1.1366+02
19	2.1904+02	2.1287+04	4.9715+04	5.3674-03	4.3898-03	1.1426+02
20	2.1903+02	2.1282+04	4.9708+04	5.3686-03	4.3902-03	1.1425+02
21	2.1904+02	2.1284+04	4.9714+04	5.3682-03	4.3898-03	1.1425+02
22	1.8874+02	2.1054+04	4.2711+04	5.3789-03	4.4013-03	1.1325+02
23	1.8873+02	2.1052+04	4.2706+04	5.3794-03	4.4017-03	1.1325+02
24	1.8873+02	2.1053+04	4.2705+04	5.3791-03	4.4018-03	1.1325+02
25	1.7090+02	2.0966+04	3.8570+04	5.3903-03	4.4122-03	1.1301+02
26	1.7090+02	2.0965+04	3.8569+04	5.3906-03	4.4123-03	1.1301+02
27	1.7091+02	2.0970+04	3.8572+04	5.3894-03	4.4121-03	1.1302+02
28	1.4330+02	2.1078+04	3.2175+04	5.4115-03	4.4332-03	1.1406+02
29	1.4330+02	2.1078+04	3.2176+04	5.4115-03	4.4331-03	1.1406+02
30	1.4329+02	2.1075+04	3.2173+04	5.4121-03	4.4333-03	1.1406+02

LIQUID-LIQUID RUNS CORRECTED K FLOW

	389 NPE K1	398 NRENA2	400 NRE K2	703 NPRNA2	705 NPR K2	706 NPENA2
31	1.6246+02	2.8713+04	3.6765+04	5.3645-03	4.4009-03	1.5403+02
32	1.6247+02	2.8711+04	3.6770+04	5.3648-03	4.4005-03	1.5403+02
33	1.6247+02	2.8715+04	3.6769+04	5.3643-03	4.4006-03	1.5403+02
34	1.7682+02	2.8873+04	4.0167+04	5.3468-03	4.3849-03	1.5438+02
35	1.7682+02	2.8870+04	4.0168+04	5.3473-03	4.3848-03	1.5438+02
36	1.7681+02	2.8873+04	4.0167+04	5.3468-03	4.3848-03	1.5438+02
37	2.0255+02	2.9029+04	4.6205+04	5.3276-03	4.3682-03	1.5466+02
38	2.0256+02	2.9028+04	4.6211+04	5.3278-03	4.3678-03	1.5465+02
39	2.0256+02	2.9032+04	4.6211+04	5.3272-03	4.3678-03	1.5466+02
40	2.3316+02	2.9100+04	5.3508+04	5.2984-03	4.3436-03	1.5418+02
41	2.3317+02	2.9102+04	5.3516+04	5.2982-03	4.3430-03	1.5419+02
42	2.3318+02	2.9107+04	5.3517+04	5.2974-03	4.3430-03	1.5419+02
43	2.5648+02	2.9463+04	5.9376+04	5.2468-03	4.3064-03	1.5458+02
44	2.5649+02	2.9461+04	5.9386+04	5.2469-03	4.3059-03	1.5458+02
45	2.5649+02	2.9466+04	5.9386+04	5.2462-03	4.3059-03	1.5459+02
46	2.7808+02	2.9931+04	6.5031+04	5.1893-03	4.2640-03	1.5532+02
47	2.7808+02	2.9931+04	6.5025+04	5.1893-03	4.2643-03	1.5532+02
48	2.7808+02	2.9928+04	6.5026+04	5.1897-03	4.2642-03	1.5532+02
49	3.0800+02	3.0242+04	7.2407+04	5.1635-03	4.2418-03	1.5615+02
50	3.0799+02	3.0244+04	7.2402+04	5.1631-03	4.2420-03	1.5615+02
51	3.0800+02	3.0245+04	7.2413+04	5.1630-03	4.2415-03	1.5615+02
52	3.3159+02	3.0549+04	7.8598+04	5.1172-03	4.2075-03	1.5632+02
53	3.3161+02	3.0553+04	7.8611+04	5.1166-03	4.2070-03	1.5633+02
54	3.3161+02	3.0554+04	7.8614+04	5.1165-03	4.2069-03	1.5633+02
55	3.4545+02	3.0483+04	8.2586+04	5.0840-03	4.1718-03	1.5497+02
56	3.4545+02	3.0485+04	8.2588+04	5.0837-03	4.1718-03	1.5498+02
57	3.4545+02	3.0484+04	8.2586+04	5.0838-03	4.1718-03	1.5498+02
58	3.4206+02	3.0442+04	8.2697+04	5.0648-03	4.1201-03	1.5418+02
59	3.4207+02	3.0441+04	8.2702+04	5.0650-03	4.1199-03	1.5418+02
60	3.4204+02	3.0440+04	8.2679+04	5.0651-03	4.1207-03	1.5418+02

LIQUID-LIQUID RUNS CORRECTED K FLOW

	389 NPE K1	398 NRENA2	400 NRE K2	703 NPRNA2	705 NPR K2	706 NPENA2
61	3.2466+02	3.0389+04	7.8362+04	5.0689-03	4.1265-03	1.5404+02
62	3.2465+02	3.0390+04	7.8354+04	5.0688-03	4.1268-03	1.5404+02
63	3.2465+02	3.0390+04	7.8352+04	5.0689-03	4.1269-03	1.5404+02
64	3.0242+02	3.0579+04	7.2636+04	5.0852-03	4.1459-03	1.5550+02
65	3.0243+02	3.0580+04	7.2651+04	5.0851-03	4.1453-03	1.5550+02
66	3.0243+02	3.0580+04	7.2647+04	5.0851-03	4.1455-03	1.5550+02
67	2.7041+02	2.9952+04	6.4223+04	5.1316-03	4.1912-03	1.5370+02
68	2.7040+02	2.9950+04	6.4214+04	5.1319-03	4.1916-03	1.5370+02
69	2.7039+02	2.9945+04	6.4202+04	5.1325-03	4.1922-03	1.5369+02
70	2.3924+02	2.9024+04	5.5486+04	5.2620-03	4.2916-03	1.5272+02
71	2.3926+02	2.9026+04	5.5506+04	5.2617-03	4.2905-03	1.5273+02
72	2.3925+02	2.9024+04	5.5494+04	5.2619-03	4.2911-03	1.5272+02
73	2.3872+02	2.3544+04	5.4874+04	5.3184-03	4.3295-03	1.2522+02
74	2.3872+02	2.3545+04	5.4878+04	5.3182-03	4.3293-03	1.2522+02
75	2.3871+02	2.3543+04	5.4868+04	5.3187-03	4.3299-03	1.2522+02
76	2.7965+02	2.3679+04	6.4442+04	5.3130-03	4.3210-03	1.2580+02
77	2.7966+02	2.3683+04	6.4455+04	5.3123-03	4.3204-03	1.2581+02
78	2.7965+02	2.3681+04	6.4451+04	5.3126-03	4.3206-03	1.2581+02
79	3.0521+02	2.3819+04	7.0636+04	5.2923-03	4.3036-03	1.2606+02
80	3.0521+02	2.3814+04	7.0639+04	5.2932-03	4.3035-03	1.2605+02
81	3.0522+02	2.3818+04	7.0644+04	5.2925-03	4.3033-03	1.2606+02
82	3.3645+02	2.4292+04	7.8532+04	5.2488-03	4.2675-03	1.2751+02
83	3.3644+02	2.4294+04	7.8522+04	5.2485-03	4.2679-03	1.2751+02
84	3.3656+02	2.4297+04	7.8563+04	5.2481-03	4.2671-03	1.2751+02
85	1.1551+02	2.4685+04	2.6736+04	5.2047-03	4.3074-03	1.2848+02
86	1.1552+02	2.4691+04	2.6742+04	5.2038-03	4.3067-03	1.2848+02
87	1.1551+02	2.4689+04	2.6740+04	5.2040-03	4.3069-03	1.2848+02
88	9.4334+01	2.4562+04	2.1809+04	5.2049-03	4.3125-03	1.2784+02
89	9.4337+01	2.4562+04	2.1810+04	5.2050-03	4.3123-03	1.2784+02
90	9.4339+01	2.4563+04	2.1812+04	5.2048-03	4.3121-03	1.2784+02

LIQUID-LIQUID RUNS CORRECTED K FLOW

	389 NPE K1	398 NRENA2	400 NRE K2	703 NPRNA2	705 NPR K2	706 NPENA2
91	8.0824+01	2.5135+04	1.8756+04	5.1773-03	4.2957-03	1.3013+02
92	8.0824+01	2.5134+04	1.8755+04	5.1775-03	4.2959-03	1.3013+02
93	8.0818+01	2.5130+04	1.8752+04	5.1781-03	4.2965-03	1.3013+02
94	1.5861+02	4.1477+03	3.8310+04	5.0157-03	4.1265-03	2.0803+01
95	1.5862+02	4.1468+03	3.8314+04	5.0164-03	4.1261-03	2.0802+01
96	1.5861+02	4.1474+03	3.8314+04	5.0159-03	4.1262-03	2.0803+01
97	1.6876+02	4.1881+03	4.1117+04	4.9822-03	4.0912-03	2.0866+01
98	1.9328+02	4.1720+03	4.7277+04	4.9649-03	4.0767-03	2.0713+01
99	2.1464+02	4.2124+03	5.2807+04	4.9395-03	4.0537-03	2.0807+01
100	2.1465+02	4.2121+03	5.2809+04	4.9397-03	4.0536-03	2.0806+01
101	2.1464+02	4.2114+03	5.2803+04	4.9402-03	4.0540-03	2.0805+01
102	2.4373+02	4.2336+03	6.0139+04	4.9269-03	4.0428-03	2.0859+01
103	2.4373+02	4.2342+03	6.0144+04	4.9264-03	4.0426-03	2.0860+01
104	2.4373+02	4.2339+03	6.0142+04	4.9267-03	4.0427-03	2.0859+01
105	2.6037+02	3.9838+03	6.4685+04	4.8935-03	4.0162-03	1.9495+01
106	2.6038+02	3.9836+03	6.4692+04	4.8937-03	4.0160-03	1.9495+01
107	2.6038+02	3.9840+03	6.4689+04	4.8934-03	4.0161-03	1.9495+01
108	2.9400+02	3.9589+03	7.3477+04	4.8645-03	3.9931-03	1.9258+01
109	2.9401+02	3.9594+03	7.3481+04	4.8640-03	3.9930-03	1.9259+01
110	2.9401+02	3.9585+03	7.3478+04	4.8648-03	3.9931-03	1.9257+01

LIQUID-LIQUID RUNS CORRECTED K FLOW

	707	405	406	408	418	419
	NPE K2	DTW 1	DTW 2	QNA	QL	QL+QNA
1	3.5048+02	2.1697+01	1.3449+01	9.5902+03	1.1065+03	1.0697+04
2	3.5048+02	2.1664+01	1.3376+01	9.2082+03	1.1061+03	1.0314+04
3	3.5047+02	2.1627+01	1.3375+01	9.4876+03	1.1064+03	1.0594+04
4	3.3934+02	2.0969+01	1.2777+01	8.9733+03	1.1029+03	1.0076+04
5	3.3933+02	2.0802+01	1.2731+01	9.1693+03	1.1028+03	1.0272+04
6	3.3933+02	2.0807+01	1.2708+01	8.9547+03	1.1029+03	1.0058+04
7	3.1448+02	1.9985+01	1.1910+01	8.8006+03	1.0720+03	9.8726+03
8	3.1448+02	1.9961+01	1.1893+01	8.6240+03	1.0717+03	9.6956+03
9	3.1447+02	2.0153+01	1.1959+01	8.5136+03	1.0716+03	9.5852+03
10	2.8869+02	1.9692+01	1.1349+01	8.5482+03	1.0505+03	9.5987+03
11	2.8869+02	1.9728+01	1.1379+01	8.3419+03	1.0505+03	9.3924+03
12	2.8868+02	1.9805+01	1.1405+01	8.4265+03	1.0502+03	9.4767+03
13	2.6349+02	1.6788+01	9.2723+00	6.6962+03	1.0572+03	7.7534+03
14	2.6349+02	1.6817+01	9.2752+00	6.5190+03	1.0575+03	7.5764+03
15	2.6349+02	1.6843+01	9.2797+00	6.4632+03	1.0574+03	7.5206+03
16	2.4309+02	1.6596+01	8.8549+00	6.6076+03	1.0553+03	7.6629+03
17	2.4309+02	1.6690+01	8.8595+00	6.4484+03	1.0550+03	7.5035+03
18	2.4309+02	1.6602+01	8.8642+00	6.7372+03	1.0551+03	7.7924+03
19	2.1824+02	1.6590+01	8.3409+00	6.2455+03	1.0490+03	7.2945+03
20	2.1823+02	1.6582+01	8.3682+00	6.6121+03	1.0488+03	7.6609+03
21	2.1824+02	1.6589+01	8.3767+00	6.4430+03	1.0488+03	7.4918+03
22	1.8798+02	1.6153+01	7.5376+00	6.4212+03	1.0425+03	7.4637+03
23	1.8798+02	1.6173+01	7.5425+00	6.4679+03	1.0425+03	7.5104+03
24	1.8798+02	1.6202+01	7.5283+00	6.4679+03	1.0423+03	7.5102+03
25	1.7018+02	1.6020+01	7.0042+00	6.3853+03	1.0353+03	7.4206+03
26	1.7018+02	1.6026+01	7.0161+00	6.4877+03	1.0352+03	7.5229+03
27	1.7018+02	1.6051+01	6.9816+00	6.0409+03	1.0351+03	7.0759+03
28	1.4264+02	1.5475+01	5.9365+00	6.2192+03	1.0245+03	7.2437+03
29	1.4264+02	1.5478+01	5.9426+00	6.2004+03	1.0245+03	7.2249+03
30	1.4264+02	1.5464+01	5.9520+00	6.4356+03	1.0241+03	7.4598+03

LIQUID-LIQUID RUNS CORRECTED K FLOW

	707 NPE K2	405 DTW 1	406 DTW 2	408 QNA	418 QL	419 QL+QNA
31	1.6180+02	1.4967+01	6.1991+00	4.4543+03	1.0530+03	5.5073+03
32	1.6180+02	1.4955+01	6.2439+00	4.7326+03	1.0537+03	5.7864+03
33	1.6180+02	1.4990+01	6.2142+00	4.4538+03	1.0003+03	5.4541+03
34	1.7613+02	1.5046+01	6.7244+00	4.4865+03	1.0665+03	5.5530+03
35	1.7613+02	1.4968+01	6.7428+00	4.7388+03	1.0663+03	5.8051+03
36	1.7613+02	1.4898+01	6.6906+00	4.6868+03	1.0671+03	5.7539+03
37	2.0184+02	1.4915+01	7.2978+00	4.3869+03	1.0785+03	5.4654+03
38	2.0184+02	1.4807+01	7.3040+00	4.6132+03	1.0791+03	5.6923+03
39	2.0184+02	1.4834+01	7.2841+00	4.3995+03	1.0790+03	5.4785+03
40	2.3241+02	1.4908+01	7.9616+00	4.6268+03	1.0953+03	5.7221+03
41	2.3242+02	1.4915+01	7.9874+00	4.5768+03	1.0954+03	5.6722+03
42	2.3242+02	1.4992+01	7.9819+00	4.4267+03	1.0958+03	5.5225+03
43	2.5570+02	1.5065+01	8.3229+00	4.4091+03	1.1218+03	5.5309+03
44	2.5571+02	1.5038+01	8.3517+00	4.6714+03	1.1221+03	5.7935+03
45	2.5571+02	1.5080+01	8.3351+00	4.3966+03	1.1222+03	5.5188+03
46	2.7729+02	1.4876+01	8.5891+00	4.3742+03	1.1531+03	5.5273+03
47	2.7729+02	1.4929+01	8.5922+00	4.3368+03	1.1530+03	5.4898+03
48	2.7729+02	1.4890+01	8.5977+00	4.4743+03	1.1529+03	5.6272+03
49	3.0714+02	1.5881+01	9.4841+00	4.8534+03	1.1679+03	6.0212+03
50	3.0713+02	1.5900+01	9.4640+00	4.8909+03	1.1682+03	6.0592+03
51	3.0714+02	1.5865+01	9.4750+00	4.9536+03	1.1683+03	6.1219+03
52	3.3070+02	1.6124+01	9.8699+00	5.2450+03	1.1960+03	6.4410+03
53	3.3072+02	1.6191+01	9.9031+00	5.1069+03	1.1960+03	6.3028+03
54	3.3072+02	1.6170+01	9.8979+00	5.1189+03	1.1961+03	6.3150+03
55	3.4454+02	1.6305+01	1.0110+01	5.5287+03	1.2219+03	6.7507+03
56	3.4454+02	1.6201+01	1.0055+01	5.4429+03	1.2217+03	6.6646+03
57	3.4454+02	1.6230+01	1.0065+01	5.5532+03	1.2218+03	6.7749+03
58	3.4072+02	2.3473+01	1.4767+01	1.0591+04	1.2416+03	1.1832+04
59	3.4072+02	2.3439+01	1.4772+01	1.0542+04	1.2414+03	1.1784+04
60	3.4070+02	2.3466+01	1.4745+01	1.0591+04	1.2415+03	1.1833+04

LIQUID-LIQUID RUNS CORRECTED K FLOW

	707	405	406	408	418	419
	NPE K2	DTW 1	DTW 2	QNA	QL	QL+QNA
61	3.2336+02	2.2846+01	1.4193+01	1.0111+04	1.2392+03	1.1350+04
62	3.2335+02	2.2865+01	1.4177+01	1.0062+04	1.2392+03	1.1301+04
63	3.2335+02	2.2909+01	1.4196+01	9.9893+03	1.2388+03	1.1228+04
64	3.0115+02	2.2681+01	1.3746+01	1.0076+04	1.2267+03	1.1302+04
65	3.0116+02	2.2570+01	1.3724+01	9.9773+03	1.2271+03	1.1204+04
66	3.0116+02	2.2649+01	1.3746+01	1.0014+04	1.2267+03	1.1241+04
67	2.6917+02	2.2853+01	1.3284+01	1.0616+04	1.1929+03	1.1809+04
68	2.6916+02	2.2801+01	1.3252+01	1.0567+04	1.1926+03	1.1760+04
69	2.6915+02	2.2827+01	1.3254+01	1.0543+04	1.1917+03	1.1734+04
70	2.3812+02	2.1638+01	1.1923+01	8.5989+03	1.0905+03	9.6895+03
71	2.3815+02	2.1526+01	1.1941+01	8.1789+03	1.0906+03	9.2695+03
72	2.3813+02	2.1669+01	1.1962+01	8.4260+03	1.0907+03	9.5167+03
73	2.3758+02	2.2395+01	1.2186+01	1.0823+04	1.0571+03	1.1880+04
74	2.3758+02	2.2302+01	1.2161+01	1.0751+04	1.0571+03	1.1808+04
75	2.3757+02	2.2338+01	1.2161+01	1.0965+04	1.0569+03	1.2022+04
76	2.7845+02	2.2716+01	1.3208+01	1.1165+04	1.0604+03	1.2225+04
77	2.7847+02	2.2559+01	1.3157+01	1.0889+04	1.0604+03	1.1949+04
78	2.7846+02	2.2616+01	1.3180+01	1.1053+04	1.0605+03	1.2113+04
79	3.0399+02	2.2686+01	1.3689+01	1.0548+04	1.0722+03	1.1620+04
80	3.0399+02	2.2698+01	1.3737+01	1.0721+04	1.0725+03	1.1794+04
81	3.0400+02	2.2758+01	1.3745+01	1.0578+04	1.0726+03	1.1651+04
82	3.3513+02	2.3968+01	1.4882+01	1.1696+04	1.1105+03	1.2807+04
83	3.3512+02	2.4064+01	1.4891+01	1.1562+04	1.1104+03	1.2673+04
84	3.3524+02	2.4086+01	1.4925+01	1.1562+04	1.1103+03	1.2673+04
85	1.1516+02	8.4610+00	2.7907+00	2.1629+03	1.1525+03	3.3154+03
86	1.1517+02	8.4523+00	2.7982+00	1.8421+03	1.1523+03	2.9944+03
87	1.1517+02	8.4338+00	2.7900+00	1.9663+03	1.1524+03	3.1187+03
88	9.4049+01	7.5084+00	2.0142+00	1.8948+03	1.1569+03	3.0517+03
89	9.4051+01	7.5127+00	2.0336+00	1.9154+03	1.1570+03	3.0724+03
90	9.4053+01	7.5141+00	2.0390+00	1.9360+03	1.1570+03	3.0930+03

LIQUID-LIQUID RUNS CORRECTED K FLOW

	707	405	406	408	418	419
	NPE K2	DTW 1	DTW 2	QNA	QL	QL+QNA
91	8.0571+01	7.0999+00	1.6004+00	1.2972+03	1.1815+03	2.4787+03
92	8.0570+01	7.1107+00	1.6037+00	1.3600+03	1.1818+03	2.5418+03
93	8.0566+01	7.0991+00	1.5854+00	1.6948+03	1.1816+03	2.8763+03
94	1.5808+02	1.1828+01	4.1046+00	5.7942+03	7.5923+02	6.5535+03
95	1.5809+02	1.1866+01	4.1840+00	5.8565+03	7.5948+02	6.6159+03
96	1.5809+02	1.1849+01	4.1425+00	5.8237+03	7.5966+02	6.5833+03
97	1.6822+02	1.1764+01	4.2940+00	5.7329+03	1.3273+03	7.0602+03
98	1.9273+02	1.1702+01	4.5820+00	5.7100+03	1.3438+03	7.0538+03
99	2.1407+02	1.1854+01	4.9503+00	5.8261+03	1.3697+03	7.1958+03
100	2.1407+02	1.1846+01	4.9704+00	5.8473+03	1.3697+03	7.2170+03
101	2.1406+02	1.1846+01	4.9808+00	5.9027+03	1.3694+03	7.2720+03
102	2.4313+02	1.2024+01	5.1757+00	5.9497+03	1.3828+03	7.3326+03
103	2.4314+02	1.2049+01	5.1679+00	5.9368+03	1.3822+03	7.3190+03
104	2.4313+02	1.2061+01	5.1804+00	5.9612+03	1.3826+03	7.3438+03
105	2.5979+02	1.1629+01	4.9642+00	5.6316+03	1.4136+03	7.0452+03
106	2.5980+02	1.1674+01	5.0068+00	5.6710+03	1.4133+03	7.0843+03
107	2.5980+02	1.1739+01	4.9913+00	5.6967+03	1.4137+03	7.1105+03
108	2.9340+02	1.1935+01	5.0404+00	5.7825+03	1.4414+03	7.2239+03
109	2.9341+02	1.1969+01	5.0292+00	5.7779+03	1.4415+03	7.2195+03
110	2.9341+02	1.1955+01	5.0717+00	5.8305+03	1.4415+03	7.2720+03

LIQUID-LIQUID RUNS CORRECTED K FLOW

	422	442	443	444	445	446
	DQ PCT	TWI 1	TWO 1	DTK-W1	DTW-N1	HK1
1	1.3609+01	7.3777+02	7.1608+02	1.2717+01	2.5357+00	2.2575+03
2	1.6842+01	7.3780+02	7.1614+02	1.2656+01	2.2737+00	2.2649+03
3	1.4196+01	7.3772+02	7.1610+02	1.2615+01	2.4138+00	2.2683+03
4	1.5798+01	7.3632+02	7.1536+02	1.2184+01	2.1931+00	2.2766+03
5	1.3271+01	7.3614+02	7.1534+02	1.2149+01	2.4189+00	2.2650+03
6	1.5279+01	7.3609+02	7.1529+02	1.2174+01	2.2492+00	2.2610+03
7	1.2705+01	7.2529+02	7.0530+02	1.1907+01	2.2546+00	2.2167+03
8	1.4320+01	7.2522+02	7.0526+02	1.1925+01	2.1973+00	2.2106+03
9	1.6241+01	7.2526+02	7.0511+02	1.1918+01	2.0816+00	2.2333+03
10	1.3454+01	7.1797+02	6.9828+02	1.1888+01	2.1866+00	2.1853+03
11	1.5671+01	7.1796+02	6.9823+02	1.2015+01	2.1397+00	2.1661+03
12	1.5184+01	7.1787+02	6.9806+02	1.2013+01	2.0984+00	2.1749+03
13	1.8214+01	7.1922+02	7.0244+02	1.0355+01	1.7211+00	2.1396+03
14	2.0398+01	7.1931+02	7.0249+02	1.0324+01	1.7050+00	2.1498+03
15	2.1163+01	7.1930+02	7.0246+02	1.0336+01	1.6612+00	2.1506+03
16	1.7959+01	7.1854+02	7.0195+02	1.0432+01	1.8369+00	2.0994+03
17	2.0298+01	7.1864+02	7.0195+02	1.0450+01	1.6535+00	2.1076+03
18	1.6483+01	7.1854+02	7.0194+02	1.0470+01	1.8330+00	2.0925+03
19	2.1900+01	7.1688+02	7.0029+02	1.0721+01	1.5454+00	2.0416+03
20	1.7586+01	7.1689+02	7.0031+02	1.0610+01	1.8084+00	2.0618+03
21	1.9596+01	7.1687+02	7.0028+02	1.0753+01	1.6965+00	2.0353+03
22	1.7443+01	7.1443+02	6.9827+02	1.0896+01	1.8076+00	1.9550+03
23	1.6999+01	7.1441+02	6.9824+02	1.0820+01	1.8761+00	1.9712+03
24	1.7176+01	7.1439+02	6.9819+02	1.0812+01	1.7689+00	1.9763+03
25	1.7362+01	7.1197+02	6.9594+02	1.0986+01	1.7501+00	1.9223+03
26	1.6158+01	7.1195+02	6.9592+02	1.0996+01	1.7913+00	1.9213+03
27	2.1685+01	7.1200+02	6.9595+02	1.1001+01	1.5821+00	1.9236+03
28	1.7339+01	7.0712+02	6.9165+02	1.0867+01	1.6639+00	1.8759+03
29	1.7581+01	7.0721+02	6.9173+02	1.0809+01	1.7482+00	1.8865+03
30	1.4589+01	7.0714+02	6.9168+02	1.0807+01	1.8109+00	1.8850+03

LIQUID-LIQUID RUNS CORRECTED K FLOW

	422	442	443	444	445	446
	DQ PCT	TWI 1	TWO 1	DTK-W1	DTW-N1	HK1
31	3.5054+01	7.1604+02	7.0107+02	9.7388+00	9.7104-01	2.0273+03
32	3.1495+01	7.1603+02	7.0108+02	9.8988+00	1.0362+00	1.9931+03
33	3.5780+01	7.1609+02	7.0110+02	9.7979+00	9.5441-01	2.0183+03
34	3.4580+01	7.1994+02	7.0489+02	9.9568+00	1.1843+00	1.9946+03
35	3.1057+01	7.1989+02	7.0492+02	1.0010+01	1.3305+00	1.9738+03
36	3.1374+01	7.1983+02	7.0493+02	9.9698+00	1.2174+00	1.9724+03
37	3.5089+01	7.2379+02	7.0888+02	9.7112+00	1.2714+00	2.0286+03
38	3.1729+01	7.2378+02	7.0897+02	9.8014+00	1.3960+00	1.9953+03
39	3.4551+01	7.2376+02	7.0892+02	9.8217+00	1.2302+00	1.9949+03
40	3.2215+01	7.2992+02	7.1501+02	9.7116+00	1.4736+00	2.0294+03
41	3.2879+01	7.2999+02	7.1507+02	9.8119+00	1.4932+00	2.0097+03
42	3.5084+01	7.3009+02	7.1509+02	9.7560+00	1.3642+00	2.0317+03
43	3.5702+01	7.4044+02	7.2537+02	9.3725+00	1.3129+00	2.1285+03
44	3.2363+01	7.4052+02	7.2548+02	9.4392+00	1.4582+00	2.1095+03
45	3.5917+01	7.4059+02	7.2551+02	9.3734+00	1.3458+00	2.1304+03
46	3.5346+01	7.5209+02	7.3721+02	9.3902+00	1.4661+00	2.1015+03
47	3.6036+01	7.5213+02	7.3720+02	9.2787+00	1.4655+00	2.1344+03
48	3.4178+01	7.5207+02	7.3718+02	9.3476+00	1.5200+00	2.1131+03
49	3.4352+01	7.5821+02	7.4233+02	9.5206+00	1.4528+00	2.2148+03
50	3.3983+01	7.5825+02	7.4235+02	9.4122+00	1.4013+00	2.2431+03
51	3.3120+01	7.5831+02	7.4244+02	9.4806+00	1.4848+00	2.2219+03
52	3.1042+01	7.6784+02	7.5171+02	9.3622+00	1.5276+00	2.2898+03
53	3.2900+01	7.6790+02	7.5171+02	9.4884+00	1.4028+00	2.2688+03
54	3.2675+01	7.6793+02	7.5176+02	9.4804+00	1.4402+00	2.2677+03
55	2.8693+01	7.7782+02	7.6152+02	9.4184+00	1.5387+00	2.3052+03
56	2.9190+01	7.7779+02	7.6158+02	9.4233+00	1.5205+00	2.2892+03
57	2.8071+01	7.7784+02	7.6161+02	9.3586+00	1.5618+00	2.3092+03
58	1.1896+01	7.9172+02	7.6825+02	1.4380+01	3.2780+00	2.1769+03
59	1.2171+01	7.9172+02	7.6828+02	1.4436+01	3.3599+00	2.1653+03
60	1.1849+01	7.9166+02	7.6820+02	1.4239+01	3.3132+00	2.1977+03

LIQUID-LIQUID RUNS CORRECTED K FLOW

	422	442	443	444	445	446
	DQ PCT	TWI 1	TWO 1	DTK-W1	DTW-N1	HK1
61	1.3039+01	7.9004+02	7.6719+02	1.4495+01	3.3785+00	2.1014+03
62	1.3496+01	7.9002+02	7.6716+02	1.4425+01	3.2968+00	2.1135+03
63	1.4268+01	7.9005+02	7.6714+02	1.4391+01	3.3169+00	2.1225+03
64	1.2293+01	7.8510+02	7.6242+02	1.4583+01	3.4180+00	2.0723+03
65	1.2690+01	7.8515+02	7.6258+02	1.4667+01	3.5160+00	2.0503+03
66	1.2691+01	7.8521+02	7.6256+02	1.4594+01	3.4970+00	2.0678+03
67	8.0495+00	7.7307+02	7.5022+02	1.5081+01	3.5758+00	2.0154+03
68	8.2411+00	7.7294+02	7.5014+02	1.5053+01	3.5499+00	2.0146+03
69	8.5522+00	7.7280+02	7.4998+02	1.5041+01	3.5091+00	2.0184+03
70	2.0260+01	7.4466+02	7.2302+02	1.4966+01	2.7004+00	1.9149+03
71	2.3533+01	7.4452+02	7.2299+02	1.5405+01	2.6147+00	1.8507+03
72	2.1895+01	7.4456+02	7.2289+02	1.5248+01	2.5637+00	1.8822+03
73	4.3186+00	7.3406+02	7.1167+02	1.4909+01	3.4029+00	1.9861+03
74	4.5230+00	7.3397+02	7.1167+02	1.5014+01	3.3633+00	1.9641+03
75	2.7987+00	7.3403+02	7.1169+02	1.4816+01	3.4804+00	1.9935+03
76	3.4763+00	7.3539+02	7.1267+02	1.4356+01	3.3967+00	2.0925+03
77	5.1906+00	7.3538+02	7.1282+02	1.4463+01	3.3953+00	2.0628+03
78	4.0215+00	7.3539+02	7.1277+02	1.4429+01	3.4140+00	2.0729+03
79	9.1356+00	7.3927+02	7.1659+02	1.4577+01	3.1142+00	2.0595+03
80	7.7272+00	7.3936+02	7.1667+02	1.4553+01	3.3903+00	2.0639+03
81	9.1942+00	7.3944+02	7.1669+02	1.4558+01	3.2646+00	2.0686+03
82	5.4188+00	7.4963+02	7.2566+02	1.4409+01	3.4720+00	2.2045+03
83	6.8743+00	7.4968+02	7.2562+02	1.4275+01	3.3801+00	2.2341+03
84	6.9896+00	7.4982+02	7.2573+02	1.4372+01	3.4097+00	2.2211+03
85	3.3818+01	7.4297+02	7.3451+02	6.5500+00	1.2376+00	1.7118+03
86	4.0363+01	7.4308+02	7.3462+02	6.6708+00	1.1643+00	1.6792+03
87	3.7657+01	7.4310+02	7.3467+02	6.5529+00	1.2537+00	1.7056+03
88	3.4688+01	7.4199+02	7.3448+02	6.0609+00	1.1233+00	1.6415+03
89	3.4084+01	7.4204+02	7.3452+02	6.1147+00	1.1750+00	1.6280+03
90	3.3587+01	7.4209+02	7.3458+02	6.1314+00	1.1879+00	1.6239+03

LIQUID-LIQUID RUNS CORRECTED K FLOW

	422 DQ PCT	442 TWI 1	443 TWO 1	444 DTK-W1	445 DTW-N1	446 HK1
91	4.7202+01	7.4678+02	7.3968+02	6.4921+00	6.3832-01	1.4502+03
92	4.5896+01	7.4683+02	7.3972+02	6.4317+00	7.1481-01	1.4660+03
93	3.8688+01	7.4681+02	7.3971+02	6.2136+00	8.2788-01	1.5151+03
94	9.0695+00	7.8994+02	7.7811+02	1.2251+01	2.9981+00	1.2884+03
95	7.8028+00	7.8996+02	7.7810+02	1.2435+01	3.2779+00	1.2733+03
96	8.4969+00	7.8996+02	7.7811+02	1.2376+01	3.0908+00	1.2775+03
97	8.4935-01	7.9992+02	7.8815+02	1.2356+01	3.2248+00	1.2723+03
98	-4.3479-01	8.0523+02	7.9353+02	1.1750+01	3.7257+00	1.3320+03
99	-2.0906+00	8.1389+02	8.0203+02	1.1643+01	4.4736+00	1.3633+03
100	-2.7610+00	8.1389+02	8.0205+02	1.1687+01	4.5719+00	1.3573+03
101	-4.0460+00	8.1381+02	8.0196+02	1.1648+01	4.6780+00	1.3618+03
102	-2.6972+00	8.1798+02	8.0595+02	1.1038+01	4.4700+00	1.4596+03
103	-2.0282+00	8.1804+02	8.0599+02	1.1071+01	4.3533+00	1.4581+03
104	-2.4418+00	8.1806+02	8.0600+02	1.1028+01	4.4569+00	1.4654+03
105	2.4621-01	8.2766+02	8.1603+02	1.1056+01	3.8788+00	1.4113+03
106	-1.7424-01	8.2778+02	8.1611+02	1.1076+01	4.0639+00	1.4142+03
107	2.3949-01	8.2782+02	8.1608+02	1.1006+01	3.9454+00	1.4311+03
108	1.6315+00	8.3684+02	8.2490+02	1.0243+01	3.5801+00	1.5654+03
109	2.2942+00	8.3688+02	8.2491+02	1.0264+01	3.4470+00	1.5666+03
110	6.6334-01	8.3687+02	8.2491+02	1.0246+01	3.7343+00	1.5676+03

LIQUID-LIQUID RUNS CORRECTED K FLOW

	448	449	453	455	464	465
	Q/A01	HNA1	NUK1	NUNA1	TWI 2	TWO 2
1	1.0444+04	4.1187+03	5.0774+00	6.1145+00	7.3240+02	7.1895+02
2	1.0428+04	4.5866+03	5.0940+00	6.8099+00	7.3245+02	7.1908+02
3	1.0410+04	4.3126+03	5.1012+00	6.4026+00	7.3234+02	7.1896+02
4	1.0091+04	4.6014+03	5.1167+00	6.8301+00	7.3098+02	7.1821+02
5	1.0011+04	4.1385+03	5.0902+00	6.1425+00	7.3079+02	7.1806+02
6	1.0014+04	4.4522+03	5.0812+00	6.6084+00	7.3071+02	7.1800+02
7	9.6019+03	4.2588+03	4.9621+00	6.2991+00	7.1981+02	7.0790+02
8	9.5907+03	4.3649+03	4.9486+00	6.4560+00	7.1971+02	7.0782+02
9	9.6827+03	4.6516+03	4.9994+00	6.8800+00	7.1973+02	7.0777+02
10	9.4512+03	4.3223+03	4.8793+00	6.3772+00	7.1210+02	7.0076+02
11	9.4683+03	4.4251+03	4.8367+00	6.5290+00	7.1208+02	7.0070+02
12	9.5049+03	4.5295+03	4.8562+00	6.6827+00	7.1205+02	7.0064+02
13	8.0599+03	4.6831+03	4.7768+00	6.9208+00	7.1371+02	7.0444+02
14	8.0742+03	4.7356+03	4.7996+00	6.9987+00	7.1378+02	7.0451+02
15	8.0865+03	4.8677+03	4.8015+00	7.1940+00	7.1376+02	7.0448+02
16	7.9669+03	4.3370+03	4.6859+00	6.4081+00	7.1269+02	7.0384+02
17	8.0124+03	4.8456+03	4.7046+00	7.1600+00	7.1276+02	7.0390+02
18	7.9701+03	4.3482+03	4.6708+00	6.4246+00	7.1267+02	7.0380+02
19	7.9627+03	5.1527+03	4.5548+00	7.6096+00	7.1042+02	7.0208+02
20	7.9584+03	4.4009+03	4.5998+00	6.4987+00	7.1044+02	7.0207+02
21	7.9618+03	4.6931+03	4.5409+00	6.9305+00	7.1043+02	7.0205+02
22	7.7496+03	4.2873+03	4.3581+00	6.3266+00	7.0736+02	6.9982+02
23	7.7593+03	4.1358+03	4.3941+00	6.1027+00	7.0729+02	6.9975+02
24	7.7733+03	4.3944+03	4.4054+00	6.4844+00	7.0730+02	6.9977+02
25	7.6830+03	4.3901+03	4.2817+00	6.4730+00	7.0445+02	6.9745+02
26	7.6860+03	4.2907+03	4.2795+00	6.3263+00	7.0436+02	6.9734+02
27	7.6982+03	4.8657+03	4.2846+00	7.1747+00	7.0441+02	6.9743+02
28	7.4159+03	4.4570+03	4.1711+00	6.5619+00	6.9886+02	6.9292+02
29	7.4178+03	4.2430+03	4.1946+00	6.2468+00	6.9887+02	6.9293+02
30	7.4108+03	4.0923+03	4.1912+00	6.0247+00	6.9878+02	6.9282+02

LIQUID-LIQUID RUNS CORRECTED K FLOW

	448	449	453	455	464	465
	Q/A01	HNA1	NUK1	NUNA1	TWI 2	TWO 2
31	7.1826+03	7.3969+03	4.5201+00	1.0929+01	7.0838+02	7.0218+02
32	7.1773+03	6.9265+03	4.4439+00	1.0234+01	7.0830+02	7.0206+02
33	7.1940+03	7.5376+03	4.5001+00	1.1137+01	7.0842+02	7.0220+02
34	7.2250+03	6.1008+03	4.4536+00	9.0255+00	7.1272+02	7.0599+02
35	7.1878+03	5.4023+03	4.4071+00	7.9919+00	7.1270+02	7.0596+02
36	7.1539+03	5.8762+03	4.4039+00	8.6933+00	7.1263+02	7.0594+02
37	7.1668+03	5.6371+03	4.5352+00	8.3511+00	7.1741+02	7.1011+02
38	7.1147+03	5.0963+03	4.4609+00	7.5499+00	7.1727+02	7.0996+02
39	7.1278+03	5.7940+03	4.4599+00	8.5837+00	7.1737+02	7.1009+02
40	7.1699+03	4.8656+03	4.5468+00	7.2234+00	7.2417+02	7.1620+02
41	7.1737+03	4.8044+03	4.5030+00	7.1325+00	7.2418+02	7.1619+02
42	7.2108+03	5.2858+03	4.5523+00	7.8476+00	7.2428+02	7.1629+02
43	7.2575+03	5.5279+03	4.7860+00	8.2373+00	7.3513+02	7.2681+02
44	7.2440+03	4.9678+03	4.7436+00	7.4026+00	7.3519+02	7.2684+02
45	7.2646+03	5.3981+03	4.7905+00	8.0442+00	7.3531+02	7.2697+02
46	7.1790+03	4.8967+03	4.7450+00	7.3272+00	7.4719+02	7.3860+02
47	7.2048+03	4.9162+03	4.8192+00	7.3564+00	7.4717+02	7.3858+02
48	7.1859+03	4.7276+03	4.7711+00	7.0740+00	7.4711+02	7.3851+02
49	7.6710+03	5.2801+03	5.0119+00	7.9155+00	7.5342+02	7.4393+02
50	7.6805+03	5.4811+03	5.0757+00	8.2171+00	7.5341+02	7.4394+02
51	7.6633+03	5.1613+03	5.0280+00	7.7376+00	7.5344+02	7.4397+02
52	7.7989+03	5.1054+03	5.1992+00	7.6792+00	7.6326+02	7.5339+02
53	7.8314+03	5.5825+03	5.1517+00	8.3971+00	7.6329+02	7.5338+02
54	7.8212+03	5.4307+03	5.1494+00	8.1688+00	7.6336+02	7.5346+02
55	7.8984+03	5.1333+03	5.2529+00	7.7469+00	7.7331+02	7.6320+02
56	7.8477+03	5.1614+03	5.2164+00	7.7896+00	7.7336+02	7.6331+02
57	7.8619+03	5.0339+03	5.2620+00	7.5971+00	7.7336+02	7.6329+02
58	1.1388+04	3.4742+03	4.9945+00	5.2520+00	7.8502+02	7.7026+02
59	1.1371+04	3.3844+03	4.9679+00	5.1161+00	7.8500+02	7.7022+02
60	1.1385+04	3.4361+03	5.0419+00	5.1942+00	7.8490+02	7.7015+02

LIQUID-LIQUID RUNS CORRECTED K FLOW

	448	449	453	455	464	465
	Q/A01	HNA1	NUK1	NUNA1	TWI 2	TWO 2
61	1.1082+04	3.2801+03	4.8185+00	4.9565+00	7.8318+02	7.6899+02
62	1.1091+04	3.3642+03	4.8460+00	5.0837+00	7.8321+02	7.6904+02
63	1.1112+04	3.3502+03	4.8666+00	5.0625+00	7.8317+02	7.6897+02
64	1.0994+04	3.2164+03	4.7434+00	4.8525+00	7.7789+02	7.6414+02
65	1.0940+04	3.1114+03	4.6933+00	4.6942+00	7.7792+02	7.6419+02
66	1.0978+04	3.1393+03	4.7334+00	4.7363+00	7.7794+02	7.6420+02
67	1.1057+04	3.0923+03	4.5941+00	4.6452+00	7.6515+02	7.5187+02
68	1.1032+04	3.1078+03	4.5920+00	4.6685+00	7.6502+02	7.5177+02
69	1.1045+04	3.1474+03	4.6005+00	4.7277+00	7.6487+02	7.5162+02
70	1.0426+04	3.8609+03	4.3207+00	5.7456+00	7.3628+02	7.2436+02
71	1.0372+04	3.9668+03	4.1764+00	5.9033+00	7.3632+02	7.2438+02
72	1.0441+04	4.0727+03	4.2473+00	6.0607+00	7.3627+02	7.2431+02
73	1.0773+04	3.1657+03	4.4646+00	4.6910+00	7.2577+02	7.1359+02
74	1.0727+04	3.1896+03	4.4150+00	4.7264+00	7.2573+02	7.1357+02
75	1.0745+04	3.0873+03	4.4809+00	4.5747+00	7.2572+02	7.1356+02
76	1.0929+04	3.2174+03	4.7051+00	4.7693+00	7.2798+02	7.1477+02
77	1.0854+04	3.1967+03	4.6385+00	4.7388+00	7.3068+02	7.1752+02
78	1.0881+04	3.1873+03	4.6610+00	4.7247+00	7.2805+02	7.1487+02
79	1.0921+04	3.5069+03	4.6375+00	5.2061+00	7.3241+02	7.1872+02
80	1.0927+04	3.2230+03	4.6476+00	4.7843+00	7.3443+02	7.2069+02
81	1.0956+04	3.3561+03	4.6583+00	4.9821+00	7.3268+02	7.1894+02
82	1.1555+04	3.3282+03	4.9820+00	4.9562+00	7.4304+02	7.2815+02
83	1.1602+04	3.4325+03	5.0488+00	5.1115+00	7.4300+02	7.2811+02
84	1.1613+04	3.4058+03	5.0198+00	5.0720+00	7.4316+02	7.2823+02
85	4.0789+03	3.2958+03	3.8486+00	4.9274+00	7.3717+02	7.3438+02
86	4.0750+03	3.5000+03	3.7756+00	5.2329+00	7.3724+02	7.3445+02
87	4.0659+03	3.2433+03	3.8349+00	4.8491+00	7.3727+02	7.3448+02
88	3.6193+03	3.2220+03	3.6887+00	4.8172+00	7.3618+02	7.3417+02
89	3.6215+03	3.0822+03	3.6585+00	4.6081+00	7.3623+02	7.3420+02
90	3.6222+03	3.0491+03	3.6493+00	4.5588+00	7.3627+02	7.3423+02

LIQUID-LIQUID RUNS CORRECTED K FLOW

	448	449	453	455	464	465
	Q/A01	HNA1	NUK1	NUNA1	TWI 2	TWO 2
91	3.4250+03	5.3656+03	3.2648+00	8.0384+00	7.4097+02	7.3937+02
92	3.4302+03	4.7988+03	3.3005+00	7.1891+00	7.4098+02	7.3937+02
93	3.4247+03	4.1368+03	3.4106+00	6.1971+00	7.4099+02	7.3941+02
94	5.7419+03	1.9152+03	2.9517+00	2.9051+00	7.8719+02	7.8308+02
95	5.7603+03	1.7573+03	2.9175+00	2.6653+00	7.8720+02	7.8301+02
96	5.7519+03	1.8610+03	2.9270+00	2.8228+00	7.8722+02	7.8308+02
97	5.7190+03	1.7734+03	2.9255+00	2.6990+00	7.9741+02	7.9311+02
98	5.6935+03	1.5282+03	3.0679+00	2.3296+00	8.0334+02	7.9876+02
99	5.7748+03	1.2909+03	3.1500+00	1.9731+00	8.1233+02	8.0738+02
100	5.7707+03	1.2622+03	3.1361+00	1.9292+00	8.1232+02	8.0735+02
101	5.7706+03	1.2336+03	3.1463+00	1.8853+00	8.1226+02	8.0728+02
102	5.8612+03	1.3112+03	3.3767+00	2.0069+00	8.1683+02	8.1165+02
103	5.8728+03	1.3491+03	3.3733+00	2.0648+00	8.1685+02	8.1168+02
104	5.8791+03	1.3191+03	3.3903+00	2.0190+00	8.1684+02	8.1166+02
105	5.6763+03	1.4634+03	3.2765+00	2.2480+00	8.2686+02	8.2190+02
106	5.6985+03	1.4022+03	3.2834+00	2.1539+00	8.2691+02	8.2191+02
107	5.7302+03	1.4524+03	3.3226+00	2.2310+00	8.2699+02	8.2200+02
108	5.8334+03	1.6294+03	3.6455+00	2.5108+00	8.3626+02	8.3122+02
109	5.8500+03	1.6972+03	3.6484+00	2.6153+00	8.3634+02	8.3131+02
110	5.8434+03	1.5648+03	3.6507+00	2.4111+00	8.3631+02	8.3123+02

LIQUID-LIQUID RUNS CORRECTED K FLOW

	466 DTK-W2	467 DTW-N2	468 HK2	469 Q/AO2	470 HNA2	472 NUK 2
1	6.8818+00	2.5574+00	2.5841+03	6.4695+03	2.5297+03	5.7890+00
2	6.8378+00	2.3654+00	2.5866+03	6.4345+03	2.7202+03	5.7946+00
3	6.8422+00	2.4380+00	2.5847+03	6.4338+03	2.6390+03	5.7901+00
4	6.4364+00	2.3115+00	2.6245+03	6.1455+03	2.6587+03	5.8757+00
5	6.4828+00	2.4190+00	2.5961+03	6.1226+03	2.5311+03	5.8116+00
6	6.5468+00	2.2476+00	2.5661+03	6.1117+03	2.7192+03	5.7445+00
7	6.1606+00	2.2661+00	2.5517+03	5.7188+03	2.5236+03	5.6896+00
8	6.2247+00	2.1756+00	2.5216+03	5.7102+03	2.6246+03	5.6224+00
9	6.1512+00	2.1434+00	2.5661+03	5.7424+03	2.6791+03	5.7216+00
10	5.9321+00	2.1653+00	2.5221+03	5.4428+03	2.5137+03	5.6079+00
11	6.0546+00	2.0963+00	2.4777+03	5.4575+03	2.6034+03	5.5094+00
12	5.9501+00	2.1631+00	2.5270+03	5.4699+03	2.5287+03	5.6187+00
13	5.0291+00	1.6306+00	2.4316+03	4.4489+03	2.7283+03	5.4082+00
14	5.0010+00	1.6237+00	2.4462+03	4.4505+03	2.7409+03	5.4406+00
15	5.0173+00	1.5828+00	2.4394+03	4.4526+03	2.8131+03	5.4256+00
16	4.8544+00	1.6819+00	2.4055+03	4.2482+03	2.5258+03	5.3479+00
17	4.8548+00	1.5601+00	2.4066+03	4.2505+03	2.7244+03	5.3505+00
18	4.9114+00	1.6472+00	2.3801+03	4.2526+03	2.5817+03	5.2913+00
19	4.7995+00	1.3570+00	2.2911+03	4.0004+03	2.9480+03	5.0894+00
20	4.6677+00	1.5887+00	2.3634+03	4.0133+03	2.5262+03	5.2498+00
21	4.7934+00	1.4822+00	2.3038+03	4.0174+03	2.7104+03	5.1176+00
22	4.4440+00	1.4739+00	2.2351+03	3.6135+03	2.4517+03	4.9591+00
23	4.4108+00	1.4998+00	2.2534+03	3.6158+03	2.4109+03	4.9994+00
24	4.3732+00	1.4619+00	2.2685+03	3.6090+03	2.4687+03	5.0328+00
25	4.1171+00	1.4414+00	2.2409+03	3.3564+03	2.3286+03	4.9663+00
26	4.1884+00	1.3997+00	2.2065+03	3.3621+03	2.4021+03	4.8900+00
27	4.2097+00	1.2532+00	2.1846+03	3.3457+03	2.6696+03	4.8416+00
28	3.5020+00	1.2963+00	2.2312+03	2.8427+03	2.1929+03	4.9342+00
29	3.5046+00	1.3075+00	2.2319+03	2.8456+03	2.1763+03	4.9357+00
30	3.5273+00	1.3201+00	2.2210+03	2.8500+03	2.1589+03	4.9114+00

LIQUID-LIQUID RUNS CORRECTED K FLOW

	466 DTK-W2	467 DTW-N2	468 HK2	469 Q/AO2	470 HNA2	472 NUK 2
31	3.5615+00	8.6631-01	2.2944+03	2.9727+03	3.4315+03	5.0908+00
32	3.7570+00	7.9965-01	2.1907+03	2.9941+03	3.7443+03	4.8609+00
33	3.6104+00	8.3861-01	2.2688+03	2.9799+03	3.5534+03	5.0342+00
34	3.9484+00	1.0222+00	2.2464+03	3.2267+03	3.1566+03	4.9925+00
35	3.9995+00	1.0999+00	2.2236+03	3.2354+03	2.9414+03	4.9420+00
36	4.0451+00	9.6999-01	2.1815+03	3.2103+03	3.3097+03	4.8484+00
37	4.1635+00	1.2015+00	2.3135+03	3.5042+03	2.9165+03	5.1505+00
38	4.4220+00	1.0921+00	2.1800+03	3.5070+03	3.2112+03	4.8536+00
39	4.3201+00	1.0978+00	2.2254+03	3.4975+03	3.1860+03	4.9546+00
40	4.6631+00	1.3012+00	2.2557+03	3.8266+03	2.9408+03	5.0346+00
41	4.7990+00	1.2457+00	2.1990+03	3.8391+03	3.0819+03	4.9083+00
42	4.7161+00	1.1950+00	2.2361+03	3.8364+03	3.2105+03	4.9912+00
43	4.5501+00	1.3447+00	2.4207+03	4.0070+03	2.9800+03	5.4237+00
44	4.6381+00	1.4057+00	2.3830+03	4.0209+03	2.8603+03	5.3394+00
45	4.5173+00	1.3991+00	2.4419+03	4.0130+03	2.8682+03	5.4715+00
46	4.8217+00	1.4386+00	2.3618+03	4.1428+03	2.8798+03	5.3148+00
47	4.7475+00	1.4280+00	2.3996+03	4.1443+03	2.9022+03	5.3996+00
48	4.8359+00	1.4306+00	2.3572+03	4.1469+03	2.8986+03	5.3042+00
49	5.0178+00	1.5264+00	2.5082+03	4.5785+03	2.9996+03	5.6570+00
50	4.9617+00	1.4651+00	2.5311+03	4.5688+03	3.1184+03	5.7087+00
51	5.0610+00	1.4785+00	2.4844+03	4.5741+03	3.0937+03	5.6034+00
52	5.0335+00	1.6243+00	2.6058+03	4.7717+03	2.9376+03	5.8978+00
53	5.1561+00	1.4972+00	2.5524+03	4.7877+03	3.1977+03	5.7773+00
54	5.1216+00	1.5550+00	2.5683+03	4.7852+03	3.0773+03	5.8133+00
55	5.1901+00	1.5942+00	2.5923+03	4.8945+03	3.0701+03	5.8886+00
56	5.1549+00	1.6283+00	2.5958+03	4.8680+03	2.9895+03	5.8967+00
57	5.1415+00	1.6221+00	2.6053+03	4.8730+03	3.0042+03	5.9182+00
58	8.1773+00	2.9097+00	2.4063+03	7.1583+03	2.4601+03	5.4950+00
59	8.2623+00	2.9324+00	2.3824+03	7.1609+03	2.4420+03	5.4406+00
60	8.1148+00	2.8933+00	2.4213+03	7.1479+03	2.4705+03	5.5289+00

LIQUID-LIQUID RUNS CORRECTED K FLOW

	466	467	468	469	470	472
	DTK-W2	DTW-N2	HK2	Q/AO2	HNA2	NUK 2
61	8.2096+00	2.8736+00	2.3032+03	6.8788+03	2.3938+03	5.2562+00
62	8.0930+00	2.8746+00	2.3338+03	6.8711+03	2.3903+03	5.3259+00
63	8.1142+00	2.8390+00	2.3308+03	6.8804+03	2.4235+03	5.3191+00
64	7.9853+00	2.9037+00	2.2917+03	6.6572+03	2.2927+03	5.2195+00
65	8.1315+00	2.9043+00	2.2469+03	6.6467+03	2.2886+03	5.1178+00
66	8.0525+00	2.9062+00	2.2725+03	6.6573+03	2.2907+03	5.1762+00
67	7.8138+00	3.0094+00	2.2591+03	6.4217+03	2.1339+03	5.1216+00
68	7.8217+00	2.9685+00	2.2514+03	6.4063+03	2.1581+03	5.1040+00
69	7.8171+00	2.9328+00	2.2531+03	6.4073+03	2.1847+03	5.1075+00
70	7.7118+00	2.0005+00	2.0456+03	5.7389+03	2.8687+03	4.5902+00
71	8.0017+00	1.9719+00	1.9744+03	5.7476+03	2.9148+03	4.4310+00
72	7.8629+00	1.9463+00	2.0128+03	5.7576+03	2.9582+03	4.5168+00
73	7.1601+00	2.7824+00	2.2482+03	5.8561+03	2.1047+03	5.0251+00
74	7.2632+00	2.7356+00	2.2116+03	5.8439+03	2.1362+03	4.9436+00
75	7.1245+00	2.8141+00	2.2547+03	5.8439+03	2.0766+03	5.0395+00
76	7.4477+00	2.8531+00	2.3431+03	6.3486+03	2.2251+03	5.2420+00
77	4.9333+00	5.4598+00	3.5239+03	6.3243+03	1.1583+03	7.8839+00
78	7.4962+00	2.8795+00	2.3231+03	6.3352+03	2.2001+03	5.1973+00
79	8.0904+00	2.5607+00	2.2369+03	6.5837+03	2.5711+03	5.0132+00
80	6.1137+00	4.7235+00	2.9706+03	6.6071+03	1.3988+03	6.6578+00
81	7.9245+00	2.8178+00	2.2932+03	6.6109+03	2.3461+03	5.1395+00
82	7.9713+00	3.1085+00	2.4720+03	7.1687+03	2.3061+03	5.5609+00
83	7.8965+00	3.0058+00	2.4970+03	7.1731+03	2.3864+03	5.6168+00
84	7.9548+00	3.0405+00	2.4844+03	7.1896+03	2.3646+03	5.5888+00
85	2.2249+00	3.4061-01	1.6612+03	1.3446+03	3.9475+03	3.7215+00
86	2.3680+00	2.2259-01	1.5650+03	1.3482+03	6.0571+03	3.5064+00
87	2.2753+00	3.0395-01	1.6240+03	1.3442+03	4.4226+03	3.6384+00
88	1.7444+00	1.8068-01	1.5292+03	9.7039+02	5.3708+03	3.4240+00
89	1.7484+00	2.2250-01	1.5403+03	9.7973+02	4.4032+03	3.4490+00
90	1.7760+00	2.0785-01	1.5204+03	9.8235+02	4.7263+03	3.4045+00

LIQUID-LIQUID RUNS CORRECTED K FLOW

	466	467	468	469	470	472
	DTK-W2	DTW-N2	HK2	Q/AO2	HNA2	NUK 2
91	1.8211+00	-2.1560-01	1.1647+03	7.7161+02	-3.5789+03	2.6123+00
92	1.7884+00	-1.7833-01	1.1885+03	7.7321+02	-4.3358+03	2.6657+00
93	1.5913+00	-2.0584-02	1.3204+03	7.6438+02	-3.7134+04	2.9614+00
94	4.1927+00	1.0977+00	1.3062+03	1.9923+03	1.8150+03	2.9809+00
95	4.2861+00	1.2529+00	1.3024+03	2.0308+03	1.6209+03	2.9724+00
96	4.2524+00	1.1536+00	1.2997+03	2.0106+03	1.7429+03	2.9662+00
97	4.4969+00	1.1893+00	1.2759+03	2.0873+03	1.7550+03	2.9229+00
98	4.3431+00	1.7159+00	1.4109+03	2.2292+03	1.2991+03	3.2388+00
99	4.4494+00	2.2809+00	1.4898+03	2.4115+03	1.0573+03	3.4313+00
100	4.4923+00	2.3296+00	1.4816+03	2.4213+03	1.0394+03	3.4123+00
101	4.4265+00	2.4380+00	1.5067+03	2.4263+03	9.9520+02	3.4701+00
102	4.2516+00	2.4241+00	1.6312+03	2.5230+03	1.0408+03	3.7627+00
103	4.3206+00	2.2962+00	1.6027+03	2.5191+03	1.0971+03	3.6972+00
104	4.2880+00	2.3631+00	1.6188+03	2.5252+03	1.0686+03	3.7342+00
105	4.6531+00	1.7236+00	1.4316+03	2.4234+03	1.4060+03	3.3150+00
106	4.7073+00	1.7869+00	1.4273+03	2.4442+03	1.3679+03	3.3050+00
107	4.5855+00	1.7728+00	1.4607+03	2.4366+03	1.3744+03	3.3823+00
108	4.2823+00	1.5570+00	1.5816+03	2.4639+03	1.5825+03	3.6743+00
109	4.2557+00	1.5072+00	1.5879+03	2.4585+03	1.6312+03	3.6891+00
110	4.2480+00	1.6840+00	1.6042+03	2.4791+03	1.4721+03	3.7269+00

LIQUID-LIQUID RUNS CORRECTED K FLOW

	474	487	490
	NUNA 2	HKOMIN	NUKMIN
1	3.7593+00	1.8831+03	4.2269+00
2	4.0429+00	1.9209+03	4.3118+00
3	3.9220+00	1.9048+03	4.2755+00
4	3.9503+00	1.9302+03	4.3297+00
5	3.7604+00	1.8898+03	4.2387+00
6	4.0401+00	1.9094+03	4.2826+00
7	3.7360+00	1.8646+03	4.1658+00
8	3.8855+00	1.8676+03	4.1725+00
9	3.9661+00	1.9021+03	4.2495+00
10	3.7120+00	1.8467+03	4.1148+00
11	3.8446+00	1.8396+03	4.0990+00
12	3.7341+00	1.8524+03	4.1273+00
13	4.0350+00	1.8355+03	4.0900+00
14	4.0538+00	1.8459+03	4.1132+00
15	4.1605+00	1.8536+03	4.1305+00
16	3.7346+00	1.7858+03	3.9780+00
17	4.0286+00	1.8205+03	4.0556+00
18	3.8174+00	1.7815+03	3.9686+00
19	4.3567+00	1.7853+03	3.9743+00
20	3.7330+00	1.7624+03	3.9233+00
21	4.0054+00	1.7588+03	3.9155+00
22	3.6202+00	1.6776+03	3.7310+00
23	3.5599+00	1.6808+03	3.7378+00
24	3.6452+00	1.6993+03	3.7789+00
25	3.4356+00	1.6590+03	3.6859+00
26	3.5440+00	1.6530+03	3.6726+00
27	3.9390+00	1.6826+03	3.7384+00
28	2.2303+00	1.6276+03	3.6092+00
29	3.2060+00	1.6246+03	3.6026+00
30	3.1801+00	1.6153+03	3.5818+00

LIQUID-LIQUID RUNS CORRECTED K FLOW

	474 NUNA 2	487 HKOMIN	490 NUKMIN
31	5.0722+00	1.8445+03	4.1025+00
32	5.5345+00	1.8052+03	4.0153+00
33	5.2526+00	1.8401+03	4.0930+00
34	4.6720+00	1.7835+03	3.9730+00
35	4.3534+00	1.7431+03	3.8831+00
36	4.8985+00	1.7587+03	3.9177+00
37	4.3227+00	1.7946+03	4.0036+00
38	4.7594+00	1.7474+03	3.8985+00
39	4.7223+00	1.7737+03	3.9571+00
40	4.3680+00	1.7628+03	3.9420+00
41	4.5775+00	1.7450+03	3.9025+00
42	4.7689+00	1.7832+03	3.9880+00
43	4.4428+00	1.8677+03	4.1922+00
44	4.2644+00	1.8280+03	4.1032+00
45	4.2763+00	1.8637+03	4.1833+00
46	4.3115+00	1.8184+03	4.0988+00
47	4.3449+00	1.8440+03	4.1564+00
48	4.3395+00	1.8183+03	4.0985+00
49	4.4992+00	1.9224+03	4.3429+00
50	4.6775+00	1.9533+03	4.4126+00
51	4.6404+00	1.9218+03	4.3419+00
52	4.4210+00	1.9693+03	4.4644+00
53	4.8127+00	1.9773+03	4.4827+00
54	4.6315+00	1.9694+03	4.4648+00
55	4.6358+00	1.9823+03	4.5101+00
56	4.5142+00	1.9719+03	4.4864+00
57	4.5364+00	1.9797+03	4.5041+00
58	3.7219+00	1.7738+03	4.0601+00
59	3.6945+00	1.7574+03	4.0227+00
60	3.7375+00	1.7839+03	4.0830+00

LIQUID-LIQUID RUNS CORRECTED K FLOW

	474 NUNA 2	487 HKOMIN	490 NUKMIN
61	3.6200+00	1.7051+03	3.9006+00
62	3.6149+00	1.7212+03	3.9372+00
63	3.6650+00	1.7258+03	3.9477+00
64	3.4615+00	1.6797+03	3.8352+00
65	3.4554+00	1.6547+03	3.7784+00
66	3.4585+00	1.6690+03	3.8110+00
67	3.2081+00	1.6300+03	3.7056+00
68	3.2444+00	1.6311+03	3.7078+00
69	3.2843+00	1.6375+03	3.7221+00
70	4.2722+00	1.6232+03	3.6525+00
71	4.3409+00	1.5831+03	3.5627+00
72	4.4054+00	1.6124+03	3.6283+00
73	3.1215+00	1.6180+03	3.6269+00
74	3.1683+00	1.6056+03	3.5990+00
75	3.0799+00	1.6153+03	3.6206+00
76	3.3014+00	1.6931+03	3.7974+00
77	1.7187+00	1.6717+03	3.7494+00
78	3.2644+00	1.6773+03	3.7621+00
79	3.8205+00	1.6980+03	3.8146+00
80	2.0784+00	1.6749+03	3.7627+00
81	3.4861+00	1.6907+03	3.7982+00
82	3.4377+00	1.7775+03	4.0077+00
83	3.5574+00	1.8075+03	4.0752+00
84	3.5249+00	1.7963+03	4.0503+00
85	5.9033+00	1.4402+03	3.2322+00
86	9.0588+00	1.4301+03	3.2098+00
87	6.6142+00	1.4321+03	3.2143+00
88	8.0316+00	1.3852+03	3.1073+00
89	6.5846+00	1.3660+03	3.0642+00
90	7.0679+00	1.3607+03	3.0524+00

LIQUID-LIQUID RUNS CORRECTED K FLOW

	474 NUNA 2	487 HKOMIN	490 NUKMIN
91	-5.3627+00	1.3207+03	2.9678+00
92	-6.4968+00	1.3197+03	2.9656+00
93	-5.5640+01	1.3373+03	3.0049+00
94	2.7595+00	1.0351+03	2.3669+00
95	2.4643+00	1.0078+03	2.3044+00
96	2.6498+00	1.0223+03	2.3377+00
97	2.6774+00	1.0090+03	2.3158+00
98	1.9853+00	1.0113+03	2.3255+00
99	1.6202+00	9.8491+02	2.2720+00
100	1.5927+00	9.7563+02	2.2506+00
101	1.5249+00	9.7158+02	2.2412+00
102	1.5971+00	1.0389+03	2.3999+00
103	1.6837+00	1.0465+03	2.4177+00
104	1.6399+00	1.0436+03	2.4110+00
105	2.1657+00	1.0447+03	2.4222+00
106	2.1069+00	1.0346+03	2.3989+00
107	2.1171+00	1.0534+03	2.4426+00
108	2.4456+00	1.1599+03	2.6980+00
109	2.5209+00	1.1727+03	2.7278+00
110	2.2749+00	1.1489+03	2.6722+00

TABLE 2: CONDENSING DATA REDUCTION
(Part 1. List of Symbols)

Column	Symbol	Identification
113-149	TCN	Temperature of thermocouple N, ^{o}F
161-185	TCNC	Corrected temperature of thermocouple N, ^{o}F
196	TKI	Inlet potassium temperature, ^{o}F
198	TKO	Outlet potassium temperature, ^{o}F
201	TNAO	Outlet sodium temperature, ^{o}F
204	TNAI	Inlet sodium temperature, ^{o}F
205	DTNA	Sodium temperature increase, ^{o}F
214	WNA	Sodium flow rate, lb/hr
216	TNAM	Sodium mean temperature, ^{o}F
217	CPNA	Sodium specific heat, Btu/lb - ^{o}F
219	QNA	Sodium heat gain, Btu/hr
235	QC	Condenser load, Btu/hr
220	Q/AA	Average heat flux, Btu hr-ft^2
239	WK	Potassium flow rate, lb/hr
240	PI	Inlet potassium vapor pressure, lb/in^2
241	PO	Outlet potassium vapor pressure, lb/in^2
242	DPC	Condensing pressure drop
351	TWIT*	Inner wall temperature at top axial station, ^{o}F
362	Q/AT*	Heat flux at inner wall at top axial station, Btu/hr-ft^2
364	TWOT*	Outer wall temperature at top axial station, ^{o}F
369	HCONT*	Condensing heat transfer coefficient at top axial station, Btu/hr-ft^2 - ^{o}F
371	NUCT*	Nusselt's condensing ratio at top axial station, dimensionless
393	TWIB*	Inner wall temperature at bottom axial station, ^{o}F
404	Q/AB*	Heat flux at inner wall at bottom axial station, Btu/hr-ft^2
406	TWOB*	Outer wall temperature at bottom axial station, ^{o}F
409	HCONB*	Condensing heat transfer coefficient at bottom axial station, Btu/hr-ft^2-^{o}F
411	NUCB*	Nusselt's condensing ratio at bottom axial station, dimensionless

* These values were also calculated accounting for the thermocouple standardizations obtained in the vapor standardization runs. The values of the parameters utilizing the thermocouple standardization are indicated in the columns in which the notation for the above parameters are followed by a C, e.g., TWITC is the Inner Wall Temperature at top axial station utilizing the standardized correction factor, ^{o}F.

TABLE 2:
CONDENSING DATA REDUCTION
(Part 2, Tabulated Data)

	110	111	113	115	117	119
	DATE	TIME	TC1	TC2	TC3	TC4
1	1.2043+04	2.3000+03	1.1688+03	1.1684+03	1.1661+03	1.1671+03
2	1.2043+04	2.3000+03	1.1687+03	1.1684+03	1.1662+03	1.1671+03
3	1.2043+04	2.3000+03	1.1687+03	1.1685+03	1.1662+03	1.1671+03
4	1.2043+04	2.3000+03	1.1688+03	1.1686+03	1.1662+03	1.1671+03
5	1.2073+04	2.0000+01	1.2041+03	1.2039+03	1.2020+03	1.2031+03
6	1.2073+04	2.0000+01	1.2042+03	1.2038+03	1.2022+03	1.2032+03
7	1.2073+04	2.0000+01	1.2043+03	1.2041+03	1.2021+03	1.2032+03
8	1.2073+04	2.0000+01	1.2042+03	1.2040+03	1.2021+03	1.2032+03
9	1.2073+04	1.3000+02	1.2370+03	1.2368+03	1.2355+03	1.2364+03
10	1.2073+04	1.3000+02	1.2372+03	1.2370+03	1.2355+03	1.2364+03
11	1.2073+04	1.3000+02	1.2370+03	1.2368+03	1.2354+03	1.2364+03
12	1.2073+04	1.3000+02	1.2371+03	1.2370+03	1.2356+03	1.2365+03
13	1.2073+04	2.2000+02	1.2584+03	1.2580+03	1.2568+03	1.2577+03
14	1.2073+04	2.2000+02	1.2585+03	1.2582+03	1.2569+03	1.2579+03
15	1.2073+04	2.2000+02	1.2584+03	1.2582+03	1.2568+03	1.2578+03
16	1.2073+04	2.3000+02	1.2580+03	1.2578+03	1.2565+03	1.2574+03
17	1.2073+04	2.3000+02	1.2579+03	1.2575+03	1.2565+03	1.2573+03
18	1.2073+04	2.3000+02	1.2581+03	1.2578+03	1.2565+03	1.2574+03

CONDENSING DATA REDUCTION

	121	123	125	127	129	131
	TC5	TC6	TC7	TC8	TC9	TC10
1	1.1469+03	1.1449+03	1.1457+03	1.1409+03	1.1376+03	1.1392+03
2	1.1469+03	1.1449+03	1.1458+03	1.1409+03	1.1377+03	1.1392+03
3	1.1468+03	1.1449+03	1.1459+03	1.1408+03	1.1377+03	1.1392+03
4	1.1470+03	1.1450+03	1.1459+03	1.1409+03	1.1376+03	1.1392+03
5	1.1843+03	1.1824+03	1.1834+03	1.1800+03	1.1768+03	1.1784+03
6	1.1844+03	1.1824+03	1.1833+03	1.1801+03	1.1766+03	1.1782+03
7	1.1843+03	1.1823+03	1.1834+03	1.1800+03	1.1767+03	1.1783+03
8	1.1842+03	1.1823+03	1.1833+03	1.1799+03	1.1766+03	1.1782+03
9	1.2181+03	1.2161+03	1.2172+03	1.2142+03	1.2109+03	1.2125+03
10	1.2181+03	1.2161+03	1.2172+03	1.2142+03	1.2107+03	1.2124+03
11	1.2181+03	1.2160+03	1.2171+03	1.2141+03	1.2106+03	1.2123+03
12	1.2181+03	1.2160+03	1.2172+03	1.2141+03	1.2106+03	1.2123+03
13	1.2388+03	1.2365+03	1.2376+03	1.2343+03	1.2309+03	1.2326+03
14	1.2387+03	1.2366+03	1.2376+03	1.2344+03	1.2309+03	1.2325+03
15	1.2385+03	1.2365+03	1.2376+03	1.2342+03	1.2308+03	1.2325+03
16	1.2379+03	1.2359+03	1.2370+03	1.2335+03	1.2301+03	1.2318+03
17	1.2381+03	1.2359+03	1.2369+03	1.2335+03	1.2301+03	1.2319+03
18	1.2380+03	1.2359+03	1.2369+03	1.2335+03	1.2300+03	1.2317+03

CONDENSING DATA REDUCTION

	133	135	137	139	143	145
	TC11	TC12	TC13	TC14	TC16	TC17
1	1.1610+03	1.1603+03	1.1578+03	1.1565+03	1.1596+03	1.1575+03
2	1.1610+03	1.1604+03	1.1578+03	1.1566+03	1.1597+03	1.1575+03
3	1.1610+03	1.1605+03	1.1579+03	1.1566+03	1.1597+03	1.1575+03
4	1.1611+03	1.1604+03	1.1578+03	1.1565+03	1.1595+03	1.1576+03
5	1.1979+03	1.1974+03	1.1951+03	1.1940+03	1.1966+03	1.1947+03
6	1.1982+03	1.1976+03	1.1950+03	1.1939+03	1.1966+03	1.1948+03
7	1.1980+03	1.1975+03	1.1952+03	1.1940+03	1.1966+03	1.1947+03
8	1.1979+03	1.1974+03	1.1951+03	1.1940+03	1.1965+03	1.1947+03
9	1.2318+03	1.2314+03	1.2289+03	1.2278+03	1.2303+03	1.2286+03
10	1.2319+03	1.2313+03	1.2289+03	1.2277+03	1.2303+03	1.2286+03
11	1.2318+03	1.2312+03	1.2288+03	1.2278+03	1.2303+03	1.2287+03
12	1.2319+03	1.2314+03	1.2289+03	1.2277+03	1.2303+03	1.2287+03
13	1.2529+03	1.2523+03	1.2499+03	1.2487+03	1.2514+03	1.2496+03
14	1.2531+03	1.2524+03	1.2497+03	1.2486+03	1.2515+03	1.2497+03
15	1.2530+03	1.2524+03	1.2498+03	1.2485+03	1.2513+03	1.2496+03
16	1.2526+03	1.2519+03	1.2492+03	1.2480+03	1.2509+03	1.2491+03
17	1.2524+03	1.2518+03	1.2493+03	1.2481+03	1.2509+03	1.2490+03
18	1.2525+03	1.2517+03	1.2492+03	1.2481+03	1.2510+03	1.2490+03

CONDENSING DATA REDUCTION

	147	149	161	163	165	167
	TC18	TC19	TC1C	TC2C	TC3C	TC4C
1	1.1569+03	1.1523+03	1.1688+03	1.1684+03	1.1674+03	1.1670+03
2	1.1569+03	1.1523+03	1.1687+03	1.1684+03	1.1674+03	1.1670+03
3	1.1570+03	1.1524+03	1.1687+03	1.1685+03	1.1675+03	1.1670+03
4	1.1570+03	1.1524+03	1.1688+03	1.1686+03	1.1675+03	1.1670+03
5	1.1941+03	1.1900+03	1.2041+03	1.2040+03	1.2032+03	1.2030+03
6	1.1943+03	1.1902+03	1.2042+03	1.2039+03	1.2034+03	1.2031+03
7	1.1942+03	1.1900+03	1.2043+03	1.2042+03	1.2034+03	1.2032+03
8	1.1941+03	1.1900+03	1.2042+03	1.2041+03	1.2034+03	1.2031+03
9	1.2279+03	1.2241+03	1.2370+03	1.2370+03	1.2366+03	1.2364+03
10	1.2280+03	1.2240+03	1.2372+03	1.2372+03	1.2367+03	1.2364+03
11	1.2279+03	1.2239+03	1.2370+03	1.2370+03	1.2366+03	1.2363+03
12	1.2280+03	1.2240+03	1.2371+03	1.2372+03	1.2368+03	1.2364+03
13	1.2488+03	1.2448+03	1.2584+03	1.2582+03	1.2579+03	1.2577+03
14	1.2488+03	1.2447+03	1.2585+03	1.2584+03	1.2580+03	1.2578+03
15	1.2488+03	1.2447+03	1.2584+03	1.2584+03	1.2579+03	1.2578+03
16	1.2482+03	1.2441+03	1.2580+03	1.2580+03	1.2576+03	1.2574+03
17	1.2482+03	1.2441+03	1.2579+03	1.2577+03	1.2576+03	1.2572+03
18	1.2482+03	1.2440+03	1.2581+03	1.2580+03	1.2576+03	1.2573+03

CONDENSING DATA REDUCTION

	169	171	173	175	179	181
	TC11C	TC12C	TC13C	TC14C	TC16C	TC17C
1	1.1605+03	1.1596+03	1.1571+03	1.1554+03	1.1599+03	1.1574+03
2	1.1605+03	1.1596+03	1.1571+03	1.1555+03	1.1600+03	1.1574+03
3	1.1605+03	1.1597+03	1.1572+03	1.1554+03	1.1600+03	1.1574+03
4	1.1606+03	1.1597+03	1.1571+03	1.1554+03	1.1598+03	1.1575+03
5	1.1974+03	1.1967+03	1.1944+03	1.1929+03	1.1968+03	1.1946+03
6	1.1976+03	1.1969+03	1.1943+03	1.1928+03	1.1968+03	1.1947+03
7	1.1975+03	1.1968+03	1.1945+03	1.1929+03	1.1969+03	1.1946+03
8	1.1974+03	1.1967+03	1.1944+03	1.1929+03	1.1968+03	1.1945+03
9	1.2313+03	1.2307+03	1.2282+03	1.2267+03	1.2305+03	1.2284+03
10	1.2314+03	1.2306+03	1.2281+03	1.2267+03	1.2305+03	1.2284+03
11	1.2313+03	1.2305+03	1.2280+03	1.2267+03	1.2305+03	1.2285+03
12	1.2314+03	1.2307+03	1.2282+03	1.2267+03	1.2305+03	1.2285+03
13	1.2523+03	1.2516+03	1.2491+03	1.2477+03	1.2516+03	1.2494+03
14	1.2525+03	1.2517+03	1.2490+03	1.2476+03	1.2516+03	1.2495+03
15	1.2525+03	1.2517+03	1.2491+03	1.2475+03	1.2515+03	1.2494+03
16	1.2520+03	1.2512+03	1.2484+03	1.2470+03	1.2511+03	1.2489+03
17	1.2518+03	1.2511+03	1.2485+03	1.2471+03	1.2511+03	1.2488+03
18	1.2520+03	1.2510+03	1.2484+03	1.2471+03	1.2512+03	1.2488+03

CONDENSING DATA REDUCTION

	183	185	196	198	201	204
	TC18C	TC19C	TKI	TKO	TNAO	TNAI
1	1.1571+03	1.1519+03	1.1686+03	1.1672+03	1.1458+03	1.1393+03
2	1.1571+03	1.1519+03	1.1686+03	1.1672+03	1.1458+03	1.1393+03
3	1.1571+03	1.1520+03	1.1686+03	1.1673+03	1.1459+03	1.1392+03
4	1.1571+03	1.1520+03	1.1687+03	1.1672+03	1.1460+03	1.1392+03
5	1.1943+03	1.1896+03	1.2040+03	1.2031+03	1.1833+03	1.1784+03
6	1.1945+03	1.1897+03	1.2041+03	1.2033+03	1.1834+03	1.1783+03
7	1.1944+03	1.1896+03	1.2042+03	1.2033+03	1.1833+03	1.1783+03
8	1.1943+03	1.1896+03	1.2042+03	1.2032+03	1.1833+03	1.1782+03
9	1.2281+03	1.2236+03	1.2370+03	1.2365+03	1.2171+03	1.2125+03
10	1.2283+03	1.2235+03	1.2372+03	1.2365+03	1.2171+03	1.2125+03
11	1.2281+03	1.2234+03	1.2370+03	1.2364+03	1.2171+03	1.2123+03
12	1.2282+03	1.2235+03	1.2371+03	1.2366+03	1.2171+03	1.2124+03
13	1.2490+03	1.2443+03	1.2583+03	1.2578+03	1.2376+03	1.2326+03
14	1.2491+03	1.2442+03	1.2585+03	1.2579+03	1.2376+03	1.2326+03
15	1.2490+03	1.2442+03	1.2584+03	1.2578+03	1.2375+03	1.2325+03
16	1.2485+03	1.2435+03	1.2580+03	1.2575+03	1.2370+03	1.2318+03
17	1.2484+03	1.2436+03	1.2578+03	1.2574+03	1.2370+03	1.2318+03
18	1.2485+03	1.2435+03	1.2580+03	1.2575+03	1.2370+03	1.2317+03

CONDENSING DATA REDUCTION

	205	214	216	217	219	235
	DTNA	WNA	TNAM	CPNA	QNA	QC
1	6.5961+00	3.9151+03	1.1425+03	3.0000-01	7.7473+03	1.0323+04
2	6.5819+00	3.9151+03	1.1426+03	3.0000-01	7.7307+03	1.0307+04
3	6.6384+00	3.9151+03	1.1426+03	3.0000-01	7.7971+03	1.0374+04
4	6.7231+00	3.9151+03	1.1426+03	3.0000-01	7.8966+03	1.0474+04
5	4.9573+00	4.4514+03	1.1809+03	3.0000-01	6.6200+03	9.3705+03
6	5.0285+00	4.4514+03	1.1808+03	3.0000-01	6.7152+03	9.4654+03
7	5.0143+00	4.4514+03	1.1808+03	3.0000-01	6.6961+03	9.4464+03
8	5.0427+00	4.4514+03	1.1807+03	3.0000-01	6.7342+03	9.4842+03
9	4.6154+00	4.4929+03	1.2148+03	3.0007-01	6.2225+03	9.1086+03
10	4.6724+00	4.4929+03	1.2148+03	3.0007-01	6.2993+03	9.1857+03
11	4.7578+00	4.4929+03	1.2147+03	3.0007-01	6.4145+03	9.3009+03
12	4.7578+00	4.4929+03	1.2147+03	3.0007-01	6.4145+03	9.3012+03
13	5.0142+00	4.5153+03	1.2351+03	3.0018-01	6.7962+03	9.7693+03
14	5.0570+00	4.5153+03	1.2351+03	3.0018-01	6.8541+03	9.8271+03
15	5.0142+00	4.5153+03	1.2350+03	3.0018-01	6.7962+03	9.7690+03
16	5.1567+00	4.5167+03	1.2344+03	3.0017-01	6.9913+03	9.9624+03
17	5.1424+00	4.5167+03	1.2344+03	3.0017-01	6.9720+03	9.9430+03
18	5.2279+00	4.5167+03	1.2343+03	3.0017-01	7.0879+03	1.0059+04

CONDENSING DATA REDUCTION

	220	239	240	241	242	351
	Q/AA	WK	PI	PO	DPC	TWI T
1	2.1028+04	1.1842+01	3.6989+00	3.6636+00	3.5325-02	1.1640+03
2	2.0996+04	1.1824+01	3.6973+00	3.6641+00	3.3226-02	1.1640+03
3	2.1132+04	1.1901+01	3.6978+00	3.6651+00	3.2704-02	1.1641+03
4	2.1337+04	1.2017+01	3.7015+00	3.6646+00	3.6906-02	1.1642+03
5	1.9088+04	1.0812+01	4.6785+00	4.6500+00	2.8522-02	1.2007+03
6	1.9282+04	1.0922+01	4.6792+00	4.6552+00	2.3966-02	1.2011+03
7	1.9243+04	1.0900+01	4.6837+00	4.6546+00	2.9179-02	1.2007+03
8	1.9320+04	1.0944+01	4.6818+00	4.6533+00	2.8528-02	1.2007+03
9	1.8555+04	1.0567+01	5.7685+00	5.7502+00	1.8317-02	1.2347+03
10	1.8712+04	1.0657+01	5.7746+00	5.7510+00	2.3645-02	1.2347+03
11	1.8947+04	1.0790+01	5.7685+00	5.7487+00	1.9836-02	1.2346+03
12	1.8947+04	1.0791+01	5.7731+00	5.7540+00	1.9088-02	1.2348+03
13	1.9901+04	1.1377+01	6.5757+00	6.5550+00	2.0635-02	1.2557+03
14	2.0019+04	1.1444+01	6.5824+00	6.5609+00	2.1485-02	1.2561+03
15	1.9900+04	1.1377+01	6.5782+00	6.5576+00	2.0637-02	1.2561+03
16	2.0294+04	1.1601+01	6.5648+00	6.5433+00	2.1461-02	1.2556+03
17	2.0255+04	1.1578+01	6.5572+00	6.5399+00	1.7250-02	1.2552+03
18	2.0490+04	1.1713+01	6.5648+00	6.5425+00	2.2300-02	1.2554+03

CONDENSING DATA REDUCTION

	362	364	369	371	393	404
	Q/A T	TWO T	HCON T	NUC T	TWI B	Q/A B
1	1.6663+04	1.1523+03	4.0046+03	1.1214-02	1.1638+03	2.3673+04
2	1.6448+04	1.1525+03	3.9750+03	1.1131-02	1.1639+03	2.3844+04
3	1.6603+04	1.1524+03	4.0628+03	1.1377-02	1.1638+03	2.3526+04
4	1.7074+04	1.1522+03	4.1971+03	1.1753-02	1.1637+03	2.3328+04
5	1.4963+04	1.1903+03	4.8708+03	1.3692-02	1.2004+03	2.1600+04
6	1.6129+04	1.1899+03	5.8699+03	1.6500-02	1.2003+03	2.0936+04
7	1.5102+04	1.1903+03	4.7764+03	1.3427-02	1.2004+03	2.1506+04
8	1.5144+04	1.1902+03	4.8145+03	1.3534-02	1.2003+03	2.1238+04
9	1.5636+04	1.2239+03	7.2454+03	2.0486-02	1.2340+03	2.0899+04
10	1.5986+04	1.2237+03	7.2115+03	2.0391-02	1.2340+03	2.0912+04
11	1.5650+04	1.2238+03	7.0683+03	1.9986-02	1.2341+03	2.1432+04
12	1.6038+04	1.2238+03	7.4673+03	2.1114-02	1.2341+03	2.1057+04
13	1.5973+04	1.2448+03	6.6090+03	1.8757-02	1.2553+03	2.2234+04
14	1.7145+04	1.2443+03	7.7599+03	2.2024-02	1.2554+03	2.2707+04
15	1.7218+04	1.2443+03	8.1231+03	2.3055-02	1.2552+03	2.2252+04
16	1.7467+04	1.2437+03	7.9100+03	2.2449-02	1.2550+03	2.3029+04
17	1.6243+04	1.2441+03	6.6322+03	1.8822-02	1.2549+03	2.2766+04
18	1.6714+04	1.2439+03	6.7701+03	1.9214-02	1.2550+03	2.3329+04

CONDENSING DATA REDUCTION

	406	409	411	428	438	440
	TWO B	HCON B	NUC B	TWI TC	Q/A TC	TWO TC
1	1.1472+03	6.1043+03	1.7093-02	1.1638+03	1.8683+04	1.1507+03
2	1.1472+03	6.3147+03	1.7682-02	1.1638+03	1.8467+04	1.1509+03
3	1.1473+03	6.0688+03	1.6994-02	1.1639+03	1.8623+04	1.1509+03
4	1.1474+03	5.8250+03	1.6311-02	1.1640+03	1.9093+04	1.1506+03
5	1.1854+03	7.1176+03	2.0008-02	1.2005+03	1.6826+04	1.1888+03
6	1.1858+03	6.4635+03	1.8169-02	1.2009+03	1.7993+04	1.1884+03
7	1.1855+03	6.7691+03	1.9029-02	1.2005+03	1.6965+04	1.1888+03
8	1.1855+03	6.5324+03	1.8363-02	1.2005+03	1.7007+04	1.1887+03
9	1.2196+03	7.8661+03	2.2241-02	1.2344+03	1.7340+04	1.2225+03
10	1.2196+03	7.7370+03	2.1877-02	1.2345+03	1.7691+04	1.2223+03
11	1.2194+03	8.5714+03	2.4236-02	1.2344+03	1.7355+04	1.2224+03
12	1.2196+03	7.8243+03	2.2124-02	1.2346+03	1.7743+04	1.2223+03
13	1.2400+03	8.3116+03	2.3590-02	1.2555+03	1.7578+04	1.2434+03
14	1.2399+03	8.5087+03	2.4150-02	1.2558+03	1.8749+04	1.2430+03
15	1.2400+03	8.0151+03	2.2748-02	1.2558+03	1.8824+04	1.2429+03
16	1.2392+03	8.4962+03	2.4112-02	1.2554+03	1.9074+04	1.2423+03
17	1.2392+03	8.4993+03	2.4120-02	1.2550+03	1.7851+04	1.2427+03
18	1.2390+03	8.9140+03	2.5298-02	1.2551+03	1.8321+04	1.2425+03

CONDENSING DATA REDUCTION

	442	444	463	473	475	477
	HCONTC	NUC TC	TWI BC	Q/A BC	TWO BC	HCONBC
1	4.3263+03	1.2114-02	1.1644+03	2.5627+04	1.1464+03	7.7967+03
2	4.2991+03	1.2038-02	1.1645+03	2.5798+04	1.1464+03	8.1002+03
3	4.3878+03	1.2287-02	1.1644+03	2.5481+04	1.1466+03	7.7559+03
4	4.5187+03	1.2653-02	1.1643+03	2.5283+04	1.1466+03	7.4077+03
5	5.1457+03	1.4465-02	1.2009+03	2.3482+04	1.1846+03	9.4015+03
6	6.1091+03	1.7173-02	1.2008+03	2.2819+04	1.1850+03	8.4453+03
7	5.0496+03	1.4195-02	1.2009+03	2.3389+04	1.1847+03	8.8597+03
8	5.0867+03	1.4299-02	1.2008+03	2.3120+04	1.1848+03	8.5191+03
9	7.2385+03	2.0467-02	1.2345+03	2.2738+04	1.2188+03	1.0510+04
10	7.2085+03	2.0383-02	1.2345+03	2.2751+04	1.2188+03	1.0296+04
11	7.0789+03	2.0016-02	1.2346+03	2.3270+04	1.2186+03	1.1592+04
12	7.4390+03	2.1034-02	1.2346+03	2.2897+04	1.2188+03	1.0417+04
13	6.5609+03	1.8621-02	1.2557+03	2.4043+04	1.2393+03	1.0882+04
14	7.5863+03	2.1532-02	1.2559+03	2.4517+04	1.2391+03	1.1127+04
15	7.9044+03	2.2434-02	1.2557+03	2.4062+04	1.2392+03	1.0412+04
16	7.7230+03	2.1918-02	1.2554+03	2.4838+04	1.2384+03	1.1065+04
17	6.5857+03	1.8690-02	1.2553+03	2.4576+04	1.2385+03	1.1107+04
18	6.7101+03	1.9043-02	1.2555+03	2.5138+04	1.2383+03	1.1684+04

CONDENSING DATA REDUCTION

479

NUC BC

1	2.1832-02
2	2.2682-02
3	2.1718-02
4	2.0743-02
5	2.6428-02
6	2.3740-02
7	2.4906-02
8	2.3948-02
9	2.9716-02
10	2.9112-02
11	3.2777-02
12	2.9455-02
13	3.0884-02
14	3.1581-02
15	2.9552-02
16	3.1404-02
17	3.1521-02
18	3.3160-02

APPENDIX D. A CALORIMETRIC METHOD FOR THE MEASUREMENT OF ALKALI METAL FLOW RATE

In most heat transfer experiments, accurate determination of flow rate is an absolute requirement. In low temperature systems with noncorrosive fluids, flow rate is usually measured by a pressure drop device such as an orifice or venturimeter. In the case of alkali metal investigations, when both high temperature and chemical reactivity are involved, accurate flow rate measurement becomes a major problem. For measurements within ±20%, electromagnetic, flowmeters are normally used because this type flowmeter does not involve a penetration of the system. For investigations where accuracy exceeding ±5% is required, a calibrated electromagnetic flowmeter or an alternative flow measurement device is required. Several methods are available for the calibration of this type flowmeter e.g., a pressure drop device, such as a venturi meter or a calorimetric device.

Considerable problems are inherent with any device requiring accurate pressure measurement in an alkali metal system; because of exposure to alkali metal and/or high temperature, commonly used pressure measuring devices are inapplicable. The calorimetric method was chosen since the measurement of a temperature difference in a flowing single-phase alkali metal stream has demonstrated accuracy within ±0.4°F for differences from 2 to 8°F

The design of the calorimeter used in the calibration of the electromagnetic flowmeter in the 50 kw facility is shown in Figure D-1. This design was selected for two reasons:

1) The device is applicable for flow in either direction.

2) An immersion heater used for heat input to the calorimeter assures that substantially all the heat input to the calorimeter will go into the potassium sensible heat.

To determine the flow rate accurately, three parameters must be known:

1) Heat input to the calorimeter, q_w, Btu/sec

2) Specific heat of potassium, Cp, Btu/lb°F

3) Potassium temperature difference across the calorimeter, $T_o - T_i$, °F

The heat input to the calorimeter is measured by a standardized General Electric Single Phase Wattmeter, Type P-3, which has an indicated accuracy of $\pm 1/4\%$ of full scale. The specific heat of liquid potassium has been reported in reference 21. The values are correct within $\pm 2\%$ up to 900°F. These values are correlated by

$$Cp = 0.202 - .5093(10^{-4})T + 0.3385(10^{-7})T^2$$

The sensitivity of Cp to values of error in temperature level is apparent from the value of the derivative

$$dCp/dT = -.51(10^{-4}) + .68(10^{-7})T$$

At 900°F, this value is $5(10^{-5})$. For a 5°F error in average temperature level, therefore the error in Cp is approximately $3(10^{-4})$ Btu/lb-°F. The percentage error in Cp caused by this error in temperature level is less than 0.2%. Consequently, because of the insensitivity of the value of Cp to changes in temperature level, the error associated with the accurate evaluation of the temperature level is not an important consideration.

Recognizing these considerations, the accuracy of the calorimetric method is highly dependent on the evaluation of the potassium temperature increase, caused by the heat input to the calorimeter. With no heat input to the calorimeter, the potassium loses a certain amount of heat to the surroundings. This is a function of temperature difference between the calorimeter shell and the surroundings and can be expressed

$$q_L = (W\ C_p)_L\ (T_{im} - T_{om} + \triangle)_L \qquad (1)$$

With heat input to the calorimeter and with the same average temperature difference,

$$q_{wm} - q_L = (WC_p)_{wm}\ (T_{om} - T_{im} - \triangle)_{wm} \qquad (2)$$

This assumes that the heat lost by the potassium, as it passes through the calorimeter, is a function of the average temperature of the potassium only, i.e., the effective shell temperature of the calorimeter, and not a function of heat put into the calorimeter with the immersion heater. Since, as shown in Figure D-1, the heated length of the immersion heater is surrounded entirely by potassium, this assumption can be demonstrated true with neglible error. To equate q_L in equations 1 and 2 requires two data runs at the same average calorimeter shell temperature, one with and one without heat input. The expression for the heat loss, q_L, from equation 1 is then substituted into equation 2 to yield

$$q_{wm} = (WC_p)_{wm} (T_{om} - T_{im} - \Delta)_{wm} + (WC_p)_L (T_{im} - T_{om} + \Delta)_L \quad (3)$$

$$q_{wm} = (WC_p)_{wm} \left[(T_{om} - T_{im} - \Delta)_{wm} + \frac{(WC_p)_L}{(WC_p)_{wm}} (T_{im} - T_{om} + \Delta)_L \right] \quad (4)$$

Employing equation 4 depends upon the particular facility in which the measurements are made. In the 50 kw facility, where an electromagnetic flowmeter can be used to equate the flows during a heat loss and heat input run, it is quite possible to set $(WCp)_L/WCp)_{wm} = 1$ and equation 4 yields

$$q_{wm} = (WC_p)_{wm} \left[(T_{om} - T_{im} - \Delta)_{wm} + (T_{im} - T_{om} + \Delta)_L \right] \quad (5)$$

Since the thermocouple error Δ should not be a function of the calorimeter heat input, equation 5 gives

$$W = \frac{q_{wm}}{C_p \left[(T_{om} - T_{im})_{wm} + (T_{im} - T_{om})_L \right]} \quad (6)$$

Since the RHS of equation 6 contains only measured values of temperature and flow and since the specific heat of the potassium can be calculated from the average measured potassium temperature, the flow rate (W) can be accurately determined. As previously cited, the errors associated with the measured values of q_{wm} and Cp are: error in $q_{wm} = \pm 0.5\%$ (0.25% of full scale but assume only that wattmeter reading is always taken in upper half of range); error in Cp = $\pm 2.2\%$.

As previously mentioned, the error in the measured temperature difference with values of $(T_i - T_o)$ exceeding flow rate 25°F should be less than ± 0.4°F, or $\pm 1.6\%$.

The standard error in the calculation of (W) is

$$\sigma \leqq \sqrt{(.5)^2 + (2.2)^2 + (1.6)^2}$$

$$\sigma \leqq \sqrt{7.65}$$

$$\sigma \leqq \pm 2.8\%$$

This method of calibrating an electromagnetic flowmeter was used in the 50 kw facility during November for these conditions:

Flow rate, lb/sec.	0.14 to 0.31
Temperature difference, °F.	11.5 to 43.4
Average temperature, °F.	600 to 700
Wattmeter input, Btu/sec	0.76 to 1.6

Four pairs of runs were made. These indicated that the ratio of the flow rate calculated from the calorimeter to that calculated from the electromagnetic flowmeter was 1.145 with a standard error of 0.014 or ±1.3%.

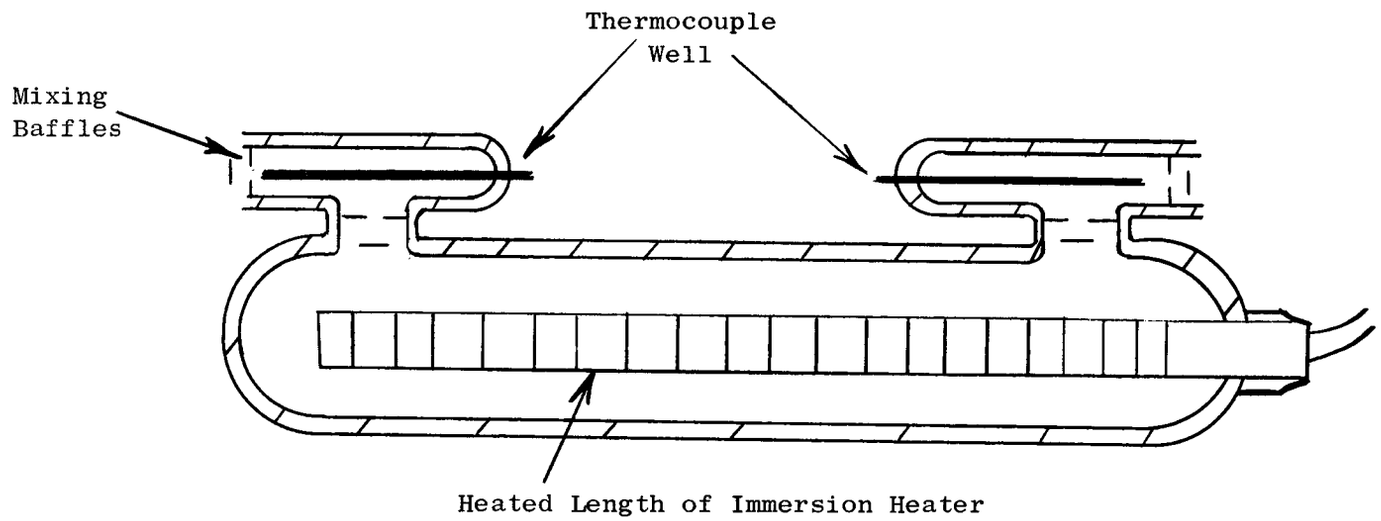

Figure D-1. 50 KW Facility Thermal Calorimeter

APPENDIX E. DERIVATION OF THE EXPRESSION FOR THE TWO-PHASE GRADIENT FROM CONTINUITY AND MOMENTUM CONSIDERATIONS

The system to be analyzed is shown in Figure 62. The assumptions and conditions of the analysis are given below:

Assumptions:

1) The velocity and density of each phase are functions only of the axial distance L, i.e., they are independent of R and θ .

2) The system is in steady state operation.

3) The pressure is a function only of the axial distance L, i.e., it is independent of R and θ .

4) The wall shear stress (T_w) is a function only of L, i.e., it is independent of θ .

Geometry Conditions:

1) Constant area duct A_T = Constant

2) $A_f + A_g = A_T$

Continuity Equation

$$\frac{d}{dt}\iiint_{cv} \rho \, dv + \oiint_{cs} \rho \bar{V} \, d\bar{A} = 0 \qquad (1)$$

Using the assumptions given above, equation 1 becomes

$$\rho_f V_f A_f + \rho_g V_g A_g = m \qquad \text{(a constant)} \qquad (2)$$

Linear Momentum Equation

$$\overset{+}{\rightarrow}\uparrow \quad \Sigma \bar{F} = \frac{d}{dt}\iiint_{cv} \rho \bar{V} \, dv + \oiint_{c.s} \bar{V} \left(\rho \bar{V} \cdot dA\right) \qquad (3)$$

Using the assumptions given above, equation 3 becomes

$$P_L A_T - P_{L+\Delta L} A_T - \int_L^{L+\Delta L} \tau_w p \, dL - \left\{ \int_L^{L+\Delta L} (\rho_g A_g + \rho_f A_f) \, dL \right\} \frac{g}{g_c} \sin\phi$$

$$= \left\{ \left(\frac{\rho_f V_f^2 A_f}{g_c \beta_f} \right)_{L+\Delta L} - \left(\frac{\rho_f V_f^2 A_f}{g_c \beta_f} \right)_L \right\} + \left\{ \left(\frac{\rho_g V_g^2 A_g}{g_c \beta_g} \right)_{L+\Delta L} - \left(\frac{\rho_g V_g^2 A_g}{g_c \beta_g} \right)_L \right\} \tag{4}$$

where a shape factor β has been introduced to account for those cases in which the velocity of each phase is not constant over a given cross-sectional area.

$$\beta = V_A^2 A \Big/ \int_A V^2 dA \tag{5}$$

where $V_A = \int V dA \Big/ \int dA$

$$\text{since} \quad \sqrt{\frac{\int V^2 dA}{\int dA}} \geq \frac{\int V dA}{\int_A dA} \tag{6}$$

$$\text{then} \quad \frac{\int_A V^2 dA}{\int_A dA} \geq \left[\frac{\int_A V dA}{\int dA} \right]^2 = V_A^2$$

$$\beta = V_A^2 A \Big/ \int_A V^2 dA \leq 1 \tag{7}$$

Dividing equation 4 by (ΔL) (A_T) and taking the limit as $\Delta L \to 0$ yields

$$-\frac{dP}{dL} - \frac{\tau_w p}{A_T} - \left(\frac{g}{g_c} \sin\phi\right)\left(\rho_g \frac{A_g}{A_T} + \rho_f \frac{A_f}{A_T}\right) = \frac{1}{g_c A_T} \frac{d}{dL}\left[\frac{\rho_f V_f^2 A_f}{\beta_f}\right] + \frac{1}{g_c A_T} \frac{d}{dL}\left[\frac{\rho_g V_g^2 A_g}{\beta_g}\right] \tag{8}$$

$$\frac{dP}{dL} = -\frac{1}{g_c A_T} \frac{d}{dL}\left[\frac{m_f V_f}{\beta_f} + \frac{m_g V_g}{\beta_g}\right] - \frac{p}{A_T} \tau_w - \frac{g}{g_c} \sin\phi \left(\rho_g R_g + \rho_f R_f\right) \tag{9}$$

Define the hydraulic diameter as follows:

$$D_H = (4) \frac{\text{(Cross-Sectional Area)}}{\text{(Wetted Perimeter)}} = \frac{4 A_T}{p} \tag{10}$$

Introducing 10 and the definition of the flowing quality into 9 yields

$$\frac{dP}{dL} = \frac{G}{g_c}\frac{d}{dL}\left[\frac{(1-x)V_f}{\beta_f} + \frac{xV_g}{\beta_g}\right] - \frac{4}{D_H}\tau_w - \frac{g}{g_c}\sin\phi\left(\rho_g R_g + \rho_f R_f\right) \tag{11}$$

$$\frac{dP}{dL} = \frac{G^2}{g_c}\frac{d}{dL}\left[\frac{(1-x)^2}{\rho_f R_f \beta_f} + \frac{x^2}{\rho_g R_g \beta_g}\right] - \frac{4}{D_H}\tau_w - \frac{g}{g_c}\sin\phi\left(\rho_f R_f + \rho_g R_g\right) \tag{12}$$

---

* This relationship is a special case of the Schwarz Inequality. (Reference 22).

APPENDIX F. DERIVATION OF THE RELATIONSHIP BETWEEN SLIP, VOID FRACTION, AND FLOWING QUALITY

The following equations will be needed in the present derivations.

Continuity equation:

$$m = m_f + m_g = \rho_f V_f A_f + \rho_g V_g A_g \tag{1}$$

The geometry condition:

$$A_f + A_g = A_T = \text{Constant} \tag{2}$$

Definition of the slip ratio:

$$K = V_g / V_f \tag{3}$$

Definition of the flowing quality:

$$X = m_g / m_T \tag{4}$$

Definition of the void fraction:

$$R_g = A_g / A_T \tag{5}$$

From equations 2 and 5,

$$A_f + A_g = A_T$$

$$\frac{A_f}{A_T} + \frac{A_g}{A_T} = 1$$

then $$\underline{R_g + R_f = 1} \tag{6}$$

From equations 1 through 5,

$$X = \frac{m_g}{m_T} = \rho_g V_g A_g / G A_T \tag{7}$$

$$V_g = X G / \rho_g R_g$$

$$m_f + m_g = m_T \; ; \quad \frac{m_f}{m_t} + \frac{m_g}{m_t} = 1$$

$$\frac{m_f}{m_T} = 1 - m_g / m_T = 1 - X$$

$$m_f = (1-X) m_T = \left(\frac{1-X}{X}\right) m_g$$

$$V_f = (1-X) G A_T / \rho_f A_f \tag{8}$$

$$V_f = (1-X) G / \rho_f R_f$$

Substituting equations 7 and 8 into the definition of slip yields

$$K = \frac{V_g}{V_f} = \left(X G / \rho_g R_g\right) \Big/ \frac{(1-X) G}{R_f \rho_f} = \frac{\rho_f}{\rho_g} \left(\frac{X}{1-X}\right) \frac{R_f}{R_g} \tag{9}$$

$$K = \left(\frac{\rho_f}{\rho_g}\right)\left(\frac{X}{1-X}\right)\left(\frac{1-R_g}{R_g}\right)$$

APPENDIX G. EXPRESSIONS FOR THE SLIP AND SHAPE FACTOR IN TERMS OF THE ENTRAINMENT FRACTION FOR THE MODIFIED ANNULAR FLOW MODEL

The equations given in Appendix F, the definitions of β given in Appendix E, and the entrainment fraction defined below will be needed in this derivation:

Definition of the entrainment fraction:

$$E = m_{f(g)} / m_f \tag{1}$$

$$m_f = m_{f(a)} + m_{f(g)}$$

$$1 = \frac{m_{f(a)}}{m_f} + \frac{m_{f(g)}}{m_f} = \frac{m_{f(a)}}{m_f} + E$$

$$\therefore \frac{m_{f(a)}}{m_f} = 1 - E$$

$$\frac{m_{f(a)}}{m_f} = 1 - E = \frac{\rho_f V_{f(a)} A_{f(a)}}{(1-x) G A_T} \tag{2}$$

$$\frac{A_{f(a)}}{A_T} = \frac{(1-x)}{\rho_f} \frac{(1-E)}{V_{f(a)}} G$$

$$E = \frac{m_{f(g)}}{m_f} = \frac{\rho_f V_g A_{f(g)}}{(1-x) G A_T} \tag{3}$$

$$\frac{A_{f(g)}}{A_T} = \frac{(1-x)(E) G}{\rho_f V_g} \tag{4}$$

$$R_g = \frac{A_g}{A_T} = \frac{A_T - A_f}{A_T} = 1 - \frac{A_f}{A_T}$$

$$1 - R_g = \frac{A_f}{A_T} = \frac{A_{f(a)}}{A_T} + \frac{A_{f(g)}}{A_T}$$

$$1 - R_g = \frac{(1-x) G}{\rho_f} \left[\frac{(1-E)}{V_{f(a)}} + \frac{E}{V_g} \right] \tag{5}$$

From equation 7, Appendix F,

$$V_g = X G / \rho_g R_g$$

$$\frac{(1-R_g)}{(1-X)}\left(\frac{\rho_f}{G}\right)\frac{V_{f(a)}}{1-E} = 1 + \left(\frac{E}{1-E}\right)\frac{V_{f(a)}}{V_g}$$

$$V_{f(a)}\left[\frac{(1-R_g)\rho_f}{(1-X)(1-E)G} - \frac{E\rho_g R_g}{X(1-E)G}\right] = 1$$

$$V_{f(a)} = \frac{G X (1-E)}{\rho_g R_g (K-E)} \tag{6}$$

$$\frac{V_g}{V_{f(a)}} = \left(\frac{X G}{\rho_g R_g}\right)\left(\frac{\rho_g R_g (K-E)}{G X (1-E)}\right)$$

$$\frac{V_g}{V_{f(a)}} = \frac{K-E}{1-E} \tag{7}$$

Define a modified slip K'

$$K' = \frac{V_g}{V_{f(a)}} = \frac{K-E}{1-E} \tag{8}$$

The definition of β given in Appendix E was

$$\beta = V_A^2 A \Big/ \int_A V^2 \, dA$$

$$\beta_f = V_{Af}^2 A_f \Big/ \int_A V_f^2 \, dA_f \tag{9}$$

$$V_{Af} = (1-x)G / \rho_f R_f \tag{10}$$

$$\beta_f = V_{Af}^2 A_f \Big/ V_{f(a)}^2 A_{f(a)} + V_g^2 . A_{f(g)}$$

$$\beta_f = \frac{V_{Af}^2}{\left[V_{f(a)}^2 \frac{A_{f(a)}}{A_T} + V_g^2 \frac{A_{fg}}{A_T} \right] \frac{A_T}{A_f}} \tag{11}$$

Substituting equations 3 and 4 into equation 11 yields the following:

$$\beta_f = \frac{V_{Af}^2 R_f}{V_{f(a)}^2 \left[\frac{(1-x)(1-E)G}{\rho_f V_{f(a)}} \right] + V_g^2 \left[\frac{(1-x)EG}{\rho_f V_g} \right]}$$

$$\beta_f = \frac{\rho_f (1-x)^2 G^2 R_f / \rho_f^2 R_f^2}{(1-x)G \left(\frac{G x (1-E)}{\rho_g R_g (K-E)} \right) \left(1 - E + E \left(\frac{K-E}{1-E} \right) \right)}$$

$$\beta_f = \frac{K-E}{K\left[1 + E(K-2)\right]} \tag{12}$$

APPENDIX H. THE DETERMINATION OF EXPRESSIONS FOR SEVERAL OF THE DENSITIES IN TERMS OF THE SLIP RATIO

In equation 2 of Section V, the density ($\hat{\rho}$) was defined as follows:

$$\frac{1}{\hat{\rho}} = \frac{(1-x)^2}{\rho_f R_f} + \frac{x^2}{\rho_g R_g} \tag{1}$$

$$\frac{1}{\hat{\rho}} = \frac{1}{R_g}\left[\frac{x^2}{\rho_g} + \frac{(1-x)^2}{\rho_f}\frac{R_g}{R_f}\right]$$

Using the expression for the slip ratio given by equation 8 of Section V in the above equation yields

$$\frac{1}{\hat{\rho}} = \frac{1}{R_g}\left[\frac{x^2}{\rho_g} + \frac{(1-x)^2}{\rho_f}\left(\frac{1}{K}\frac{x}{1-x}\frac{\rho_f}{\rho_g}\right)\right]$$

$$\frac{K}{\hat{\rho}} = \frac{x}{\rho_g R_g}\left[x(K-1)+1\right]$$

Substituting for R_g from equation 9 of Section V, the following results are obtained:

$$\frac{K}{\hat{\rho}} = \frac{x}{\rho_g}\left(\frac{\rho_f x + K\rho_g(1-x)}{\rho_f x}\right)\left(x(K-1)+1\right)$$

$$\frac{K}{\hat{\rho}} = \left[(1-x)\frac{K}{\rho_f} + \frac{x}{\rho_g}\right]\left[1 + x(K-1)\right] \tag{2}$$

In equation 3, Section V, the density ($\bar{\rho}$) was defined in the following manner:

$$\frac{1}{\bar{\rho}} = \frac{1}{\rho_g R_g + \rho_f R_f} = \frac{1}{\rho_g}\left[\frac{1}{R_g + \rho_f/\rho_g(1-R_g)}\right] \tag{3}$$

$$\frac{1}{\bar{\rho}} = \frac{1}{\rho_g}\left[\frac{1}{R_g(1-\rho_f/\rho_g) + \rho_f/\rho_g}\right]$$

Substituting for R_g from equation 9 of Section V, the following results are obtained:

$$\frac{1}{\bar{\rho}} = \frac{1}{\rho_g}\left[\frac{1}{\dfrac{1-\rho_f/\rho_g}{1+K(\rho_f/\rho_g)\left(\frac{1-x}{x}\right)} + \dfrac{\rho_f}{\rho_g}}\right]$$

(4)

$$\frac{1}{\bar{\rho}} = \frac{1}{\rho_g}\left[(1-x)\frac{\rho_g}{\rho_f} + \frac{x}{K}\right]\left[\frac{K}{x+K(1-x)}\right]$$

APPENDIX I. THE DETERMINATION OF THE DERIVATIVE OF $1/\hat{\rho}$ WITH RESPECT TO THE SLIP RATIO

In equation 18 of the Analysis Section, the following expression for $1/\hat{\rho}$ in terms of the slip ratio is given

$$\frac{1}{\hat{\rho}} = \frac{1}{\rho_g}\left[(1-x)\frac{\rho_g}{\rho_f} + \frac{x}{K}\right]\left[1 + x(K-1)\right] \tag{1}$$

$$\frac{1}{\hat{\rho}} = \left[\frac{(1-x)K}{\rho_f} + \frac{x}{\rho_g}\right]\left[\frac{1}{K} + x - \frac{x}{K}\right]$$

$$\frac{\partial(1/\hat{\rho})}{\partial K} = \left[\frac{(1-x)K}{\rho_f} + \frac{x}{\rho_g}\right]\left[-\frac{1}{K^2} + \frac{x}{K^2}\right] + \left[\frac{1}{K} + x - \frac{x}{K}\right]\left[\frac{1-x}{\rho_f}\right]$$

$$= \frac{x}{\rho_g K^2} + \frac{x^2}{\rho_g K^2} + \frac{x}{\rho_f} - \frac{x^2}{\rho_f} = \frac{1}{\rho_g K^2}(x^2 - x) - \frac{1}{\rho_f}(x^2 - x)$$

$$\frac{\partial(1/\hat{\rho})}{\partial K} = (x^2 - x)\left[\frac{1}{\rho_g K^2} - \frac{1}{\rho_f}\right] = (x - x^2)\left[\frac{1}{\rho_f} - \frac{1}{\rho_g K^2}\right] \tag{2}$$

APPENDIX J. THE RELATIONSHIP BETWEEN THE SLIP RATIO AND THE ACCELERATION FACTOR

Define an acceleration factor (a) as follows:

$$a = V_{f2} / V_{f1} \tag{1}$$

Assume that the fluid entering the boiler at station 1 is saturated liquid (zero quality) and that the boiler cross-sectional area is constant.

$$m_f = (1-x)m = (1-x)GA_T$$

$$\rho_{f2} V_{f2} A_{f2} = (1-x) V_{f1} \rho_{f1} A_T$$

$$a = \frac{V_{f2}}{V_{f1}} = \frac{\rho_{f1}}{\rho_{f2}} \left(\frac{1-x}{R_f} \right) \tag{2}$$

$$a = \left(\rho_{f1} / \rho_{f2} \right) \left(\frac{1-x}{1-R_g} \right) \tag{3}$$

Substituting for R_g in terms of the slip gives the following:

$$K = \left(\frac{x}{1-x} \right) \left(\frac{\rho_{f2}}{\rho_{g2}} \right) \left(\frac{R_f}{R_g} \right) = \frac{x}{1-x} \left(\frac{\rho_{f2}}{\rho_{g2}} \right) \frac{\rho_{f1}}{\rho_{f2}} \left(\frac{1-x}{a} \right) \left(\frac{1}{1 - \frac{\rho_{f1}}{\rho_{f2}} \left(\frac{1-x}{a} \right)} \right)$$

$$K = \frac{\rho_{f2}}{\rho_{g2}} \left(\frac{x}{\rho_{f2}/\rho_{f1}\, a - (1-x)} \right) \tag{4}$$

Equation 4 can be simplified further if it is assumed that $\rho_{f1} = \rho_{f2}$

$$K = \left(\rho_{f2} / \rho_{g2} \right) \left(\frac{x}{a - (1-x)} \right) \tag{5}$$

Note that if $a \geq 1$, then

$$K_{max} = \left(\frac{\rho_{f1}}{\rho_{g2}} \right) \left(\frac{x}{x} \right) = \frac{\rho_f}{\rho_g} \tag{6}$$

APPENDIX K. PROOF THAT THE VALUE OF $1/\hat{\rho}$ IS IDENTICAL FOR A SLIP OF ONE AND A SLIP EQUAL TO ρ_f/ρ_g.

From equation 18 of the Analysis Section,

$$\frac{1}{\hat{\rho}} = \frac{1}{\rho_g}\left[(1-x)\frac{\rho_g}{\rho_f} + \frac{x}{K}\right]\left[1 + x(K-1)\right] \tag{1}$$

for $K = 1$

$$\frac{1}{\hat{\rho}} = \frac{1}{\rho_g}\left[(1-x)\frac{\rho_g}{\rho_f} + x\right] \tag{2}$$

for $K = \rho_f/\rho_g$

$$\frac{1}{\hat{\rho}} = \frac{1}{\rho_g}\left[(1-x)\frac{\rho_g}{\rho_f} + \frac{x}{\rho_f/\rho_g}\right]\left[1 + x\left(\frac{\rho_f}{\rho_g} - 1\right)\right]$$

$$\frac{1}{\hat{\rho}} = \frac{1}{\rho_g}\left[\left(\frac{\rho_g}{\rho_f}\right)(1 - x + x)\right]\left[(1-x) + x\frac{\rho_f}{\rho_g}\right]$$

$$\frac{1}{\hat{\rho}} = \frac{1}{\rho_g}\left[(1-x)\frac{\rho_g}{\rho_f} + x\right] \tag{3}$$

The proof is completed by noting that 2 and 3 are identical.

DISTRIBUTION FOR QUARTERLY AND FINAL REPORTS
CONTRACT NAS3-2528
January 1, 1964

NASA
Washington, D. C. 20546
Attn: William H. Woodward (RN)

NASA
Washington, D. C. 20546
Attn: Dr. Fred Schulman (RN)

NASA
Washington, D. C. 20546
Attn: James J. Lynch (RNP)

NASA
Washington, D. C. 20546
Attn: George C. Deutsch (RR)

NASA
Ames Research Center
Moffet Field, California 94035
Attn: Librarian

NASA
Goddard Space Flight Center
Greenbelt, Maryland 20771
Attn: Librarian

NASA
Langley Research Center
Hampton, Virginia 23365
Attn: Librarian

NASA
Lewis Research Center
21000 Brookpark Road
Cleveland, Ohio 44135
Attn: Librarian (3-7)

NASA
Lewis Research Center
21000 Brookpark Road
Cleveland, Ohio 44135
Attn: Dr. Bernard Lubarsky (86-1)

Nasa
Lewis Research Center
21000 Brookpark Road
Cleveland, Ohio 44135
Attn: Seymour Lieblein (7-1)

NASA
Lewis Research Center
21000 Brookpark Road
Cleveland, Ohio 44135
Attn: Warren H. Lowdermilk (106-1)

NASA
Lewis Research Center
21000 Brookpark Road
Cleveland, Ohio 44135
Attn: Dr. Louis Rosenblum (106-1)

NASA
Lewis Research Center
21000 Brookpark Road
Cleveland, Ohio 44135
Attn: Robert Siegel (49-2)

NASA
Lewis Research Center
21000 Brookpark Road
Cleveland, Ohio 44135
Attn: Robert Y. Wong (5-9)

NASA
Manned Spacecraft Center
Houston, Texas 77001
Attn: Librarian

NASA
George C. Marshall Space Flight Center
Huntsville, Alabama 35812
Attn: Librarian

NASA
George C. Marshall Space Flight Center
Huntsville, Alabama 35812
Attn: Ernst Stuhlinger

NASA
George C. Marshall Space Flight Center
Huntsville, Alabama 35812
Attn: Russell H. Shelton

NASA
Lewis Research Center
21000 Brookpark Road
Cleveland, Ohio 44135
Attn: Henry O. Slone (86-5)

NASA
Lewis Research Center
21000 Brookpark Road
Cleveland, Ohio 44135
Attn: Solomon Weiss (54-1)

NASA
Lewis Research Center
21000 Brookpark Road
Cleveland, Ohio 44135
Attn: John E. Dilley (86-1)

NASA
Lewis Research Center
21000 Brookpark Road
Cleveland, Ohio 44135
Attn: Patent Counsel (77-1)

NASA
Lewis Research Center
21000 Brookpark Road
Cleveland, Ohio 44135
Attn: Harold J. Christenson (5-3)

NASA
Lewis Research Center
21000 Brookpark Road
Cleveland, Ohio 44135
Attn: Robert G. Dorsch (11-1)

NASA
Lewis Research Center
21000 Brookpark Road
Cleveland, Ohio 44135
Attn: Robert E. English (86-1)

NASA
Lewis Research Center
21000 Brookpark Road
Cleveland, Ohio 44135
Attn: James P. Lewis (11-1)

NASA
Jet Propulsion Laboratory
4800 Oak Grove Drive
Pasadena, California 91103
Attn: Librarian

NASA
Jet Propulsion Laboratory
4800 Oak Grove Drive
Pasadena, California 91103
Attn: John Paulson

NASA
Western Operations Office
150 Pico Boulevard
Santa Monica, California 90406
Attn: John Keeler

NASA
Lewis Research Center
21000 Brookpark Road
Cleveland, Ohio 44135
Attn: Daniel Bernatowicz (100-1)

NASA
Lewis Research Center
21000 Brookpark Road
Cleveland, Ohio 44135
Attn: Ruth N. Weltmann (86-5) (6)

NASA
Lewis Research Center
21000 Brookpark Road
Cleveland, Ohio 44135
Attn: H. G. Hurrell (100-1)

NASA
Lewis Research Center
21000 Brookpark Road
Cleveland, Ohio 44135
Attn: D. Namkoong (86-1)

NASA
Lewis Research Center
21000 Brookpark Road
Cleveland, Ohio 44135
Attn: L. Gertsma (86-1)

NASA
Lewis Research Center
21000 Brookpark Road
Cleveland, Ohio 44135
Attn: Roger F. Mather (86-5)

NASA
Scientific & Technical Information Facility
Box 5700
Bethesda, Maryland 20014
Attn: NASA Representative (2)

NASA
Scientific & Technical Information
Washington, D. C. 20546
Attn: Code AFFSS-A

Air Force Systems Command
Aeronautical Systems Division
Wright-Patterson Air Force Base, Ohio 45433
Attn: R. J. Benzing (ASRCNL)

Air Force Systems Command
Aeronautical Systems Division
Wright-Patterson Air Force Base, Ohio 45433
Attn: Bernard Chasman (ASRCEA)

Air Force Systems Command
Aeronautical Systems Division
Wright-Patterson Air Force Base, Ohio 45433
Attn: George E. Thompson (ASRMFP-1)

Snap 50 Spur Office
U. S. Atomic Energy Commission
Washington, D. C. 20545
Attn: Herbert D. Rochen
NASA-AEC, Deputy

Snap 50 Spur Office
U. S. Atomic Energy Commission
Washington, D. C. 20545
Attn: Gerald Leighton

U. S. Atomic Energy Commission
Technical Reports Library
Washington, D. C. 20545
Attn: J. M. O'Leary (2)

U. S. Atomic Energy Commission
Technical Information Service
Extension
P. O. Box 62
Oak Ridge, Tennessee 37831 (2)

U. S. Atomic Energy Commission
Washington, D. C. 20545
Attn: R. M. Scroggins

U. S. Atomic Energy Commission
CANEL Project Office
P. O. Box 1102
Middletown, Connecticut 06458
Attn: C. E. McCalley

U. S. Atomic Energy Commission
Reactor Experiment Branch
Washington, D. C. 20545
Attn: T. W. McIntosh

Argonne National Laboratory
P. O. Box 299
Lemont, Illinois 60439
Attn: Librarian

Argonne National Laboratory
9700 South Cass Avenue
Argonne, Illinois 60440
Attn: John F. Marchaterre

Brookhaven National Laboratory
Upton, Long Island, New York 11973
Attn: Librarian

Brookhaven National Laboratory
Upton, Long Island, New York 11973
Attn: Dr. O. E. Dwyer

Oak Ridge National Laboratory
Oak Ridge, Tennessee 37831
Attn: Herbert W. Hoffman

Oak Ridge National Laboratory
Oak Ridge, Tennessee 37831
Attn: W. D. Manly

U. S. Naval Research Laboratory
Washington, D. C. 20390
Attn: C. T. Ewing

Columbia University
Department of Chemical Engineering
New York, N.Y. 10027
Attn: Dr. Charles F. Bonilla

Massachusetts Institute of Technology
Cambridge, Massachusetts 02139
Attn: Dr. Warren M. Rohsenow

University of Michigan
Department of Chemical and
Metallurgical Engineering
Ann Arbor, Michigan 48103
Attn: Dr. Richard E. Balzhiser

Southern Methodist University
Engineering School
Dallas, Texas 75222
Attn: Dr. Harold A. Blum

University of Wisconsin
Madison, Wisconsin 53706
Attn: Dr. Max W. Carbon

Advanced Technology Laboratories
Division of American Standard
369 Whisman Road
Mountain View, California 94040
Attn: Library

Aerojet-General Corporation
P. O. Box 296
Azusa, California 91702
Attn: Librarian (2)

Aerojet-General Nucleonics
P. O. Box 77
San Ramon, California 94583
Attn: Librarian (2)

Aerojet-General Nucleonics
P. O. Box 77
San Ramon, California 94583
Attn: John R. Payne

AiResearch Manufacturing Company
Sky Harbor Airport
402 South 36th Street
Phoenix, Arizona 85009
Attn: Librarian (2)

AiResearch Manufacturing Company
Sky Harbor Airport
402 South 36th Street
Phoenix, Arizona 85009
Attn: E. A. Kovacevich

AiResearch Manufacturing Company
9851-9951 Sepulveda Blvd.
Los Angeles, California 90045
Attn: Librarian

AiResearch Manufacturing Company
9851-9951 Sepulveda Blvd.
Los Angeles, California 90045
Attn: James J. Killackey

Atomics International
8900 DeSoto Avenue
Canoga Park, California 91303
Attn: Louis Bernath

Avco
Research & Advanced Development
Department
201 Lowell Street
Wilmington, Massachusetts 01800
Attn: Librarian

Babcock and Wilcox Company
Research Center
Alliance, Ohio
Attn: W. Markert, Jr.

Batelle Memorial Institute
505 King Avenue
Columbus, Ohio 43201
Attn: Alexis W. Lemmon, Jr.

Curtiss-Wright Corporation
Research Division
Tuehanna, Pennsylvania
Attn: S. Lombardo

Electro-Optical Systems, Inc.
Advanced Power Systems Division
Pasadena, California
Attn: Joseph Neustein

Euratom
Common Research Center of Ispra
Casella postale no. 1
Ispara (Varese)
Italy
Attn: Dr. Bernard P. Milliot
Heat Transfer Division

General Atomic
John Jay Hopkins Laboratory
P. O. Box 608
San Diego, California 92112
Attn: Librarian

General Motors Corporation
Allison Division
Indianapolis, Indiana 46206
Attn: Librarian

Geoscience Ltd.
8686 Dunaway Drive
La Jolla, California 92037
Attn: H. F. Poppendiek

Hughes Aircraft Company
Engineering Division
Culver City, California 90230
Attn: Tom B. Carvey, Jr.

Jacobs Engineering Company
774 East Green Street
Pasadena, California
Attn: Wayne Cochran

Marquardt Aircraft Company
P. O. Box 2013
Van Nuys, California
Attn: Librarian

Materials Research Corporation
Orangeburg, New York
Attn: Vernon E. Adler

The Martin Company
Nuclear Division
P. O. Box 5042
Baltimore, Maryland 21220
Attn: Librarian

MSA Research Corporation
Gallery, Pennsylvania 16024
Attn: Frederick Tepper

Plasmadyne Corporation
3839 South Main Street
Santa Anna, California
Attn: Librarian

Pratt & Whitney Aircraft
400 Main Street
East Hartford, Connecticut 06108
Attn: Librarian (2)

Pratt & Whitney Aircraft
400 Main Street
East Hartford, Connecticut 06108
Attn: Richard Curry

Pratt & Whitney Aircraft
400 Main Street
East Hartford, Connecticut 06108
Attn: Eugene Szetela

Pratt & Whitney Aircraft Division
CANEL-Connecticut Operation
P. O. Box 611
Middletown, Connecticut 06458
Attn: Librarian (2)

Pratt & Whitney Aircraft
CANEL-Connecticut Operation
Middletown, Connecticut 06458
Attn: Mr. Herbert Means

Rocketdyne
Canoga Park, California 91303
Attn: Librarian

Southwest Research Institute
8500 Culebra Road
San Antonio, Texas 78206
Attn: Dr. W. D. Weatherford, Jr.

Sundstrand Denver
2480 West 70th Avenue
Denver, Colorado 80221
Attn: Librarian

Thompson-Ramo-Wooldridge, Inc.
New Devices Laboratories
7209 Platt Avenue
Cleveland, Ohio 44115
Attn: Librarian

Thompson-Ramo-Wooldridge, Inc.
New Devices Laboratories
7209 Platt Avenue
Cleveland, Ohio 44115
Attn: A. Ziobro

Union Carbide Nuclear Company
P. O. Box X
Oak Ridge, Tennessee 37831
Attn: X-10 Laboratory Records
Department (2)

United Nuclear Corporation
Development Division
5 New Street
White Plains, New York
Attn: Librarian

Westinghouse Electric Corporation
Astronuclear Laboratory
P. O. Box 10864
Pittsburgh, Pennsylvania 15236
Attn: Librarian

Westinghouse Electric Corporation
Aero-Space Department
Lima, Ohio 45801
Attn: Librarian

General Atomic
John Jay Hopkins Laboratory
P. O. Box 608
San Diego, California 92112
Attn: Librarian (2)

General Dynamics/General Atomic
P. O. Box 608
San Diego, California 92112
Attn: Librarian (2)

California Institute of Technology
Jet Propulsion Laboratory
4800 Oak Grove Drive
Pasadena, California 91103
Attn: Mr. Gerald M. Kikin

A. L. Clarkson
3325 Wilshire Blvd.
General Electric Company
Los Angeles, California 90005

Research Institute of Temple
University
4150 Henry Avenue
Philadelphia, Pennsylvania 19144
Attn: A. V. Grosse

Professor W. E. Hilding
Department of Mechanical Engineering
University of Connecticut
Storrs, Connecticut 06268

Reactor Engineering Argonne
Materials Laboratory
Argonne, Illinois 60440
Attn: Ralph P. Stein

Knolls Atomic Power Laboratory
P. O. Box 1072
Schenectady, New York 12301
Attn: Document Librarian

S. V. Manson & Company, Inc.
38-41 Morlot Avenue
Fair Lawn, New Jersey 07410
Attn: S. V. Manson

General Electric Company
P. O. Box 100
Richland, Washington 99352
Attn: Technical Information Operation
Dr. T. T. Claudson

North American Aviation, Incorporated
Atomics International Division
Canoga Park, California
Attn: Paul Cohn